Electronic Theses and Dissertations   Graduate School

2011

New Synthetic Methodologies for the Construction and Optimization of Natural Products

Amir E. Wahba

Follow this and additional works at: https://egrove.olemiss.edu/etd

Part of the Pharmacy and Pharmaceutical Sciences Commons

NEW SYNTHETIC METHODOLOGIES FOR THE CONSTRUCTION AND

OPTIMIZATION OF NATURAL PRODUCTS

A Dissertation
Presented in Partial Fulfillment of the Requirements for the Degree Doctor Philosophy in
Pharmaceutical Sciences (with Emphasis in Pharmacognosy)
The University of Mississippi

by

AMIR E. WAHBA

August 2011

ABSTRACT

Toxicity associated with bioactive natural products is considered a major obstacle in the process of drug discovery. Manzamine A (MA) is one such candidate that requires optimization to overcome the toxicity problem. The manzamine alkaloids represent a unique class of natural products that have shown a diverse range of bioactivities including antimicrobial, antiparasitic, cytotoxicity, anti-inflammatory, pesticidial and was shown to possess activity against HIV-1 and AIDS opportunistic infections.[1] The greatest potential for the manzamine alkaloids appears to be against malaria and neuroinflammation.[1,14,45] Experimental and modeling studies suggested that the planer β-carboline moiety can act as DNA intercalator and hence induce toxicity.[14] Thus either modification or the replacement of the β-carboline moiety with other heterocycles could eliminate DNA intercalation and will be a straightforward step toward generating manzamine-like analogs with similar or better biological activities and reduced toxicity.

An optimized purification approach, that utilized an acid-base treatment of the acetone extract of the Indonesian sponge *Acanthostrongylophora sp.,* have been used to obtain a 100 g scale of pure manzamine A and 8-hydroxymanzamine A. Further purification of the more polar fractions led to the isolation of the known manzamines: manzamine F, 12,34-oxamanzamine E, 31-keto-12,34-oxa-32,33-dihydroircinal A, along with two new manzamine-related analogs, acantholactone with unprecedented δ-lactone and 2,21,28-trioxomanzamine J.

Twenty manzamine A amides were synthesized through the nitration, reduction and acylation of C-6 and C-8 of the β-carboline moiety. These analogs were evaluated for in vitro

antimalarial and antimicrobial activities. The amides of MA showed significantly reduced cytotoxicity against Vero cells, although were less active than MA. Two amides 6-cyclohexyamidomanzamine A and 8-*n*-hexamidomanzamine A showed potent antimalarial activity in vitro against *Plasmodium falciparum* and were further evaluated in vivo in *Plasmodium berghei* infected mice. Oral administration of these analogs at the dose of 30 mg/kg (once daily for three days) caused parasitemia suppression of 24% and 62%, respectively, with no apparent toxicity.

Aminomanzmaines were observed to be unstable in solution and this instability affected the yield of the amides. This instability inspired the development of a simple and practical approach for the one-pot conversion of nitroarenes into amide derivatives. HOAc/Zn were utilized as a reducing agent and acyl chloride/Et$_3$N were used as the acylating agent in DMF with good yield (~60%) of the amide. This method was applicable to 6-nitromanzamine A, where the yield of 6-cyclohexamidemanzamine A was significantly improved (56%) by this approach relative to starting with 6-aminomanzamine A (17%). *N*-Alkylation of the aminomanzamines was also problematic because of the instability issue. Utilizing the same reducing system (HOAc/Zn), a simple, mild, cost effective, and green approach for the reductive mono *N*-alkylation of nitroarenes was developed. Carbonyl compounds were utilized as the alkyl source in methanol. Excellent yields were obtained with stoichiometric control of mono over dialkylated products. In order to show the general applicability of our optimized conditions, five natural products: harmane, estradiol, quinine, manzamine F and curcudiol were nitrated and modified

using our green *N*-alkylation strategy. Our new reductive alkylation conditions were well tolerated by the nitrated natural products and afforded moderate to excellent yields.

The straightforward oxidation of ircinal A to ircinoic acid inspired utilizing the decarboxylative cross coupling (DCCC) approach for the replacement of the β-carboline moiety with other heterocycles. Optimization of the DCCC reaction was completed using (*S*)-perillic acid as a model compound; however, failed with ircinoic acid. We then switched to the ircinal derived triflate and Suzuki coupling approach. Our proposed scheme was based on Birch reduction of ircinal A followed by an oxidative deformylation that should generate the corresponding oxo derivative that could be converted to the derived triflate. New and unexpected sequences of reactions were observed in the Birch reduction of ircinal A under atmospheric air. A sequential Birch reduction-elimination-oxidative deformylation occurred and yielded the unexpected ircinal-derived enone. Further optimizations are needed to convert the new enone to the corresponding triflate.

DEDICATION

I dedicated this work to my wife Hoda Gebril and my children Malek and Omar, without their encouragement, support and love I would not be able to finish this work. It is also dedicated to my family, my father, my mother and my brothers and sister.

LIST OF ABBREVIATIONS AND SYMBOLS

AIDS: Acquired Immunodeficiency Syndrome

CD_3OD: Deuterated Methanol

CD: Circular Dichroism

COSY: COrrelation SpectroscopY

DEPT: Distortionless Enhancement by Polarization Transfer

DCCC: Decarboxylative Cross Coupling

DCM: DiChloroMethane

DMSO: DiMethyl SulfOxide

DMF: DiMethyl Formamide

EC_{50}: Effective Concentration, 50%

EtOAc: Ethyl Acetate

GSK-3: Glycogen Synthase Kinase

HOAc: Acetic acid

HMBC: Heteronuclear Multiple Bond Coherence

HMQC: Heteronuclear Multiple Quantum Coherence

HPLC: High Pressure Liquid Chromatography

HRESIMS: High Resolution Electrospray Ionization Mass Spectrometry

HSQC: Heteronuclear Single Quantum Coherence

HIV: Human Immunodeficiency Virus

IC50: Inhibitory Concentration, 50%

IR: Infrared

LC-MS: Liquid Chromatography–Mass Spectrometry

LD50: Lethal Dose, 50%

LDH: Lactate DeHydrogenase

MA: Manzamine A

MOA: Mechanisms Of Action

MS: Mass Spectrometry

MeOH: Methanol

MIC: Minimum Inhibitory Concentration

NA: Not Active

NMR: Nuclear Magnetic Resonance

NOE: Nuclear Overhauser Effect

NOESY: Nuclear Overhauser Effect SpectroscopY

ROESY: Rotating frame Overhause Effect SpectroscopY

SI: Selectivity Index

TLC: Thin-Layer Chromatography

TOF: Time-Of-Flight

TXB_2: Thromboxane B_2

VLC: Vacuum Liquid Chromatography

ACKNOWLEDGMENTS

TABLE OF CONTENTS

LIST OF TABLES

LIST OF FIGURES

Review

New One-Pot Methodologies for the Modification or Synthesis of Alkaloid Scaffolds

Amir E. Wahba [1] **and Mark T. Hamann** [1,2,3,]*

CHAPTER I

NEW ONE-POT METHODOLOGIES FOR THE MODIFICATION OR SYNTHESIS OF

ALKALOIDS SCAFFOLDS

Published in Marine Drugs, 2010, 8, 2395-2416.

Authors: Amir E. Wahba and Mark T. Hamann

Abstract: There are several avenues by which promising bioactive natural products can be produced in sufficient quantities to enable lead optimization and medicinal chemistry studies. Total synthesis of natural products is an important, but sometimes difficult, approach and requires the development of innovative synthetic methodologies to simplify the synthesis of complex molecules. Various classes of natural product alkaloids are both common and widely distributed in plants, bacteria, fungi, insects and marine organisms. This mini-review will discuss the scope, mechanistic insights and enantioselectivity aspects of selected examples of recently developed one-pot methods that have been published in 2009 for the synthesis of substituted piperidines, quinolizidines, pyrrolidines, hexahydropyrrolizines, octahydroindolizines, and γ-lactams. In addition, progress on the synthesis of β-carboline (manzamine) alkaloids will also be discussed.

I.1. Introduction

The challenging task of developing a drug candidate from a natural source to clinical usage has many obstacles. Toxicity, development of resistance associated with the drug candidate, and providing a sufficient amount of material needed for preclinical and clinical studies, all represent major challenges. Although nature has been generous in providing structurally diverse molecules with varying biological activities, it is not always possible to obtain the required quantities of the target drug candidate. This lack of material has inspired innovative chemistry that develops new methodologies, catalysts, and inventive synthetic routes for the synthesis and modification of natural products.

Our research program has been involved in isolation and optimization process of a number of marine alkaloids and peptides. Among the most intriguing is manzamine A (**1**) with impressive antimalarial activity. A number of chemical stability challenges associated with its chemical modification require significant attention due to the complexity of the structure. This compound can be readily isolated from a marine sponge in good yields.[1] This inspired the development of new one-pot synthetic methodologies and conditions which are applicable to **1** and to other bioactive natural products.

During lead optimization of the manzamine alkaloids, the importance of one-pot methods for scaling certain drug leads became apparent. One-pot reactions are reactions in which two or more bond-forming transformations take place under the same reaction conditions without adding additional reagents or catalysts.[2] These reactions have numerous applications in the field of total synthesis of natural products, particularly in avoiding the costly protection/deprotection processes and purification of intermediates.[2–6] The importance of these reactions to the organic synthesis community is illustrated by the numerous reviews that have discussed different aspects

of these reactions.[2-11] Most of these reviews discuss one-pot reactions that were developed during the total synthesis of selected examples of natural products (either as designed or serendipitous developments) such as Nicolaou's[4-6] and Tietze's[2,3] reviews. Although outstanding one-pot transformations designed for total synthesis of natural products were highlighted in these reviews, other one-pot transformations designed for other purposes were omitted. Synthesis of heterocycles by one-pot methodologies were discussed in detail in Padwa's reviews.[9,10] Specific reviews on the construction of alkaloids are not found with the exception of Kobayashi's review that discussed new methodologies developed for the total synthesis of some select examples of alkaloids.[11]

Owing to the growing interest in marine alkaloids, a detailed discussion of select, newly developed one-pot methodologies that have been utilized for modification of marine alkaloids or the synthesis of common alkaloid moieties emphasizing asymmetric synthesis, are presented here. This mini-review discusses applications, mechanistic insights and enantioselectivity of recently developed one-pot methods that have been published during 2009. Those reports that could be applied in the synthesis of marine alkaloid scaffolds (*i.e.*, alkaloid moieties found in marine alkaloids) are emphasized. This mini-review will also cover our results for manzamine alkaloids, as well as detailed asymmetric one-pot methods for the synthesis of substituted piperidines, quinolizidines, pyrrolidines, hexahydropyrrolizines, octahydroindolizines and γ-lactams.

I.2. New One-Pot Methods Used in the Modification of Marine Alkaloids

One-pot reductive amidation of nitroarenes

4

Manzamine alkaloids are a unique class of compounds that contain a complicated ring system coupled with a β-carboline moiety (Figure I.1). The first representative of this family is manzamine A (**1**), which was first isolated by Higa and co-workers in 1986.[11] This class of alkaloids has shown a wide range of biological activities (antimicrobial, antiparasitic, cytotoxicity, anti-inflammatory and pesticidal) and has also shown activity against HIV-1 and AIDS opportunistic infections.[12] The most potent activity for the manzamine alkaloids appears to be against malaria. Manzamine A (**1**) and its natural analog 8-hydroxymanzamine A (**2**) exhibited improved potency against malarial parasites both in vitro and in vivo relative to chloroquine and artemisinin.[13] However, toxicity associated with high dose schedules limited the development of this class of compounds as new antimalarial drugs.
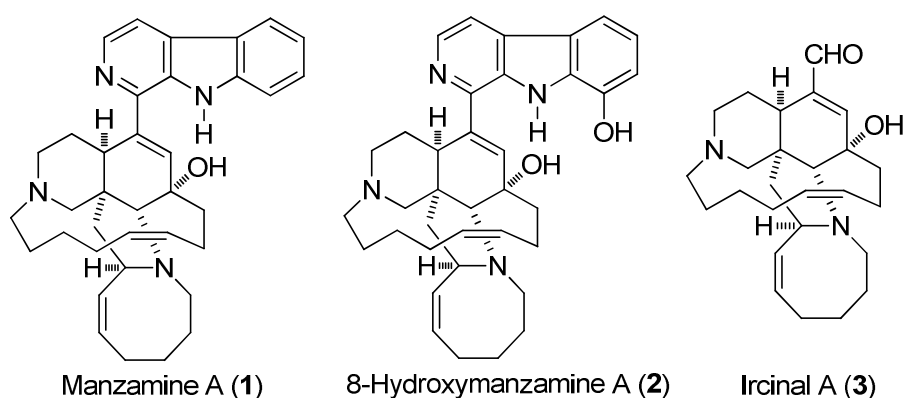
Figure I.1. Manzamine alkaloids.

Since the mechanism of action of manzamine alkaloids as antimalarial agents is not clear; several structure activity relationship (SAR) and optimization studies using **1**, **2** or **3** as starting materials have been completed.[14-18] Nitration of **1** yielded 6- and 8- nitromanzamines and after reduction afforded the corresponding aminomanzamines (Scheme I.1). Aminomanzamines are not stable, making them unsuitable for further amidation and *N*-alkylation reactions. However, 20 amide analogs were successfully synthesized in low yield.[15]

5
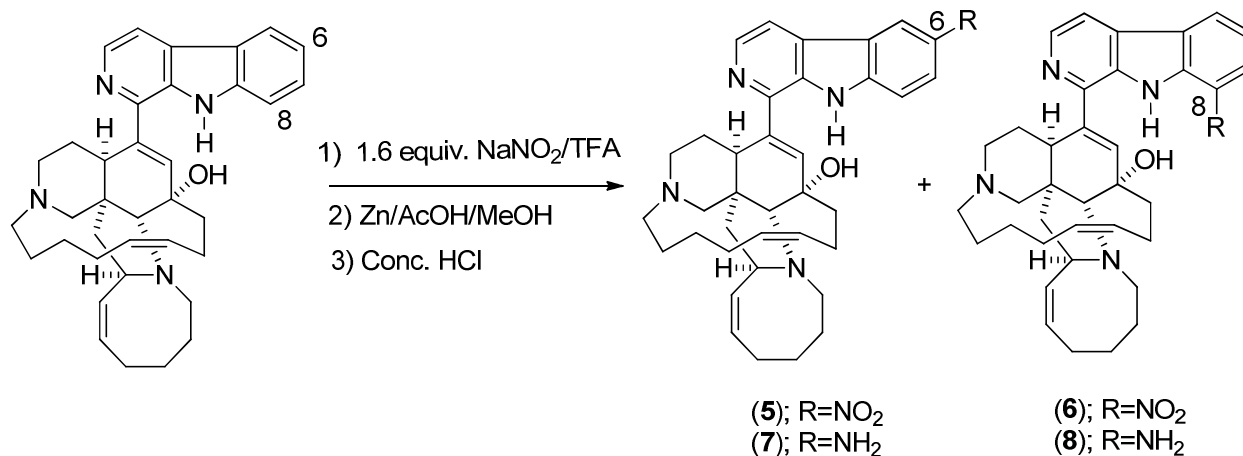
Scheme I.1. Nitration of manzamine A.

Inspired by the instability of aminomanzamines (**7** and **8**) and by the low yields of amidomanzamine derivatives, a one-pot reductive amidation method was developed for the conversion of nitroarenes to the corresponding amides.[19] Reduction of the nitro group generally requires a protic solvent as a carrier of the hydrogen generated *in situ*. However, amidation reactions using acyl chloride require aprotic solvents as well as dry conditions to prevent side reactions with the solvent. In addition, an amidation reaction using acyl chlorides requires basic conditions in which the base will neutralize the hydrochloric acid liberated from the reaction as a by-product. Because of this, a 3° amine base (triethylamine, Et_3N) was added in the reduction step where equimolecular amounts of acetic acid and zinc are used in addition to the acyl chloride. Once the amine is formed *in situ*, it immediately reacted with the acyl chloride facilitated by the tertiary amine. Dimethylformamide (DMF) was shown to be the best choice of solvent for this reaction (Scheme I.2). Using the optimized conditions, several nitroarenes were screened for one-pot conversion to amides. All reagents were added at once and complete

conversion of the starting materials to the corresponding amines and amides was observed with ~60% yield of the amides.
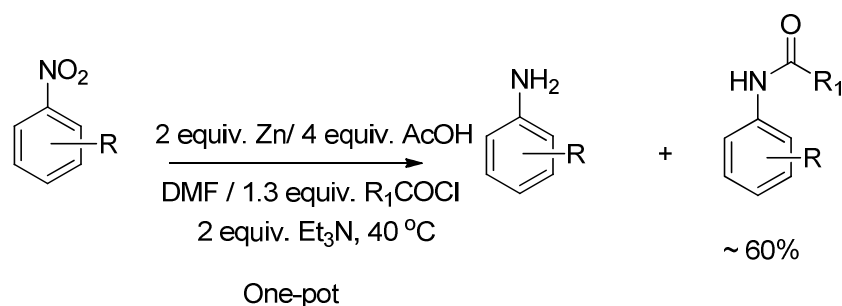
Scheme I.2. Optimized one-pot conditions for the reductive amidation of nitroarenes.

As a validation of this method, a one-pot approach was used for the synthesis of 6-cyclohexamidomanzamine A (**9**). This amide showed potent antimalarial activity in vitro with an IC_{50} of 0.032 μM against the D6 clone of *Plasmodium falciparum*, and was synthesized from 6-aminomanzamine A (**7**) through the normal amidation pathway with low yield (17%).[15] Starting with 6-nitromanzamine A (**5**), and using the optimized one-pot reductive amidation method, the yield of amide **9** was increased to 56% (Scheme I.3). It was surprising that the reductive amidation of **5** proceeded without the addition of a 3° amine. A reasonable explanation for this observation is that **5** has two internal 3° amino functionalities which could possibly facilitate the reductive amidation reaction. To validate this, harmane was nitrated to produce the closely related model compounds, 6- and 8- nitroharmanes. When optimized one-pot reductive amidation conditions were applied to nitroharmanes without the addition of Et_3N, no amides were obtained, only aminoharmanes (Scheme I.4, Equation 1); however, by adding Et_3N the amide derivatives of harmane were isolated in good yield (60%) (Scheme I.4, Equation 2). These experimental results validated the hypothesis regarding the 3° amino capacity of manzamine alkaloids.

Although this method was developed particularly for the modification of manzamine alkaloids, it has clear utility in the synthesis of other alkaloids. The nitration of several biologically active natural products, as well as currently utilized drugs to generate the starting nitro materials for this one-pot reductive amidation method is ongoing. The goal is to show the general and practical applications for this method, as well as generating a library of compounds for further optimization and biological evaluation.
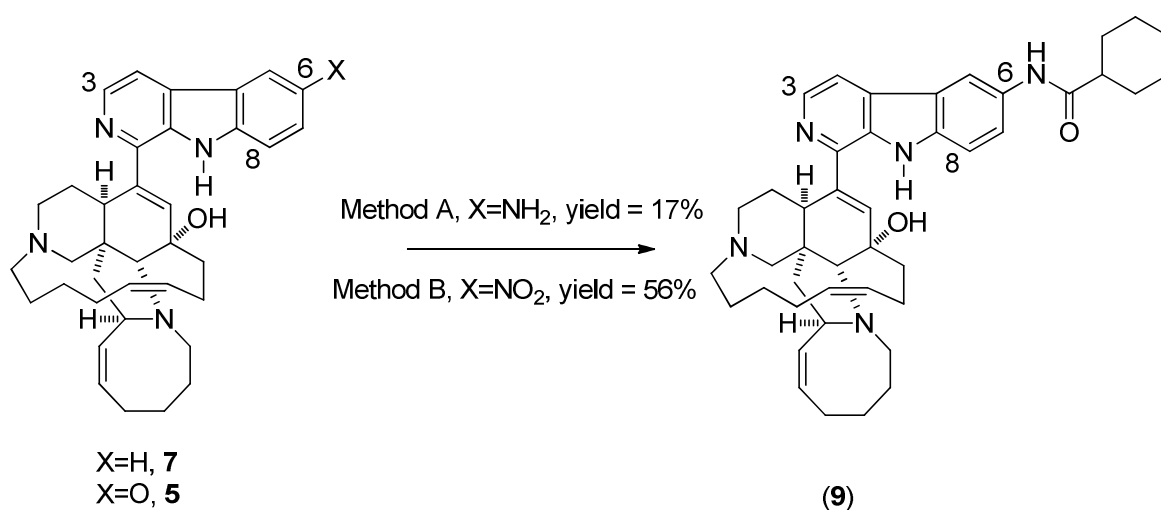
Scheme I.3. Synthesis of 6-cyclohexamidomanzamine A (**9**) by direct and reductive amidation approaches. Method A: 1.2 equiv. cyclohexylcarbonyl chloride, 1.1 equiv. Et$_3$N, cat. DMAP, THF, rt, 1 h; Method B: 2 equiv. Zn/4 equiv. HOAc, 2 equiv. Et$_3$N, 1.2 equiv. cyclohexylcarbonyl chloride, DMF, 40 °C, one-pot.
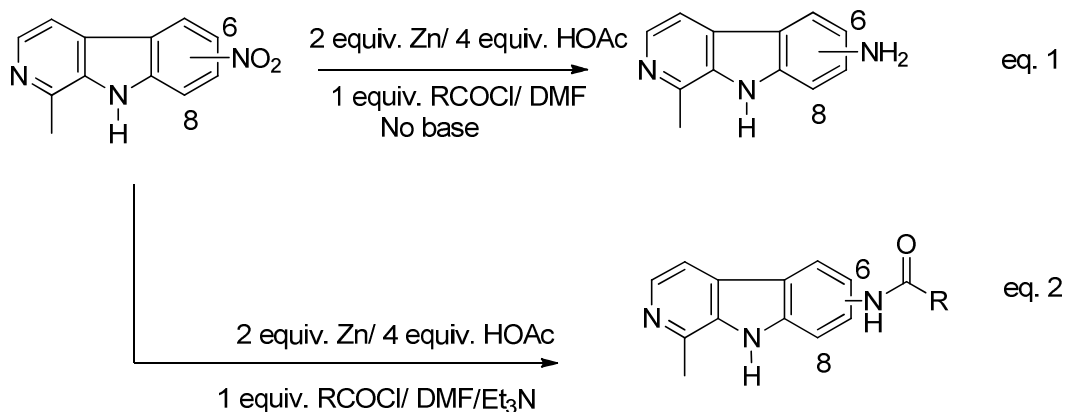
Scheme I.4. Validation of the internal 3° amino functionalities in manzamine A using nitroharmane as a model compounds.

I.3. New One-Pot Reactions Used in the Asymmetric Construction of Some Important Alkaloid Moieties

I.3.1. One-pot asymmetric synthesis of substituted piperidines

Piperidine containing alkaloids are common in marine environments.[20-22] Although there have been several synthetic methods[23-25] reported for construction of this moiety, stereoselectivity remains a challenging task especially when three or more stereogenic centers or quaternary substituted carbons are present. The Shi group developed a novel cascade approach for the stereoselective synthesis of the piperidine moiety, based on their development of an intermolecular cross-double-Michael addition between α,β-unsaturated carbonyl compounds and nitroalkenes, facilitated by amines as Lewis bases (LB).[26] Allylic nitro products are generated in the process via β-elimination of LB (Figure I.2). The new cascade reaction encouraged Shi's group to extend the cascade by involving an activated electrophilic intermediate for the construction of nitrogen containing heterocycles with two or more stereogenic centers.

9
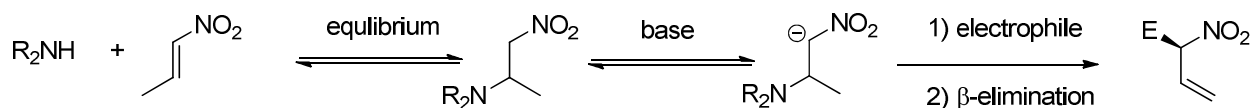
Figure I.2. Intermolecular cross-double-Michael addition facilitated by amines via β elimination.

Based on their previous results, which showed that addition of the amine to nitroalkene is fast, they proposed a one-pot cascade approach for the asymmetric synthesis of the piperidine moiety.[27] They postulated that adduct **A** (Figure I.3), the addition product of the amine with nitroalkene, was suitable for Michael addition type reaction with an activated carbonyl to generate adduct **B.** Ring closure then provides the substituted piperidine motif in a one-pot approach with the generation of two stereogenic centers. To validate this proposed one-pot cascade sequence, nitrostyrene was allowed to react with methyl vinyl ketone (MVK) in the presence of a primary amine (Scheme I.5). Being a complex mixture with many possible side reactions (*i.e.*, Baylis-Hillman reaction), it was surprising that substituted piperidines, **13a** and **13b**, were obtained in excellent yields and good diastereoselectivities with no side products. Solvent optimization of these one-pot conditions showed that THF gave the best yields with good diastereoselectivities (97%, dr = 7:1 for **13a**; 85%, dr = 15:1 for **13b**). Formation of **13** confirmed the formation of adduct **B** (Figure I.3), which was trapped by a sequential Henry-aldol cyclization. Although three stereogenic centers were generated in piperidine **13** only two C-4 diastereoisomers were obtained, of which the *cis* isomer of C-3 nitro and C-4 hydroxy groups was the major product.
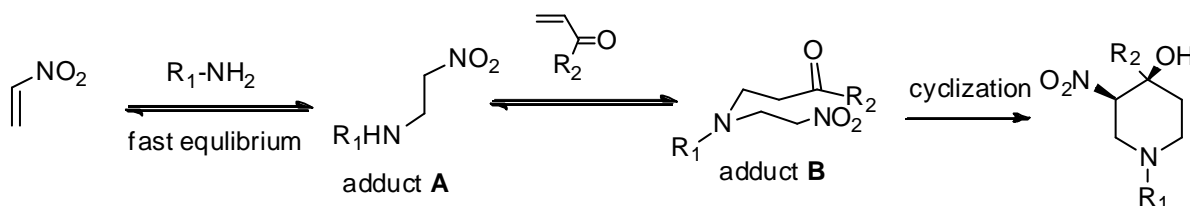
Figure I.3. Proposed one-pot cascade piperidine synthesis.
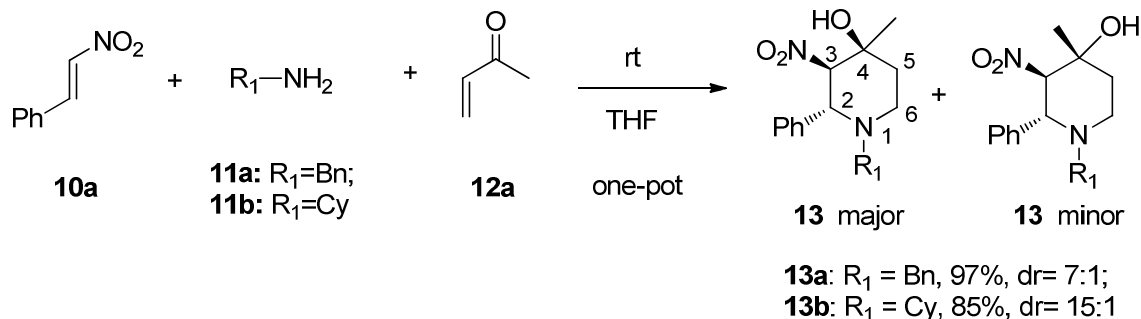
Scheme I.5. Optimized one-pot condensation for the asymmetric synthesis of piperidine moiety.

This one-pot reaction was compatible with a variety of nitroalkenes, amines and activated carbonyls. Different aryl and alkyl substituted nitroalkenes generated variation at C-2. Moreover, both alkyl and aryl ketones were suitable for this cascade one-pot process giving different choices of substituents at C-4. Substituents at C-5 were possible through α-substituted enones, while β-substituted enones delivered variation at C-6 only when ammonia was used. It is interesting that only C-4 isomers were obtained in all cases.

The aza-Michael adduct **B** (Figure I.3) was not observed in their mechanistic studies (using ^{1}H-NMR); moreover, the piperidine products were stable under strong basic conditions. These results strongly suggested that the irreversible Henry-aldol cyclization was the rate determining step, which accounts for the piperidine diastereoselectivity through the chair-like transition state. With the formation of the C-2 stereogenic center during the amine conjugate addition, it is possible that the stereochemistry of the final piperidine product could be selectively induced by chiral amines through its involvement in spatial arrangement of chair-like transition states. In this case, a new stereogenic center at the exocyclic C-7 will be introduced in the piperidine product,

which may result in the formation of four diastereoisomers. To investigate this proposed chirality induction, arylethanamines **14a–c** were applied in the one-pot piperidine synthesis and as expected, piperidines **15a–c** were obtained in good yields (Scheme I.6). The results showed excellent diastereoselectivity at C-4 in **15a** and **15b** with dr > 10:1. In addition, modest chirality induction by the C-7 center was observed with dr = 4:1.
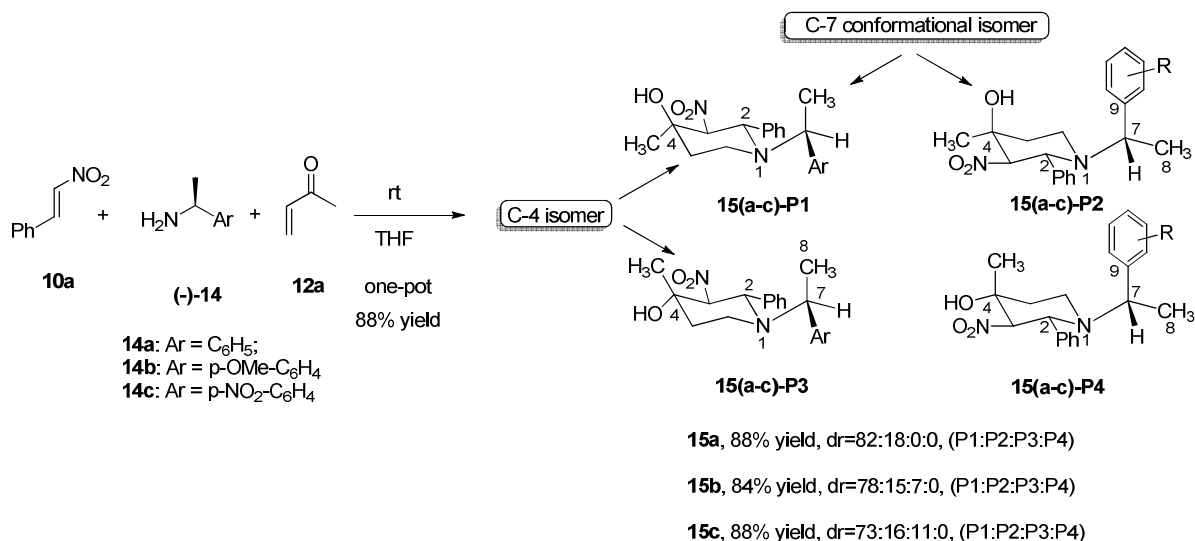
Scheme I.6. Chirality induction by chiral amines.

X-ray analysis of the piperidine crystals revealed that exocyclic C-7 adopted a staggered conformation with respect to the ring. Moreover, the chemical shifts of C-8 and C-9 were significantly shifted upfield in an anti-parallel position relative to the nitrogen lone pair electrons. This data suggest that N1-C7 σ-bond rotation was restricted. Based on these results, a Henry-aldol cyclization chair transition state was proposed in Figure I.4. The N-1 nitrogen lone pair electrons were placed in the axial position and the preferred staggered N1-C7 conformation could be achieved when the small group at C-7 was placed anti (axial orientation) to N-1 nitrogen lone pair. Three *syn*-pentane interactions were expected in this staggered conformation (as shown in Figure I.4); however, placement of the small group on C-7 anti to the lone pair will

minimize these interactions. This proposed transition state was consistent with experimental observations. Also, stability of this transition state could be influenced by the n-σ* electronic interaction between the nitrogen lone pair and the exocyclic axial small group.
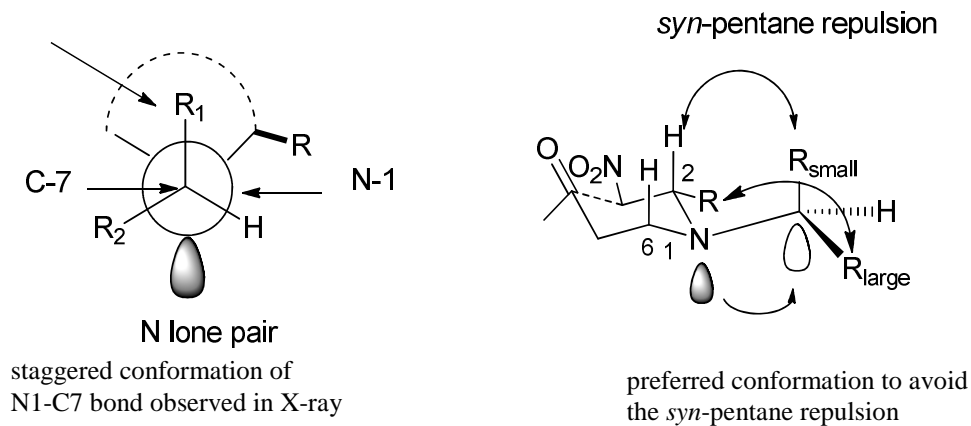
Figure I.4. Proposed chair transition state and the exocyclic chirality induction.

To validate the importance of this n-σ* electronic interaction in chirality enhancement, methyl group in the chiral amine was replaced with a carboxylate group which is less bulky and would produce a stronger n-σ* interaction. As expected, the reaction of the amino esters **16a**, **b** with enone **12a** and nitroarene **10a** yielded the corresponding piperidine products in moderate yields (Scheme I.7). Interestingly, piperidines **17a**, **b** were obtained in diastereomerically pure form. Complete chirality induction was achieved through control via exocyclic asymmetry. This new one-pot method opens the door for the asymmetric synthesis of several natural products that contain a piperidine moiety.
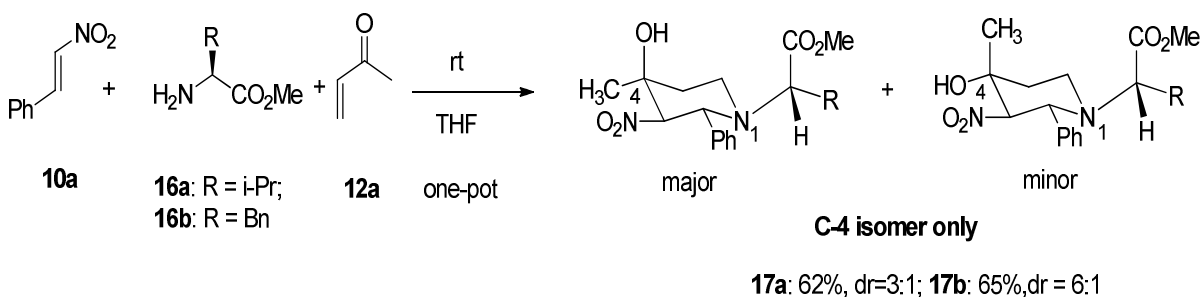
Scheme I.7. Enhanced exocyclic stereochemistry control by amino esters.

I.3.2. One-pot organo-catalytic synthesis of quinolizidine derivatives

An elegant one-pot method was recently developed by Franzen and Fisher[28] for the asymmetric synthesis of substituted quinolizidines. This moiety is widely represented in several alkaloids isolated from plants, ants and marine organisms. Their retrosynthetic analysis for the indolo[2,3-*a*]quinolizidine skeleton is shown in Figure I.5. They postulated that the stereogenic center 12b could be generated through the asymmetric acyliminium ion cyclization of the imine (**19**). This imine could be obtained from the aldehyde precursor **20**, in which the aldehyde is apparently the adduct of an enantioselective Michael addition.
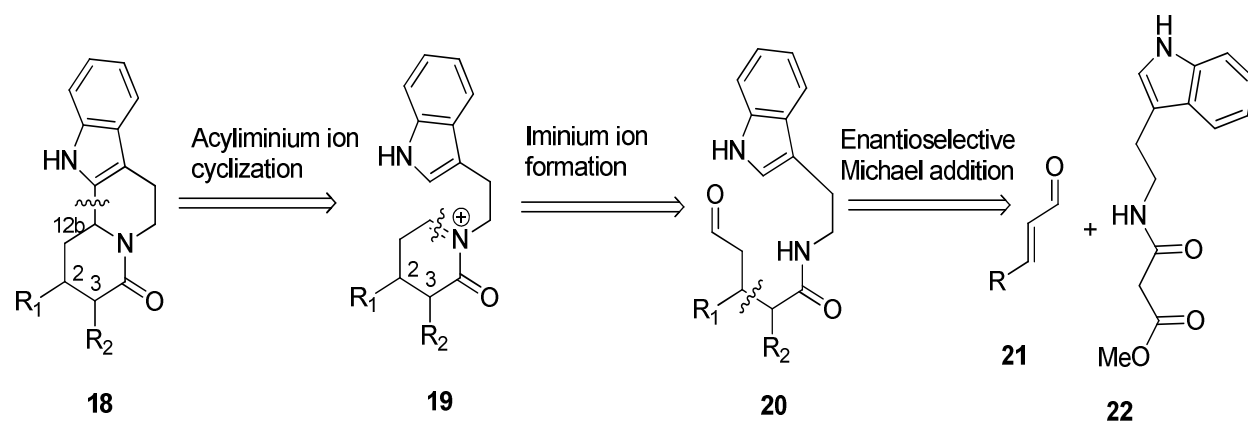
Figure I.5. Retrosynthetic analysis of the indolo[2,3-*a*]quinolizidine skeleton.

This retro-analysis required the addition of an activated amide **22** to the unsaturated aldehyde **21**, which has not yet been reported. To accomplish their synthetic plan, they optimized the enantioselective Michael addition of cinnamic aldehyde **23** and an activated indol substituted amide **22,** using different proline derivatives as organocatalysts (Figure I.6), exploring different solvents, temperatures, as well as various acids needed for the cyclization step of the acyliminium ion (Scheme I.7). Dichloromethane (DCM) was the solvent of choice and yielded compounds **24a** and **24b** with full conversion at room temperature, but with low enantioselectivity (88% ee). Enantioselectivity was increased to 94% by lowering the temperature to 3 °C, while further cooling (−20 °C) resulted in only 5% conversion. The proline derivative (*S*)-**A** showed the best selectivity, **B** was less selective and less active, while **C** and **D** were inactive for this reaction. When trifluoroacetic acid (TFA) was used in the acid-catalyzed cyclization of the acyliminium ion, indoloquinolidine products were obtained nonselectively as a 1:1 mixture. However, some

selectivity of **24a** over **24b** was observed when HCl was used. It was also noted that cooling down the reaction mixture prior to the addition of HCl increased the selectivity up to 85:15. The optimized conditions are highlighted in Scheme I.7.
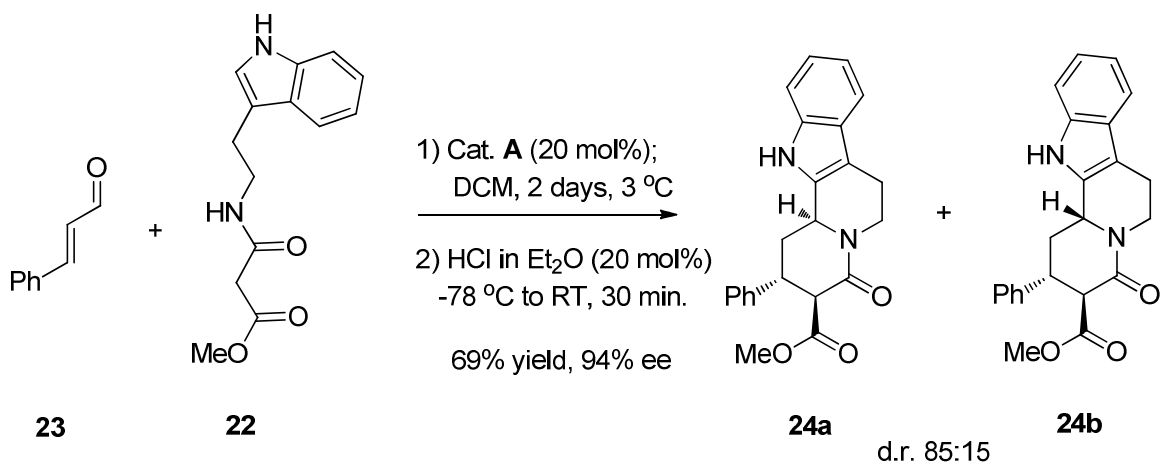
Scheme I.7. Optimized one-pot, two step conditions for the synthesis of indoloquinolizidine derivatives.
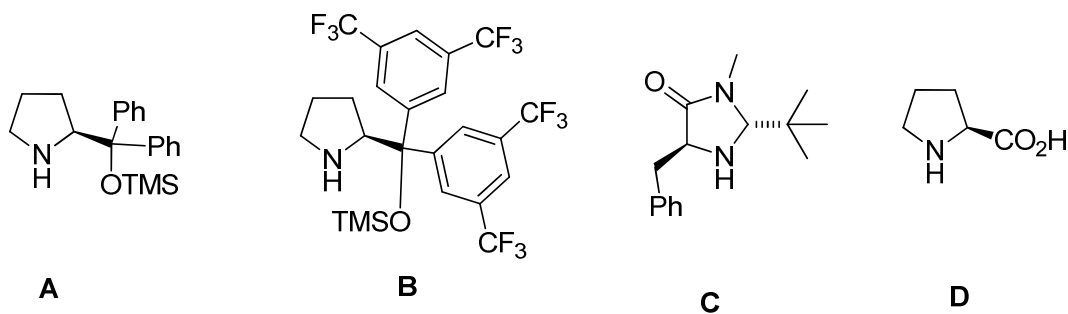
Figure I.6. Organocatalysts used for the optimization of the one-pot conditions.

This one-pot, two step method was applied to several aromatic α,β-unsaturated aldehydes with good to excellent enantioselectivity. The indolyl moiety of **22** was replaced with an electron-rich phenyl group, which should give direct access to the benzo[*a*]quinolizidine

skeleton. Reaction between **23** and the activated amide **25,** in the presence of the organocatalyst **A,** and subsequent addition of HCl, afforded the benzo[*a*]quinolizidines **26a** and **26b** with good to high enantioselectivity (Scheme I.8). It was noted that the formation of the benzo[*a*]quinolizidine moiety required stronger acidic conditions (40 mol%) relative to the indolo[2,3-*a*]quinolizidine (20 mol%). This is explained by the poorer nucleophilicity of the phenyl ring compared to the 3-indolyl moiety.
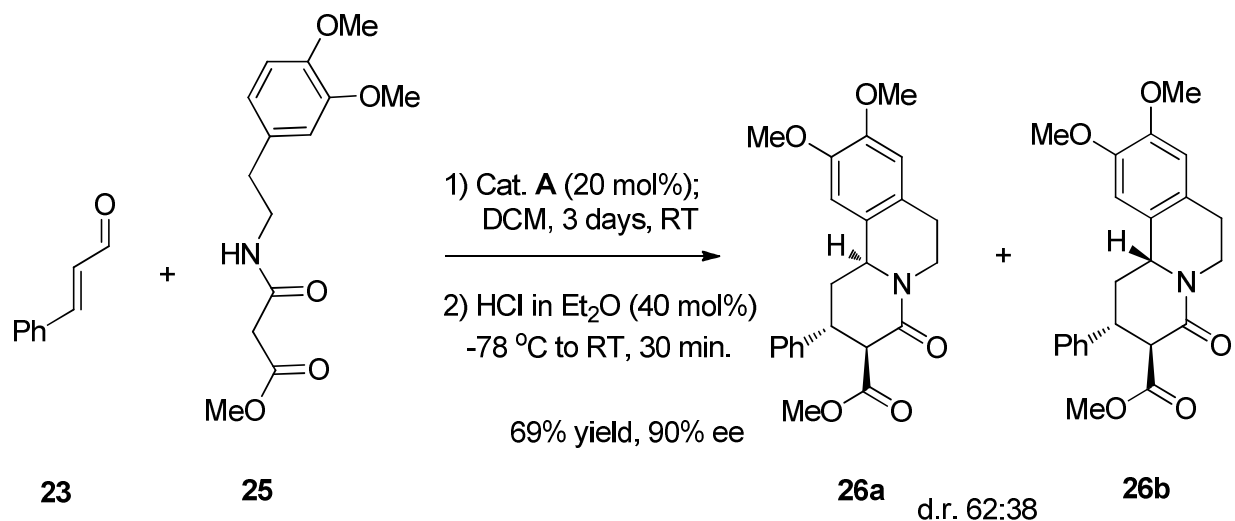
Scheme I.8. Optimized one-pot, two step synthesis of benzo[*a*]quinolizidine.

The absolute configuration of one of the benzo[*a*]quinolizidine derivatives was established by X-ray analysis as 2*R*,3*S*,11b*S*, which provided important mechanistic insight (Scheme I.9). The aryl groups in the catalyst will shield the *Re* face of the iminium intermediate **27**, which will help to establish *S* configuration on C-2 through the unshielded *Si* face. Intramolecular imine formation with epimerization of the stereochemically labile C-3 stereogenic center will establish the thermodynamically more stable 2*R*,3*S*-*trans* configuration of the intermediate imine **28**. This

acyliminium ion undergoes an electrophilic aromatic substitution with the aromatic moiety to give quinolizidine products.
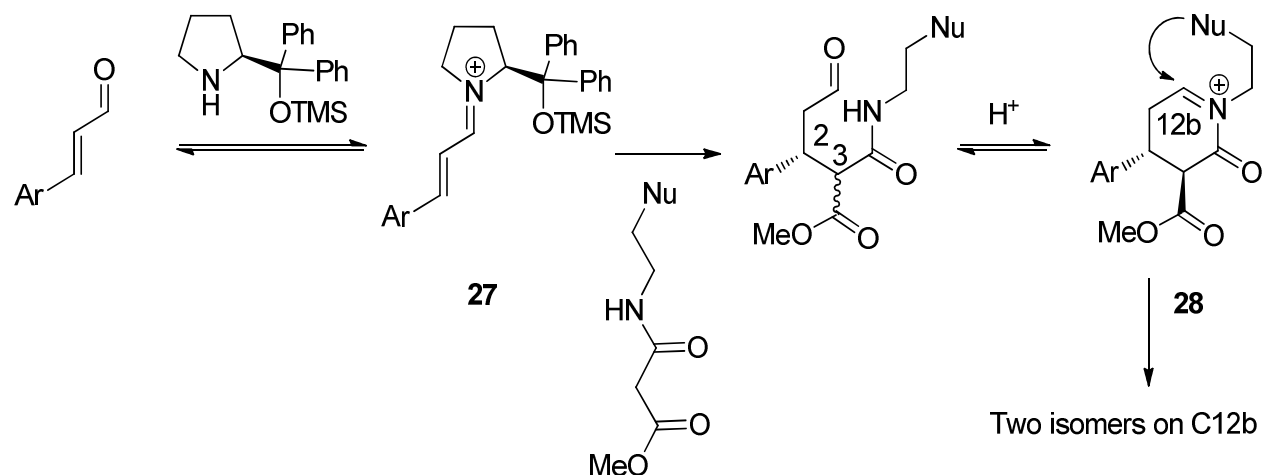
Scheme I.9. Proposed mechanism for the one-pot formation of quinolizidine moiety.

The excellent diastereoselectivity observed in the acid catalyzed cyclization could be explained based on the reaction conditions. Considering the synthesis of indoloquinolizidines **24a** and **24b** (Scheme I.7), the major isomer was **24a** with the indolyl moiety in an axial orientation. Although the formation of **24a** resembles a higher energy product, reaction via the transition state I (Scheme I.10) is under kinetic control (−78 °C), owing to less steric hindrance from the equatorial α–protons relative to the theromodynamic equatorial product.
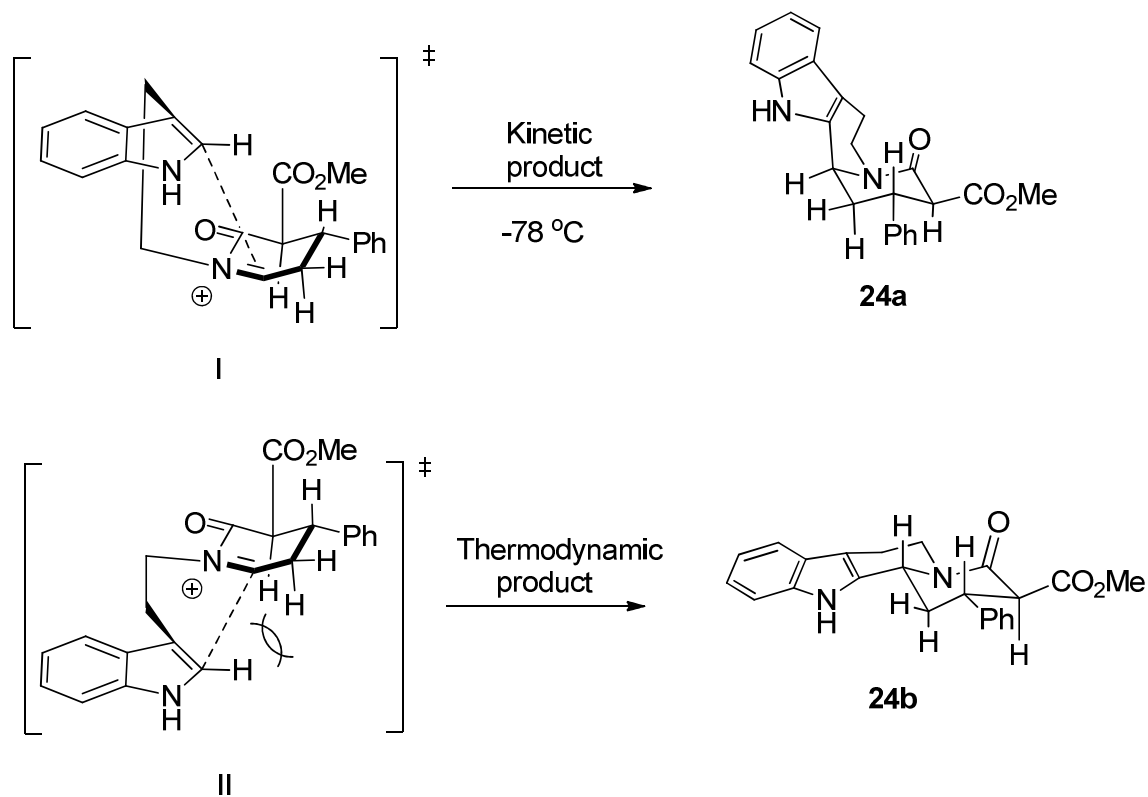
Scheme I.10. Kinetic *versus* thermodynamic product formation in the cyclization of the acyliminium ion.

As a possible application of this one-pot method in the total synthesis of biologically active marine alkaloids, the tricyclic core of schulzenine alkaloids could be readily constructed using Franzen and Fisher's method (Figure I.8). Schulzenine alkaloids were recently isolated from the marine sponge *Penares schulzei.*[29] Schulzenines A-C inhibit α-glucosidase with IC_{50} values of 48–170 nM. Figure I.9 represents the proposed one-pot reaction that could be used for the synthesis of the tricyclic core of schulzenine alkaloids.
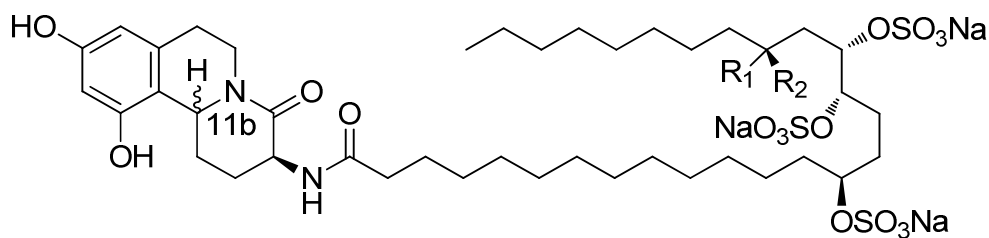
Schulzenine A: H-11b is α; R_1 = H; R_2 = CH$_3$.

Schulzenine B: H-11b is β; R_1 = R_2 = H.

Schulzenine C: H-11b is α; R_1 = R_2 = H.

Figure I.8. Schulzenine alkaloids.
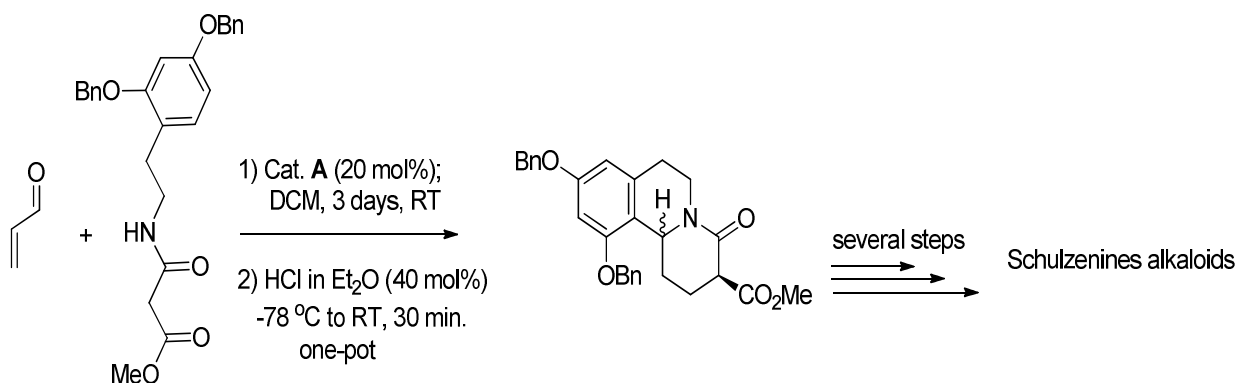
Figure I.9. Proposed one-pot synthesis of the tricyclic core of schulzenine alkaloids.

I.3.3. One-pot enantioselective synthesis of pyrrolidine, hexahydropyrrolizine and related moieties

Recently, organocatalysis has been widely used in asymmetric synthesis due to its operational simplicity, low toxicity, and ready availability compared to metal catalyzed reactions.[30] Maruoka and coworkers used an organocatalyst of type (*S*)-**34** for one-pot construction of pyrrolidine, hexahydropyrrolizines, and octahydroindolizine moieties with a high degree of stereoselectivity.[31] These core structures are commonly found in plant and marine alkaloids

20

(Figure I.10).[32,33] Their organocatalytic based retro-synthetic analysis is presented in Scheme I.11.

Bistellettazole A   Lepadiformine
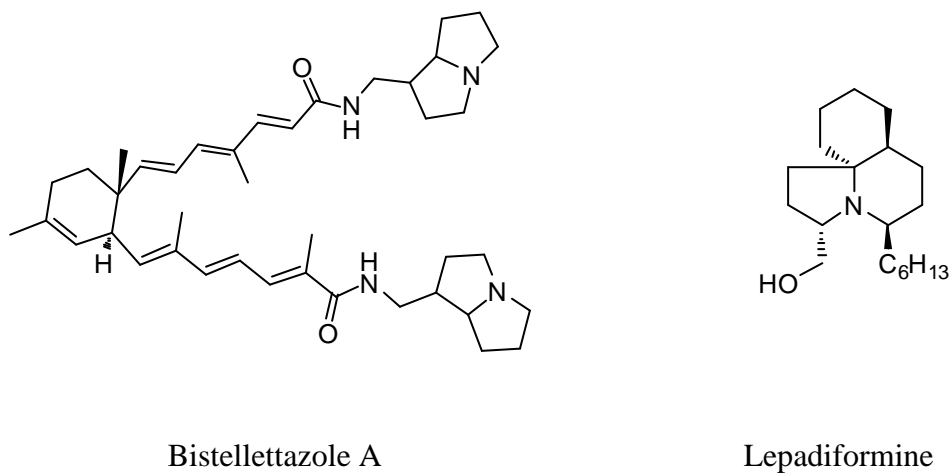
Figure I.10. Marine alkaloids that possess hexahydropyrrolizine and octahydroindolizine moieties.

(S)-**34a** (Ar = 3,4,5-F$_3$-C$_6$H$_2$)
(S)-**34b** (Ar = 3,5-(3,4,5-F$_3$-C$_6$H$_2$)$_2$-C$_6$H$_3$)
(S)-**34c** (Ar = 3,5-(3,5-(CF$_3$)$_2$-C$_6$H$_3$)$_2$-C$_6$H$_3$)

Hantzsch ester
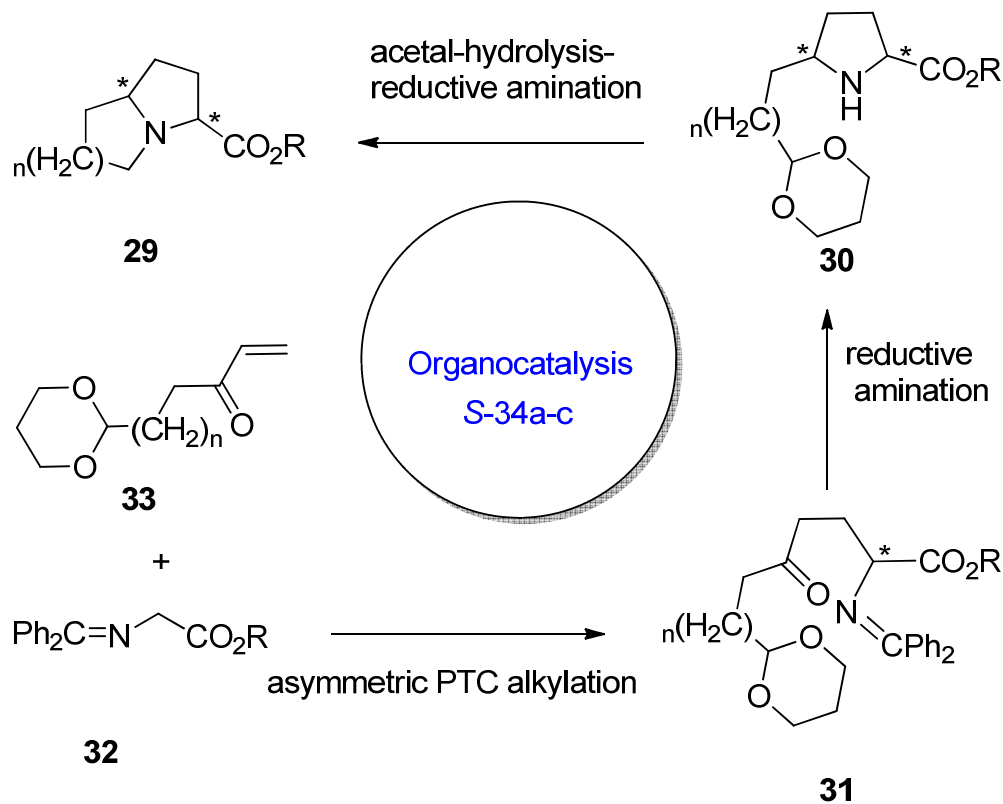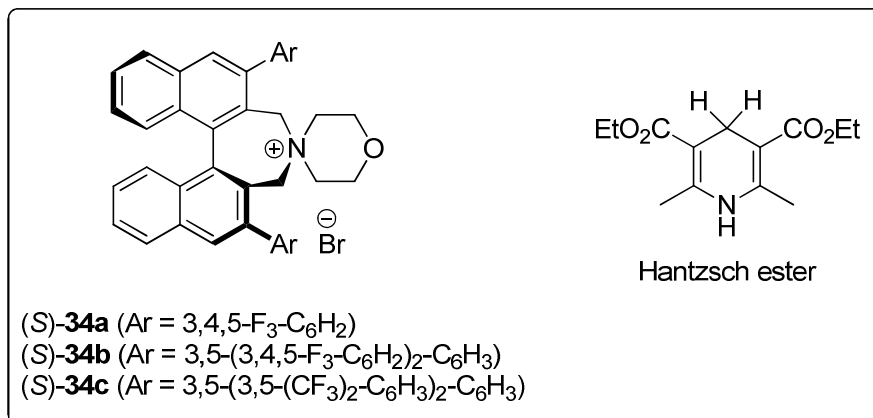
Scheme I.11. Organocatalytic retro-synthetic approach for the alkaloid core.

The key strategy is based on the asymmetric conjugate addition of the Schiff base of glycine ester **32** to α,β-unsaturated carbonyl compound **33** catalyzed by chiral phase transfer organocatalysts (S)-**34a–c**. Organocatalytic Michael addition of **32** to **33** should give adduct **31** in enantiomerically pure form. This adduct can then undergo intramolecular reductive amination facilitated by the Hantzsch ester to yield pyrrolidine derivative **30** as an intermediate. Acetal hydrolysis followed by another intramolecular reductive amination of intermediate **30** will furnish a bicyclic hexahydropyrrolizine skeleton.

First, asymmetric addition of the glycine derivative **32** to methyl vinyl ketone (MVK), under the influence of an organocatalyst of type **34** (Scheme I.12), was examined. Optimization of the reaction between **32** and MVK with K$_2$CO$_3$ and 10 mol% of CsCl at 0 °C gave the conjugate adduct **35.** This revealed that Et$_2$O and the organocatalyst (S)-**34b** gave the best yield (85%), as well as the best diastereoselectivity (94% ee). Subsequently, optimization of the intramolecular reductive amination of **35** with the Hantzsch ester for the synthesis of the substituted pyrrolidine **36** was studied. Optimization of the reaction conditions revealed that the Hantzsch ester (2

equiv.) and TFA (1 equiv.) in aqueous EtOH at 60 °C were the best conditions to build up the 2,5-disubstituted *cis*-pyrrolidine **36** stereospecifically in 84% yield.
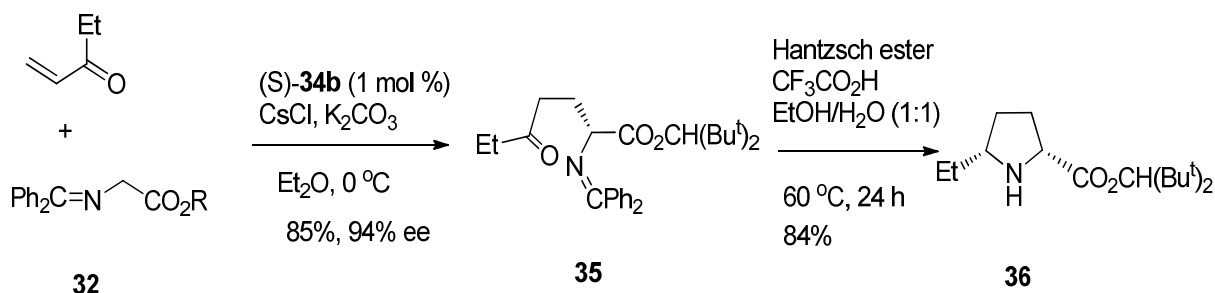
Scheme I.12. Optimized conditions for the conjugate addition and intramolecular amination steps in the synthesis of 2,5-disubstituted *cis*-pyrrolidine **36**.

Next, synthesis of the octahydroindolizine skeleton **39** using their optimized conditions (Scheme I.13) was performed. Asymmetric conjugate addition of the glycine ester **32** to the enone **37** (2 equiv.) and K_2CO_3 (5 equiv.) under the influence of the chiral phase transfer catalyst (*S*)-**34b** and CsCl in Et_2O at 0 °C for 15 h gave the conjugate adduct **38** in 88% yield with 94% ee. Hantzsch ester mediated intramolecular reductive amination with subsequent acetal hydrolysis, followed by reductive amination, was effective to give the octahydroindolizine core **39** in 70% yield. The reaction sequence was done in a one-pot approach and performed without any difficulty by sequential addition of the reagents to afford **39** in 48% overall yield.
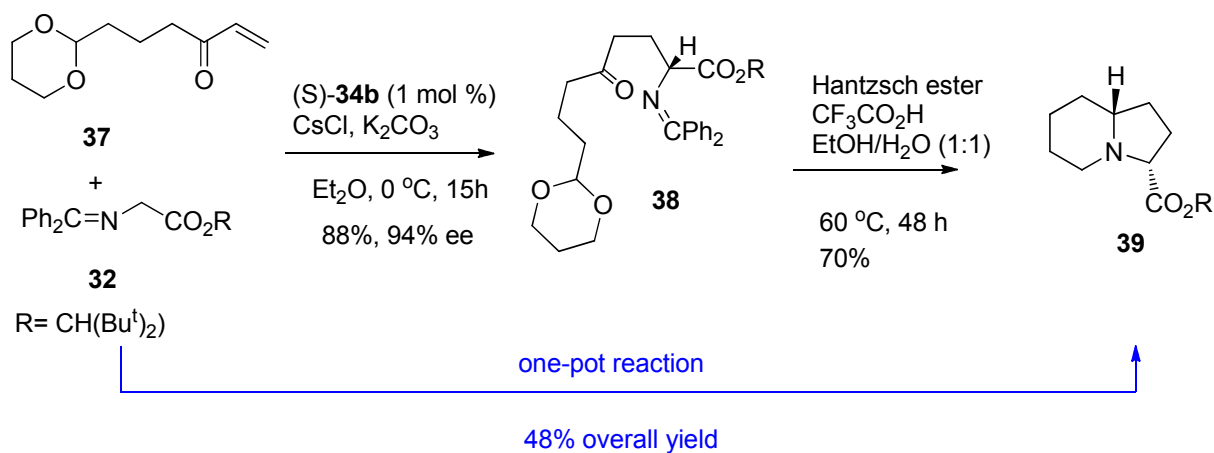
Scheme I.13. Synthesis of octahydroindolizine **39**.

Hexahydropyrrolizine **42** was also obtained under the same optimized conditions (Scheme I.14). Asymmetric conjugate addition of **32** to enone **40** yielded adduct **41** in 85% yield with 90% ee. It was noted that enantioselectivity was slightly decreased by switching the cyclic acetal moiety of **38** to a 1,3-dioxolane (78% yield, 86% ee). The hexahydropyrrolizine skeleton **42** was then formed in 55% yield by the action of Hantzsch ester mediated intramolecular reductive amination. A one-pot reaction was also possible with an overall yield of 31%.
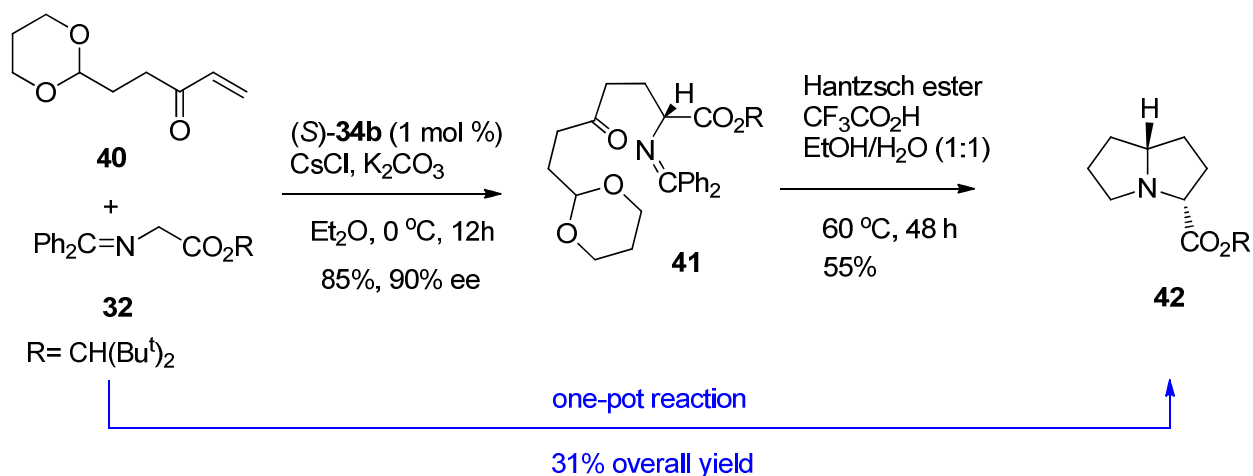
Scheme I.14. Synthesis of hexahydropyrrolizine **42**.

I.3.4. One-pot diastereoselective synthesis of γ-lactams

Cycloaddition of imines with succinic anhydride in a one-pot approach to construct the γ-lactam moiety in high yield was first reported three decades ago by Castagnoli *et al.*[34] (Scheme I.15, Equation 1). A mechanistic study was not published until 1983 when Cushman studied electronic and steric effects on the stereochemical outcome.[35] A low yield was obtained when phenyl substituted succinic anhydride was used instead of succinic anhydride (Scheme I.15, Equation 2). Also, variations in the structure of succinic anhydride were not explored in detail in this methodology. Owing to the wide abundance of the γ-lactam moiety in natural products and potential drug leads, the Shaw group has extensively studied the effect of substituents on the iminolysis of succinic anhydride derivatives. In their first report, Shaw and coworkers demonstrated the importance of electronic factors on the reactivity of phenylsuccinic anhydride when reacted with the imines derived from benzaldehyde and *o*-bromobenzaldehyde,[36] demonstrating that electron withdrawing groups in the phenyl ring led to excellent yields (>90%)

25

(Scheme I.15, Equation 3). Following this yield improvement, Shaw and coworkers reported that sulfur-substituted succinic anhydrides also gave excellent yields (90%) and showed the highest diastereoselectivity (*anti* diastereoisomer) when reacted with different imines[37] (Scheme I.15, Equation 4).

In the case of the iminolysis of maleic anhydride, a possible zwitterionic enolate intermediate could be generated through a prototropic shift which provides allylic stabilization. To validate this, Shaw and coworkers studied the cyclization of several polycyclic imines with maleic anhydride derivatives (Figure I.11) as a new one-pot synthesis of complex nitrogen heterocycles.[38] Thus, reaction of the imine **45** with maleic anhydride derivative **46** formed intermediate **47**, which could isomerize to **48**. Attack at the α- or γ- positions of the dienolate would lead to products **49a** or **49b** (Scheme I.16).

Equation 1

85%
d.r.= 83:17 anti:syn

Castagnoli *et al.,* **1969**[34]

Equation 2

36%
d.r.=86:14 anti:syn

Cushman *et al.,* **1983**[35]

Equation 3

> 90% conv.
d.r.=69:37 anti:syn

Shaw *et al.,* **2006**[36]

Equation 4

90%
d.r.=93:7 anti:syn
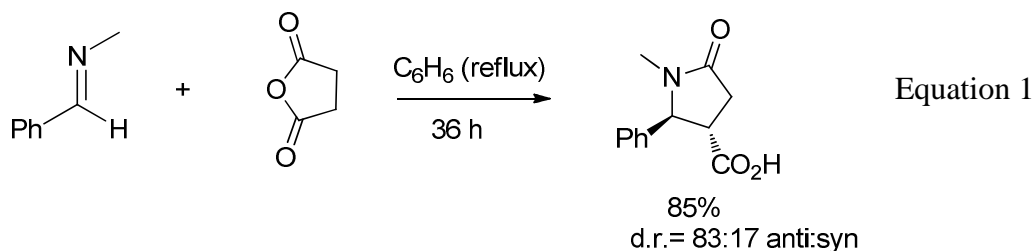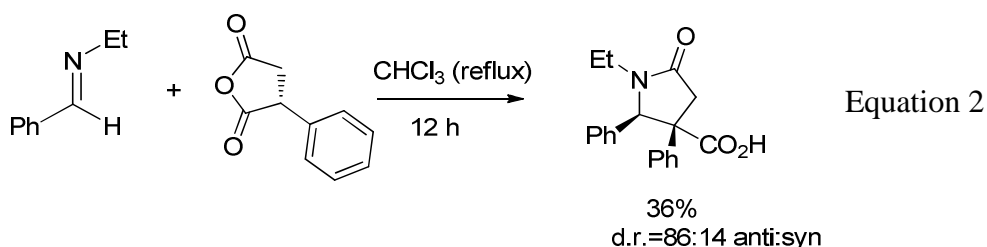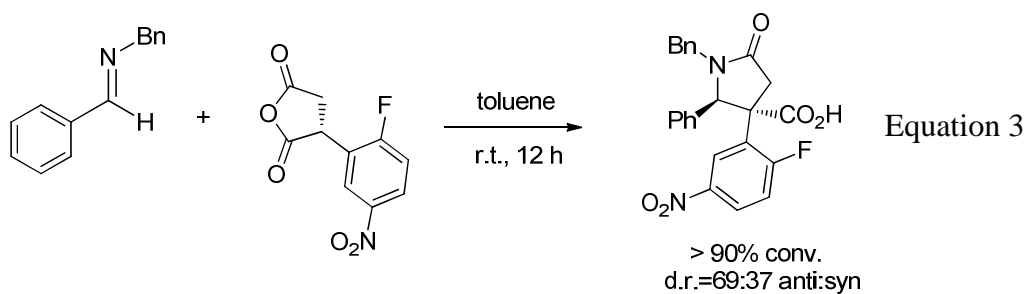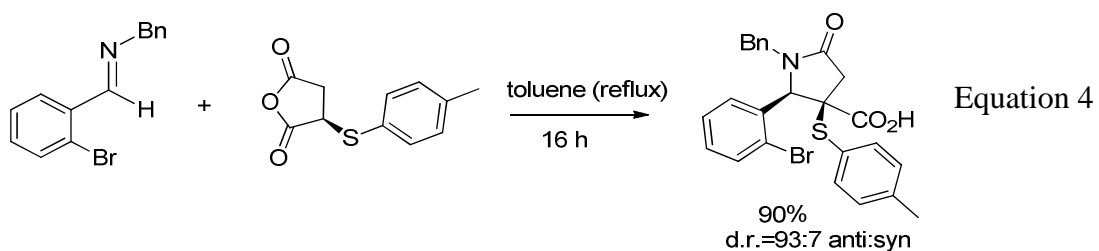
Shaw *et al.,* **2007**[37]

Scheme I.15. Milestones of the one-pot synthesis of the γ-lactam moiety.

Imines   substituted anhydride

43a   **43b**   **44a**   **44b**

43c   **43d**   **44c**   **44d**
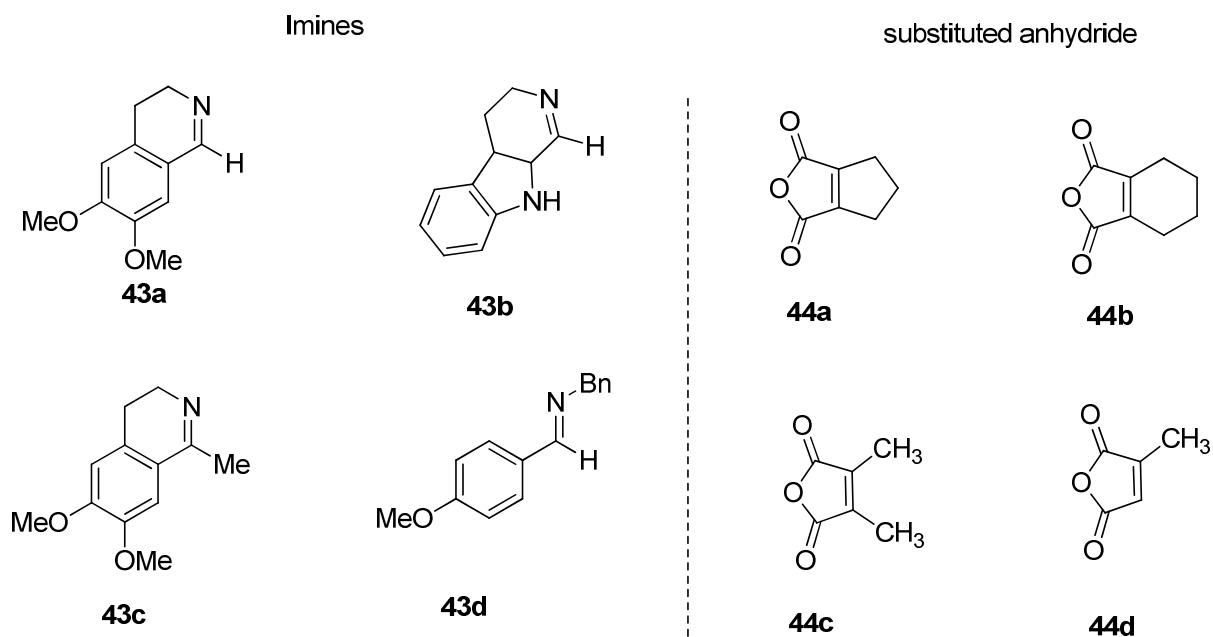
Figure I.11. Imines and substituted maleic anhydrides used by Shaw *et al.*[38]
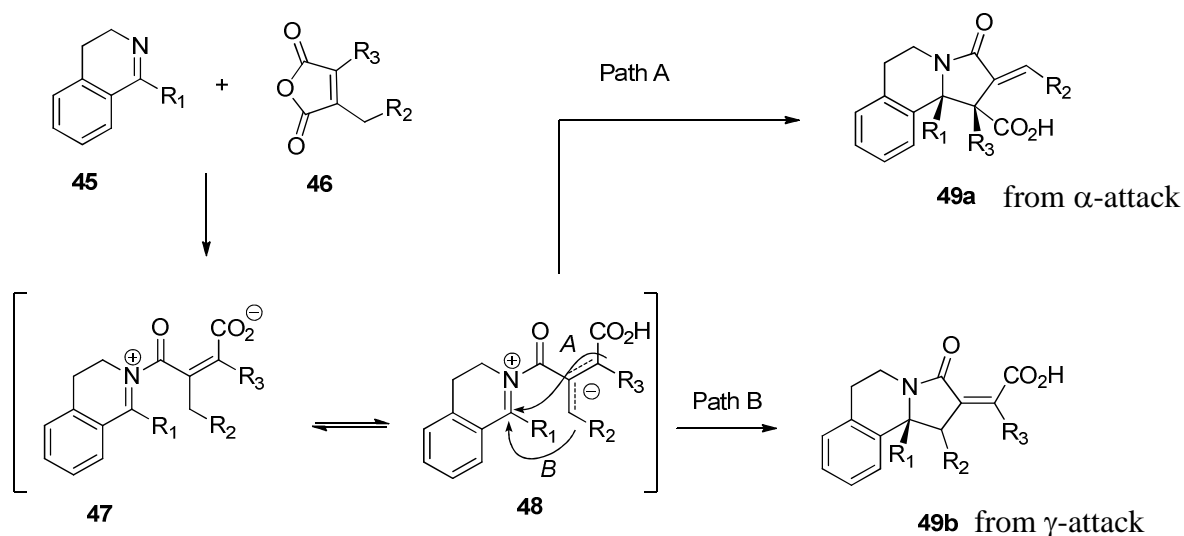
Scheme I.16. Possible cycloaddition pathways of imines with maleic anhydrides.

Tetrahydrophthalic anhydride **44b** reacted with several imines through path A to give the formal cycloaddition products with high diastereoselectivity (*anti* configuration) and acceptable yields (Scheme I.17, Equation 1 and 2). It was interesting that diastereoselectivity of the reaction of **44b** with **43b** was reversed when triethylamine and triethylammonium hydrochloride were present in the reaction mixture. Methyl and dimethyl-substituted anhydrides did not react with several imines; however, an exomethylene-substituted lactam was obtained in good yield (59%) with excellent diastereoselectivity (>95:5 *anti*:*syn*) when imine **43b** was used (Scheme I.17, Equation 3). Acyclic imines derived from aromatic aldehydes were less reactive relative to cyclic imines.
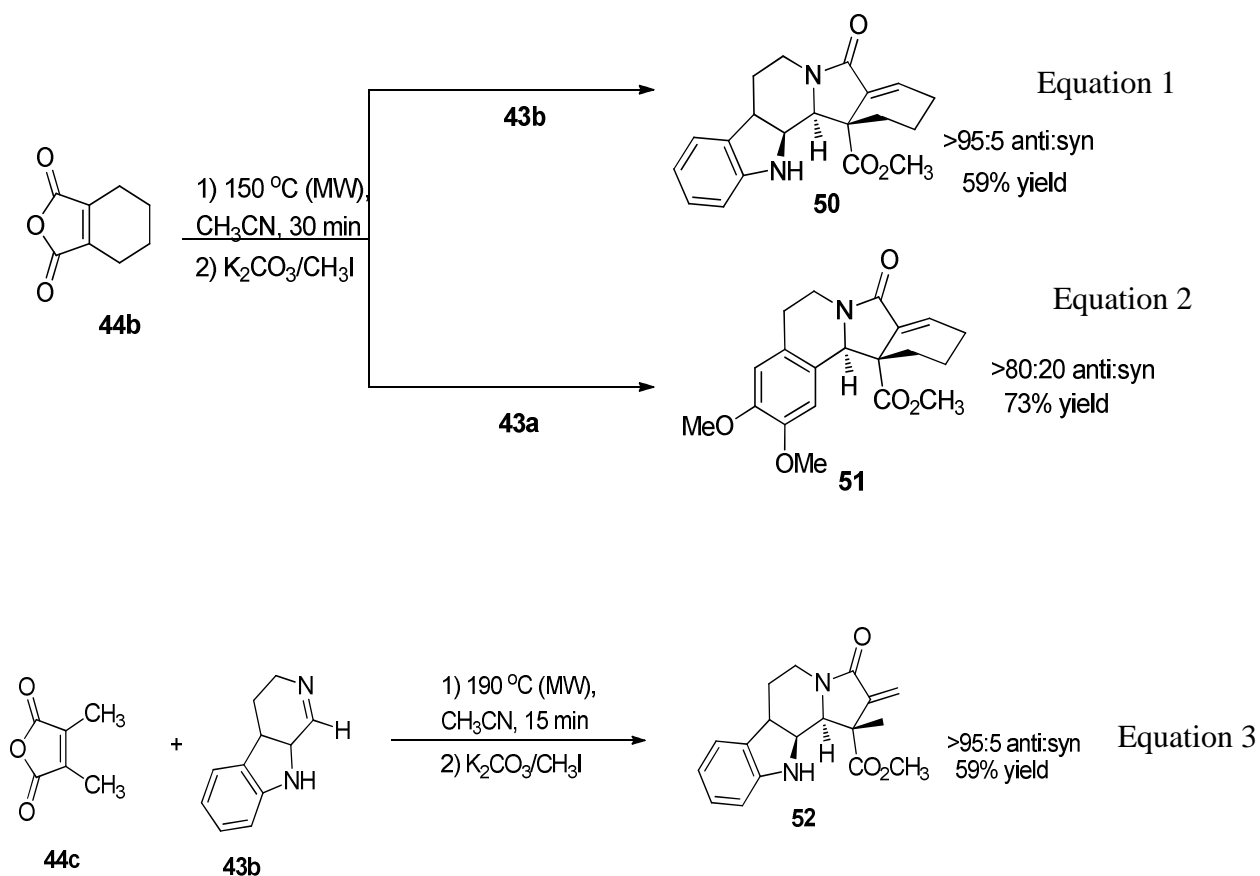
Scheme I.17. Polycyclic products from the reactions of anhydrides **44b** and **44c** with different imines.

Although the ^{1}H-NMR spectrum of the products obtained from reaction of cyclopentane-fused maleic anhydride **44a** with several imines initially appeared to be consistent with the anticipated adduct, X-ray crystallographic analysis revealed the products to be *N,O*-acetals (Scheme I.18). Mixing anhydride **44a** with imines **43a** and **43b** at room temperature yielded an immediate precipitate of *N,O*-acetals **53** and **54** in 78% and 71% yields, respectively. No γ-lactams were produced upon further heating.
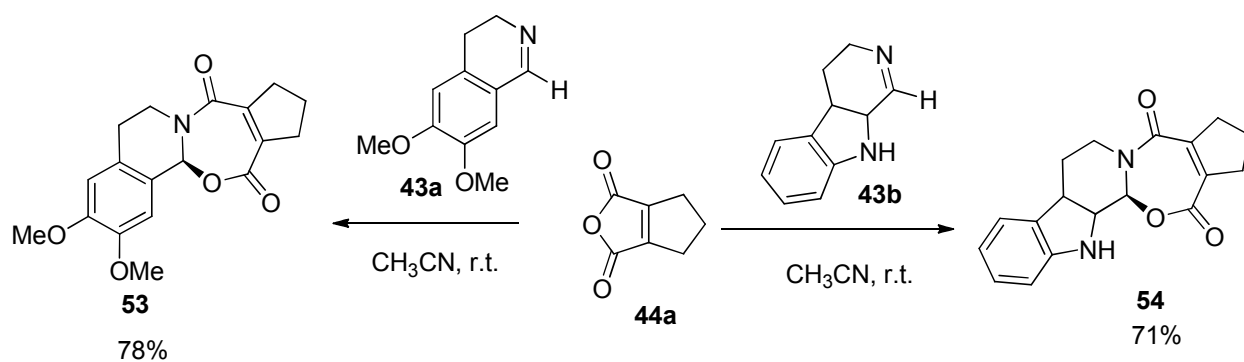
Scheme I.18. Reaction of anhydride **44a** with several imines to yield *N,O*-acetal products.

A completely different reaction manifold was observed in the reaction of ketimine **43c** with the maleic anhydride derivative **44c** (Scheme I.19). A new γ-lactam was obtained. The mechanism of formation of this new product is outlined in Scheme I.19. A prototropic shift of acylated imine **55** will yield the enamide carboxylic acid **56**, which is set up for an intramolecular Michael-type addition of the enamide to the unsaturated acid to afford a new lactam **58** through enamide **57**.
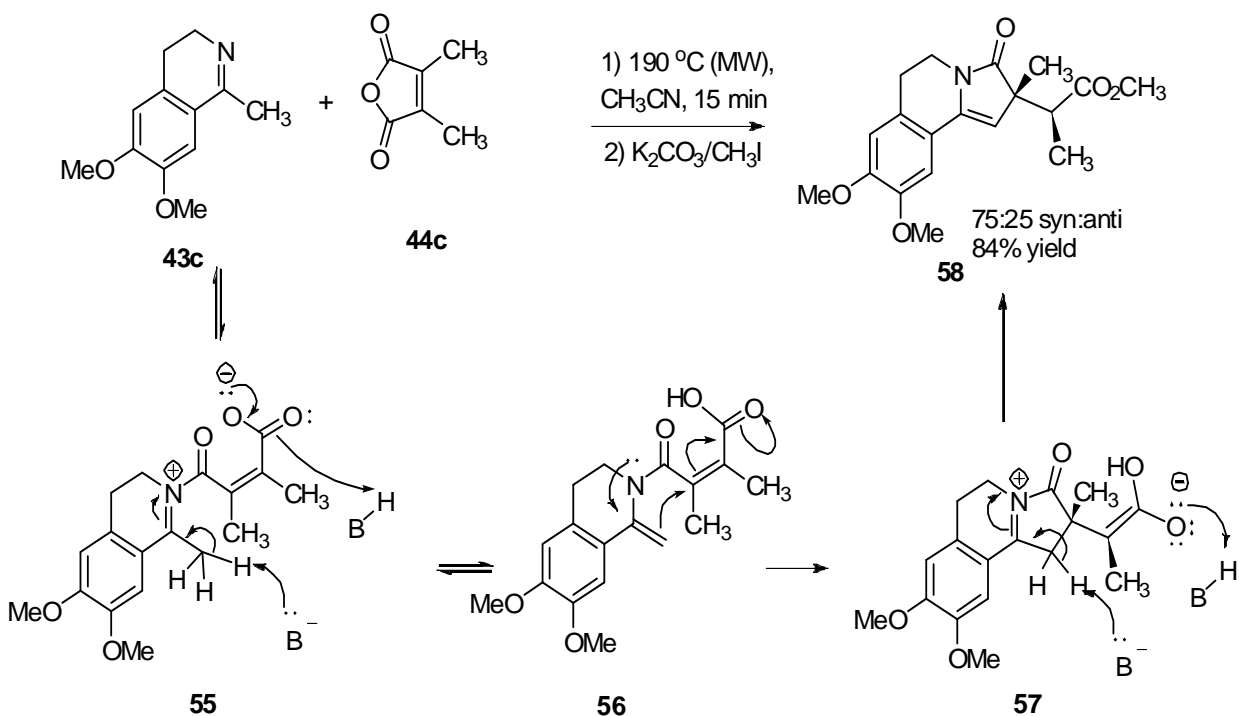
Scheme I.19. Mechanism of the formation of γ-lactam **58** obtained from the reaction of ketimine **43c** with anhydride **44c.**

Anhydrides **44d** and **44b** reacted similarly with ketimine **43c** to produce the new γ-lactams **59** and **60**, in yields of 74% and 59%, respectively (Scheme I.20). In case of the spiro γ-lactam **60**, a 50:50 mixture of diastereoisomers was obtained after 15 min of reaction time. Continued heating of **60** under reaction conditions shifted diastereoselectivity to a 70:30 mixture, favoring the *anti* isomer. Product **61** was obtained in 72% yield when anhydride **44a** was reacted with ketimine **43c**. No stereoselectivity was observed in this case.
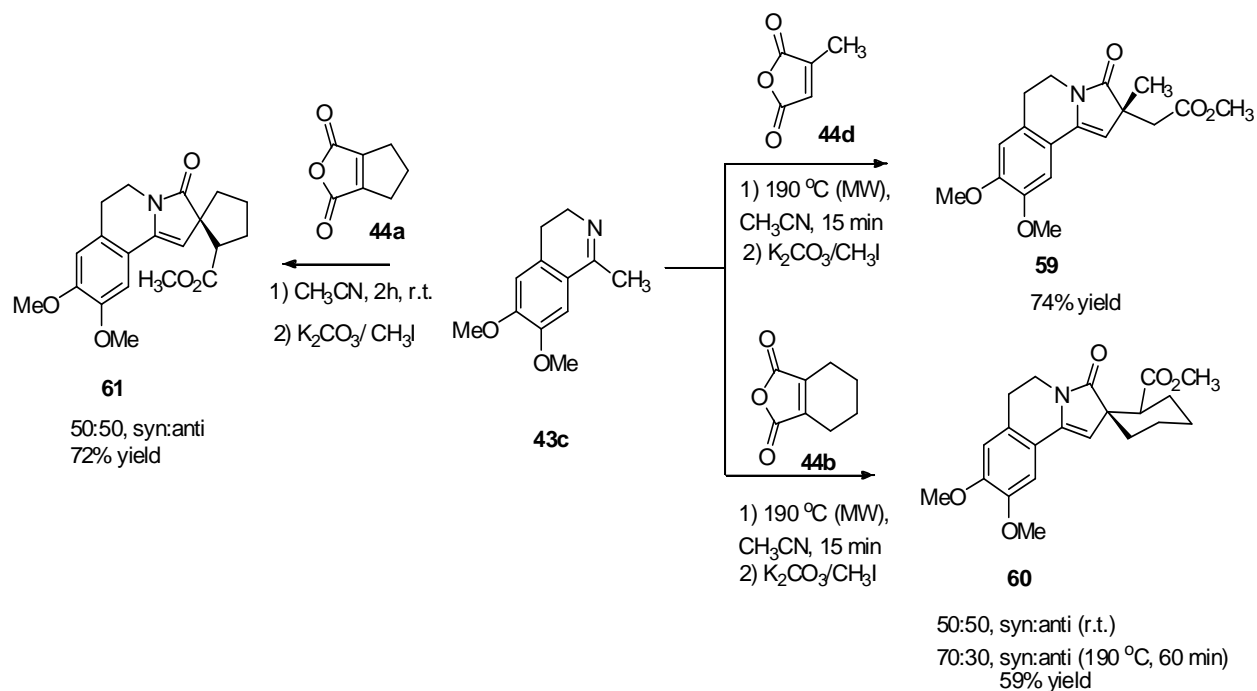
Scheme I.20. New γ-lactams obtained from the reaction of ketimine **43c** with several anhydrides.

4. Conclusion

In this mini-review, we have highlighted a number of one-pot asymmetric methodologies developed for the synthesis of important alkaloid moieties. One-pot reactions are highly practical and ideal for scaling drug leads to gram scale and greater. Manzamine alkaloids are still inspiring new chemistry in which one-pot methodologies are being developed and will be discussed in separate reports. We anticipate a greater application of these methods and similar methodologies in the field of total synthesis of marine alkaloids and have highlighted a possible route to

schulzenine alkaloids. Two or more methodologies could be combined to design a complete synthesis of a particular target. Alkaloid moieties highlighted in this mini-review (*i.e.*, substituted piperidines, quinolizidines, pyrrolidines, hexahydropyrrolizines, octahydroindolizines and γ-lactams) are common within the alkaloid family. Although there are many methods for the synthesis of these moieties, development of one-pot methodologies to obtain high yields with a high degree of enantioselectivity will provide numerous opportunities for the synthetic community.

CHAPTER II.

THE MANZAMINE ALKALOIDS

SECTION A

A SCALABLE PURIFICATION OF MANZAMINE A AND 8-HYDROXYMANZAMINE A

FROM THE INDONESIAN *ACANTHOSTRONGLYPHORA SP.* SPONGE

Introduction:

The manzamines are an intriguing group of alkaloids of marine origin (Figure II.1). Their structures are characterized by a penta- or tetracyclic nitrogen-containing ring system bound to a β-carboline moiety. Some 80 related compounds have been described from more than a dozen species of sponges since the first isolation of manzamine A (**1**) from an Okinawan genus Haliclona in 1986.[12] Manzamines exhibited diverse bioactivities including cytotoxicity,[12] fungicidal,[1] insecticidal[39] and antibacterial[40] and were shown to possess activity against HIV-1 and AIDS opportunistic infections.[1] Several manzamines were reported to modulate the generation of peroxide anion (O_2^-) and TXB_2 generated by activated rat neonatal microglia.[39,40] Manzamine A (**1**) was the most potent inhibitor and did not show in vitro toxicity to microglia.

Manzamine A (**1**): R=H
8-Hydroxymanzamine A (**2**): R=OH

Manzamine F (**3**)

Ircinal A (**4**)
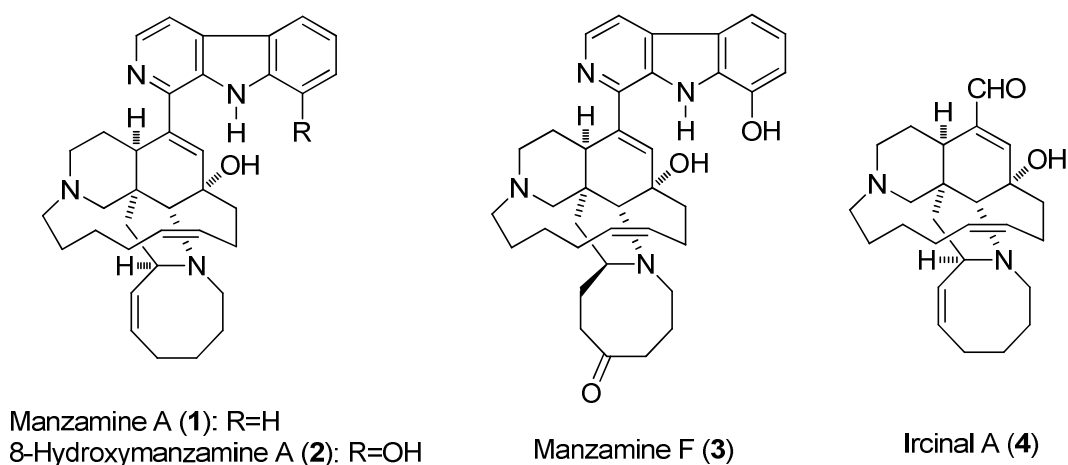
Figure II.1. Manzamine alkaloids

Manzamine A (MA) and some of its analogs were identified as a new class of glycogen synthase kinase-3 beta (GSK-3β) and cyclin-dependent kinase (CDK-5) inhibitors.[41] These two kinases belong to the cyclic-dependent, mitogen-activated, glycogen synthase and CDK-like kinases group (CMGC), which is the largest group of kinases in the *Plasmodium* kinome.[42] These two kinases are involved in tau pathological hyperphosphorylation.[43] MA was shown to be

effective in decreasing tau hyper-phosphorylation in human neuroblastoma cell lines, a demonstration of its ability to enter cells and to interfere with tau pathology.[14] Further, MA shows an interesting and selective binding for human GSK-3β (Figure II.2). All these data suggest that MA and its analogs could be used as potential therapeutic agents for Alzheimer's disease.

Recent studies indicated that the manzamines are extraordinarily active against the malaria parasite, among which MA is the most potent and shows improved activity over artemisinin and chloroquine both in vitro and in vivo.[44,45] This activity is confirmed by repeated biological evaluation in our lab and in laboratories in New Zealand, Japan, Australia, and Switzerland by corporation through a WHO program. Oral treatment with **1** (2x100 µmol/kg) and **2** (2x100 µmol/kg) showed 90% reduction in parasitemia. Mice treated with a single dose (50 or 100 µmol/kg) of **1** or **2** also showed significant improvements in survival times over mice treated with chloroquine or artemisinin.

Owing to all these promising biological activities, large amounts of MA were required for further preclinical evaluation, which include efficacy in different animal models, toxicology, pharmacokinetics, etc. On the other hand, large amounts of MA and its analogs such as 8-hydroxymanzamine A (**2**) , manzamine F (**3**), and iricinal A (**4**) are required for the structure activity relationship study and lead optimization.
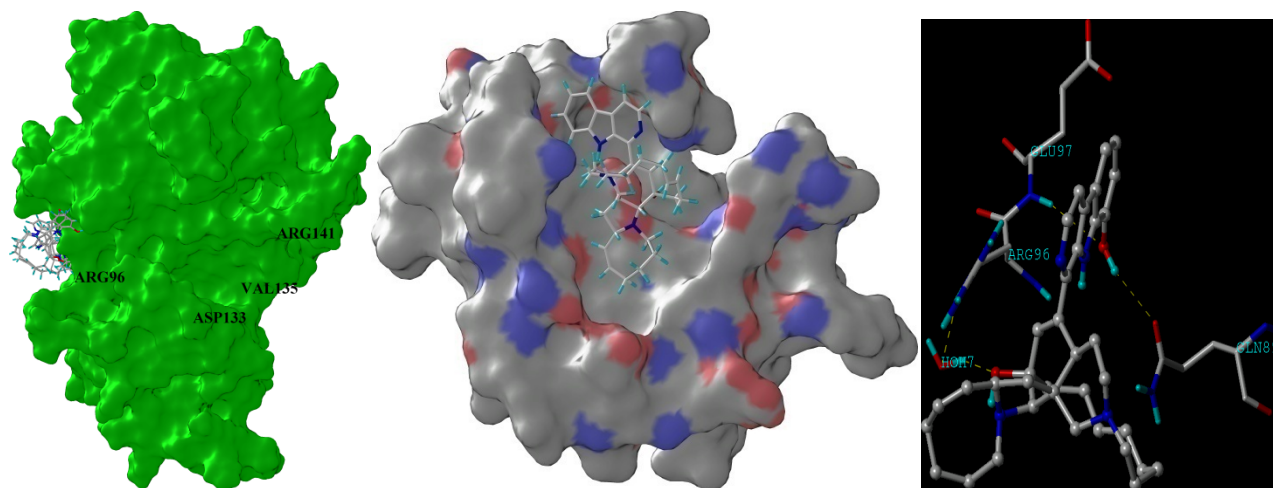
Figure II.2. (Left) Binding mode of MA and selected analogs shown in the activation loop (in the vicinity surrounded by Arg96, Arg180 and Lys205) of human GSK-3β. Also, the ATP binding region (pocket on right side of the enzyme) is shown with the key amino acids that make hinge interactions with ATP-competitive inhibitors, Asp133, Val135 and Arg141. Protein Connolly surface is shown. (Middle) Close-up view of part of GSK-3β showing MA docked into the non-ATP-noncompetitive binding site of GSK-3β enzyme (X-ray: 1I09). The red regions on the protein surface indicate hydrogen bond donors and blue regions indicate hydrogen bond acceptors. (Right) Polar interactions in a docked conformation of MA in the ATP-noncompetitive binding pocket of GSK-3β (X-ray: 1GNG).

Figure II.3. Photograph of the Indonesian sponge *Acanthostrongylophora sp.*

Results and Discussion:

Large scale preparation of natural products needs additional consideration regarding efficiency of the extraction method, solvent toxicity, and the economical factor. Although all organic solvents such as methanol, ethanol, acetone, chloroform or methylene chloride (DCM) and ethyl acetate could be used in the extraction step, miscible solvents with water are preferred to avoid extra drying of the sponge material. However, methanol and ethanol extracts usually have more impurities and are hazardous. Thus, acetone was selected as a suitable solvent for extraction of manzamine alkaloids from the sponge.

Our collaborators in Gadjah Mada University (GMU) in Indonesia have contributed a great deal to this project by providing crude extractions containing manzamine alkaloids from the marine sponge, *Acanthostrongylophora sp*. (Figure II.3), collected primarily from the Northern Sulawesi at Manado Bay (Bunaken) in Indonesia. Large quantities of the sponge were collected, using SCUBA, frozen immediately, extracted with chloroform then acetone and shipped to our lab to perform the purification.

The crude extract was first subjected to an acid-base process to remove non-alkaloidal components from alkaloids (Figure II.4). The total alkaloid obtained by this treatment is much cleaner than the crude extract, which significantly simplified the purification of pure alkaloids. The total alkaloid content is about 30% (w/w) of the crude extract.

Aluminium oxide is suitable sorbent to separate manzamine alkaloids, particularly for the separation of MA and 8-hydroxymanzamine A. However, aluminium oxide is more expensive than silica gel and is denser which means more aluminium oxide will be used. Therefore, silica gel is more favorable from the economical point of view. TLC eluent optimization revealed that *n*-hexane:acetone:Et₃N is a good solvent system to separate manzamine analogs on silica gel. To

verify this method, a batch of 200 grams of total alkaloids were loaded to a 1.5 kg silica gel VLC column and eluted with the above solvent system. Fractions were monitored by TLC. Promising separation was achieved and the majority of MA, 8-hydroxymanzamine A, and manzamine F were collected in >90% purity. A total of 24.4 grams of manzamine A (12%), 19.8 grams of 8-hydroxymanzamine A and 17.7 grams of manzamine F were obtained. No pure ircinal A was obtained under these conditions.

The fractions of MA were purified by crystallization in absolute ethanol which yielded highly pure MA as a free base which contains one molecule of ethanol in the crystal. MA free base was transferred to MA hydrochloric salt readily by adding one equivalent of 0.3% HCl in methanol and then recrystallized from DCM and methanol. Based on our experience, MA HCl salt is more stable and has higher solubility in water. The additional advantage for making the salt is that it is much easier to crystallize relative to the free base.

Experimental:

Preparation of the total alkaloids: The crude extract is dissolved in DCM, mixed with Celite 545 (Fisher Scientific) and allowed to dry under a hood. The dried mixture is packed into a 5L Buchner funnel and eluted under *vacua* using 0.2N HCl aqueous solution. The elution is monitored for precipitate formation by adding a 5% $NaHCO_3$ aqueous solution. Elution is stopped when precipitation is no longer observed. The eluent is pooled and adjusted to a pH of 8.0 using 5% $NaHCO_3$ solution. The mixture is kept cool until all the precipitate is deposited. The collected precipitate is filtered and dried affording the total alkaloids as an earthy-like powder.

Purification of manzamines: 200 grams of total alkaloids were dissolved in DCM and mixed with 100 g silica gel and was allowed to complete dryness at room temperature. The resulting mixture was loaded on a 1.5 kg silica gel VLC. Elution under vacuum starts with *n*-hexane:acetone 90:10 solvent system with 100 mL fractions until MA was visualized by TLC. Then Et$_3$N was added as well as increasing the polarity of the solvent system as follow: *n*-hexane:acetone:triethylamine 85:15:1, 75:25:1, 60:40,1 then 100% of acetone. Fractions that contain MA were combined and evaporated under vacuum**.** The same was done for **2** and **3.**

Crystalization of manzamine A: 27 g of MA free base were dissolved in DCM (20 mL) to which 0.3N HCl (5 mL) in methanol was added slowly. The solution was mixed thoroughly and was kept at room temperature for 1 h. The solution was then kept overnight in the refrigerator and the formed crystals were collected by filtration.

(+)-Manzamine A (1): $[\alpha]_D^{25}$ + 102.0 (c 1.09, CHCl$_3$); ^{1}H- and ^{13}C-NMR spectra are shown in Figure III.14. HRESIMS *m/z* 549.3589 (M+H)$^+$ (calcd for C$_{36}$H$_{45}$N$_4$O, 549.3515, Δ +0.007 mmu). The ^{1}H- and ^{13}C-NMR chemical shifts were within ±1 ppm of the reported values. X-ray crystal structure is shown in Figure II.5. The diffraction data are illustrated in Table II.1. ^{1}H- and ^{13}C-NMR spectra are shown in Figure II.6.

(+)-8-Hydroxymanzamine A (24): (24 g); pale yellow crystals obtained from methanol; $[\alpha]_D^{25}$ + 118.0 (c 1.94, CHCl$_3$); HRESIMS *m/z* 565.3539 (M + H)$^+$ (calcd for C$_{36}$H$_{45}$N$_4$O$_2$, 565.3464, Δ +0.007 mmu). The ^{1}H- and ^{13}C-NMR chemical shifts were within ±1 ppm of the reported values.

(+)-Manzamine F (2): white crystals obtained from methanol; $[\alpha]_D^{25}$ + 47.7 (c 0.67,CHCl$_3$); ^{1}H- and ^{13}C-NMR spectra are shown in Figures III.16-17. HRESIMS m/z 581.3484 (M + H)$^+$ (calcd for C$_{36}$H$_{45}$N$_4$O$_3$, 581.3413, Δ + 0.007 mmu). The ^{1}H and ^{13}C chemical shifts were within ±1 ppm

of the reported values. X-ray crystal structure is shown in Figure II.7. The diffraction data are illustrated in Table II.3.

Crude acetone extract

| Acid-base

Total alkaloids (30%)

| Silica gel VLC (1:10)

I	II	III	IV
Ircinal & **Manzamine A**	**Manzamine A**	**8-OH-MA**	**Manzamine F**

II — Manzamine A

| 1 equiv. HCl in MeOH

Manzamine A hydrochloride

| Recry.

High pure Manzamine A hydrochloride

III — 8-OH-MA

| 1 equiv. HCl in MeOH

8-OH-Manzamine A hydrochloride

| Recry.

High pure 8-OH-MA hydrochloride
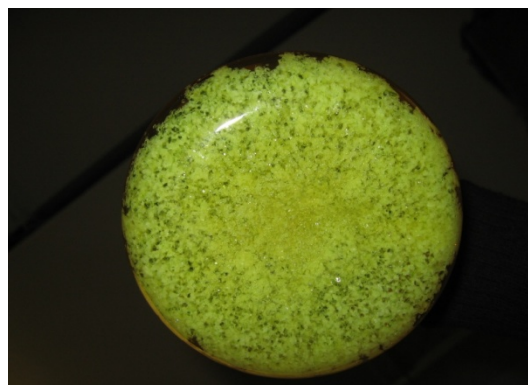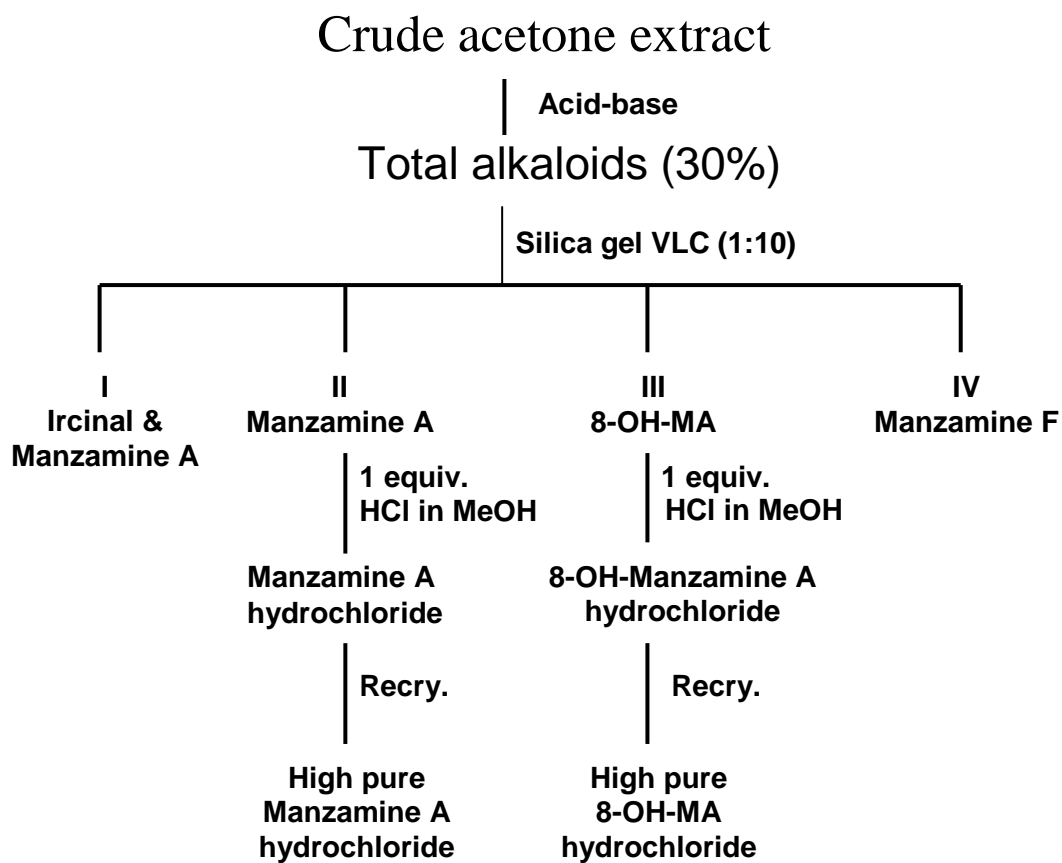
Figure II.4. Large scale purification scheme of manzamine alkaloids from the Indonesian sponge *Acanthostrongylophora* sp.
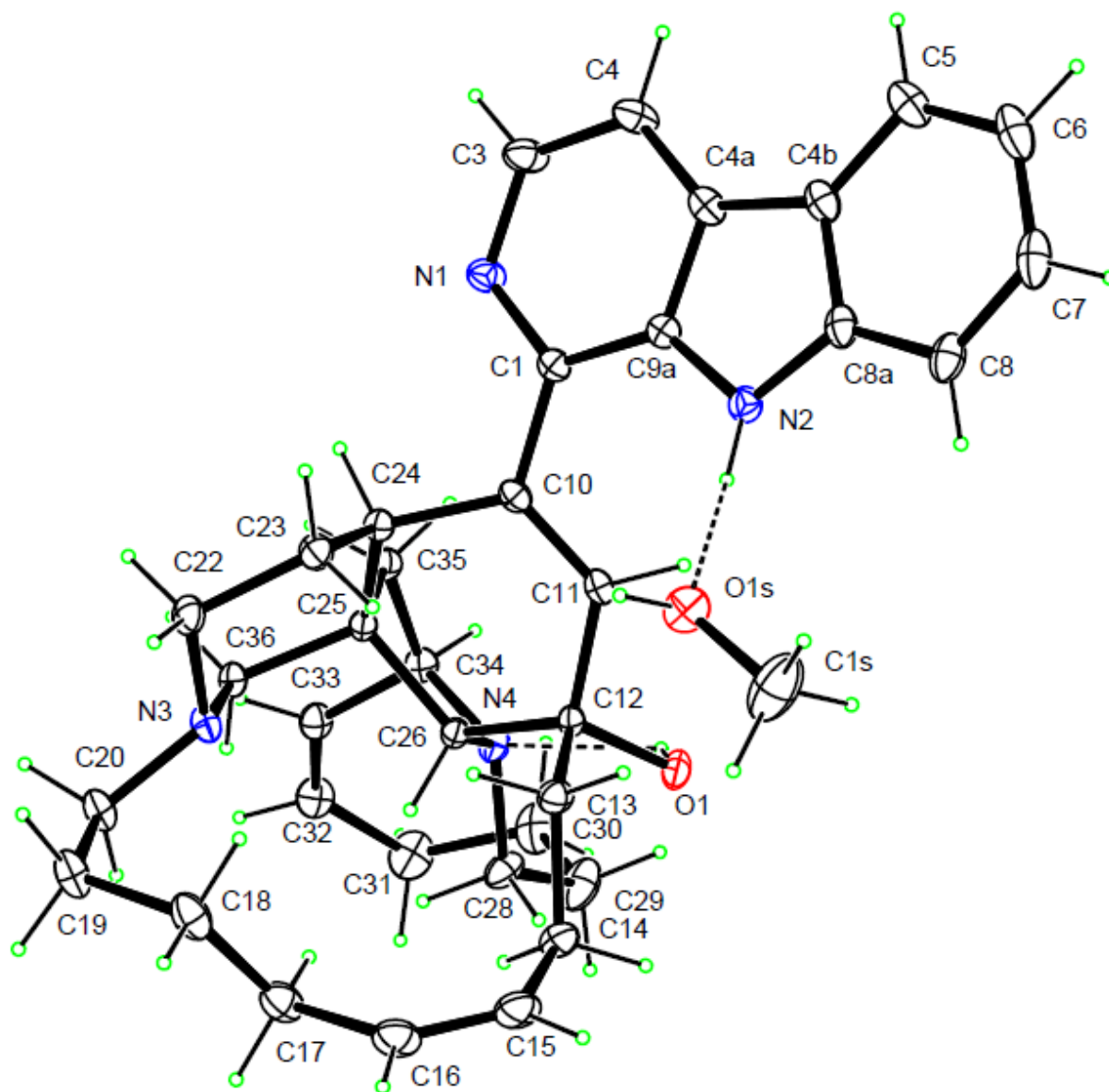
Figure II.5. ORTEP drawing of manzamine A HCl (**1**)

Table II.1. X-ray diffraction data of manzamine A HCl (**1**)

Crystal data

$C_{36}H_{44}N_4O.CH_4O$

$M_r = 580.79$

Orthorhombic

$P2_12_12_1$

$a = 9.4073\ (10)$ Å

$b = 12.2583\ (10)$ Å

$c = 28.327\ (5)$ Å

$V = 3266.6\ (7)$ Å^3

$Z = 4$

$D_x = 1.181$ Mg m^{-3}

D_m not measured

Mo $K\alpha$ radiation

$\lambda = 0.71073$ Å

Cell parameters from 5160 reflections

$\theta = 2.5$–$30.5°$

$\mu = 0.073$ mm^{-1}

$T = 105$ K

Fragment

Colorless

$0.35 \times 0.25 \times 0.20$ mm

Crystal source: local laboratory

Data collection

KappaCCD (with Oxford Cryostream) diffrac-
tometer

ω scans with κ offsets

Absorption correction: none

28546 measured reflections

5514 independent reflections

4852 reflections with

$\quad I > 2\sigma(I)$

$R_{int} = 0.027$

$\theta_{max} = 30.5°$

$h = -13 \rightarrow 13$

$k = -17 \rightarrow 17$

$l = -40 \rightarrow 40$

intensity decay: $<2\%$

Refinement

Refinement on F^2

$R[F^2 > 2\sigma(F^2)] = 0.040$

$wR(F^2) = 0.097$

$S = 1.044$

5514 reflections

399 parameters

H atoms treated by a mixture of independent
and constrained refinement

$w=1/[\sigma^2(F_o^2) + (0.0472P)^2 + 0.5834P]$

$\quad$ where $P = (F_o^2 + 2F_c^2)/3$

$(\Delta/\sigma)_{max} = 0.001$

$\Delta\rho_{max} = 0.29$ e Å^{-3}

$\Delta\rho_{min} = -0.18$ e Å^{-3}

Extinction correction: *SHELXL*

Extinction coefficient: 0.0017 (5)

Scattering factors from *International Tables
for Crystallography* (Vol. C)
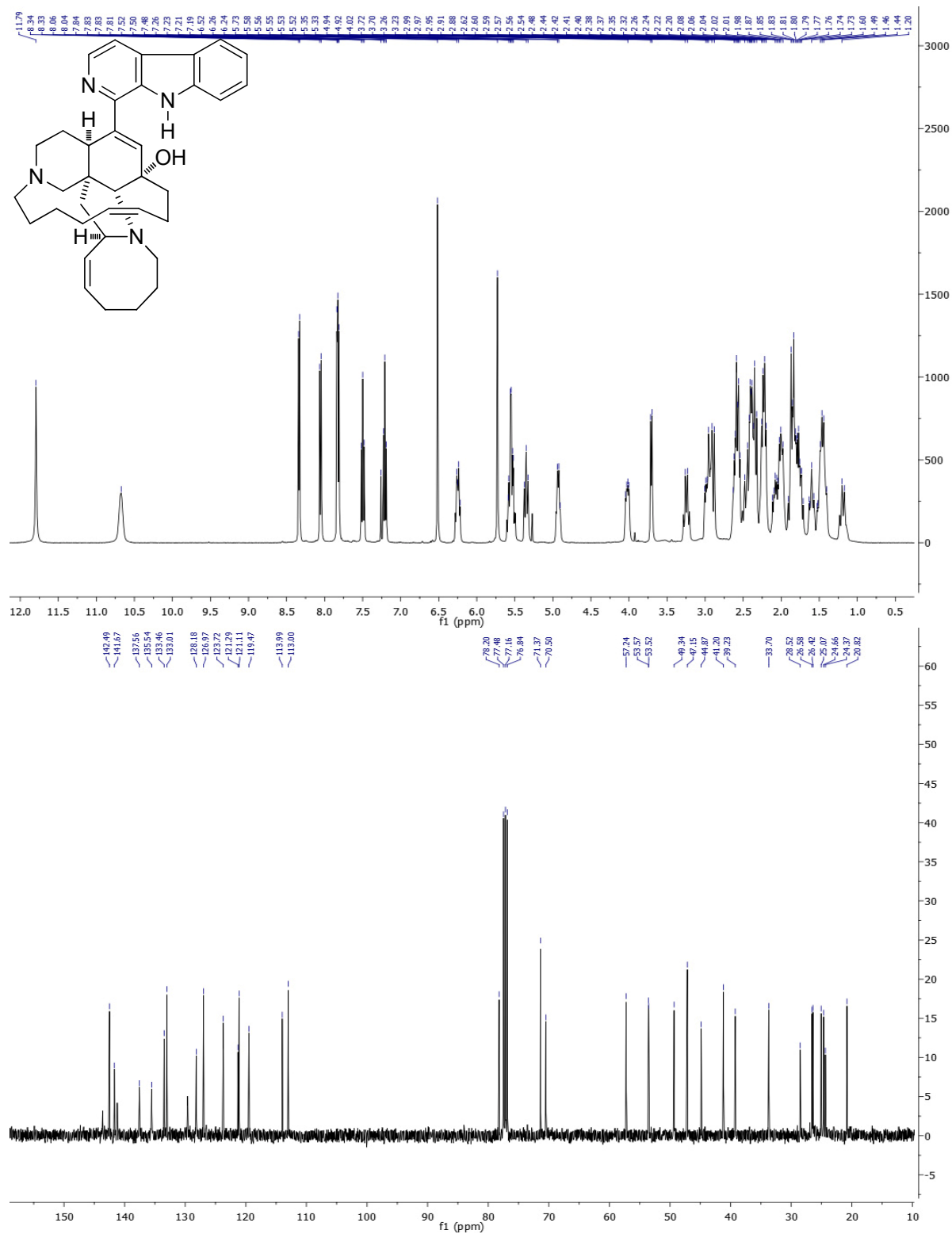
Figure II.6. ^{1}H- and ^{13}C-NMR spectra of manzamine A (**1**) in CDCl$_3$ at 400 and 100 MHz, respectively
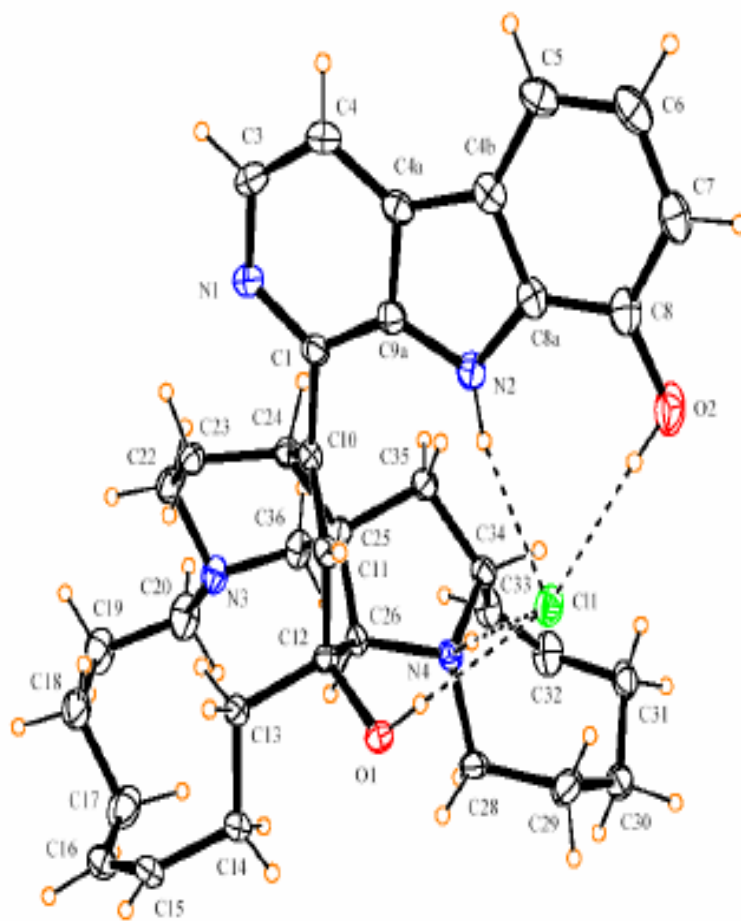
Figure II.7. ORTEP drawing of 8-hydroxymanzamine A HCl (**2**)

Table II.2. X-ray diffraction data of 8-hydroxymanzamine A HCl (**2**)

Crystal data

$C_{36}H_{45}N_4O_2^+.Cl^-$
$M_r = 601.21$
Orthorombic
$P2_12_12_1$
$a = 10.4173\ (10)\ A°$
$b = 12.2580\ (10)\ A°$
$c = 24.492\ (3)\ A°$
$V = 3127.5\ (5)\ A°$
$Z = 4$
$D_x = 1.277\ Mg\ m^{-3}$
D_m not measured

Mo $K\alpha$ radiation
$\lambda = 0.71073\ A$
Cell parameters from 6056 reflections
$\theta = 2.5\text{-}32.6°$
$\mu = 0.162\ mm^{-1}$
$T = 102\ K$
Rectangular prism
Colorless
0.35 x 0.25 x 0.20 mm

Data collection

Kappa CCD (with Oxford Cryostream) diffractometer
9404 reflections with $I > 2\sigma\ (I)$
ω scans with κ offsets
43861 measured reflections
11211 independent reflections

$R_{int} = 0.066$
$\theta max = 32.58°$
$h = -15$ to 15
$K = -18$ to 18
$l = -36$ to -37

Intensity decay $< 2\%$
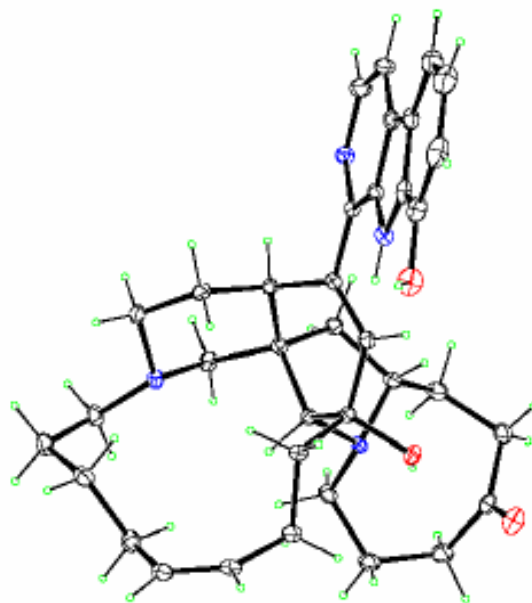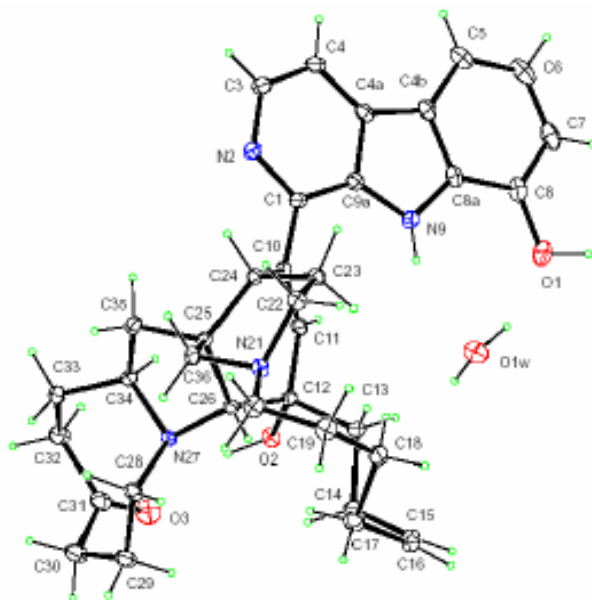
Figuer.II.8. ORTEP drawing of manzamine F (**3**)

Table II.3. X-ray diffraction data of manzamine F (**3**)

Crystal data
$C_{36}H_{44}N_4O_3.1.5(H_2O).0.5(C_2H_3N)$
$M_r = 628.30$
Monoclinic
C2
$a = 20.749$ (3) A°
$b = 12.424$ (3) A°
$c = 14.239$ (3) A°
$\beta = 114.993$ (9)°
$V = 3326.9$ (12) A°
$Z = 4$
$D_x = 1.254$ Mg m^{-3}
D_m not measured

Mo $K\alpha$ radiation
$\lambda = 0.71073$ A
Cell parameters from 5035 reflections
$\theta = 2.5$-$30.5°$
$\mu = 0.083$ mm^{-1}
$T = 110$ K
Plate
Colorless
0.35 x 0.27 x 0.08 mm

Data collection
Kappa CCD (with Oxford Cryostream) diffractometer
4686 reflections with $I > 2\sigma$ (I)
ω scans with κ offsets
27402 measured reflections
5268 independent reflections

$R_{int} = 0.031$
θmax $= 30.5°$
$h = -29$ to 28
$K = -17$ to 17
$l = -20$ to -20

Intensity decay $< 2\%$

CHAPTER II.

THE MANZAMINE ALKALOIDS

SECTION B

TWO NEW MANZAMINE ALKALOIDS FROM THE INDONESIAN

ACANTHOSTRONGLYPHORA SP. SPONGE

Submitted for publications in *Organic Letters*, 2012

Introduction:

As we discussed in section A of this chapter, we developed an efficient approach for the production of MA and other manzamine alkaloids that enable kilo gram scale purification. This approach was based on the acid-base treatment of the acetone extract of the Indonesian sponge *Acanthostrongylophora sp.*, which precipitated the alkaloids.[11] Using this approach and following the isolation scheme (Scheme II.4, page 42), we purified 100 g of MA. We envisioned the presence of some minor manzamine-related alkaloids from the fractions that eluted after 8-hydroxymanzamine A (using LCMS analysis). Although our major interest was to obtain enough MA for SAR studies, we felt that purifying the minor metabolites and elucidating their structures could add value to SAR. Herein, we describe the purification and structure elucidation of two minor new manzamine-related alkaloids **2** and **3**.

1: R=H
4: R=OH

2

3

N-oxide manzamine J (**5**)

6

7
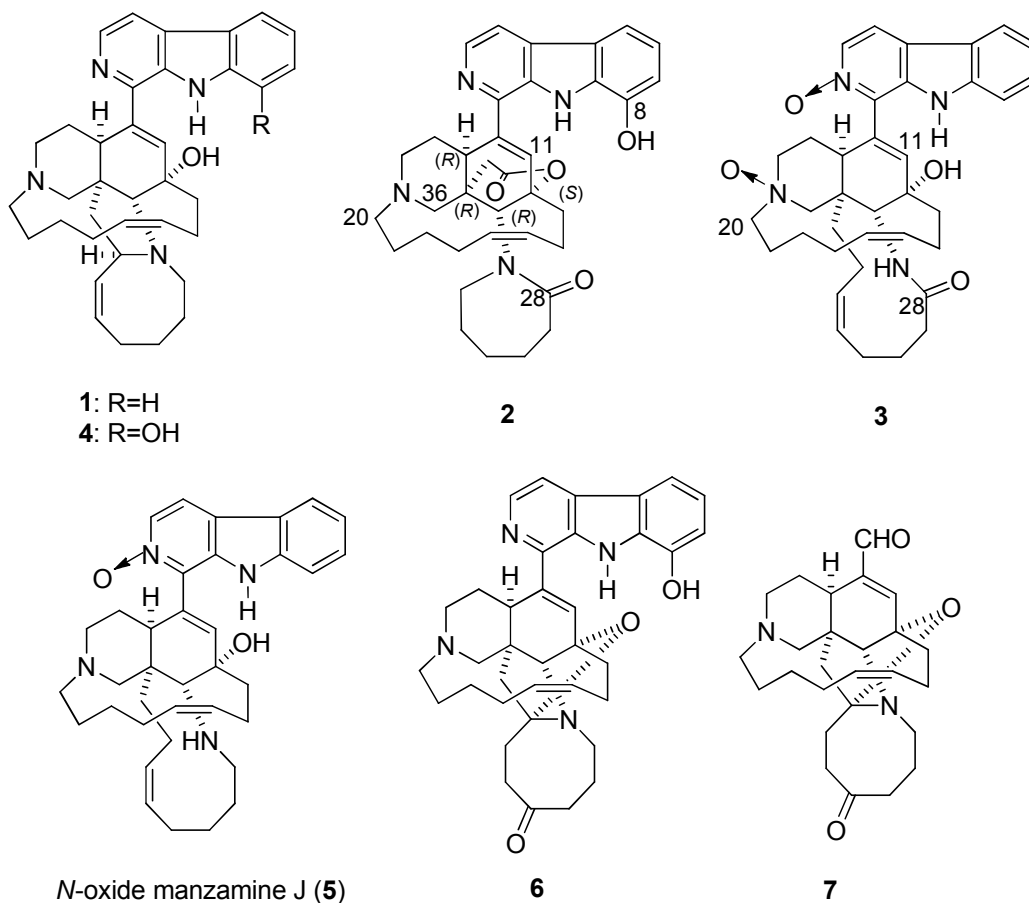
Results and discussion:

The sponge, *Acanthostrongylophora sp.*, was collected from Indonesia and successively extracted with acetone. The crude acetone extract was subjected first to an acid-base process to obtain the total alkaloid content. Using the general isolation scheme (Scheme II.4, page 42) and further purification of the more polar fractions led to the isolation of the known manzamines: manzamine A (**1**),[12] 8-hydroxymanzamine A (**4**),[13] manzamine F,[13] 12,34-oxamanzamine E (**6**),[45] 31-keto-12,34-oxa-32,33-dihydroircinal A (**7**),[58] along with two new manzamine-related analogs, acantholactone (**2**) and 2,21,28-trioxomanzamine J (**3**).

Compound **2** was obtained as a pale yellow powder from DCM, and it was revealed to have a molecular formula of $C_{36}H_{43}N_4O_4$ by HRESIMS (*m/z* 595.3416 (M+H)$^+$) combined with ^{1}H- and ^{13}C-NMR data (Table II.4). The ^{1}H-NMR resonances at δ 8.28 (1H, d, *J*=5.2), 8.04 (1H, d, *J*=5.2 Hz), 7.73 (1H, d, *J*=7.5 Hz), 7.17 (1H, t, *J*=8.0 Hz), and 7.09 (1H, d, *J*=7.2 Hz) combined with ^{13}C-NMR resonances at 136.91, 121.70, 116.46, 113.66, and 113.43 confirmed the presence of an 1,8-disubstituted β-carboline moiety with a hydroxy group at C-8 (144.42). HMBC correlations of H-11 (δ_H 6.09, δ_C 121.44) to C-12 (83.62), C-26 (70.88), C-10 (140.21), and C-24 (43.99) confirmed that the β-carboline moiety is coupled with the typical cyclohexene ring found in many manzamine alkaloids. The presence of the piperidine ring was confirmed by the HMBC correlations of H-26 (δ_H 3.86, δ_C 70.88) to C-36 (70.75), C-25 (46.76), and C-24 (43.99). The ^{13}C-NMR resonance at 56.61 (δ_H 4.69, 3.97) was assigned to C-20 which showed an HMBC correlations with the other two α-carbons of *N*-21 (C-22, 60.99; C-36, 70.75) in the piperidine ring. The presence of the 13-membered ring in the molecule was confirmed by the ^{1}H-^{1}H-COSY and HMBC correlations of the two olefinic ^{1}H-NMR resonances, H-15 (δ_H 5.47, δ_C 131.40) and

H-16 (δ_H 5.50, δ_C 131.80). The unprecedented δ-lactone ring was established based on the HMBC correlations of H-34 (δ_C 36.42) methylene resonances at δ 3.04 and 2.90 to C-24 (δ_H 4.07, 43.99), C-25 (46.76), and C-35 (ester carbonyl) (173.87). The downfield chemical shifts of C-12 (83.62), C-25 (46.76), C-36 (70.75), and C-26 (70.88) with the HMBC correlations confirmed the δ-lactone ring to be connected between C-12 and C-26. The ^{13}C-NMR spectra showed an additional carbonyl group which was shown to be the amidic carbonyl at C-28 based on the HMBC correlations of H-26 (δ_H 3.86, δ_C 70.88), H-33 (δ_H 3.80, 3.58; δ_C 55.78), and H-29 (δ_H 1.92, 1.67; δ_C 29.27) to the C-28 carbonyl (179.60). The relative configuration of acantholactone **2** was deduced from the detailed analysis of the NOESY spectrum. The chair-boat conformation of the piperidine and the cyclohexene rings were assigned based on the NOESY correlations of H-24, H-26 and H22. The new lactone ring was assigned as α-orientation relative to the cyclohexene ring based on the NOESY correlations of H-24/H-36. The clear NOESY corelation between H-20 and H-33 suggested the α-conformation of the lactam ring.

The absolute configuration of acantholactone (**2**) was established by comparing the computed electronic circular dichroism (ECD) spectra with experiment (Figure II.10). As a result of conformational analysis, six low-energy conformations were generated using the Merck Molecular Force Field (MMFF) calculations followed by the PM6 semi-empirical optimizations. The optimized structures were then used for the hybrid density-functional theory (DFT) calculation at the B3LYP/6-31G(d,p) level for the gas phase and for acetonitrile (using the Polarizable Continuum Model (PCM)).[46] The DFT optimized structures were subsequently used for the TDDFT excited-state calculations at the BHANDHLYP/TZVP level for the gas phase and for acetonitrile (PCM). The obtained rotational strengths were Boltzmann averaged and fitted to

Gaussian functions with the calculated excitation energies to simulate ECD curves of **2** which were then overlaid with the experimental ECD spectrum for comparison. Based on the relative configuration elucidated by the NMR experiments, the absolute configuration of acantholactone (**2**) was thus assigned as 12S, 24R, 25R, 26R.
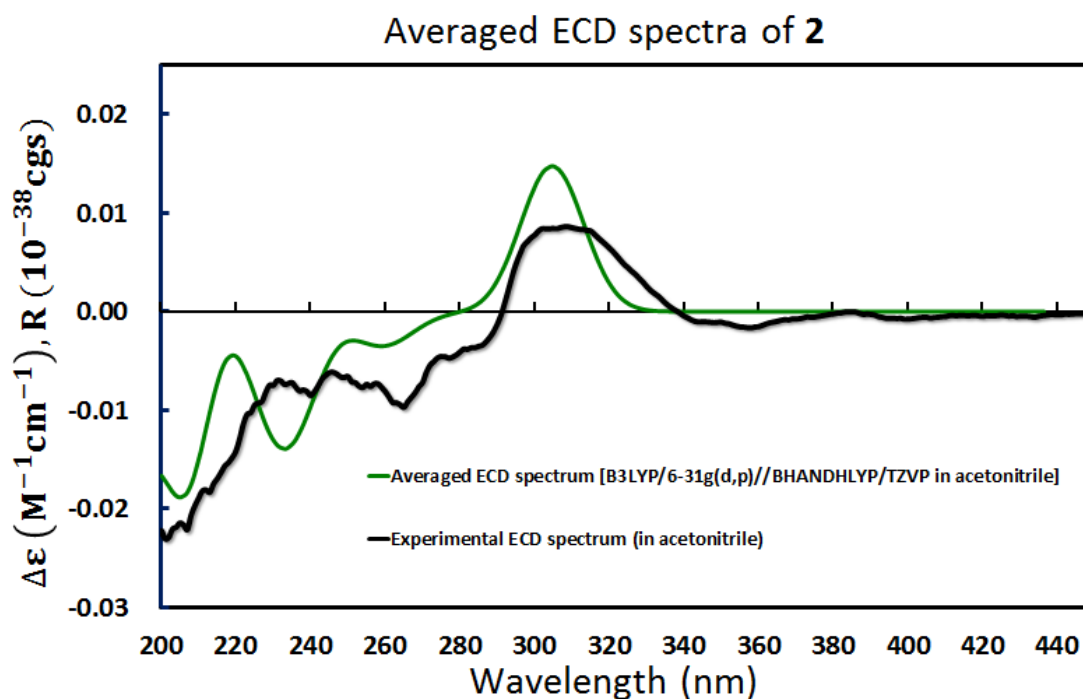
Figure II.9. Computed ECD curve (in acetonitrile) overlaid with the experimental ECD spectrum of **2**.

The molecular formula of compound **3** was determined as $C_{36}H_{45}N_4O_4$ from HRESIMS (*m/z* 597.4256 (M+H)[+]) and NMR analysis. The ^{1}H- & ^{13}C-NMR spectra of **3** revealed a classical manzamine skeleton with a substituted β-carboline moiety at C-1 (^{1}H-NMR: 8.18, 1H, d, *J*=5.4; 7.95, 1H, d, *J*=8.1; 7.64, 1H, d, *J*=5.4; 7.40,1H, t, *J*=8.0; 7.13,1H, t, *J*=7.9; 7.13, 1H, d, *J*=8.0. ^{13}C-NMR: 140.80, 139.39, 139.13, 137.03, 133.53, 129.43, 127.36, 120.76, 118.54, 112.47, 110.41) and a 3° hydroxy group at C-12 (72.99) and was similar to those of *N*-oxide manzamine J. The absence of the C-28 methylene resonance in the ^{13}C-NMR and the HMBC correlation of H-26 (δ_C 65.66, δ_H 4.42) to the carbonyl resonance at 174.97 suggested that C-28 was oxidized to form the amide functionality. ^{1}H-^{1}H COSY and HMBC correlations of the olefinic resonances, (δ_H 6.33, δ_C 148.97) and (δ_H 5.85, δ_C 120.11), as well as the absence of the C-34 methine resonance in the ^{13}C-NMR supported the opening of the eight-membered ring. The ^{13}C-NMR spectra of compound **3** showed only one oxygenated carbon resonance at 72.99 that was attributed for C-12 (bearing the 3° hydroxy group) and a carbonyl carbon (C-28, 174.97). Based on that, the remaining two oxygen atoms (from molecular formula) should be attached to nitrogen atoms. One oxygen is attached to *N*-2 of the β-carboline moiety (NMR matches with *N*-oxide manzamine J) and the other oxygen should be attached to *N*-21. The chemical shifts of C-20 (52.27) and C-22 (48.42) are similar to those published for 2,21-dioxomanzamine A.[14] Compound **3** was purified from the polar fractions of the total alkaloids extract and was found to lack the typical fluorescence on Si 60 TLC (365 nm).

Table II.4. ^{1}H, ^{13}C NMR and 2D data of compound **2** and **3** (δ in ppm, J in Hz)[a]

| Position | Acantholactone (**2**)[b] | | | | | 2,21,28-trioxomanzamine J (**3**)[c] | | |
	^{13}C-NMR	^{1}H-NMR	HMBC	COSY	NOESY	^{13}C-NMR	^{1}H-NMR	COSY
1	147.52 s	-	-	-		140.80 s	-	-
3	136.91 d	8.28 d, 5.2	3, 4a, 10	4	4, 6, 7, 11, 15, 16	137.03 d	8.18 d, 5.4	4
4	116.46 d	8.04 d, 5.2	3, 4a	3	3, 6, 7, 11	112.47 d	7.64 d, 5.4	3
4a	131.21 s	-	-	-		129.43 s	-	-
4b	130.96 s	-	-	-		133.53 s	-	-
5	113.43 d	7.73 d, 7.5	4b, 6, 7	6	6, 7, 11	120.76 d	7.95 d, 8.1	6
6	121.70 d	7.17 t, 8.0	8a, 8b	5	5, 11, 15, 16	118.54 d	7.13 t, 8	5, 7
7	113.66 d	7.07 d, 7.2	5, 8, 9	6	5, 11, 15, 16	127.36 d	7.40 t, 8	6, 8
8	144.42 s	-	-	-		110.41 d	7.13 d, 7.9	7
8a	121.92 s	-	-	-		139.39 s	-	-
9b	132.23 s	-	-	-		139.13 s	-	-
10	140.21s	-	-	-		144.34 s	-	-
11	121.44 d	6.09, s	10, 12, 24, 26	-	3, 4, 5, 6, 7, 24, 26	138.05 d	6.55 s,	-
12	83.62 s	-	-			72.99 s	-	-
13	39.15 t	2.94 m, 2.57 m	26	14		42.36 t	3.87 m, 3.51 d, 7.7	13, 14
14	28.70 t	1.91 m, 1.81 m		13, 15		25.01 t	1.73 m, 1.89 m	13, 14, 15
15	131.40 d	5.47, dd, 9.5. 4.8	14, 16	14, 16	26, 24, 17, 16	131.06 d	5.47 dd, 10.1, 5.1	13, 16
16	131.80 d	5.50 m	15, 17		26, 24, 17, 15	127.00 d	5.57 m	15, 17
17	25.52 t	1.77 m, 1.65 m	16	16, 17a	16, 15	20.62 t	2.38 m, 2.17 m	16, 18
18	27.46 t	2.47 m, 2.26 m				26.85 t	1.49 m, 1.32 m	17, 19
19	23.01 t	1.91 m, 174 m				23.39 t	1.75 m, 1.43 m	
20	56.61 t	4.69 d, 14, 3.97 m	19, 18	20a, 19		52.27 t	2.62 m, 2.52 d,	19, 20

	δC	δH	HMBC	COSY		δC	δH	COSY
								9.7, 2
21	-	-	-	-		-	-	-
22	60.99 t	4.55 m, 3.57 m	36, 23, 20	23		48.42 t	2.78 m, 1.97 m	22, 23
23	30.54 t	2.17 m, 1.51 m	24	22,24		32.59 t	2.28 dd, 11.2, 6.0, 1.60 m	22, 24
24	43.99 d	4.07, d, 4.1	12, 22, 25, 26	23	34, 16, 15, 11	39.60 d	2.28 m	23
25	46.76 s	-	-	-		46.06 s	-	-
26	70.88 d	3.86, s	12, 13, 24, 33, 36	-		65.66 d	4.42 d, 16.1	-
28	179.60 s	-	-	-		174.97	-	-
29	29.27 t	1.92 m, 1.67 m	28			33.08 t	2.21 m, 1.59 m	29, 30
30	24.04 t	1.87 m, 1.64 m				22.83 t	1.87 m, 1.47 m	31
31	26.10 t	1.76 m, 1.62 m				21.61 t	2.37 m, 2.17 m	31, 32
32	23.60 t	1.91 m, 1.74 m				148.97 d	6.33 m	31, 32, 33
33	55.78 t	3.80 d,12 , 3.58 m	26, 28, 32	32		120.11 d	5.85 dd, 10.1, 5.1	32, 34
34	36.42 t	3.04 d, 18, 2.90 d, 18	24, 26, 35	-	26, 24	29.84 t	1.43 m, 1.32 m	33, 25
35	173.87 s	-	-	-		41.43 t	2.17 m, 1.94 m	34
36	70.75 t	3.77 m, 3.49 m	12, 22, 25, 26,34	36		64.53 t	2.68 m, 2.05 d, 10.7	-

[a] 400 MHz for ^{1}H and 100 MHz for ^{13}C-NMR. Carbon multiplicities were determined by DEPT experiments. s=C, d=CH, t=CH_2. [b] NMR obtained in d_6-acetone. [c] NMR obtained in $CDCl_3$.

Experimental:

Fractions (98-120) collected from the large scale purification of MA (Scheme II.4, page 42), that came after the elution of manzamine F, were combined and subjected to a Si gel vacuum liquid chromatography and eluted in order with *n*-hexane:acetone:Et$_3$N 85:15:1, 75:25:1, 60:40,1 then 100% of acetone. The column was then washed with methanol and the 100% acetone fraction was combined with the methanol washing fraction. Further purification was carried out on a Phenomenex Luna C8 250x10 mm, 5μm Luna reverse-phase HPLC column using gradient MeOH (0.1% TFA)/water (0.1% TFA) with flow rate of 6 mL/min to gave acantholactone (**2**) and compound **3**

Acantholactone (2): 4 mg; yellow powder (DCM); $[\alpha]_D^{25}$ 31.6 (*c* 0.045, MeOH); UV (MeOH) λ$_{max}$ 352, 292, 255, 234 nm; CD (CH$_3$CN) λ$_{max}$ 306 nm (Δε +0.0084), 274 nm (Δε -0.0047), 244 nm (Δε -0.0065), 230 nm (Δε -0.0075); NMR data, see Table II.4.; HRESIMS *m/z* 595.3416 (calcd for C$_{36}$H$_{43}$N$_4$O$_4$, (M+H)$^+$, 595.3498).

2,21,28-trioxomanzamine J (3): 5 mg; $[\alpha]_D^{25}$ 16.2 (*c* 0.025, MeOH); UV (MeOH) λ$_{max}$ 346, 292, 230 nm; NMR data, see Table II.4.; HRESIMS *m/z* 597.4256 (calcd for C$_{36}$H$_{45}$N$_4$O$_4$, (M+H)$^+$, 597.4265).
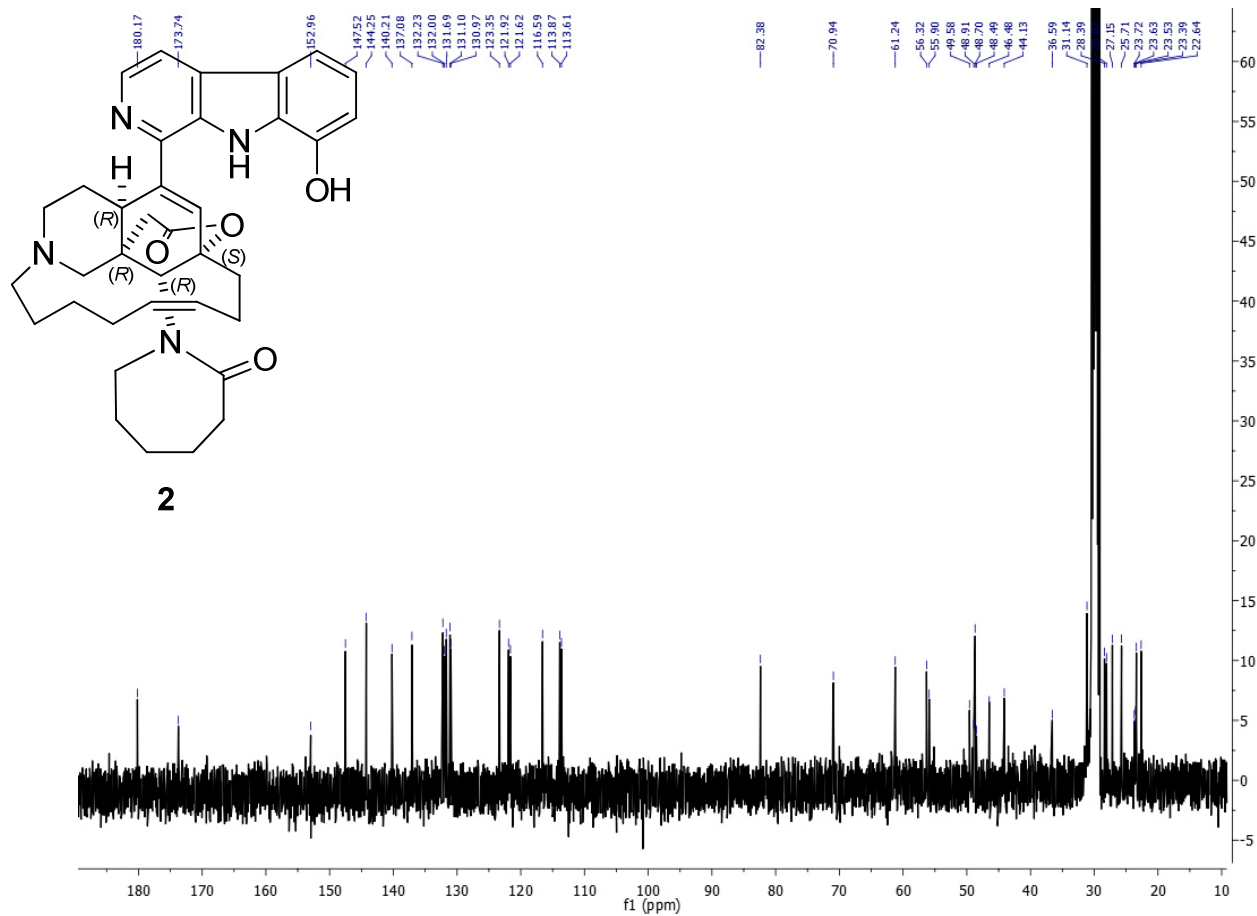
Figure II.11. ^{13}C-NMR spectra of acantholactone (**2**) in *d6*-acetone at 400 MHz.
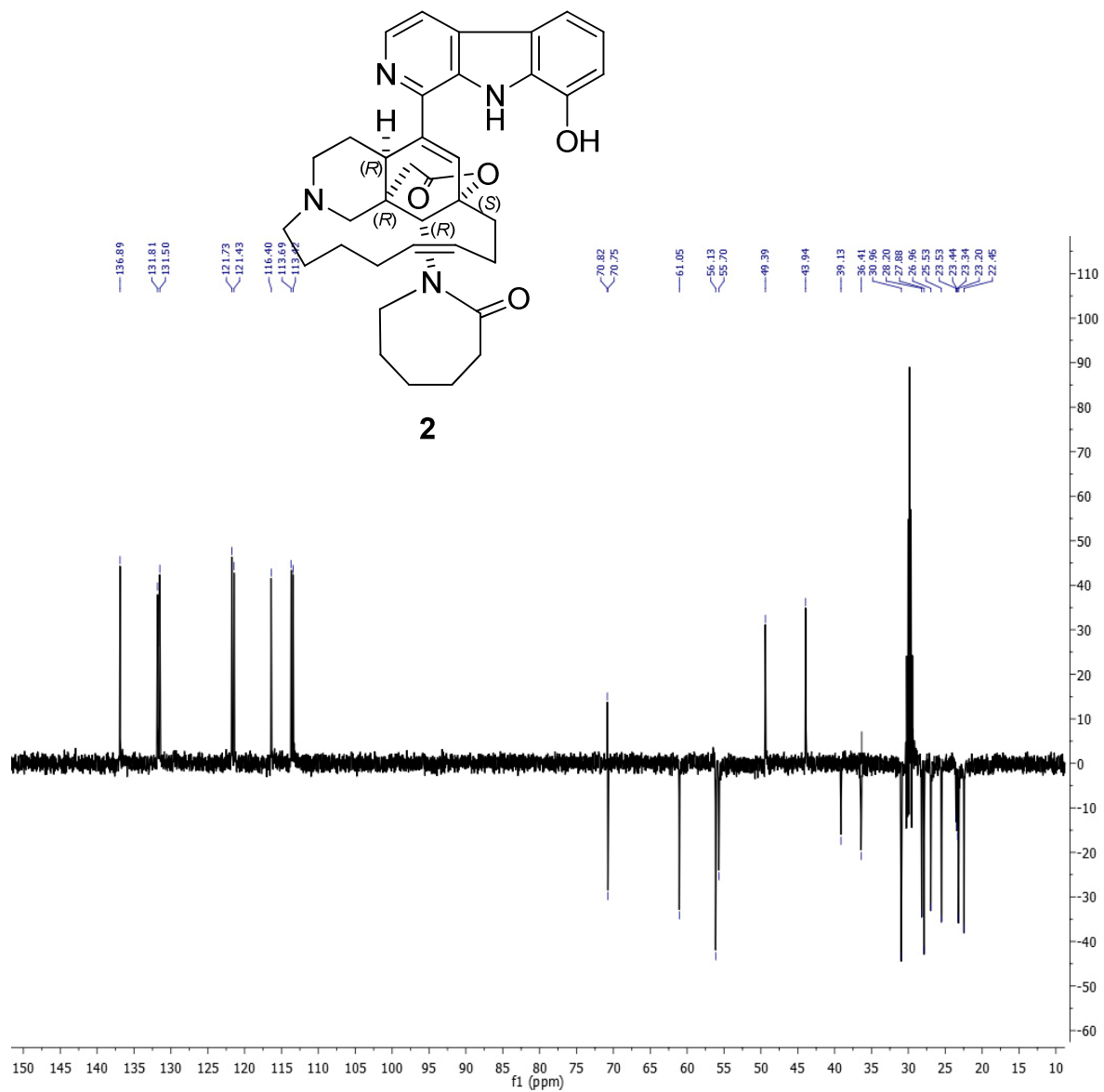
Figure II.12. [135]DEPT-NMR spectra of acantholactone (**2**) in *d6*-acetone at 400 MHz.
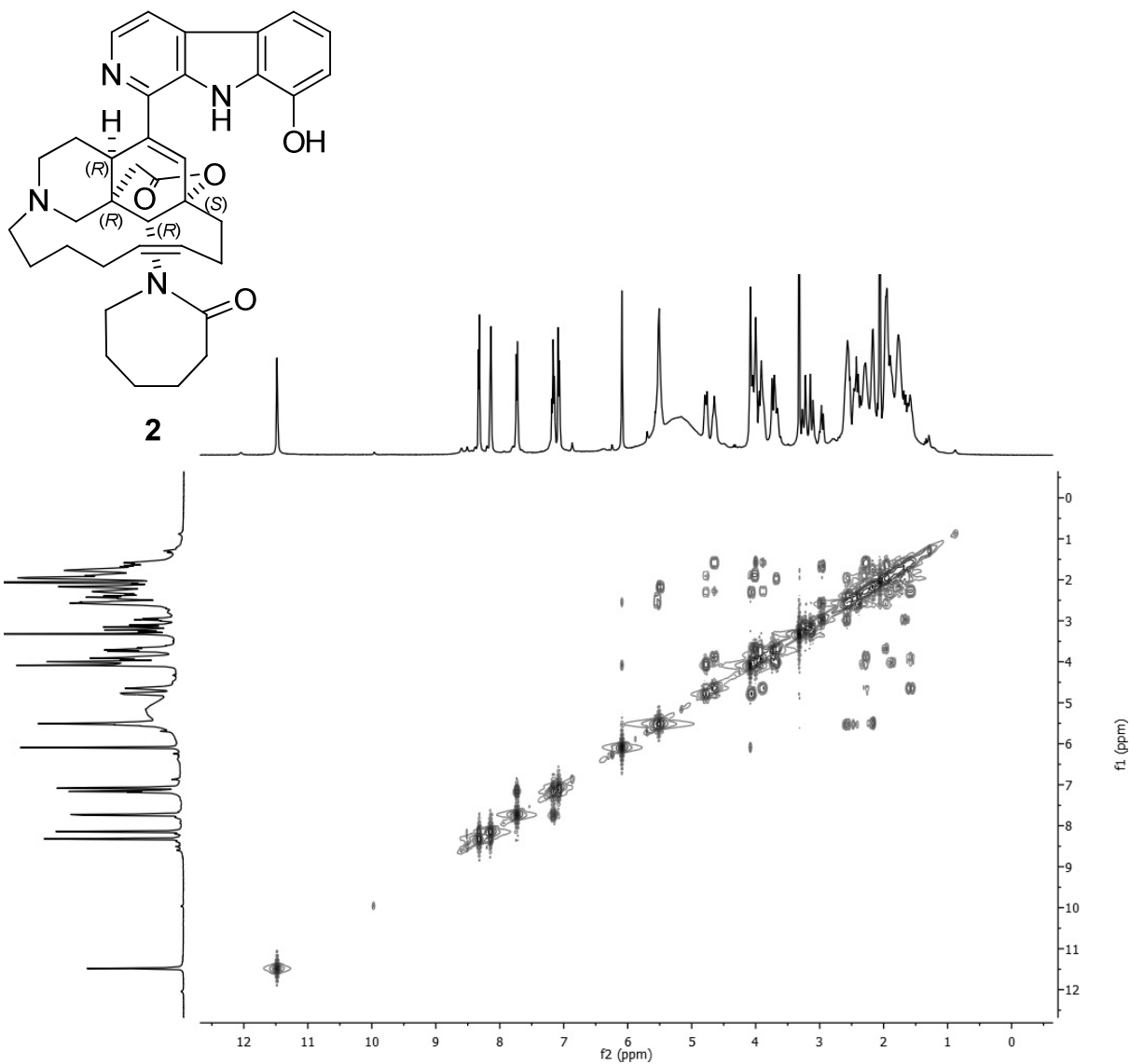
Figure II.13. ^{1}H-^{1}H COSY experiment of acantholactone (**2**) in *d6*-acetone at 400 MHz.
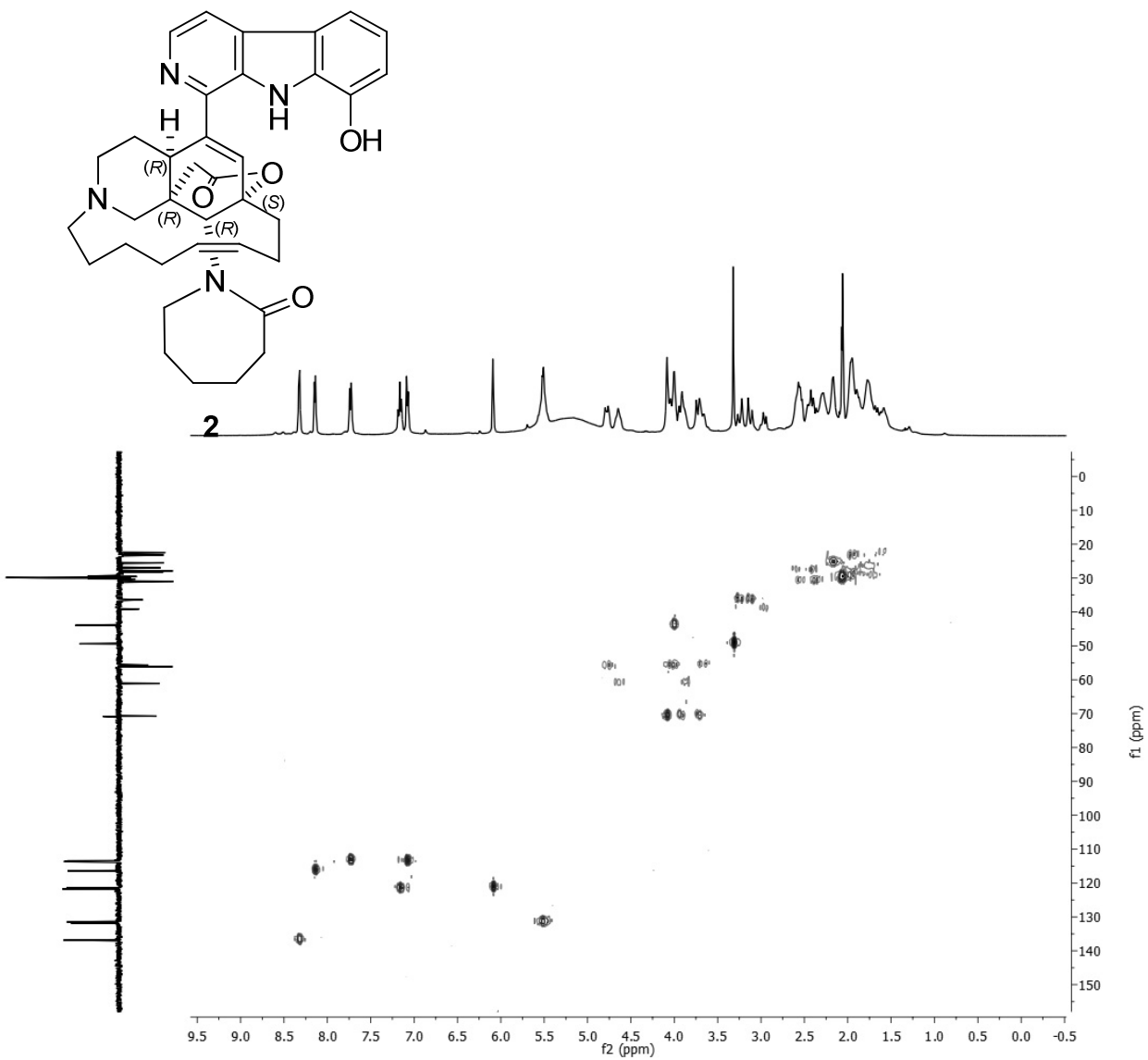
Figure II.14. HMQC experiment of acantholactone (**2**) in *d6*-acetone at 400 MHz.
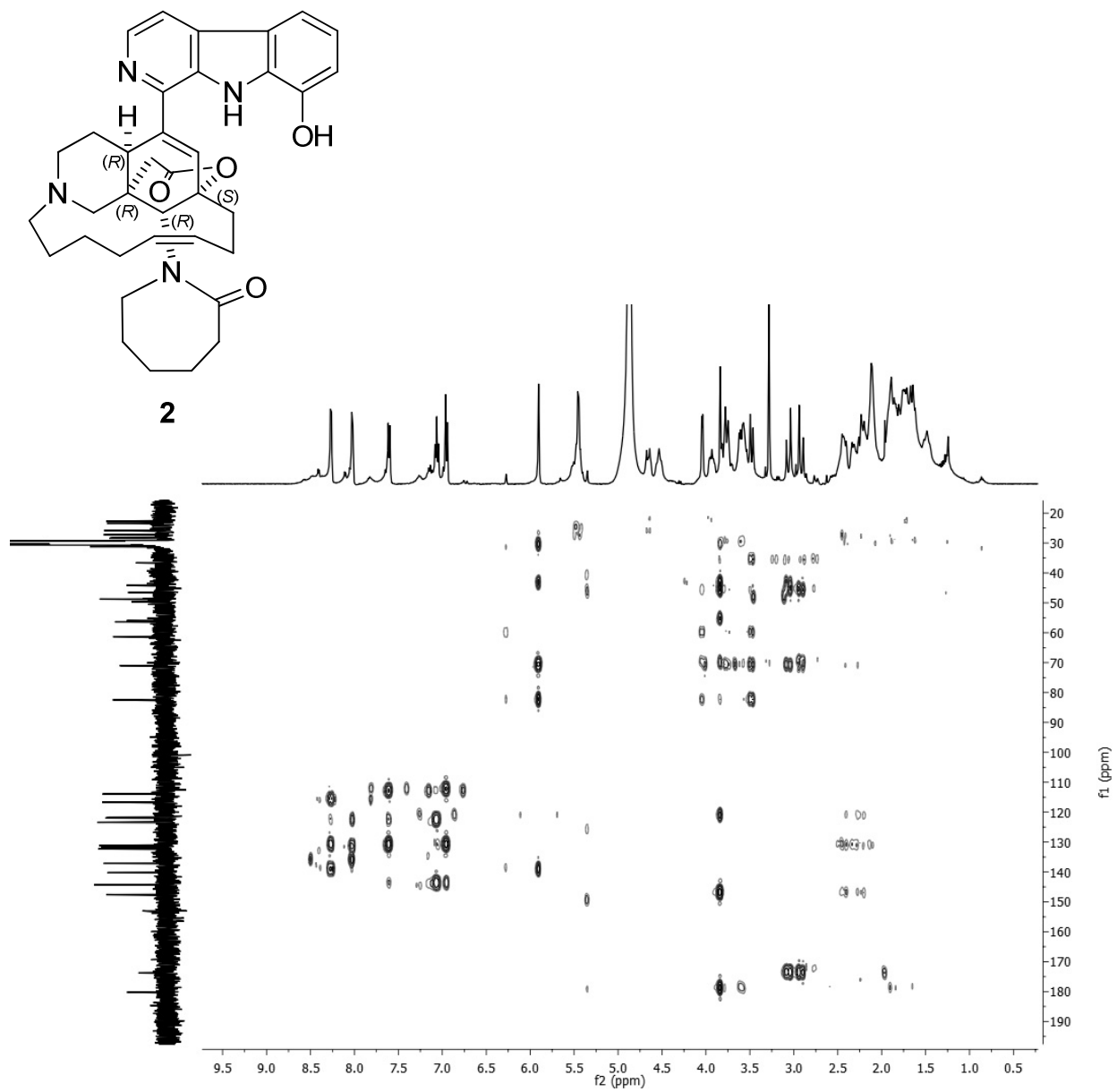
Figure II.15. HMBC experiment of acantholactone (**2**) in *d6*-acetone at 400 MHz.
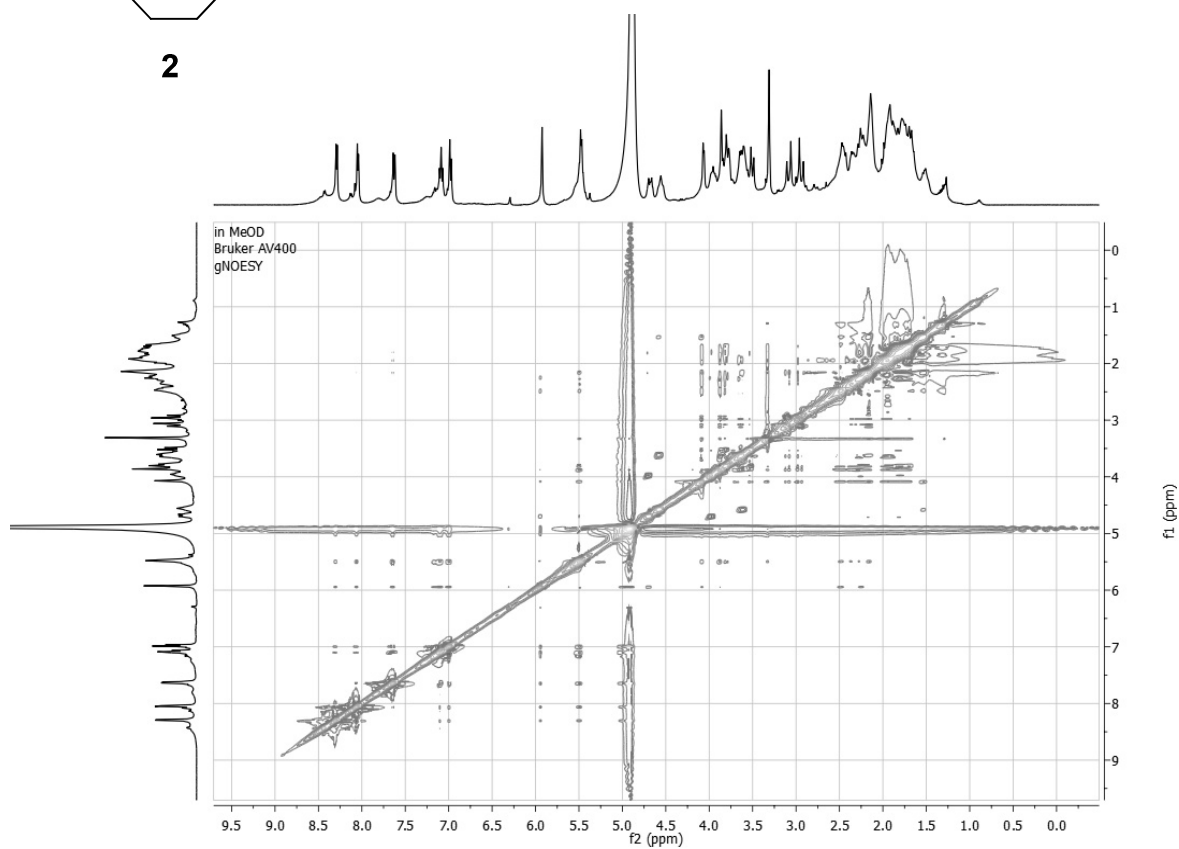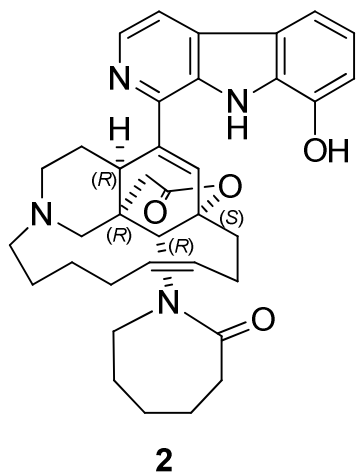
Figure II.16. NOESY experiment of acantholactone (**2**) in *d4*-methanol at 400 MHz.
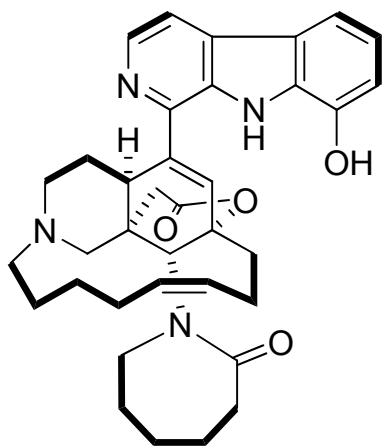
COSY correlations
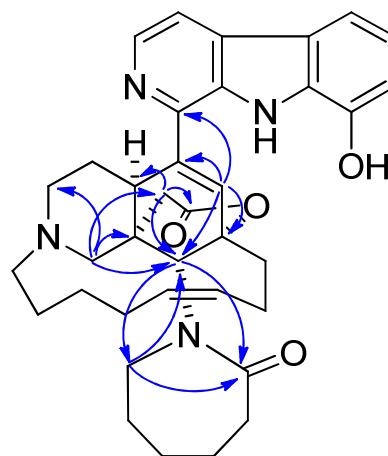
HMBC correlations
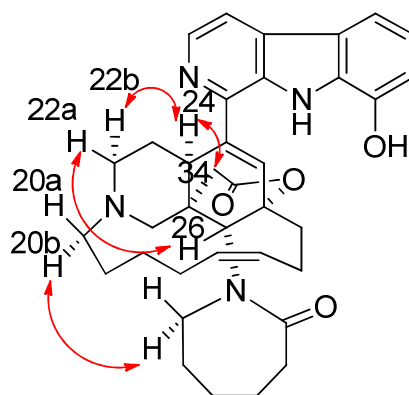
NOESY correlations

Figure II.17. Key 2D-correlations of acantholactone (**2**).
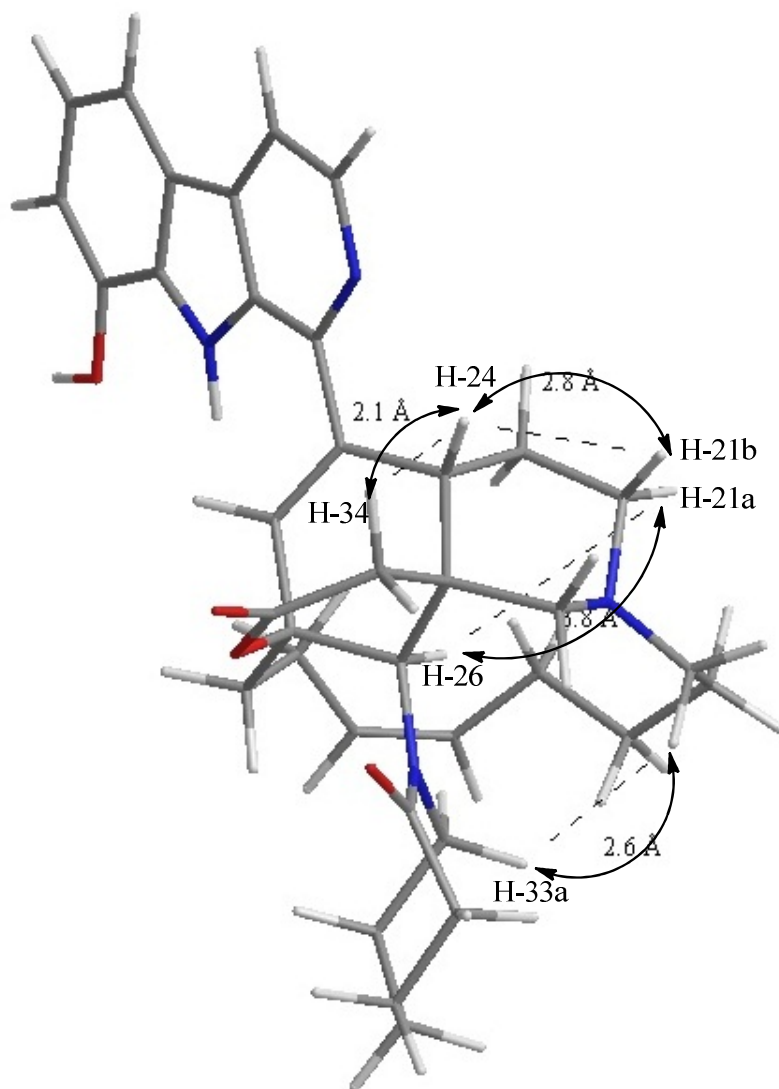
Figure II.18. 3D structure of the most stable conformer of acantholactone (**2**) with the key

NOESY correlations and the distance between the hydrogen atoms.
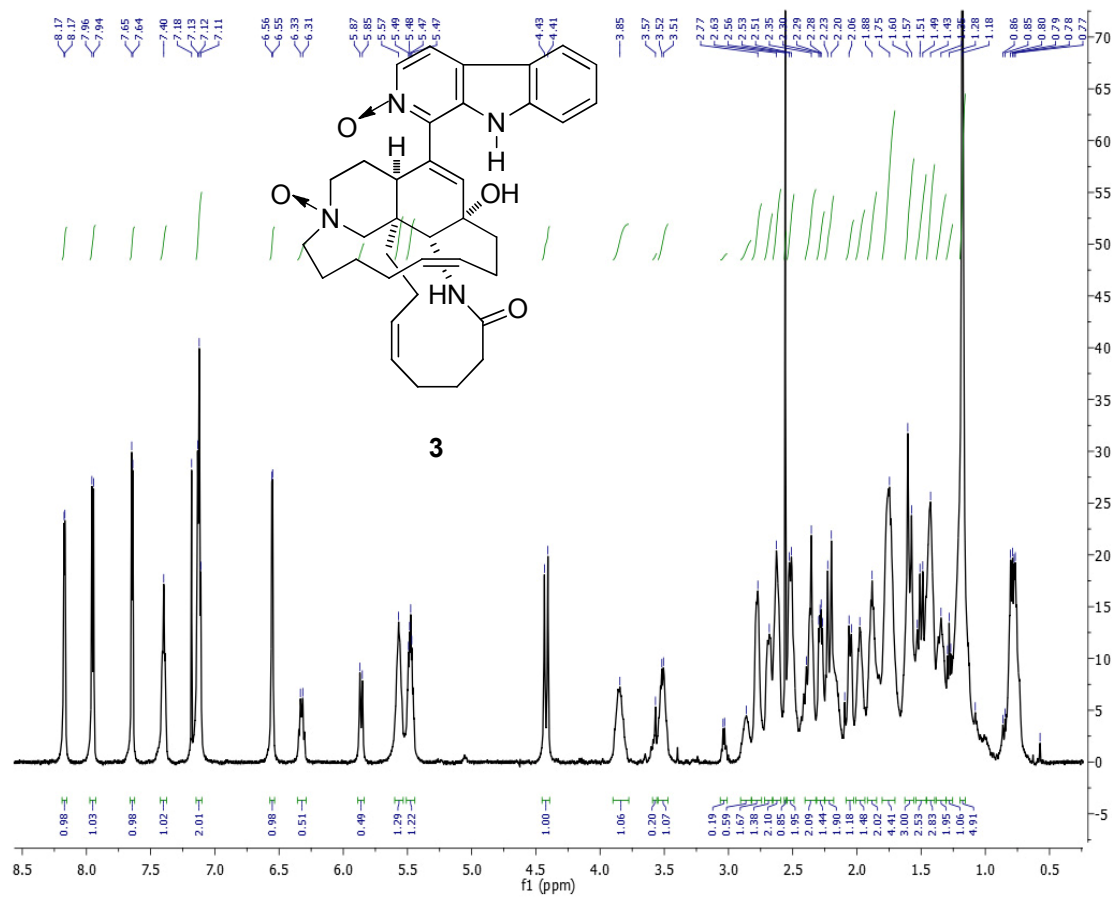
Figure II.19. ^{1}H-NMR spectra of compound **3** in CDCl$_3$ at 400 MHz.
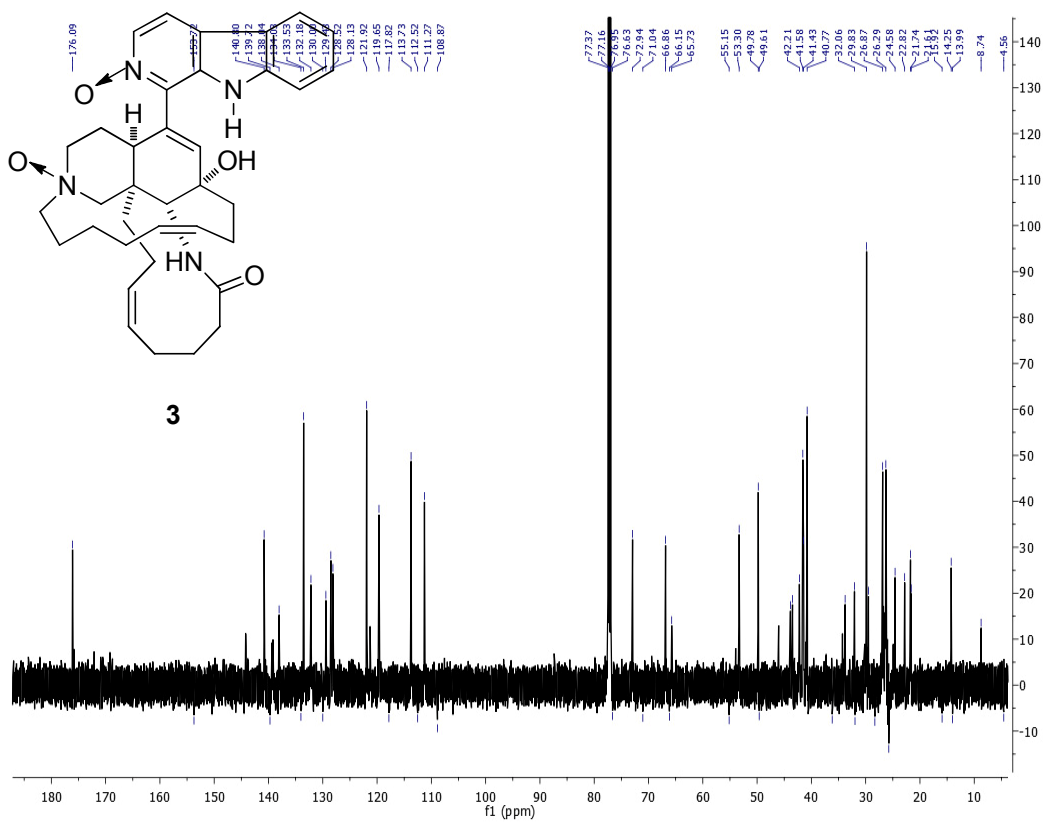
Figure II.20. ^{13}C-NMR spectra of compound **3** in CDCl$_3$ at 400 MHz.
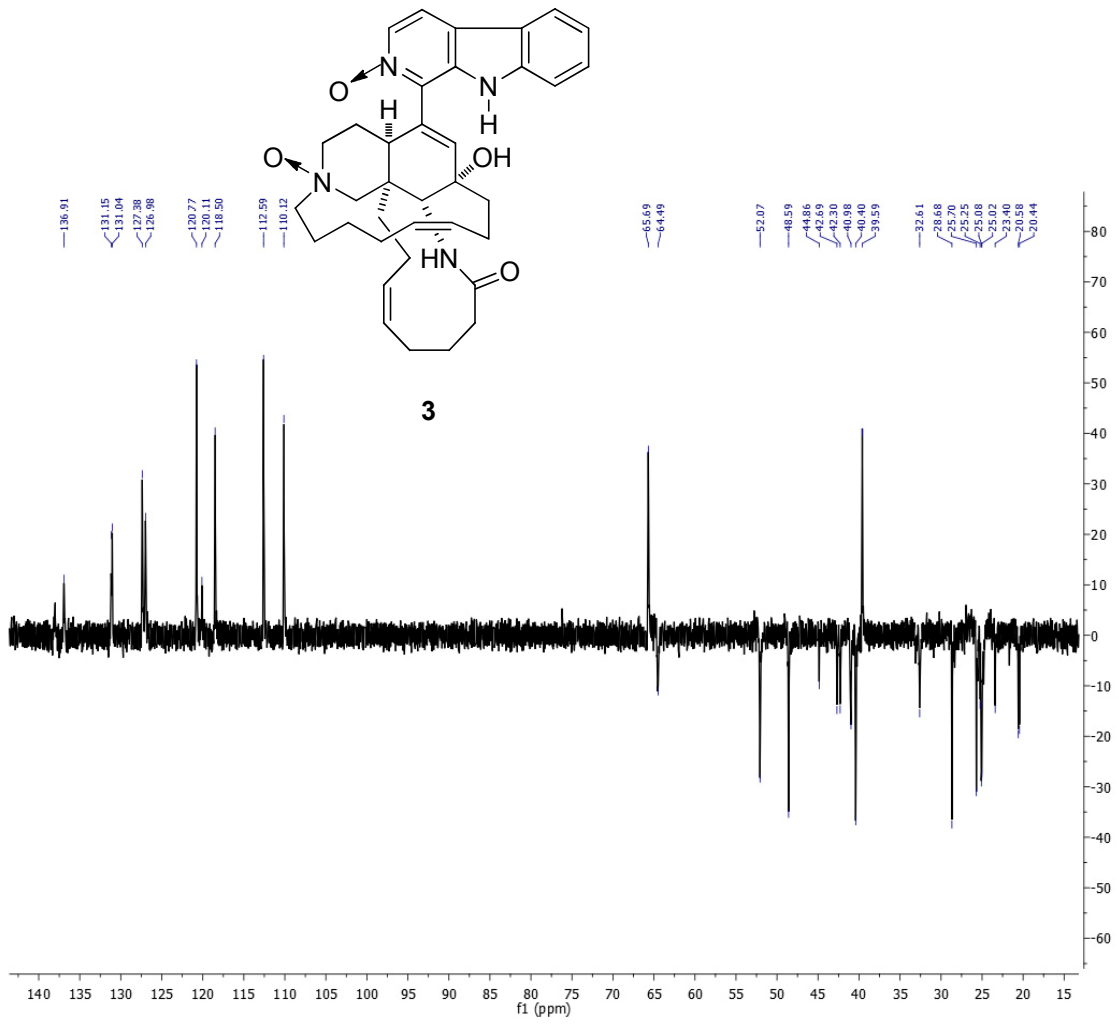
Figure II.21. [135]DEPT-NMR spectra of compound **3** in CDCl₃ at 400 MHz.
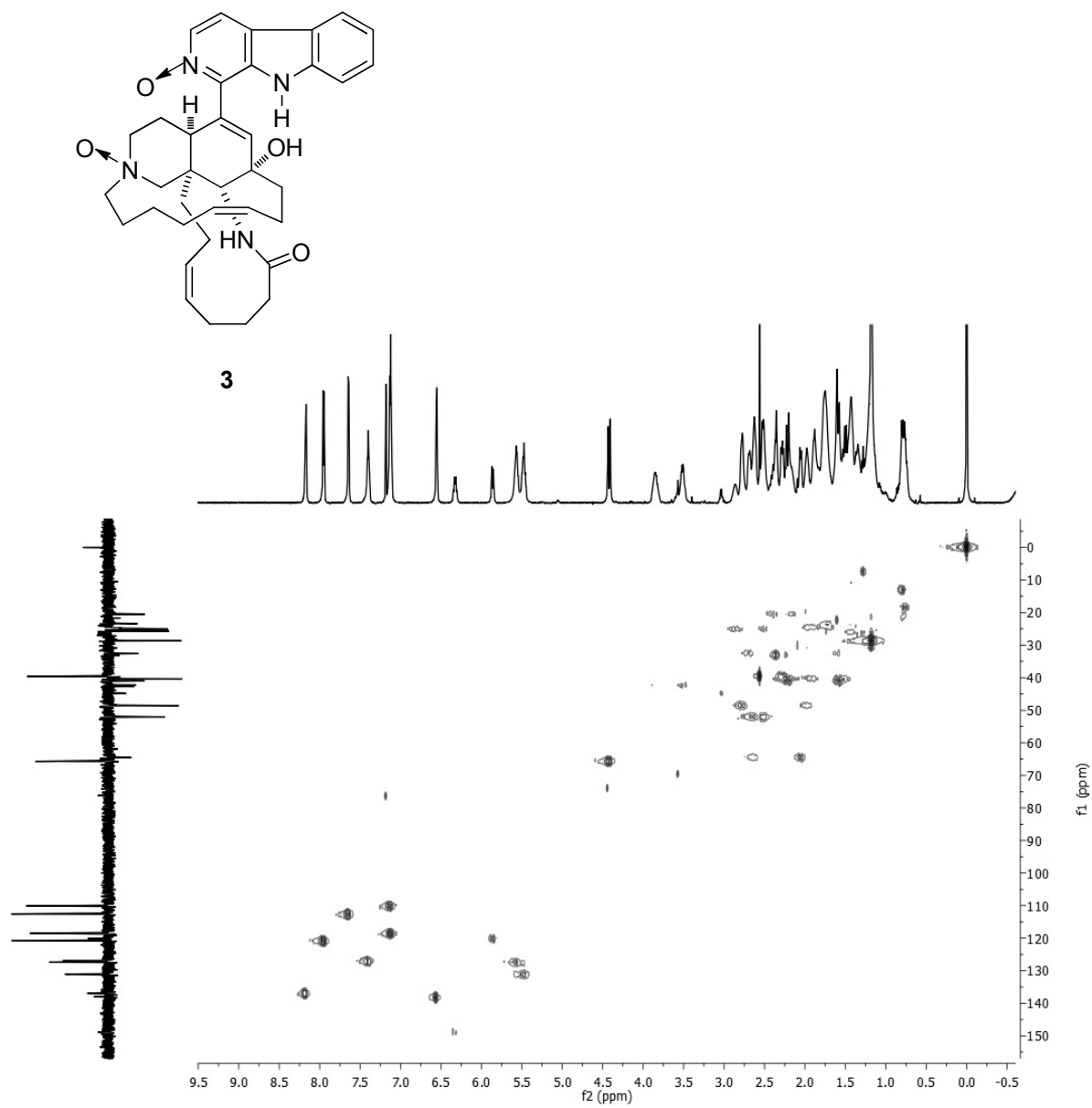
Figure II.22. HMQC experiment of compound **3** in CDCl₃ at 400 MHz.
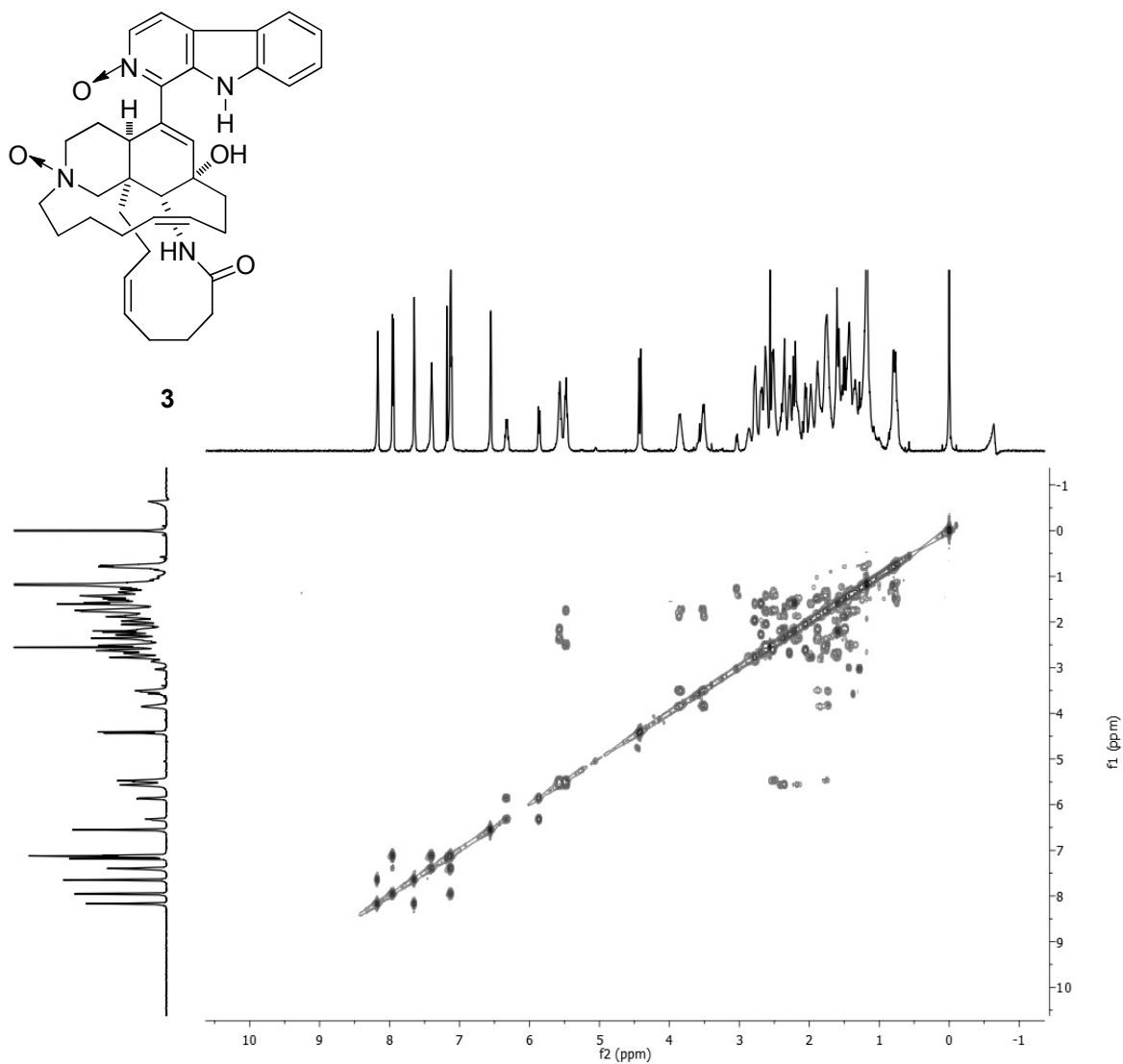
Figure II.23. ^{1}H-^{1}H COSY experiment of compound **3** in CDCl$_3$ at 400 MHz.

Structure–activity relationship studies of manzamine A: Amidation of positions 6 and 8 of the β-carboline moiety

Amir E. Wahba [a], Jiangnan Peng [a], Sucheta Kudrimoti [a], Babu L. Tekwani [b,c], Mark T. Hamann [a,b,c,*]

CHAPTER II.

THE MANZAMINE ALKALOIDS

SECTION C

STRUCTURE ACTIVITY RELATIONSHIP STUDIES OF MANZAMINE A:

AMIDATION OF POSITIONS 6 AND 8 OF THE β-CARBOLINE MOIETY

Published in Bioorganic and Medicinal Chemistry, 2009, 17, 7775-7782.

Authors: Amir E. Wahba, Jiangnan Peng, Sucheta Kudrimoti, Babu L. Tekwani, and Mark T. Hamann.

ABSTRACT: Twenty manzamine amides were synthesized and evaluated for in vitro antimalarial and antimicrobial activities. The amides of manzamine A (**1**) showed significantly reduced cytotoxicity against Vero cells, although were less active than **1**. The structure activity analysis showed that linear, short alkyl groups adjacent to the amide carbonyl at position 8 are favored for antimalarial activity, while bulky and cyclic groups at position 6 provided the most active amides. Most of the amides showed potent activity against *Mycobacterium intracellulare.* The antimicrobial activity profile for position 8 series was similar to that for the antimalarial activity profile, in which linear, slightly short alkyl groups adjacent to the amide carbonyl showed improved activity. Two amides **14** and **21**, which showed potent antimalarial activity in vitro against *Plasmodium falciparum* were further evaluated in vivo in *Plasmodium berghei* infected mice. Oral administration of **14** and **21** at the dose of 30 mg/kg (once daily for three days) caused parasitemia suppression of 24% and 62%, respectively, with no apparent toxicity.

Introduction:

By the time resistance to chloroquine has spread around the world, the era of inexpensive and available antimalarial drugs had ended.[47] This in addition to the fact that artemisinins are the only first-line antimalarial drugs that are still effective against all chloroquine-resistance malaria parasites has driven the scientific community and funding agencies to invest additional time and resources for the development of new antimalarial drugs. Malaria still causes more than one million deaths every year.[48] The process of drug discovery includes three major stages: 1) Target identification and high throughput screening of small molecules 2) lead identification and optimization, and 3) preclinical and clinical studies.[49] Nature has served as the mine for structurally diverse small molecules utilized for target identification for human diseases. Over 63% of small molecules reported between 1981 and 2006 are either natural, natural product derived or inspired from natural compounds.[49] Manzamine alkaloids (Figure II.24) represents a unique class of natural products that have shown a diverse range of bioactivities, including antimicrobial, [40,50,51,52] antiparasitic,[44] cytotoxicity,[12,53] antiinflammatory,[54,55] pesticidial,[39] and was shown to possess activity against HIV-1 and AIDS opportunistic infections.[56] They are particularly attractive candidates for optimization for the control of infectious diseases.[57] The first representative of this family is manzamine A (**1**) isolated in 1986 by Higa.[12] This family has the unique structural feature of having complex polycyclic ring systems coupled with a β-carboline moiety. Manzamine A (**1**) and its 8-hydroxy derivative (**2**), showed the most promising antimalarial activity within this class of compounds. Both showed improved potency against malaria parasite in vitro and in vivo over the clinically used drugs chloroquine and artemisinin.[57] Oral treatment of **1** (2x100 µmol/kg) and **2** (2x100 µmol/kg) showed 90% reduction in parasitemia. Mice treated with a single dose (50 or 100 µmol/kg) of **1** or **2** also showed

75

significant improvements in survival times over mice treated with chloroquine or artemisinin.[44,45] This data revealed significant promise for the development of this new class of antimalarial drugs. However, the major drawback of this class of compounds is toxicity associated with higher dosing schedules. The mechanism of action of **1** as an antimalarial agent is not clear and requires intensive SAR studies for a better understanding of the importance of each moiety of this complex molecule for the antimalarial activity. The first intensive SAR study on manzamine alkaloids was completed by our group and focused on exploring the different functional groups around the molecule.[14] This included reduction of the double bonds at the complex polycyclic ring systems, *N*-oxidation, 9-*N*-alkylation, 8-*O*-alkylation in **2** and reduction of the carbonyl group in manzamine F (**3**). In addition, ircinal (**4**) was coupled with substituted tryptamines through Pictet-Spengler cyclization. Several analogs were synthesized in this study with good antimalarial activity but without improvement in regard to cytotoxicity. Experimental evidence that manzamines arrest the cell cycle in the S phase suggests that this toxicity may be due to DNA intercalation by the planar β-carboline moiety. However, no significant modifications of the β-carboline moiety were completed until this study.

Manzamine A (**1**): R=H
8-Hydroxymanzamine A (**2**): R=OH

Manzamine F (**3**)

Ircinal A (**4**)
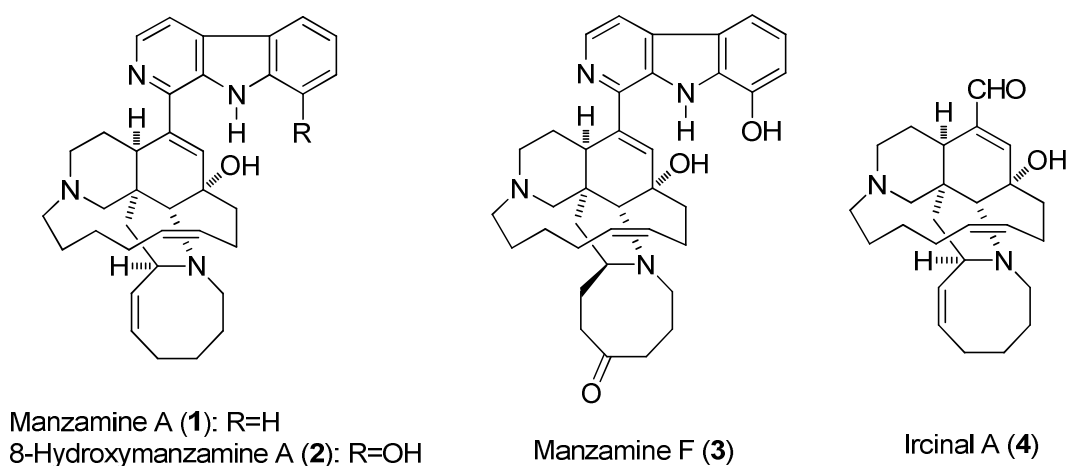
Figure II.24. Manzamine alkaloids.

In this study, we focused our modification on the β-carboline moiety of **1** as an extension to the previous study for lead optimization as antimalarial agent. Twenty amides of **1** which differ at C-6 and C-8 in the β-carboline moiety have been synthesized. These amides were evaluated for in vitro and in vivo antimalarial activity in addition to in vitro antimicrobial activity.

Results and discussion:
Chemistry:

Manzamine A (**1**) in addition to **2**, **3**, and **4** were purified from the Indonesian sponge *Acanthostrongylophora Sp*. through an optimized isolation procedure.[1] C-6 and C-8 of the β-carboline moiety in **1** could be chemically modified via electrophilic aromatic substitution reactions, due to the activation by the secondary amine functionality in the indole part of the β-carboline moiety. We began our modifications by nitrating the benzene ring of the β-carboline moiety with $NaNO_2$ in the presence of TFA (Scheme II.1). This yielded two nitro products, 6-nitromanzamine A (**3-a**), and 8-nitromanzamine A (**3-b**). Stability of these two nitromanzamine A products, and the feasibility of converting the nitro group into different functional groups were the main reasons for selecting nitromanzamines as a key intermediates for synthesizing C-6 and C-8 analogs. Large-scale nitration of **1** and purification of the nitro products **3a,b** were carried out to provide starting material for additional analogs. Both nitro products were reduced to the corresponding 6- and 8-aminomanzamine A (**4a,b**) in almost complete conversion (by LCMS). However, low yields of amines were recovered owing to their instability, even as a hydrochloric salts. In addition, aminomanzamines were unstable in solution, especially in the presence of chloroform or dichloromethane. This lack of stability created challenges in regard to yields of the amidation reaction. Adding to the challenge is the conjugation with the remaining two nitrogens

77

of the β-carboline which appears to produce a highly basic amine after reduction of the nitro group.
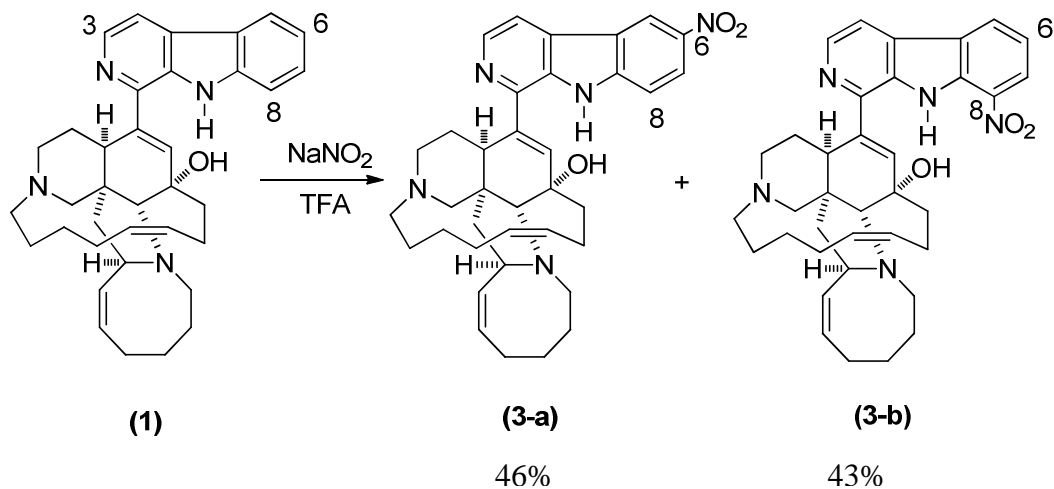
Scheme II.1. Nitration of manzamine A.

Amidation of aminomanzamines at C-6 and C-8 was carried out by reacting the amines with a slight excess of different acyl chlorides in the presence of the catalyst DMAP, and the base triethylamine at room temperature in dry THF under nitrogen atmosphere (Scheme II.2). Twenty amides were synthesized with yields ranging between ~12-17% (Table II.5). The structures of amidomanzamine A derivatives were confirmed by 1D & 2D-NMR spectroscopy.

78
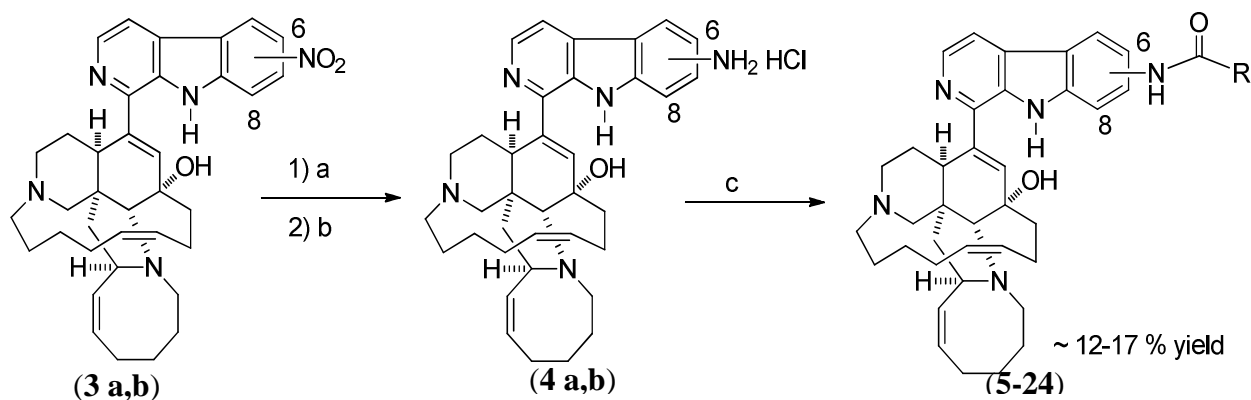
Reagents and conditions (a) Zn, HOAc/MeOH (5 %), rt, 10 min. (b) 1 equiv. (0.1M in MeOH) HCl. (c) 1.2 eqvui. RCOCl, 1 equiv. Et$_3$N, cat. DMAP, THF, rt, 1 h.

Scheme II.2. General procedure for amidation of manzamine

In vitro Antimalarial activity:

All amides were evaluated in vitro for antimalarial activity against chloroquine sensitive (D6, Sierra Leone) and resistant (W2, IndoChina) clones of *Plasmodium falciparum.* In addition they were tested for cytotoxicity on normal African green monkey kidney fibroblast cells (Vero) (Table II.6). Manzamine A (**1**) showed the highest activity with an IC$_{50}$ of 8.0 nM (D6 clone) and 11 nM (W2 clone). This activity is more potent than the standard antimalarials chloroquine and artemisinin (IC$_{50}$ values of 50 and 46 nM, respectively, against the D6 clone). Manzamine A (**1**) has a TC$_{50}$ of 365 nM against Vero cells, providing therapeutic indexes of 44 (D6 clone) and 25 (W2 clone).[45] All amides showed similar antimalarial activity against D6 and W2 clones of *P. falciparum.* Introduction of acetamido functionality at C-8 (**15**) reduced the antimalarial activity to an IC$_{50}$ of 182 nM against D6 clone. Increasing the length of the alkyl group adjacent to the amide carbonyl (2, 3, 4, 5 and 7 carbons) (**16**, **17**, **19**, **21** and **22**) in C-8 series showed improvement in in vitro antimalarial activity with IC$_{50}$ values of 123, 35, 53, 32, and 55 nM, respectively, against D6 clone. Branched alkyl groups adjacent to the amide carbonyl were not

79

favored at C-8. For example, 8-isobutamidomanzamine A (**18**) showed reduced activity with IC_{50} values of 158 and 205 nM, against D6 and W2 clones, respectively. This is relative to 8-*n*-butamidomanzamine A (**17,** 35 nM against D6), which has the same number of carbon atoms as an acyclic group. Similar results were obtained when adding bulkier groups such as *t*-butyl either directly attached to the amide carbonyl (**20,** IC_{50}=170 & 232 nM against D6 and W2 clones, respectively) or separated by one carbon as in 8-*t*-butylacetamidomanzamine A (**23,** IC_{50}=139 & 127 nM against D6 and W2 clones, respectively). Furthermore, adding a cyclohexyl group as in 8-cyclohexamidomanzamine A (**24**) markedly diminished antimalarial activity (IC_{50}=950 & 995 nM against D6 and W2 clones, respectively). This data suggests that relatively short linear alkyl groups (2-7 carbons) attached to the amide carbonyl at C-8 are preferred over branched and bulky groups for antimalarial activity.

Antimalarial activity profile for C-6 amides was opposite to that of C-8 amides. Acetamido group at C-6 drastically eliminated antimalarial activity (**5**, IC_{50}=1288 & 1982 nM against D6 and W2 clones, respectively). Increasing the number of carbons attached to the amide carbonyl (2, 3, 4, 5 and 7 carbons) **6**, **7**, **9**, **11,** and **12** also resulted in similar reduction in the antimalarial activity with IC_{50} values of 1162, 1152, 1235, 680 and 696 nM against D6, respectively. The amide with an isopropyl group attached to the amide carbonyl **8** also showed reduced antimalarial activity (IC_{50}s of 1105 & 1547 nM against D6 and W2 clones, respectively). Addition of a *t*-butyl group at C-6 slightly improved the activity as in 6-pivalamidomanzamine A (**10**) and 6-*t*-butylacetamidomanzamine A (**13**) with IC_{50} values of 231 and 211 nM against D6, compared to the linear alkyl groups. 6-Cyclohexamidomanzamine A (**14**) showed the best antimalarial activity among the C-6 amides with an IC_{50}=34 nM against D6 clone. This data

suggests that bulky groups at C-6 are preferred for antimalarial activity. It was interesting to note that all the amides did not show cytotoxicity to Vero cells.

In vivo Antimalarial activity:

With the objective of finding the analogs with reduced toxicity and equivalent or better antimalarial activity relative to manzamine A, the two most potent amides, 6-cyclohexamidomanzamine A (**14**, IC_{50} = 34 nM) and 8-*n*-hexamidomanzamine A (**21,** IC_{50} = 32 nM) were evaluated in vivo in a *Plasmodium berghei* mouse malaria model. Treatment with compounds **14** and **21** through oral administration caused only moderate suppression in parasitemia of 24% and 62%, respectively, at three doses (once daily for three days) of 30 mg/kg with no apparent toxicity. These results indicated that the amides **14** and **21** were less toxic in vivo; however, their antimalarial potency in vivo was also compromised, as compared to manzamine A.

In vitro Antimicrobial activity:

In vitro antimicrobial activities of amidomanzamines were investigated against *Candida albicans*, *E. coli, Pseudomonas aeruginosa, Cryptococcus neoformans*, *Mycobacterium intracellulare* and *Aspergillus fumigatus* (Table II.7).

1) Bioactivity against *M. intracellulare*:

Manzamine A (**1**) showed potent activity against *M. intracellulare* with an IC_{50} value of 0.64 μM which is slightly more potent than ciprofloxacin, (IC_{50}=1.06 μM). Amides at C- 6 with linear alkyl groups (**5, 6, 7, 9** and **11**) showed significantly reduced activity against *M. intracellulare* with IC_{50} values of 9.91 5.65, 4.74, 2.32 and 15.12 μM, respectively. Similar results were obtained when adding branched acyclic alkyl groups such as isopropyl (**8**, IC_{50} = 3.16 μM). 6-Cyclohexamidomanzamine A (**14**) and 6-pivalamidomanzamine A (**10**) showed improved

activities within the C-6 amides with IC_{50} values of 1.26 and 1.54 μM, respectively. These results indicate that amidation at C-6 is not favorable for activity against *M. intracellulare.* C-8 analogs showed better antimycobacterial potency compared to C-6 amides. The amide with acetamido (**15**) and propamido (**16**) groups at C-8 showed moderate activities with an IC_{50}'s of 1.65 and 1.52 μM, respectively. 8-*n*-Butamidomanzamine A (**17**), 8-isobutamidomanzamine A (**18**) and 8-*n*-pentamidomanzamine A (**19**) showed activities close to manzamine A (**1**) and the control with IC_{50} values of 0.87, 1.03 and 0.70 μM, respectively, while 8-*n*-octamidomanzamine A (**22**) was slightly more potent than manzamine (IC_{50}=0.51 μM). 8-*n*-Hexamidomanzamine A (**21**) was the most potent amide with an IC_{50} of 0.03 μM, which is one order of magnitude more potent than the control as well as **1**. Marked loss of activity in 8-cyclohexamidomanzamine A (**24**, IC_{50}=11.14 μM) suggested that linear acyclic alkyl groups as amide functionality at C-8 are more favorable than bulkier groups, which is similar to the activity profile for antimalarial activity.

2) Bioactivity against *Cryptococcus neoformans*:

All the amides were screened for anticryptococcal activity against *Cryptococcus neoformans*. The amides were either not active (**5-13** and **24**) or showed lower activity compared to **1** (IC_{50}=1.85 μM). All amides were not active against *Candida albicans, E. coli and P. aeruginosa.*

Conclusion:

In conclusion, 20 manzamine amides **5**-**24** have been synthesized and were screened in vitro for antimalarial and antibacterial activities. Amidation at C-6 and C-8 was a good choice for eliminating toxicity associated with manzamine A, since all amides (**5**-**24**) did not show cytotoxicities on Vero cells. In general, the amides were less active than **1.** Some amides such as

(**14**, **17** and **21**) showed the best antimalarial activities among the amide series with IC_{50} values of 34, 34, and 32 nM against *Plasmodium falciparum*, respectively. Our structure activity relationship study showed that linear, short alkyl groups adjacent to the amide carbonyl at C-8 are favored for antimalarial activity, while bulky and cyclic groups at C-6 appear to be the best choice for achieving better activity. Two of the most active amides, **14** and **21**, were evaluated in vivo in a *Plasmodium berghei* mouse malaria model. Oral administration of **14** and **21** at the dose of 30 mg/kg (once daily for three days) caused parasitemia suppression of 24% and 62%, respectively, with no apparent toxicity.

Most of the amides showed potent activity against *M. intracellulare.* The activity profile for the C-8 series was similar to that for the antimalarial activity profile, in which linear, slightly short alkyl groups adjacent to the amide carbonyl showed improved activity. 8-*n*-Hexamidomanzamine A (**21**) was the most potent amide with an IC_{50} of 0.03 μM which is one order of magnitude more potent than the control. The potency of **21** against *M. intracellulare* will encourage us to continue investigating this amide in animals. C-6 analogs **5**-**14** were less potent than those at C-8 against *M. intracellulare*. 6-Cyclohexamidomanzamine A (**14**) and **10** showed improved activities within C-6 series with an IC_{50} of 1.48 and 1.31 μM, respectively, which was similar to the activity profile of antimalarial activity for C-6 amides.

Experimental section:

General Experimental Procedures. The ^{1}H- and ^{13}C-NMR spectra were recorded in CDCl$_3$ or *d6*-acetone on a Bruker DRX NMR spectrometer operating at 400 MHz for ^{1}H and 100 MHz for ^{13}C. Chemical shift (δ) values are expressed in parts per million (ppm) and are referenced to the residual solvent signals of CDCl$_3$ or *d6*-acetone. UV and IR spectra were respectively obtained using a Perkin-Elmer Lambda 3B UV/VIS spectrophotometer and an AATI Mattson Genesis

series FTIR instrument. Optical rotations were measured with a JASCO DIP-310 digital polarimeter. The high resolution ESI-MS spectra were measured using a Bruker Daltonic (GmbH, Germany) micro-TOF series with electrospray ionization. TLC analysis was carried out on precoated silica gel G254 aluminum plates.

Nitration of manzamine A: manzamine A (1) (5 g, 9.12 mmol) was dissolved in TFA (133 ml. 1.79 mmol), and kept at 0 $^\circ$C with stirring for 30 minutes. Sodium nitrite (1 g, 14.5 mmol) was added in one portion and allowed to stir at 0 $^\circ$C for an additional 3 hours. The reaction mixture was poured into water and neutralized by ammonium hydroxide producing a precipitate that was filtered and dried. The crude nitro products of manzamine A (4.50 g) were loaded onto a column packed with 450 g of silica gel. 6-Nitromanzamine A (**3a**) eluted first using 99:1 DCM:MeOH followed by 8-nitromanzamine A (**3b**) after the mobile phase polarity was increased with 95:5 DCM:MeOH.

6-Nitromanzamine A (3a): (2.50 g, 46%); yellow powder; ^{1}H-NMR (CDCl$_3$) δ 9.04 (1H, d, J=2.0 Hz), 8.50 (1H, d, J=5.2 Hz) , 8.40 (1H, dd, J=9.2, 2.0 Hz), 7.89 (1H, d, J=5.2 Hz), 7.77 (1H, d, J=9.2 Hz), 6.50 (1H, s), 6.21 (1H, s), 5.62 (m), 5.42 (1H, t, J=10.8 Hz), 4.70 (br), 3.69 (s), 3.25 (1H, t, J=11.0 Hz), 2.93 (1H, d, J=9.0 Hz), 2.80~2.20 (m), 2.10~1.20 (m); ^{13}C-NMR (CDCl$_3$) δ 144.5,144.2, 142.7, 141.2, 141.1, 139.4, 135.7, 134.5, 133.2, 129.7, 127.0, 123.7, 123.5, 121.0, 118.4, 114.2, 112.9, 77.9, 71.2, 70.5, 57.6, 53.7 (2C), 49.4, 47.1, 44.9, 40.8, 39.5, 33.9, 28.7, 26.6, 26.6, 25.2, 24.8, 24.3, 20.9; HRESIMS m/z calcd for C$_{36}$H$_{44}$N$_5$O$_3$ (M+H)$^+$ 594.3444, found 594.3439.

8-Nitromanzamine A (3b): (2.35 g, 43%) yellow powder; ^{1}H-NMR (CDCl$_3$) δ 10.40 (1H, s), 8.57 (1H, d, J=5.2 Hz), 8.48 (1H, d, J=8.0 Hz), 8.45 (1H, d, J=8.1 Hz), 7.87 (1H, d, J=5.2 Hz), 7.40 (1H, t, J=8.0 Hz), 6.45 (1H, s), 5.96 (1H, m), 5.69 (1H, m), 5.55 (1H, m), 5.32 (1H, t,

J=10.0 Hz), 4.27 (1H, br), 3.58 (1H, s), 3.11 (1H, m), 2.61 (m), 2.50~1.6 (m), 1.4 (m); ^{13}C-NMR (CDCl$_3$) δ 144.6, 1443.6, 142.7, 141.4, 141.2, 139.4, 135.3, 134.6, 133.2, 130.0, 127.1, 123.8, 123.7, 121.1, 118.5, 114.4, 113.0, 77.8, 71.2, 70.6, 57.7, 53.7, 53.72, 53.68, 49.5, 47.1, 44.8, 40.5, 39.8, 34.1, 28.8, 26.7, 26.6, 25.3, 24.9, 24.3, 21.0; HRESIMS *m/z* calcd for C$_{36}$H$_{44}$N$_5$O$_3$ (M+H)$^+$ 594.3444, found 594.3439.

Reduction of nitromanzamines: 6-nitromanzamine A (**3**) or 8-nitromanzamine A (**4**) (118.6 mg, 0.21 mmol) were dissolved in methanol (5 mL). Zinc (50.0 mg) and 5% acetic acid in methanol (5 mL) were added to the nitromanzamines solution, and the reaction mixture was stirred for 10 min at room temperature. After complete conversion of the nitro products into the corresponding amine (monitored by TLC), conc. HCl was added drop wise till no further precipitate was formed. The precipitate was collected by filtration and used for the following reactions without further purification.

General preparation of the amide products. 6-Aminomanzamine A or 8-aminomanzamine A (100 mg, 0.17 mmol) and catalytic amount of DMAP were dissolved in anhydrous THF (3 mL) under nitrogen atmosphere. Et$_3$N (25 μL, 0.17 mmol) was then added, and the mixture was stirred at room temperature for 10 minutes. The desired acid chloride was added in excess, and the reaction mixture was stirred for 1 h. The completion of the reaction was monitored by TLC, then the reaction was quenched with water, and the product(s) were extracted by DCM (3x10 mL). The organic layer was dried over anhydrous sodium sulfate, and then evaporated under reduced pressure. The crude amide derivatives were first purified by silica column chromatography using *n*-hexane:acetone (9:1). Further purification was carried out on a Phenomenex Luna C8 250x10 mm, 5μm Luna reverse-phase HPLC column using gradient

CH₃CN (0.1% TFA)/water (0.1% TFA) with flow rate of 6 mL/min to gave the pure amide derivative.

6-Acetamidomanzamine A (5): (15 mg, 14%); $[\alpha]_D^{25}$ 12.9 (*c* 0.11, MeOH); UV λ_{max} (MeOH) 260, 310, 375 nm; IR: 3232 (br), 2935, 2580, 1978, 1703, 1665,1538, 1470, 1437, 1365, 1290, 1178, 1130, 1018 cm⁻¹; ¹H-NMR (CDCl₃) δ 11.32 (1H, s), 8.65 (1H, s), 8.50 (1H, s), 8.32 (1H, d, *J*=7.6 Hz), 7.79 (1H, d, *J*=7.5 Hz), 7.66 (1H, d, *J*=7.6 Hz), 7.36 (1H, d, *J*=7.6 Hz), 6.64 (1H, s), 6.28 (1H, m), 5.57 (1H, m), 5.42 (1H, t, *J*=4.0 Hz), 4.96 (1H, t, *J*=8.1 Hz), 4.04 (1H, dd, *J*=16.1, 8.0 Hz), 3.7 (1H, s), 3.37 (1H, t, *J*=12.1 Hz), 3.04 (1H, d, *J*=8.1 Hz), 2.95 (m), 2.77 (m), 2.61 (m), 2.43 (m), 2.31 (m), 2.26 (m) 2.08 (s), 2.03 (m), 1.96 (m), 1.74 (m), 1.48 (m); ¹³C-NMR (CDCl₃) δ 175.04, 166.03, 143.57, 142.05, 141.99, 138.60, 135.78, 134.48, 133.85, 133.42, 130.20, 128.08, 125.35, 122.38, 122.12, 114.63, 112.93, 77.85, 71.70, 70.50, 57.09, 53.49, 49.32, 47.07, 44.82, 31.21, 39.16, 33.62, 28.45, 26.52, 26.36, 24.99, 24.58, 24.32, 23.97, 20.73; HRESIMS *m/z* calcd for C₃₈H₄₉N₅O₂ (M+H)⁺ 606.3743, found 606.3784.

6-*n*-Propamidomanzamine A (6): (16 mg, 14%); $[\alpha]_D^{25}$ 17.1 (*c* 0.15, MeOH); ¹H-NMR (CDCl₃) δ 11.33 (1H, s), 8.66 (1H, s), 8.50 (1H, s), 8.31 (1H, d, *J*=7.6 Hz), 7.80 (1H, d, *J*=7.5 Hz), 7.67 (1H, d, *J*=7.6 Hz), 7.35 (1H, d, *J*=7.6 Hz), 6.64 (1H, s), 6.29 (1H, m), 5.56 (1H, m), 5.43 (1H, t, *J*=4.2 Hz), 4.96 (1H, t, *J*=8.0 Hz), 4.04 (1H, dd, *J*=16.1, 8.0 Hz), 3.69 (1H, s), 3.37 (1H, t, *J*=12.1 Hz), 3.04 (1H, d, *J*=8.0 Hz), 2.95 (m), 2.77 (m), 2.61 (m), 2.43 (m), 2.41 (2H, q, *J*=7.2 Hz), 2.31 (m), 2.26 (m), 2.03 (m), 1.96 (m), 1.74 (m), 1.48 (m), 1.14 (3H, t, *J*=7.2 Hz); ¹³C-NMR (CDCl₃) δ 175.04, 166.03, 143.57, 142.05, 141.99, 138.60, 135.78, 134.48, 133.85, 133.42, 130.20, 128.08, 125.35, 122.38, 122.12, 114.63, 112.93, 77.85, 71.70, 70.50, 57.09, 53.49, 49.32, 47.07, 44.82, 31.21, 39.16, 33.62, 30.36, 28.45, 26.52, 26.36, 24.99, 24.58, 24.32, 20.73, 9.86; HRESIMS *m/z* calcd for C₃₉H₅₀N₅O₂ (M+H)⁺ 620.3936, found 620.3942.

6-*n*-Butamidomanzamine A (7): (16 mg, 14%); $[\alpha]_D^{25}$ 11.9 (*c* 0.11, MeOH); ^{1}H-NMR (CDCl$_3$)

δ 11.25 (1H, s), 8.70 (1H, s), 8.50 (1H, s), 8.30 (1H, d, *J*=7.6 Hz), 7.75 (1H, d, *J*=7.5 Hz), 7.66

(1H, d, *J*=7.6 Hz), 7.36 (1H, d, *J*=7.6 Hz), 6.62 (1H, s), 6.25 (1H, m), 5.54 (1H, m), 5.39 (1H, t,

J=4.0 Hz), 4.92 (1H, t, *J*=8.0 Hz), 4.00 (1H, dd, *J*=16.1, 8.0 Hz), 3.66 (1H, s), 3.37 (1H, t,

J=12.0 Hz), 3.04 (1H, d, *J*=8.1 Hz), 2.95 (m), 2.77 (m), 2.61 (m), 2.43 (m), 2.37 (2H, t, *J*=7.0

Hz), 2.31 (m), 2.26 (m), 2.03 (m), 1.96 (m), 1.74 (m), 1.48 (m), 1.00 (3H, t, *J*=7.1 Hz); ^{13}C-NMR

(CDCl$_3$) δ 171.45, 166.03, 143.69, 141.99, 141.16, 138.32, 137.62, 134.48, 133.85, 133.42,

130.20, 128.08, 125.35, 122.38, 122.12, 114.63, 112.93, 77.85, 71.70, 70.50, 57.09, 53.49, 49.32,

47.07, 44.82, 40.09, 31.21, 39.16, 33.62, 30.36, 26.52, 26.36, 24.99, 24.58, 24.32, 20.73, 19.72,

14.52; HRESIMS *m/z* calcd for $C_{40}H_{52}N_5O_2$ (M+H)$^+$ 634.4129, found 634.4425.

6-Isobutamidomanzamine A (8): (14 mg, 12%); $[\alpha]_D^{25}$ 20.5 (*c* 0.21, MeOH); ^{1}H-NMR (CDCl$_3$)

δ 11.41 (1H, s), 8.57 (1H, s), 8.50 (1H, s), 8.30 (1H, d, *J*=7.6 Hz), 7.80 (1H, d, *J*=7.5 Hz), 7.69

(1H, d, *J*=7.6 Hz), 7.35 (1H, d, *J*=7.6 Hz), 6.59 (1H, s), 6.30 (1H, m), 5.57 (1H, m), 5.42 (1H, t,

J=4.0 Hz), 4.96 (1H, t, *J*=8.1 Hz), 4.04 (1H, dd, *J*=16.1, 8.0 Hz), 3.7 (1H, s), 3.37 (1H, t, *J*=12.0

Hz), 3.04 (1H, d, *J*=8.1 Hz), 2.95 (m), 2.77 (m), 2.61 (m), 2.43 (m), 2.63 (m), 2.31 (m), 2.26 (m),

2.03 (m), 1.96 (m), 1.74 (m), 1.48 (m), 1.29 (6H, d, *J*=7.2 Hz); ^{13}C-NMR (CDCl$_3$) δ 175.04,

166.03, 143.57, 142.05, 141.99, 138.60, 135.78, 134.48, 133.85, 133.42, 130.20, 128.08, 125.35,

122.38, 122.12, 114.63, 112.93, 77.85, 71.70, 70.50, 57.09, 53.49, 49.32, 47.07, 44.82, 40.9,

31.21, 39.16, 35.64, 33.62, 26.52, 26.36, 24.99, 24.58, 24.32, 20.73, 20.06, 19.86; HRESIMS

m/z calcd for $C_{40}H_{52}N_5O_2$ (M+H)$^+$ 634.4129, found 634.4045.

6-*n*-Pentamidomanzamine A (9): (15 mg, 13%); $[\alpha]_D^{25}$ 9.9 (*c* 0.15, MeOH); ^{1}H-NMR (CDCl$_3$) δ

11.32 (1H, s), 8.65 (1H, s), 8.50 (1H, s), 8.32 (1H, d, *J*=7.6 Hz), 7.79 (1H, d, *J*=7.5 Hz), 7.66

(1H, d, *J*=7.6 Hz), 7.36 (1H, d, *J*=7.6 Hz), 6.64 (1H, s), 6.28 (1H, m), 5.57 (1H, m), 5.42 (1H, t,

J=4.1 Hz), 4.96 (1H, t, J=8.0 Hz), 4.04 (1H, dd, J=16.0, 8.1 Hz), 3.7 (1H, s), 3.37 (1H, t, J=12.1 Hz), 3.04 (1H, d, J=8.0 Hz), 2.95 (m), 2.77 (m), 2.61 (m), 2.43 (m), 2.39 (2H, t, J=7.2 Hz), 2.31 (m), 2.26 (m), 2.03 (m), 1.96 (m), 1.74 (m), 1.48 (m), 0.99 (3H, t, J=7.1 Hz); ^{13}C-NMR (CDCl$_3$) δ 175.04, 166.03, 143.57, 142.05, 141.99, 138.60, 135.78, 134.48, 133.85, 133.42, 130.20, 128.08, 125.35, 122.38, 122.12, 114.63, 112.93, 77.85, 71.70, 70.50, 57.09, 53.49, 49.32, 47.07, 44.82, 31.21, 39.16, 37.47, 27.83, 33.62, 30.36, 29.68, 26.52, 26.36, 24.99, 24.58, 24.32, 22.44, 20.87, 13.84; HRESIMS m/z calcd for C$_{41}$H$_{54}$N$_5$O$_2$ (M+H)$^+$ 648.4277, found 648.4550.

6-Pivalamidomanzamine A (10): (14 mg, 12%); $[\alpha]_D^{25}$ 31.6 (c 0.21, MeOH); ^{1}H-NMR (CDCl$_3$) δ 11.32 (1H, s), 8.65 (1H, s), 8.50 (1H, s), 8.32 (1H, d, J=7.6 Hz), 7.79 (1H, d, J=7.5 Hz), 7.66 (1H, d, J=7.6 Hz), 7.36 (1H, d, J=7.6 Hz), 6.64 (1H, s), 6.28 (1H, m), 5.57 (1H, m), 5.42 (1H, t, J=4.0 Hz), 4.96 (1H, t, J=8.1 Hz), 4.04 (1H, dd, J=16.0, 8.0 Hz), 3.7 (1H, s), 3.37 (1H, t, J=12.1 Hz), 3.04 (1H, d, J=8.0 Hz), 2.95 (m), 2.77 (m), 2.61 (m), 2.43 (m), 2.31 (m), 2.26 (m), 2.03 (m), 1.96 (m), 1.74 (m), 1.49 (9H, s), 1.48 (m); ^{13}C-NMR (CDCl$_3$) δ 175.04, 166.03, 143.57, 142.05, 141.99, 138.60, 135.78, 134.48, 133.85, 133.42, 130.20, 128.08, 125.35, 122.38, 122.12, 114.63, 112.93, 77.85, 71.70, 70.50, 57.09, 53.49, 49.32, 47.07, 44.82, 39.31, 39.16, 33.62, 29.69, 28.45, 26.52, 26.36, 24.99, 24.58, 24.32,   20.73; HRESIMS m/z calcd for C$_{41}$H$_{54}$N$_5$O$_2$ (M+H)$^+$ 648.4277, found 648.4550.

6-n-Hexamidomanzamine A (11): (17 mg, 14%); $[\alpha]_D^{25}$ 36.1 (c 0.25, MeOH); ^{1}H-NMR (CDCl$_3$) δ 11.32 (1H, s), 8.65 (1H, s), 8.50 (1H, s), 8.32 (1H, d, J=7.6 Hz), 7.79 (1H, d, J=7.5 Hz), 7.66 (1H, d, J=7.6 Hz), 7.36 (1H, d, J=7.6 Hz), 6.64 (1H, s), 6.28 (1H, m), 5.57 (1H, m), 5.42 (1H, t, J=4.0 Hz), 4.96 (1H, t, J=8.1 Hz), 4.04 (1H, dd, J=16.0, 8.0 Hz), 3.7 (1H, s), 3.37 (1H, t, J=12.1 Hz), 3.04 (1H, d, J=8.0 Hz), 2.95 (m), 2.77 (m), 2.61 (m), 2.43 (m), 2.56 (2H, t, J=7.1 Hz), 2.31 (m), 2.26 (m), 2.03 (m), 1.96 (m), 1.74 (m), 1.48 (m), 0.94 (3H, t, J=7.0 Hz);

^{13}C-NMR (CDCl$_3$) δ 175.39, 166.03, 143.57, 142.05, 141.99, 138.60, 135.78, 134.48, 133.85, 133.42, 130.20, 128.08, 125.35, 122.38, 122.12, 114.63, 112.93, 77.85, 71.70, 70.50, 57.09, 53.49, 49.32, 47.07, 44.82, 31.21, 39.16, 37.47, 32.11, 29.68, 27.12, 26.78, 26.40, 25.54 25.28, 24.90, 23.05, 21.34, 14.22; HRESIMS m/z calcd for C$_{42}$H$_{56}$N$_5$O$_2$ (M+H)$^+$ 662.4488, found 662.4448.

6-n-Octamidomanzamine A (12): (15 mg, 12%); $[\alpha]_D^{25}$ 25.4 (c 0.12, MeOH); ^{1}H-NMR (CDCl$_3$) δ 11.32 (1H, s), 8.65 (1H, s), 8.50 (1H, s), 8.32 (1H, d, J=7.6 Hz), 7.79 (1H, d, J=7.5 Hz), 7.66 (1H, d, J=7.6 Hz), 7.36 (1H, d, J=7.6 Hz), 6.64 (1H, s), 6.28 (1H, m), 5.57 (1H, m), 5.42 (1H, t, J=4.0 Hz), 4.96 (1H, t, J=8.1 Hz), 4.04 (1H, dd, J=16.0, 8.1 Hz), 3.7 (1H, s), 3.37 (1H, t, J=12.0 Hz), 3.04 (1H, d, J=8.1 Hz), 2.95 (m), 2.77 (m), 2.61 (m), 2.43 (m), 2.46 (2H, t, J=7.2 Hz), 2.31 (m), 2.26 (m), 2.03 (m), 1.96 (m), 1.74 (m), 1.48 (m), 0.90 (3H, t, J=7.1 Hz); ^{13}C-NMR (CDCl$_3$) δ 176.14, 166.69, 143.57, 142.05, 141.99, 138.60, 135.78, 134.48, 133.85, 133.42, 130.20, 128.08, 125.35, 122.38, 122.12, 114.63, 112.93, 77.85, 71.70, 70.50, 57.09, 53.49, 49.32, 47.07, 44.82, 38.60, 37.47, 31.61, 29.68, 28.17, 26.78, 26.40, 25.54 25.28, 24.90, 22.82, 21.34, 14.47; HRESIMS m/z calcd for C$_{44}$H$_{60}$N$_5$O$_2$ (M+H)$^+$ 690.4732, found 690.4785.

6-(t-Butyl)-acetamidomanzamine A (13): (18 mg, 15%); $[\alpha]_D^{25}$ 21.5 (c 0.10, MeOH); ^{1}H-NMR (CDCl$_3$) δ 11.32 (1H, s), 8.65 (1H, s), 8.50 (1H, s), 8.32 (1H, d, J=7.6 Hz), 7.79 (1H, d, J=7.5 Hz), 7.66 (1H, d, J=7.6 Hz), 7.36 (1H, d, J=7.6 Hz), 6.64 (1H, s), 6.28 (1H, m), 5.57 (1H, m), 5.42 (1H, t, J=4.0 Hz), 4.96 (1H, t, J=8.0 Hz), 4.04 (1H, dd, J=16.0, 8.1 Hz), 3.7 (1H, s), 3.37 (1H, t, J=12.1 Hz), 3.04 (1H, d, J=8.0 Hz), 2.95 (m), 2.77 (m), 2.61 (m), 2.43 (m), 2.24 (2H, s), 2.26 (m), 2.03 (m), 1.96 (m), 1.74 (m), 1.02 (9H, s); ^{13}C-NMR (CDCl$_3$) δ 175.89, 166.03, 143.51, 142.09, 142.01, 138.60, 135.78, 134.48, 133.85, 133.42, 130.20, 128.08, 125.35, 122.38, 122.12, 114.63, 112.93, 77.85, 71.70, 70.50, 57.09, 53.49, 49.32, 47.07, 44.82, 39.3, 33.62,

31.65, 29.69, 28.80, 24.99, 24.58, 24.32, 20.73; HRESIMS *m/z* calcd for $C_{42}H_{56}N_5O_2$ (M+H)$^+$ 662.4425, found 662.4451.

6-Cyclohexamidomanzamine A (14): (20 mg, 17%); $[\alpha]_D^{25}$ 18.5 (*c* 0.13, MeOH); ^{1}H-NMR (*d6*-acetone) δ 11.33 (1H, s), 9.02 (1H, s), 8.53 (1H, s), 8.22 (1H, d, *J*=7.6 Hz), 7.76 (1H, d, *J* =7.5 Hz), 7.56 (1H, d, *J*=7.6 Hz), 7.46 (1H, d, *J*=7.6 Hz), 6.68 (1H, s), 6.08 (1H, m), 5.51 (1H, m), 5.42 (1H, t, *J*=4.0 Hz), 4.77 (1H, t, *J*=8.0 Hz), 3.84 (1H, dd, *J*=16.0, 8.1 Hz), 3.66 (1H, s), 3.26 (1H, t, *J*=12.0 Hz), 2.91 (1H, d, *J*=8.1 Hz), 2.78 (m), 2.77 (m), 2.61 (m), 2.43 (m), 2.31 (m), 2.26 (m), 2.03 (m), 1.96 (m), 1.74 (m), 1.48 (m); ^{13}C-NMR (*d6*-acetone) δ 175.04, 166.03, 143.57, 142.05, 141.99, 138.60, 135.78, 134.48, 133.85, 133.42, 130.20, 128.08, 125.35, 122.38, 122.12, 114.63, 112.93, 77.85, 71.70, 70.50, 57.09, 53.49, 49.32, 47.07, 44.82, 39.16, 33.62, 28.45, 26.52, 26.36, 24.99, 24.58, 24.32, 23.97, 20.73; HRESIMS *m/z* calcd for $C_{43}H_{56}N_5O_2$ (M+H)$^+$ 674.4434, found 674.4464.

8-Acetamidomanzamine A (15): (14 mg, 13%); $[\alpha]_D^{25}$ 16.2 (*c* 0.15, MeOH); UV λ_{max} (MeOH) 260, 310, 375 nm; IR neat: 3232, 2935, 2580, 1703, 1665, 1538, 1470, 1437, 1365, 1290, 1178, 1130, 1018 cm^{-1}; ^{1}H-NMR (CDCl$_3$) δ 11.37 (1H, s), 8.52 (1H, d, *J*=8.0 Hz), 8.33 (1H, d, *J*=7.6 Hz), 7.82 (1H, d, *J*=7.5 Hz), 7.79 (1H, d, *J*=7.6 Hz), 7.23 (1H, d, *J*=7.6 Hz), 6.64 (1H, s), 6.28 (1H, m), 5.57 (1H, m), 5.42 (1H, t, *J*=4.0 Hz), 4.96 (1H, t, *J*=8.0), 4.04 (1H, dd, *J*=16.0, 8.1 Hz) 3.7 (1H, s), 3.37 (1H, t, *J*=12.1 Hz), 3.04 (1H, d, *J*=8.0 Hz), 2.95 (m), 2.77 (m), 2.61 (m), 2.43 (m), 2.31 (m), 2.26 (m) 2.08 (3H, s), 2.03 (m), 1.96 (m), 1.74 (m), 1.48 (m); ^{13}C-NMR (CDCl$_3$) δ 174.04, 166.01, 143.27, 141.95, 141.80, 138.64, 136.00, 134.49, 133.85, 133.42, 130.20, 128.08, 125.35, 122.38, 122.12, 114.63, 112.93, 77.85, 71.70, 70.50, 57.09, 53.49, 49.32, 47.07, 44.82, 31.21, 39.16, 33.62, 28.45, 26.52, 26.36, 24.99, 24.58, 24.32, 23.97, 20.73; HRESIMS *m/z* calcd for $C_{38}H_{49}N_5O_2$ (M+H)$^+$ 606.3843, found 606.3811.

8-*n*-Propamidomanzamine A (16): (15 mg, 14%); $[\alpha]_D^{25}$ 6.1 (*c* 0.09, MeOH);); ^{1}H-NMR (CDCl$_3$) δ 11.38 (1H, s), 8.51 (1H, d, *J*=8.0 Hz), 8.36 (1H, d, *J*=7.6 Hz), 7.80 (1H, d, *J*=7.5 Hz), 7.78 (1H, d, *J*=7.6 Hz), 7.26 (1H, d, *J*=7.6 Hz), 6.68 (1H, s), 6.29 (1H, m), 5.56 (1H, m), 5.43 (1H, t, *J*=4.0 Hz), 4.96 (1H, t, *J*=8.1 Hz), 4.04 (1H, dd, *J*=16.1, 8.0 Hz) 3.69 (1H, s), 3.37 (1H, t, *J*=12.0 Hz), 3.04 (1H, d, *J*=8.0 Hz), 2.95 (m), 2.77 (m), 2.61 (m), 2.43 (m), 2.41 (2H, q, *J*=7.0 Hz), 2.31 (m), 2.26 (m), 2.03 (m), 1.96 (m), 1.74 (m), 1.48 (m), 1.14 (3H, t, *J*=7.1 Hz); ^{13}C-NMR (CDCl$_3$) δ 174.84, 166.09, 143.51, 142.25, 142.12, 138.62, 135.78, 134.48, 133.85, 133.42, 130.20, 128.08, 125.35, 122.38, 122.12, 114.63, 112.93, 77.85, 71.70, 70.50, 57.09, 53.49, 49.32, 47.07, 44.82, 31.21, 39.16, 33.62, 30.36, 28.45, 26.52, 26.36, 24.99, 24.58, 24.32, 20.78, 10.01; HRESIMS *m/z* calcd for C$_{39}$H$_{50}$N$_5$O$_2$ (M+H)$^+$ 620.3936, found 620.3981.

8-*n*-Butamidomanzamine A (17): (16 mg, 14%); $[\alpha]_D^{25}$ 13.2 (*c* 0.12, MeOH); ^{1}H-NMR (CDCl$_3$) δ 11.25 (1H, s), 8.70 (1H, s), 8.51 (1H, d, *J*=8.2 Hz), 8.36 (1H, d, *J*=7.6 Hz), 7.80 (1H, d, *J*=7.5 Hz), 7.78 (1H, d, *J*=7.6 Hz), 7.26 (1H, d, *J*=7.6 Hz), 6.62 (1H, s), 6.25 (1H, m), 5.54 (1H, m), 5.39 (1H, t, *J*=4.0 Hz), 4.92 (1H, t, *J*=8.0 Hz), 4.00 (1H, dd, *J*=16.1, 8.0 Hz), 3.66 (1H, s), 3.37 (1H, t, *J*=12.0 Hz), 3.04 (1H, d, *J*=8.1 Hz), 2.95 (m), 2.77 (m), 2.61 (m), 2.43 (m), 2.37 (2H, t, *J*=7.2 Hz), 2.31 (m), 2.26 (m), 2.03 (m), 1.96 (m), 1.74 (m), 1.48 (m), 1.00 (3H, t, *J*=7.2 Hz); ^{13}C-NMR (CDCl$_3$) δ 173.41, 143.82, 142.97, 141.90, 138.48, 135.17, 133.45, 133.29, 132.45, 130.42, 130.01, 127.30, 125.15, 123.99, 122.87, 120.67, 116.50, 114.32, 78.41, 71.70, 70.74, 63.42, 57.67, 53.88, 49.65, 47.45, 45.03, 41.44, 39.48, 34.05, 32.26, 30.36, 27.41, 26.36, 24.99, 24.58, 24.32, 20.73, 19.76, 14.42; HRESIMS *m/z* calcd for C$_{40}$H$_{52}$N$_5$O$_2$ (M+H)$^+$ 634.4011, found 634.4101.

8-Isobutamidomanzamine A (18): (16 mg, 14%); $[\alpha]_D^{25}$ 14.2 (*c* 0.10, MeOH); ^{1}H-NMR (*d6*-acetone) δ 11.41 (1H, s), 8.50 (1H, d, *J*=8.0), 8.32 (1H, d, *J*=8.1), 7.78 (1H, d, *J*=7.9), 7.77 (1H,

d, J=7.8 Hz), 7.29 (1H, d, J=7.6 Hz), 6.67 (1H, s), 6.30 (1H, m), 5.57 (1H, m), 5.42 (1H, t, J=4.2 Hz), 4.96 (1H, t, J=8.1 Hz), 4.04 (1H, dd, J=16.0, 8.1 Hz), 3.7 (1H, s), 3.37 (1H, t, J=12.1 Hz), 3.04 (1H, d, J=8.0 Hz), 2.95 (m), 2.77 (m), 2.61 (m), 2.43 (m), 2.63 (m), 2.31 (m), 2.26 (m), 2.03 (m), 1.96 (m), 1.74 (m), 1.48 (m), 1.29 (6H, d, J=7.2 Hz); ^{13}C-NMR (*d6*-acetone) δ 172.35, 143.57, 142.57, 142.14, 138.19, 135.87, 133.91, 133.78, 133.04, 129.86, 128.13, 126.75, 123.60, 120.36, 116.20, 114.02, 77.97, 71.70, 70.33, 57.35, 53.50, 49.25, 47.07, 44.63, 40.9, 39.16, 35.64, 33.75, 29.68, 28.36, 25.00, 24.34, 20.74, 20.06, 19.86; HRESIMS *m/z* calcd for $C_{40}H_{52}N_5O_2$ (M+H)$^+$ 634.4011, found 634.4095.

8-*n*-Pentamidomanzamine A (19): (17 mg,15%); $[\alpha]_D^{25}$ 17.2 (*c* 0.16, MeOH); ^{1}H-NMR (CDCl$_3$) δ 11.29 (1H, s), 8.51 (1H, d, J=8.0 Hz), 8.34 (1H, d, J=8.2 Hz), 7.80 (1H, d, J=7.9 Hz), 7.77 (1H, d, J=7.8 Hz), 7.24 (1H, d, J=7.6 Hz), 6.54 (1H, s), 6.28 (1H, m), 5.57 (1H, m), 5.42 (1H, t, J=4.1 Hz), 4.96 (1H, t, J=8.0 Hz), 4.04 (1H, dd, J=16.1, 8.0 Hz), 3.7 (1H, s), 3.37 (1H, t, J=12.0 Hz), 3.04 (1H, d, J=8.1 Hz), 2.95 (m), 2.77 (m), 2.61 (m), 2.43 (m), 2.39 (2H, t, J=7.1 Hz), 2.31 (m), 2.26 (m), 2.03 (m), 1.96 (m), 1.74 (m), 1.48 (m), 0.99 (3H, t, J=7.2); ^{13}C-NMR (CDCl$_3$) δ 172.97, 143.57, 142.60, 141.99, 138.18, 135.78, 134.88, 133.85, 133.42, 130.02, 127.22, 125.35, 123.63, 119.65, 116.18, 114.01, 78.07, 71.70, 70.40, 57.33, 53.53, 49.30, 47.07, 44.72, 41.08, 39.08, 37.07, 33.72, 31.91, 30.36, 29.68, 26.51, 26.36, 25.01, 24.59, 24.34, 22.67, 22.48, 20.75, 13.97; HRESIMS *m/z* calcd for $C_{41}H_{54}N_5O_2$ (M+H)$^+$ 648.4277, found 648.4281.

8-Pivalamidomanzamine A (20): (15 mg, 12%); $[\alpha]_D^{25}$ 17.2 (*c* 0.11, MeOH); ^{1}H-NMR (CDCl$_3$) δ 11.40 (1H, s), 8.40 (1H, d, J=8.1 Hz), 8.38 (1H, d, J=8.0 Hz), 7.84 (1H, d, J=7.9 Hz), 7.82 (1H, d, J=7.8 Hz), 7.24 (1H, d, J=7.6 Hz), 6.78 (1H, s), 6.26 (1H, m), 5.58 (1H, m), 5.36 (1H, t, J=4.0 Hz), 4.85 (1H, t, J=8.1 Hz), 4.04 (1H, dd, J=16.0, 8.1 Hz), 3.67 (1H, s), 3.21 (1H, t, J=12.1 Hz), 3.04 (1H, d, J=8.1 Hz), 2.95 (m), 2.77 (m), 2.61 (m), 2.43 (m), 2.31 (m), 2.26 (m), 2.03 (m), 1.96

(m), 1.74 (m), 1.49 (9H, s), 1.48 (m); ^{13}C-NMR (CDCl$_3$) δ 175.04, 166.03, 143.57, 142.05, 141.99, 138.27, 135.04, 134.48, 133.85, 133.86, 131.87, 127.11, 125.35, 123.99, 121.91, 116.86, 113.96, 77.23, 71.70, 70.52, 58.36, 57.11, 53.56, 49.37, 47.07, 44.59, 39.29, 38.74, 33.77, 32.76, 29.69, 28.45, 26.71, 26.36, 25.61, 24.58, 24.44, 22.68, 20.80, 14.03; HRESIMS m/z calcd for C$_{41}$H$_{54}$N$_5$O$_2$ (M+H)$^+$ 648.4277, found 648.4268.

8-n-Hexamidomanzamine A (21): (16 mg, 14%); $[\alpha]_D^{25}$ 21.1 (c 0.11, MeOH); ^{1}H-NMR ($d6$-acetone) δ 11.22 (1H, s), 8.72 (1H, d, J=8.0 Hz), 8.45 (1H, d, J=8.0 Hz), 7.99 (1H, d, J=7.9 Hz), 7.91 (1H, d, J=7.8 Hz), 7.27 (1H, d, J=7.6 Hz), 6.78 (1H, s), 6.12 (1H, m), 5.53 (1H, m), 5.16 (1H, t, J=4.0 Hz), 4.88 (1H, t, J=8.1 Hz), 4.04 (1H, dd, J=16.1, 8.0 Hz) 3.79 (1H, s), 3.41 (1H, t, J=12.0 Hz), 2.94 (1H, d, J=8.0 Hz), 2.95 (m), 2.77 (m), 2.61 (m), 2.43 (m), 2.56 (2H, t, J=7.4 Hz), 2.31 (m), 2.26 (m), 2.03 (m), 1.96 (m), 1.74 (m), 1.48 (m), 0.94 (3H, t, J=7.1 Hz); ^{13}C-NMR ($d6$-acetone) δ 173.50, 164.75, 142.69, 142.28, 142.10, 139.23, 133.93, 132.38, 130.65, 126.01, 124.70, 123.46, 119.50, 117.24, 114.89, 77.47, 71.57, 70.07, 58.06, 53.77, 53.38, 49.61, 47.18, 44.99, 40.87, 40.26, 37.56, 34.60, 30.11, 29.73, 29.53, 28.73, 27.12, 26.78, 26.40, 25.54, 24.90, 23.05, 21.34, 14.22; HRESIMS m/z calcd for C$_{42}$H$_{56}$N$_5$O$_2$ (M+H)$^+$ 662.4488, found 662.4521.

8-n-Octamidomanzamine A (22): (18 mg, 15%); $[\alpha]_D^{25}$ 19.9 (c 0.11, MeOH); ^{1}H-NMR (CDCl$_3$) δ 11.32 (1H, s), 8.61 (1H, d, J=8.1 Hz), 8.52 (1H, d, J=8.0 Hz), 7.87 (1H, d, J=7.9 Hz), 7.84 (1H, d, J=7.8 Hz), 7.23 (1H, d, J=7.6 Hz), 6.69 (1H, s), 6.28 (1H, m), 5.57 (1H, m), 5.42 (1H, t, J=4.0 Hz), 4.96 (1H, t, J=8.1 Hz), 4.04 (1H, dd, J=16.1, 8.0 Hz), 3.7 (1H, s), 3.37 (1H, t, J=12.1 Hz), 3.04 (1H, d, J=8.0 Hz), 2.95 (m), 2.77 (m), 2.61 (m), 2.43 (m), 2.46 (2H, t, J=7.1 Hz), 2.31 (m), 2.26 (m), 2.03 (m), 1.96 (m), 1.74 (m), 1.48 (m), 0.90 (3H, t, J=7.1 Hz); ^{13}C-NMR (CDCl$_3$) δ 173.54, 164.54, 142.87, 142.25, 142.04, 138.60, 136.12, 134.48, 133.85, 133.42, 130.20, 128.08, 125.35, 122.38, 122.12, 116.26, 114.33, 77.85, 71.70, 70.50, 57.09, 53.49, 49.32, 47.07, 44.82,

38.60, 37.47, 31.61, 29.68, 28.17, 26.78, 26.40, 25.54 25.28, 24.94, 22.45, 21.34, 14.51 ;

HRESIMS m/z calcd for $C_{44}H_{60}N_5O_2$ (M+H)$^+$ 690.4732, found 690.4772.

8-(*t*-Butyl)-acetamidomanzamine A (23): (16 mg, 14%); $[\alpha]_D^{25}$ 25.7 (*c* 0.12, MeOH ^{1}H-NMR

(CDCl$_3$) δ 11.32 (1H, s), 8.63 (1H, d, *J*=8.0 Hz), 8.51 (1H, d, *J*=8.1 Hz), 7.88 (1H, d, *J*=7.9 Hz),

7.86 (1H, d, *J*=7.8 Hz), 7.27 (1H, d, *J*=7.6 Hz), 6.71 (1H, s), 6.28 (1H, m), 5.57 (1H, m), 5.42

(1H, t, *J*=4.0 Hz), 4.96 (1H, t, *J*=8.1 Hz), 4.04 (1H, dd, *J*=16.0, 8.1 Hz), 3.7 (1H, s), 3.37 (1H, t,

J=12 Hz).1, 3.04 (d, *J*=8 Hz), 2.95 (m), 2.77 (m), 2.61 (m), 2.43 (m), 2.24 (2H, s), 2.26 (m), 2.03

(m), 1.96 (m), 1.74 (m), 1.02 (9H, s); ^{13}C-NMR (CDCl$_3$) δ 174.15, 164.43, 143.59, 142.41,

142.01, 138.27, 135.04, 134.48, 133.85, 132.86, 131.87, 127.11, 123.99, 122.38, 121.91, 116.86,

113.96, 77.23, 70.52, 58.35, 57.11, 53.56, 52.92, 49.37, 45.52, 44.59, 39.29, 33.77, 32.76, 29.69,

27.86, 26.71, 26.48, 25.10, 24.72, 24.44, 22.68, 20.80; HRESIMS m/z calcd for $C_{42}H_{56}N_5O_2$

(M+H)$^+$ 662.4425, found 662.4478.
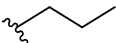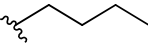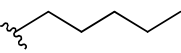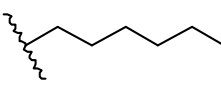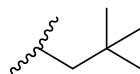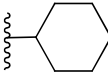
8-Cyclohexamidomanzamine A (24): (19 mg, 16%); $[\alpha]_D^{25}$ 19.5 (*c* 0.17, MeOH); ^{1}H-NMR

(CDCl$_3$) δ 11.30 (s), 9.52 (s), 8.49 (1H, d, *J*=8.0 Hz), 8.33 (1H, d, *J*=8.1 Hz), 7.79 (1H, d, *J*=7.9

Hz), 7.76 (1H, d, *J*=7.8 Hz), 7.20 (1H, d, *J*=7.6 Hz), 6.55 (s), 6.28 (m), 5.55 (m), 5.39 (1H, t,

J=4.0 Hz), 4.90 (1H, t, *J*=8.0 Hz), 4.02 (1H, dd, *J*=16.1, 8.0 Hz), 3.72 (s), 3.26 (1H, t, *J*=12.0

Hz), 2.91 (1H, d, *J*=8.0 Hz), 2.78 (m), 2.77 (m), 2.61 (m), 2.43 (m), 2.31 (m), 2.26 (m), 2.03 (m),

1.96 (m), 1.74 (m), 1.48 (m); ^{13}C-NMR (CDCl$_3$) δ 174.12, 164.03, 143.57, 142.52, 141.99,

138.13, 134.92, 134.48, 133.85, 133.00, 130.86, 128.78, 126.79, 123.64, 120.29, 119.60, 116.05,

113.97, 77.96, 77.23, 71.70, 70.48, 58.32, 57.34, 53.54, 53.39, 49.31, 45.70, 44.78, 40.98, 39.11,

33.73, 31.90, 29.81, 29.75, 29.67, 29.33, 28.48, 26.48, 26.41, 25.68, 25.64, 25.00, 24.59, 24.28,

22.66, 20.75; HRESIMS m/z calcd for $C_{43}H_{56}N_5O_2$ (M+H)$^+$ 674.4434, found 674.4432.

In vitro antimalarial and antimicrobial activities: The detailed materials and methods used for in vito antimalarial and in vitro antimicrobial assays were reported elsewhere.[58]

In vivo antimalarial activity:

In vivo antimalarial activity of compounds was determined in mice infected with *Plasmodium berghei* (NK-65 strain). Male mice (Swiss Webster strain) weighing 18-20 g were intraperitoneally inoculated with 2×10^7 parasitized red blood cells obtained from a highly infected donor mouse. Mice were divided into different groups with 5 mice in each group. Test compounds were prepared in DMSO: 0.1N HCl: Tween-80: PEG-400: water (5:1:0.5:40:53.50) and administered orally to the mice about 2 h after the infection (Day 0). The compounds were tested at three doses of 3.3, 10 and 30 mg/kg body weight. The test compounds were administered to the mice once a day for 3 consecutive days (Days 0-3). A control group was treated with equal volume of vehicle and another control group was treated with chloroquine (10 mg/kg). The mice were closely observed after every dose for any apparent signs of toxicity. Blood smears were prepared on different days (till day 28 post infection) by clipping the tail end, stained with Giemsa and observed under microscope for determination of the parasitemia. Suppression in development of parasitemia was monitored on day 5 and day 7 post infection. Mice without parasitemia until day 28 post infection were considered as cured. Treatment of mice with three doses of chloroquine caused 100% suppression of the parasitemia.

Table II.5. The synthesized manzamine A amides.

Compound	R	Entry	Yield %
6-Acetamidomanzamine A 8-Acetamidomanzamine A	CH_3	**5** **15**	14 13
6-*n*-Propamidomanzamine A 8-*n*-Propamidomanzamine A		**6** **16**	14 14
6-*n*-Butamidomanzamine A 8-*n*-Butamidomanzamine A		**7** **17**	14 14
6-Isobutamidomanzamine A 8-Isobutamidomanzamine A		**8** **18**	12 14
6-*n*-Pentamidomanzamine A 8-*n*-Pentamidomanzamine A		**9** **19**	13 15
6-Pivalamidomanzamine A 8-Pivalamidomanzamine A		**10** **20**	12 12
6-*n*-Hexamidomanzamine A 8-*n*-Hexamidomanzamine A		**11** **21**	14 14
6-*n*-Octamidomanzamine A 8-*n*-Octamidomanzmaine A		**12** **22**	12 15
6-(*t*-Butyl)-acetamidomanzamine A 8-(*t*-Butyl)-acetamidomanzamine A		**13** **23**	15 14
6-Cyclohexamidomanzamine A 8-Cyclohexamidomanzamine A		**14** **24**	17 16

Table II.6. In vitro antimalarial activity of manzamine amides against chloroquine sensitive (D6, Sierra Leone) and resistant (W2, IndoChina) strains of *Plasmodium falciparum*

Compound	Entry	*P. falciparum* (D6 Clone) IC$_{50}$ (nM)	*P. falciparum* (W2 Clone) IC$_{50}$ (nM)	Cytotoxicity (Vero) IC$_{50}$ (nM)
6-Acetamidomanzamine A	**5**	1288	1982	NC
8-Acetamidomanzamine A	**15**	182	231	NC
6-*n*-Propamidomanzamine A	**6**	1162	1937	NC
8-*n*-Propamidomanzamine A	**16**	123	87	NC
6-*n*-Butamidomanzamine A	**7**	1152	1894	NC
8-*n*-Butamidomanzamine A	**17**	35	121	NC
6-Isobutamidomanzamine A	**8**	1105	1547	NC
8-Isobutamidomanzamine A	**18**	158	205	NC
6-*n*-Pentamidomanzamine A	**9**	1235	1482	NC
8-*n*-Pentamidomanzamine A	**19**	53	49	NC
6-Pivalamidoanzamine A	**10**	231	417	NC
8-Pivalamidomanzamine A	**20**	170	232	NC
6-*n*-Hexamidomanzamine A	**11**	680	786	NC
8-*n*-Hexamidomanzamine A	**21**	32	65	NC
6-*n*-Octamidomanzamine A	**12**	696	754	NC
8-*n*-Octamidomanzamine A	**22**	55	43	NC
6-(*t*-Butyl)-acetamidomanzamine A	**13**	211	302	NC
8-(*t*-Butyl)-acetamidomanzamine A	**23**	139	127	NC
6-Cyclohexamidomanzamine A	**14**	34	53	NC
8-Cyclohexamidomanzamine A	**24**	950	995	NC

Manzamine A	**1**	8.0	11	365
8-Hydroxymanzamine A	**2**	11	14	
Chloroquine		50	484	-
Artemisinin		46	28	-

NC, no cytotoxicity up to 470 nM

Table II.7. In vitro antimicrobial data of manzamine amides (all values in μM)

Compound	Entry	IC$_{50}$/MIC			
		C. albicans	*C. neoformans*	*M. intracellulre*	*A. fumigatus*
6-Acetamidomanzamine A	**5**	-/-	-/-	9.91/16.51	-/-
8-Acetamidomanzamine A	**15**	-/-	33.35/-	1.65/2.06	-/-
6-*n*-Propamidomanzamine A	**6**	-/-	-/-	5.65/8.07	-/-
8-*n*-Propamidomanzamine A	**16**	>32.28/-	NT/NT	1.52/2.02	>32.28/-
6-*n*-Butamidomanzamine A	**7**	-/-	-/-	4.74/7.89	-/-
8-*n*-Butamidomanzamine A	**17**	-/-	23.68/-	0.87/1.97	-/-
6-Isobutamidomanzamine A	**8**	-/-	-/-	3.16/3.95	-/-
8-Isobutamidomanzamine A	**18**	-/-	3.16/-	1.03/1.97	-/-
6-*n*-Pentamidomanzamine A	**9**	-/-	-/-	2.32/3.86	-/-
8-*n*-Pentamidomanzamine A	**19**	-/-	4.63/-	0.70/0.97	-/-
6-Pivalamidomanzamine A	**10**	-/-	-/-	1.54/3.86	-/-
8-Pivalamidomanzamine A	**20**	-/-	-/-	0.54/0.97	-/-
6-*n*-Hexamidomanzamine A	**11**	-/-	-/-	15.12/30.22	-/-
8-*n*-Hexamidomanzamine A	**21**	-/-	3.78/-	0.03/0.47	-/-
6-*n*-Octamidomanzamine A	**12**	-/-	-/-	17.40/29.01	-/-
8-*n*-Octamidomanzamine A	**22**	-/-	1.01/29.01	0.51/1.81	-/-
6-(*t*-Butyl)-acetamidomanzamine A	**13**	-/-	-/-	1.36/1.89	-/-
8-(*t*-Butyl)-acetamidomanzamine A	**23**	-/-	14.36/-	1.51/3.78	-/-
6-Cyclohexamidomanzamine A	**14**	-/-	22.27/-	1.26/1.86	-/-

8-Cyclohexamidomanzamine A	**24**	-/-	-/-	11.14/14.85	-/-
Manzamine A	**1**	3.656	1.85	0.64	
8-Hydroxymanzamine A	**2**	6.20	3.55	0.177	
Amphotericin B		0.49/1.35	0.92/2.70		1.62/2.70
Ciprofloxacin				1.06	

IC_{50}, the concentration that affords 50% inhibition of growth; minimum inhibitory concentration (MIC) is the lowest test concentration that allows no detectable growth; Amphotericin B and ciprofloxacin are used as positive antifungal and antibacterial controls, respectively, "-" not active, "NT" not tested.

6-*n*-HexamidoMA (**11**)
^{1}H-NMR in CDCl$_3$
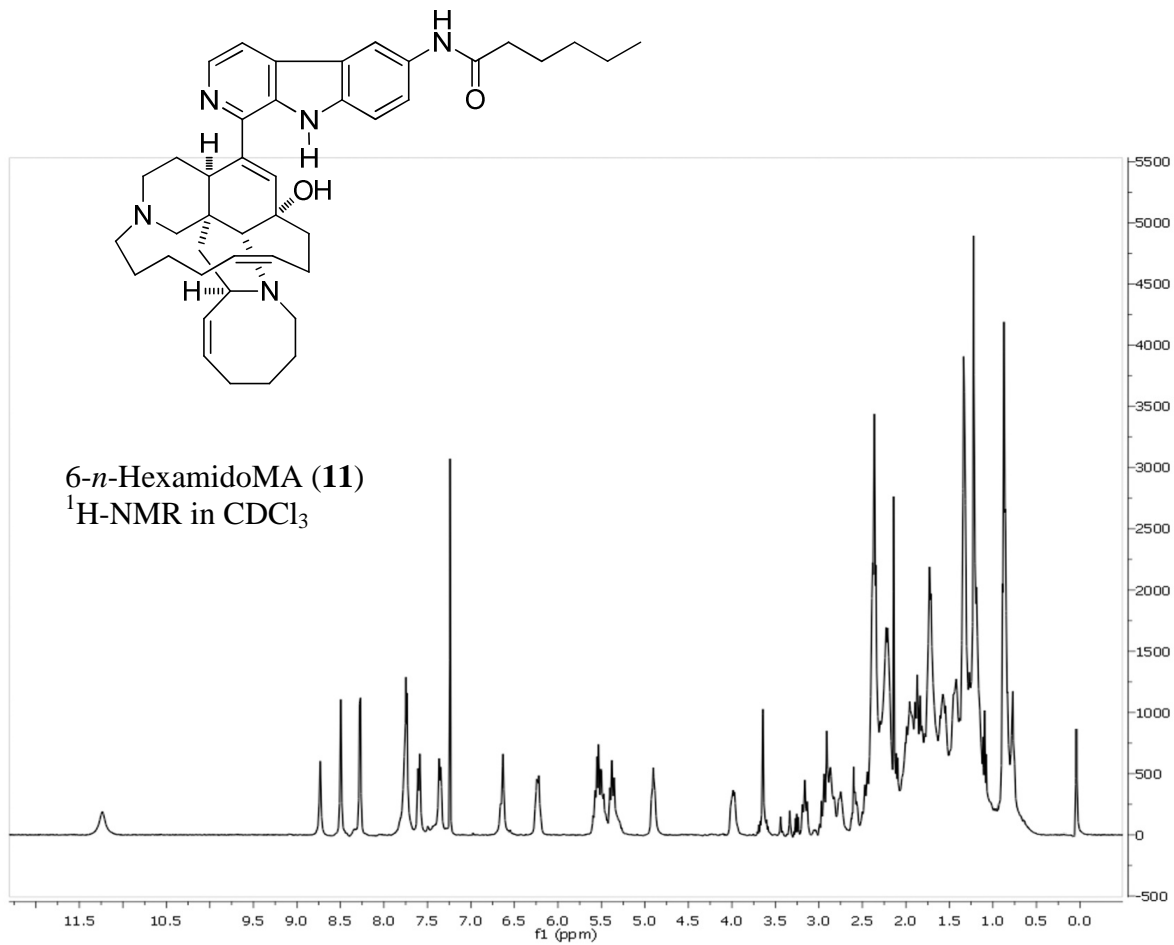
Figure II.25. ^{1}H-NMR spectra of 6-*n*-hexamidomanzamine A (**11**) in CDCl$_3$ at 400 MHz.

6-CyclohexamidoMA (**14**)
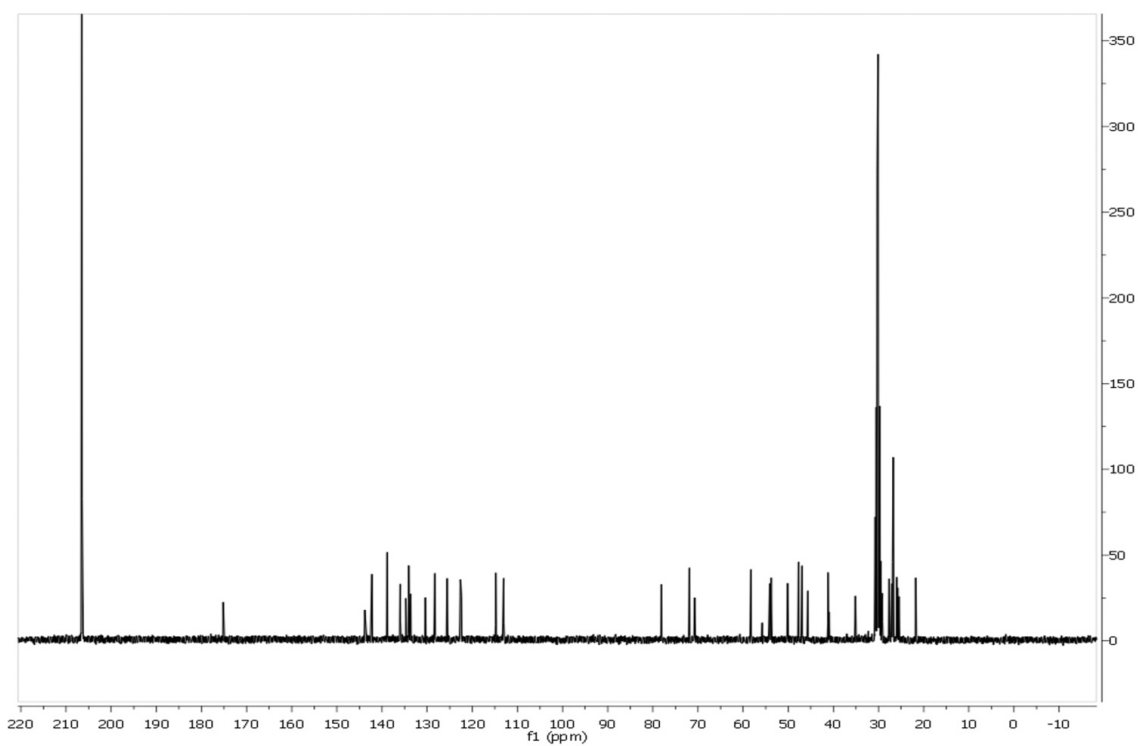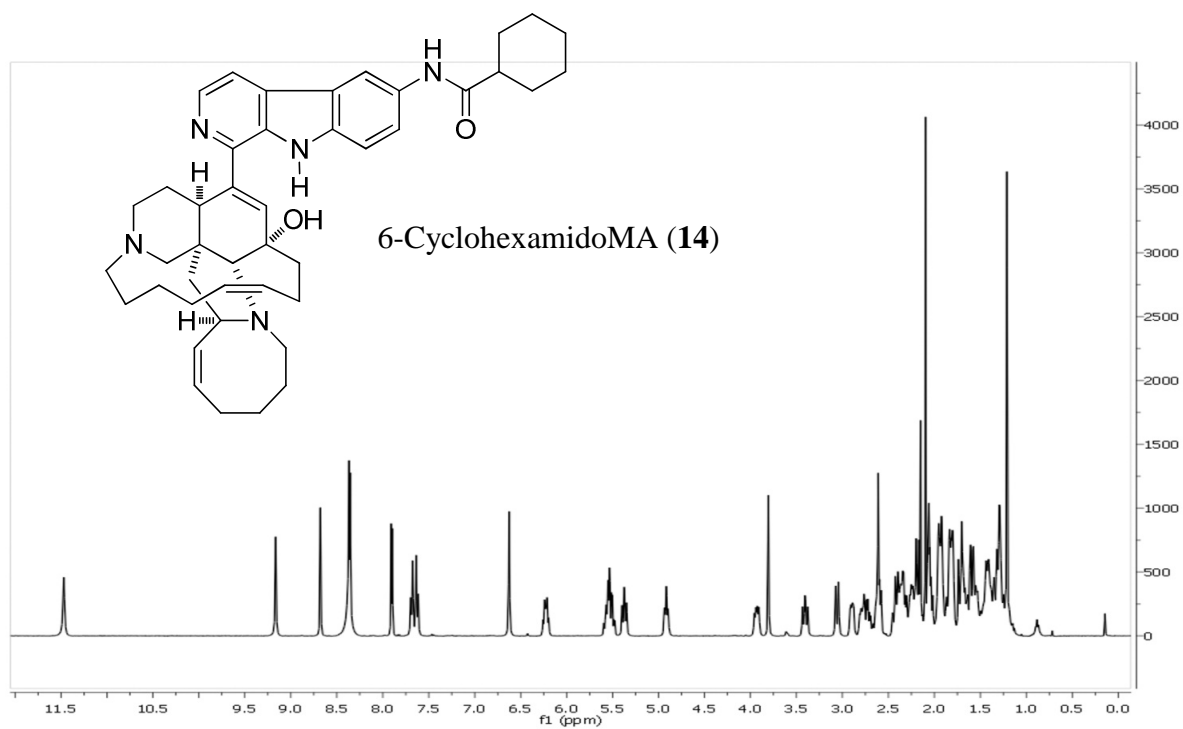
Figure II.26. ^{1}H- and ^{13}C-NMR spectra of 6-cyclohexamidomanzamine A (**14**) in *d6*-acetone at 400 and 100 MHz, respectively.
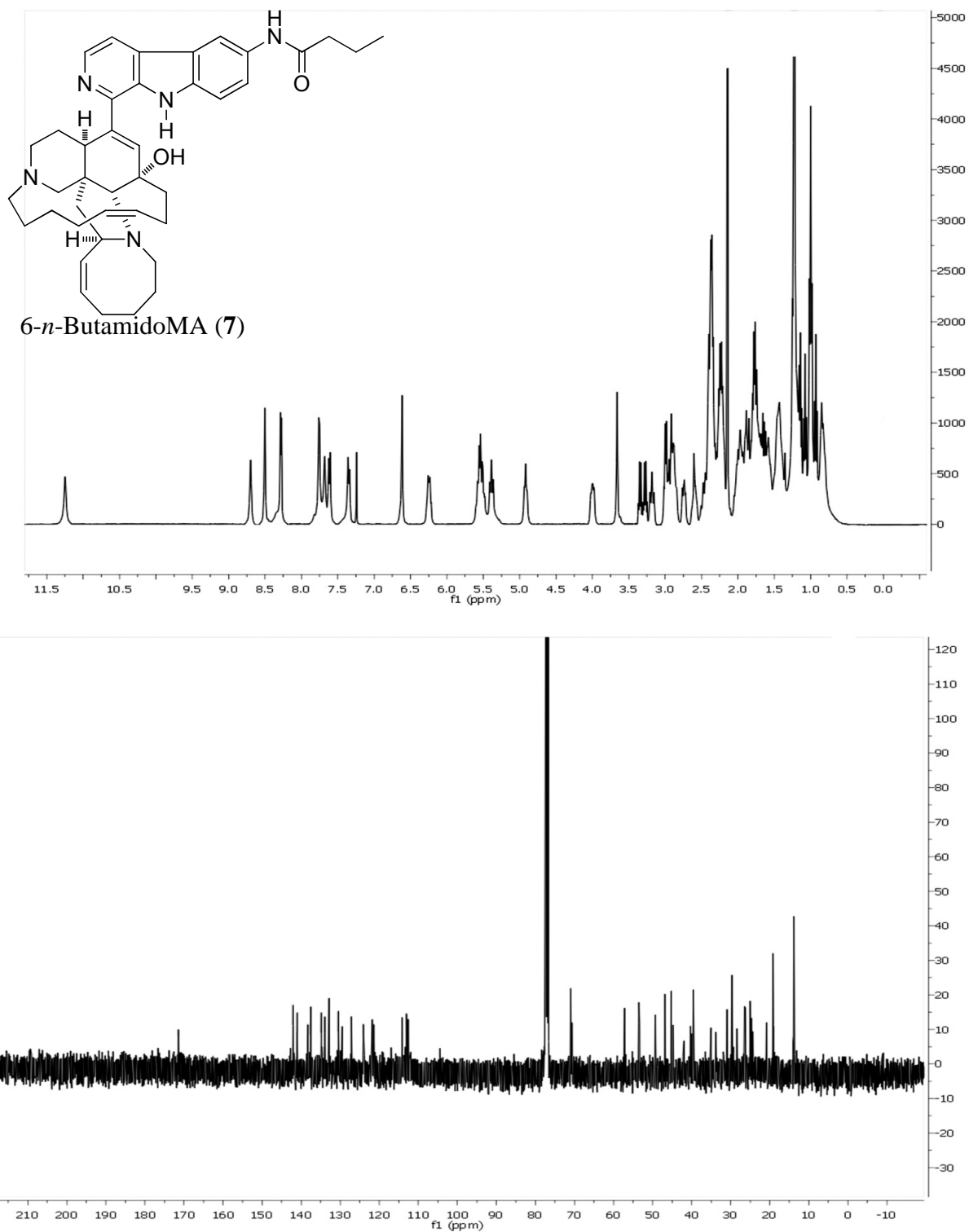
Figure II.27. ¹H- and ¹³C-NMR spectra of 6-*n*-butamidomanzamine A (**7**) in CDCl₃ at 400 and 100 MHz, respectively.

6-Isobutamide
Bruker AV400
Proton

6-IsobutamidoMA (**8**)
^{1}H-NMR in CDCl$_3$
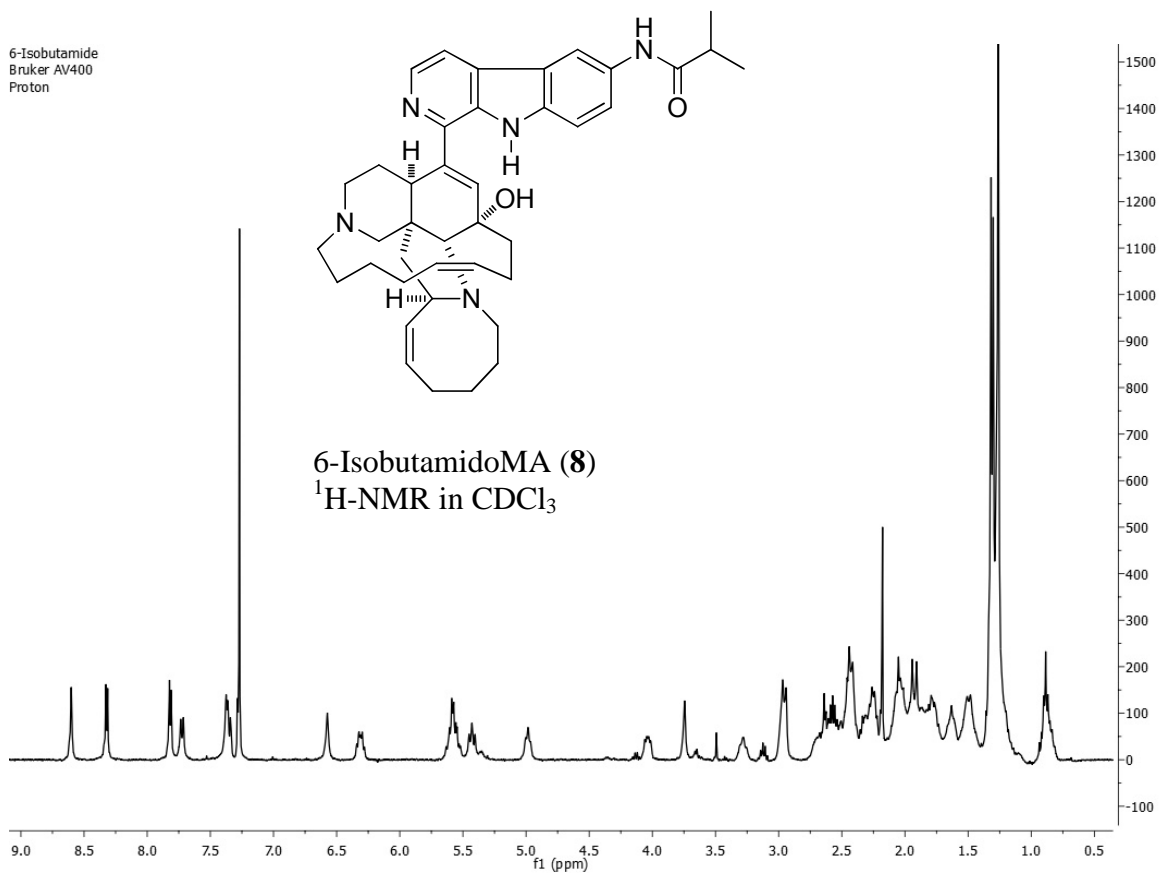
Figure II.28. ^{1}H-NMR spectra of 6-isobutamidomanzamine A (**8**) in CDCl$_3$ at 400 MHz.
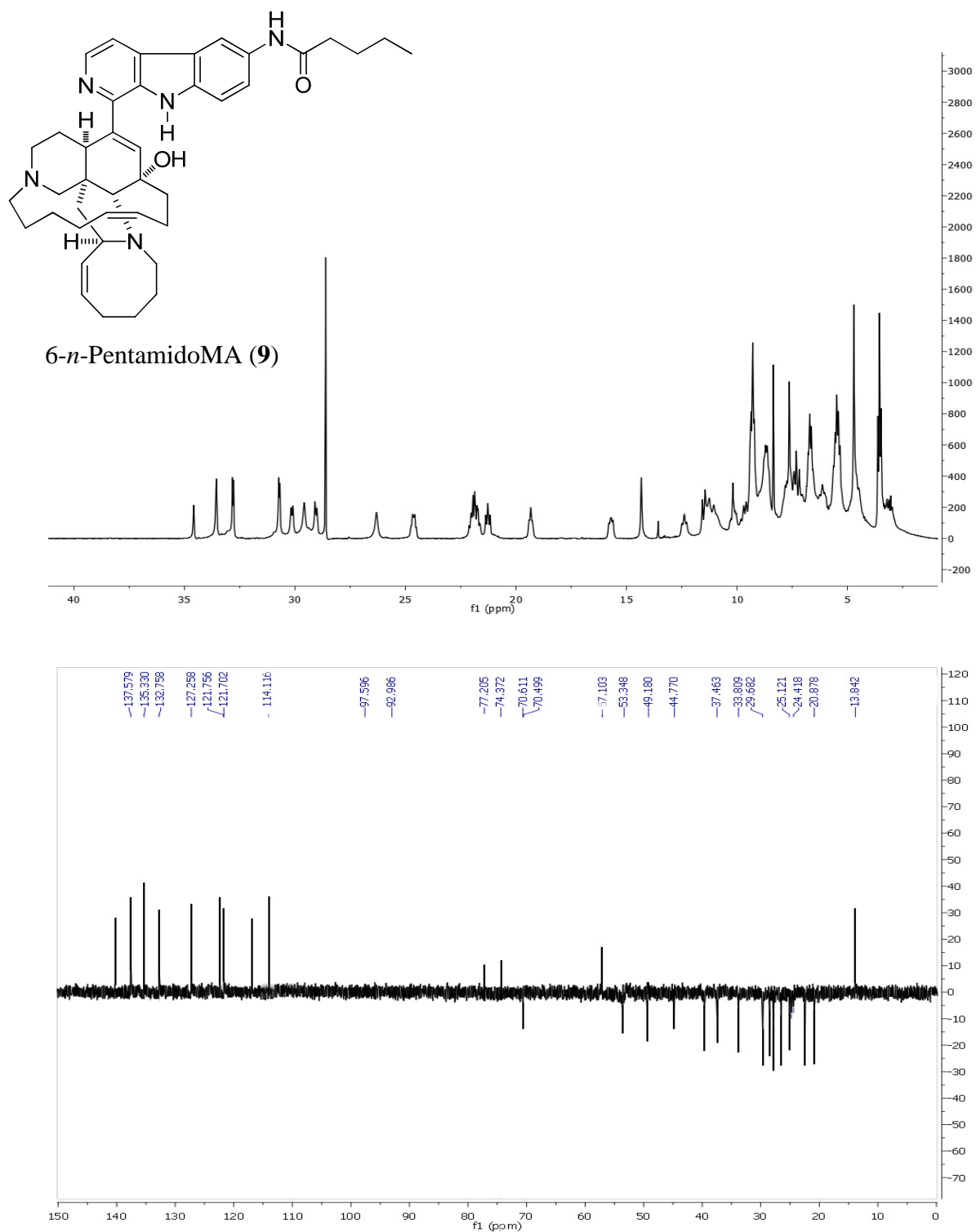
6-*n*-PentamidoMA (**9**)

Figure II.29. ^{1}H- and [135]DEPT-NMR spectra of 6-*n*-pentamidomanzamine A (**9**) in CDCl$_3$ at 400 and 100 MHz, respectively.

105
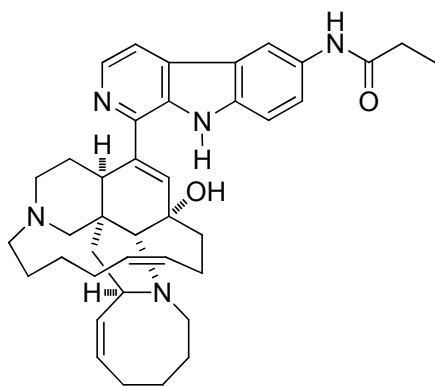
6-*n*-PropamidoMA (**6**)
^{1}H-NMR in CDCl$_3$
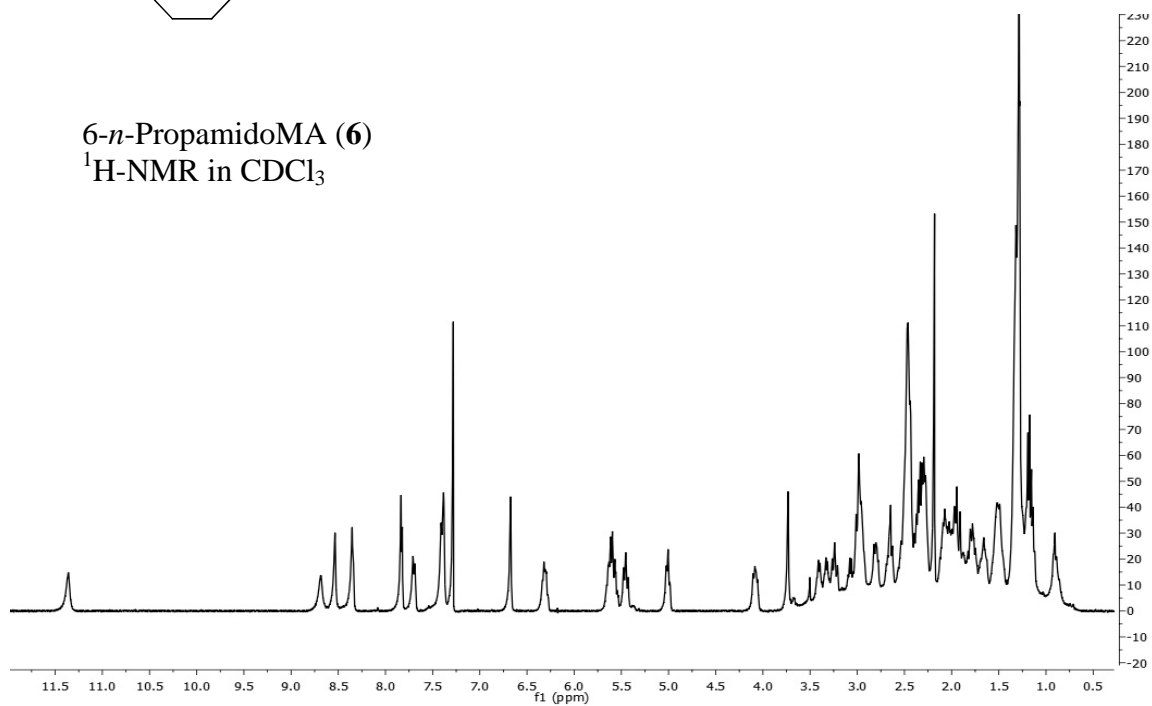
Figure II.30. ^{1}H-NMR spectra of 6-*n*-propamidomanzamine A (**6**) in CDCl$_3$ at 400 MHz.
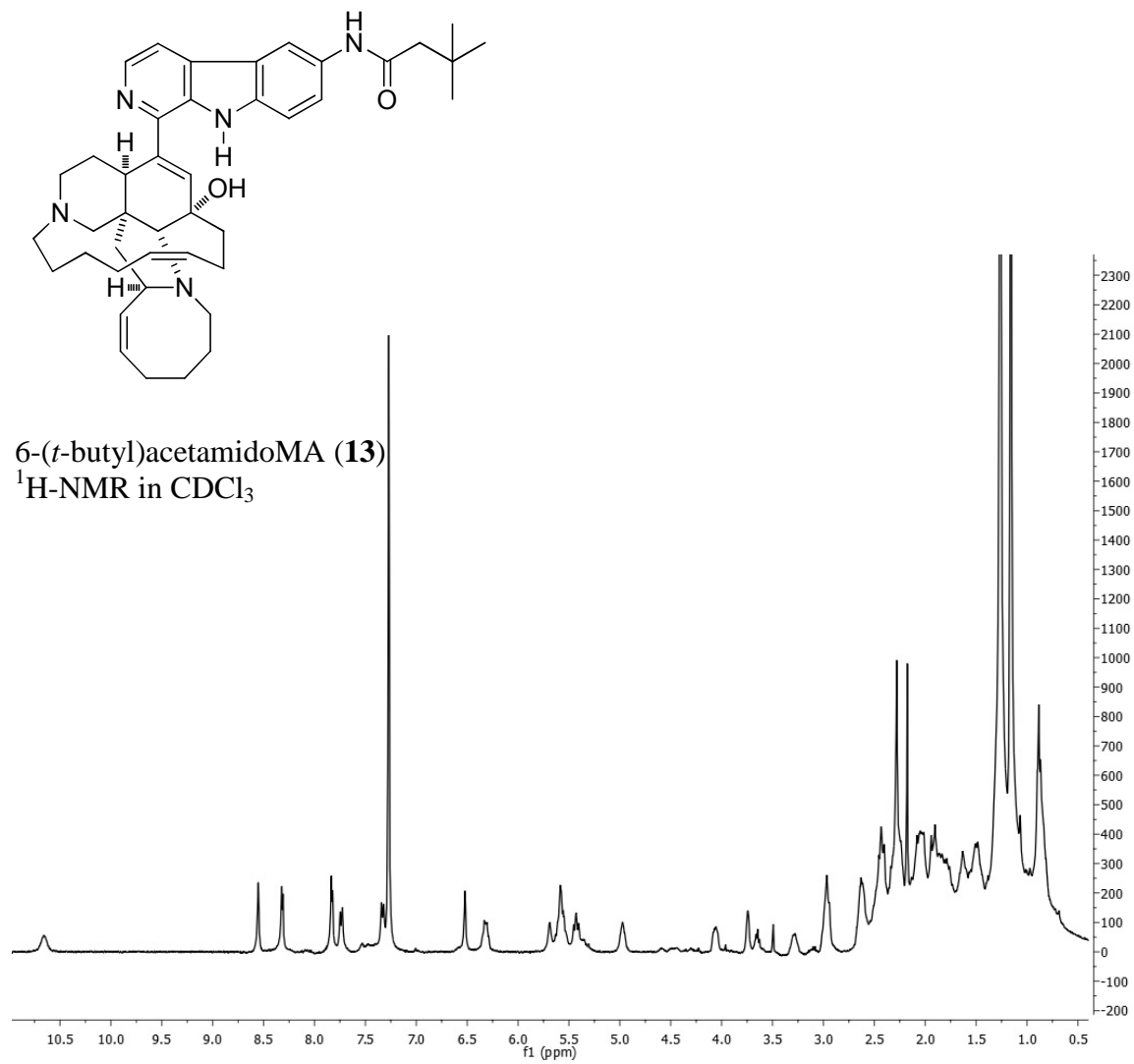
Figure II.31. ^{1}H-NMR spectra of 6-(*t*-butyl)acetamidomanzamine A (**13**) in CDCl₃ at 400 MHz.

8-CyclohexamidoMA (**24**)
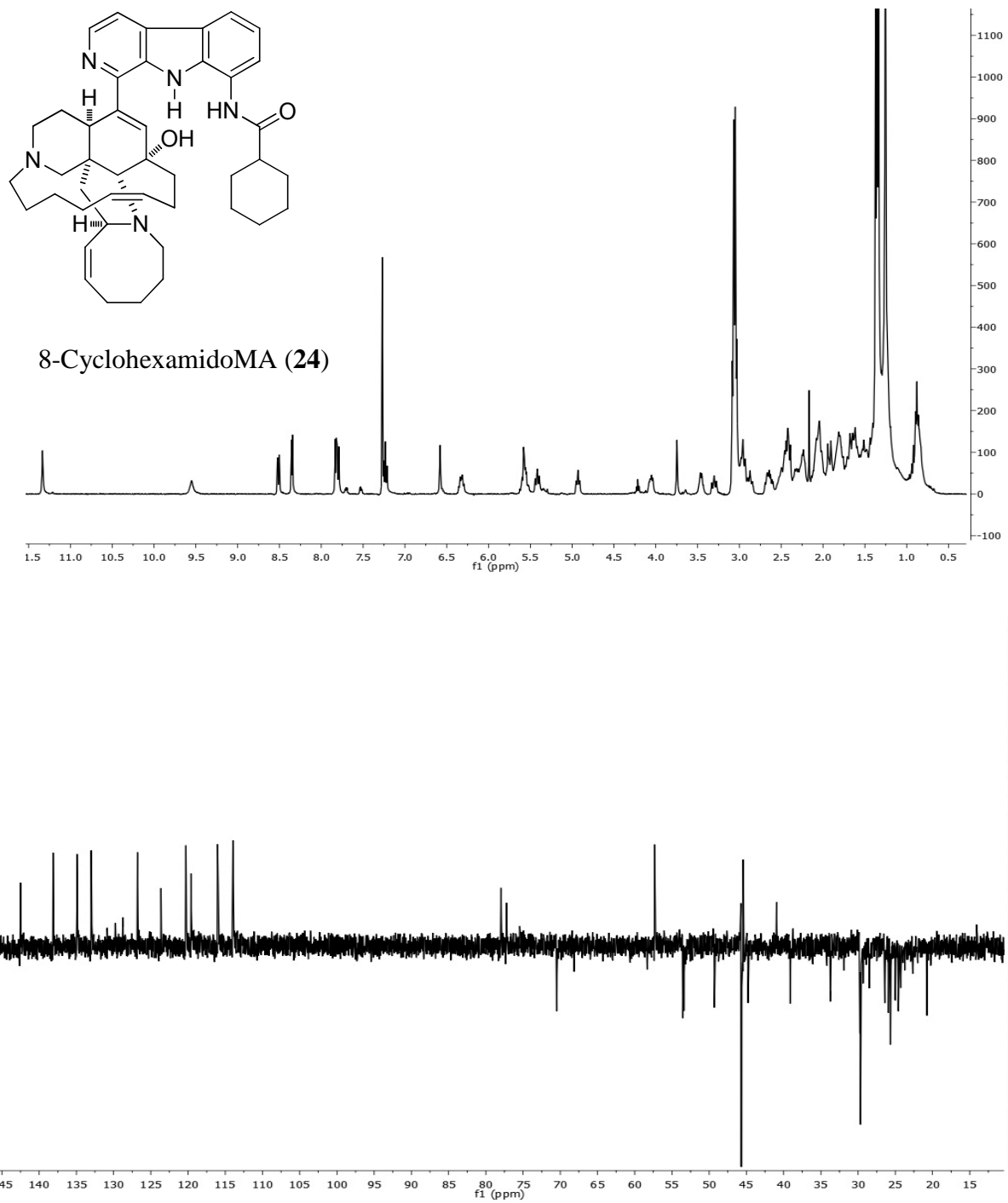
Figure II.32. ^{1}H- and [135]DEPT-NMR spectra of 8-cyclohexamidomanzamine A (**24**) in CDCl₃ at 400 and 100 MHz, respectively.
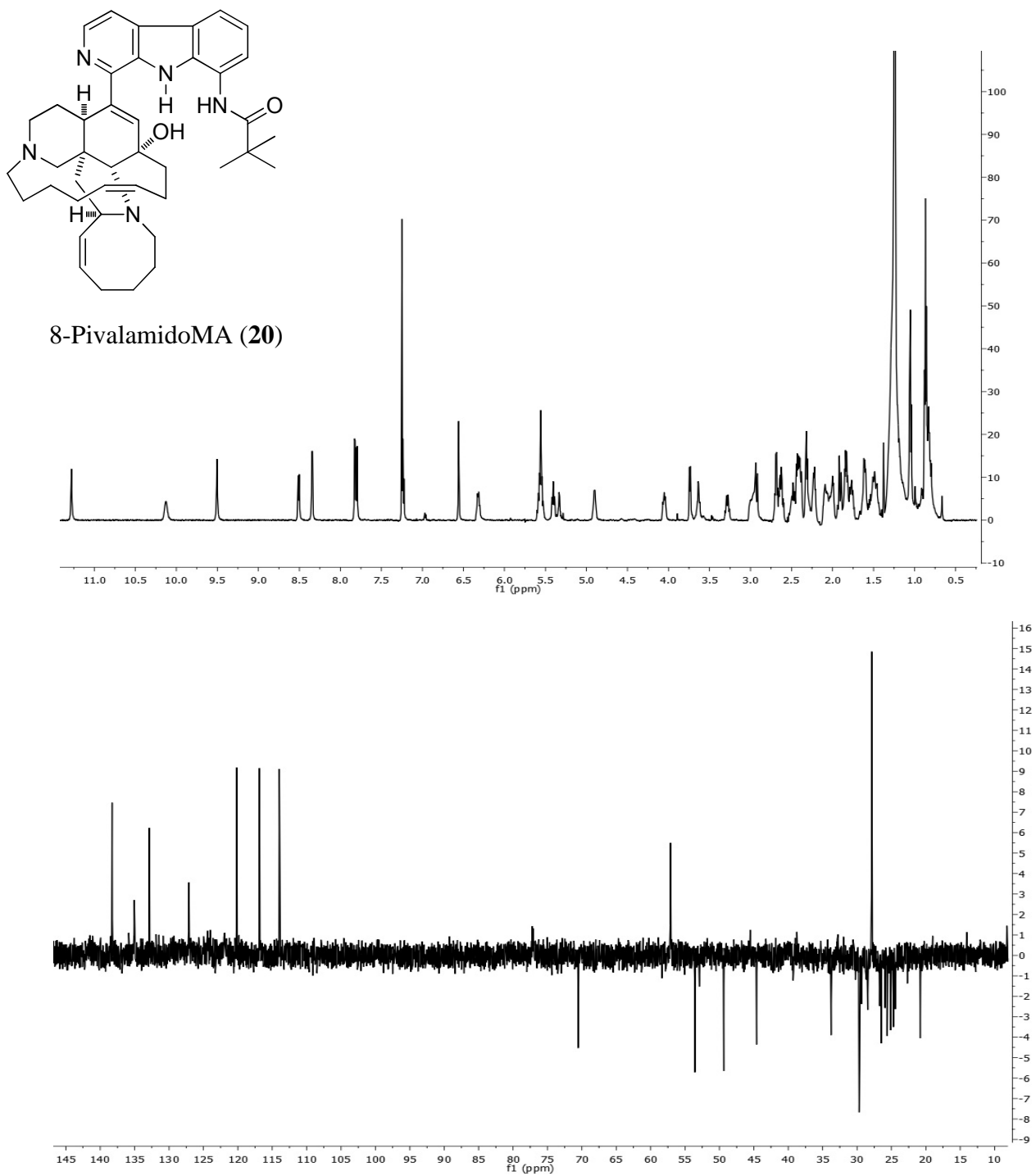
8-PivalamidoMA (**20**)

Figure II.33. ^{1}H- and [135]DEPT-NMR spectra of 8-pivalamidomanzamine A (**20**) in CDCl$_3$ at 400 and 100 MHz, respectively.
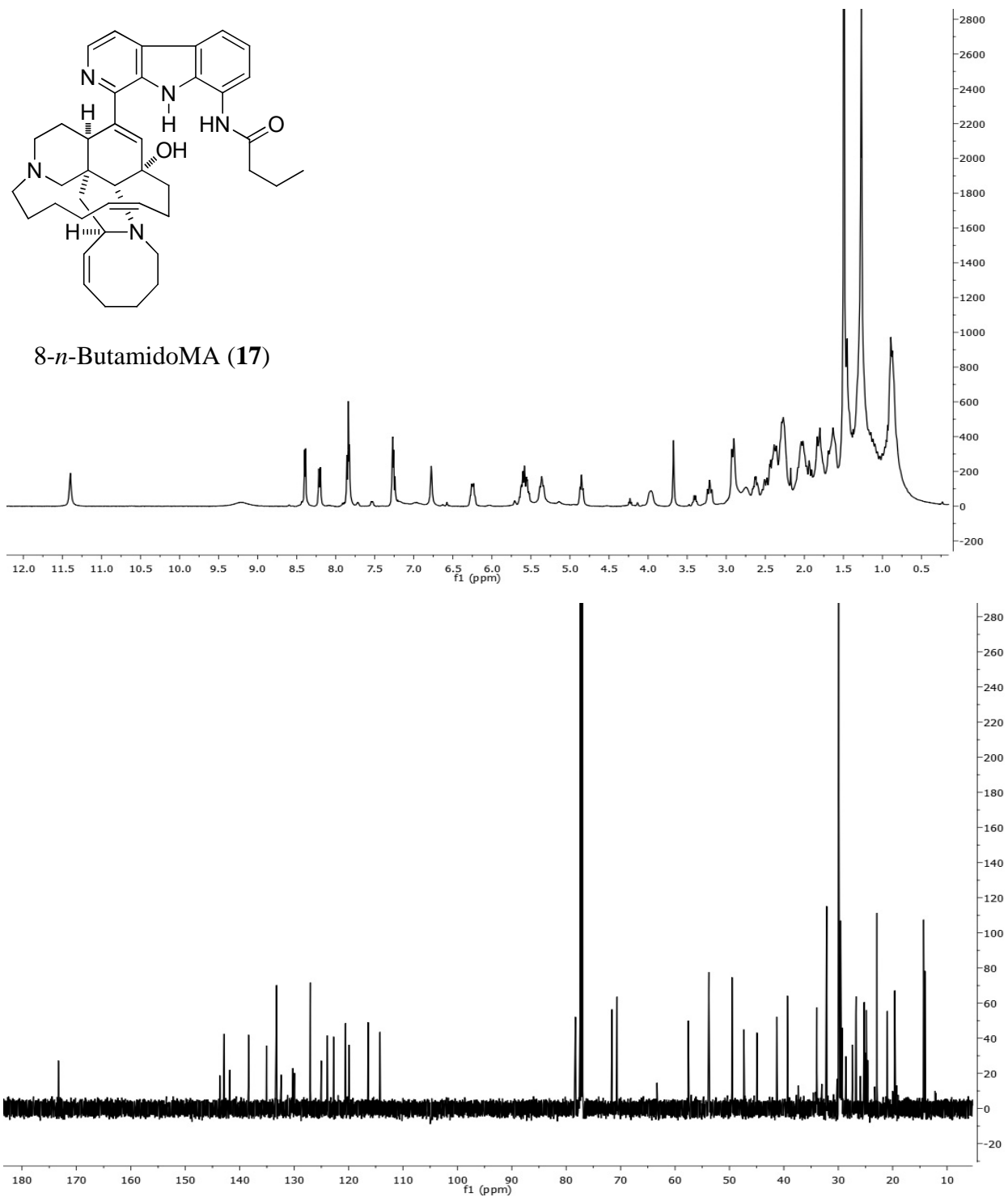
8-*n*-ButamidoMA (**17**)

Figure II.34. ^{1}H- and ^{13}C-NMR spectra of 8-*n*-butamidomanzamine A (**17**) in CDCl$_3$ at 600 and 100 MHz, respectively.

110
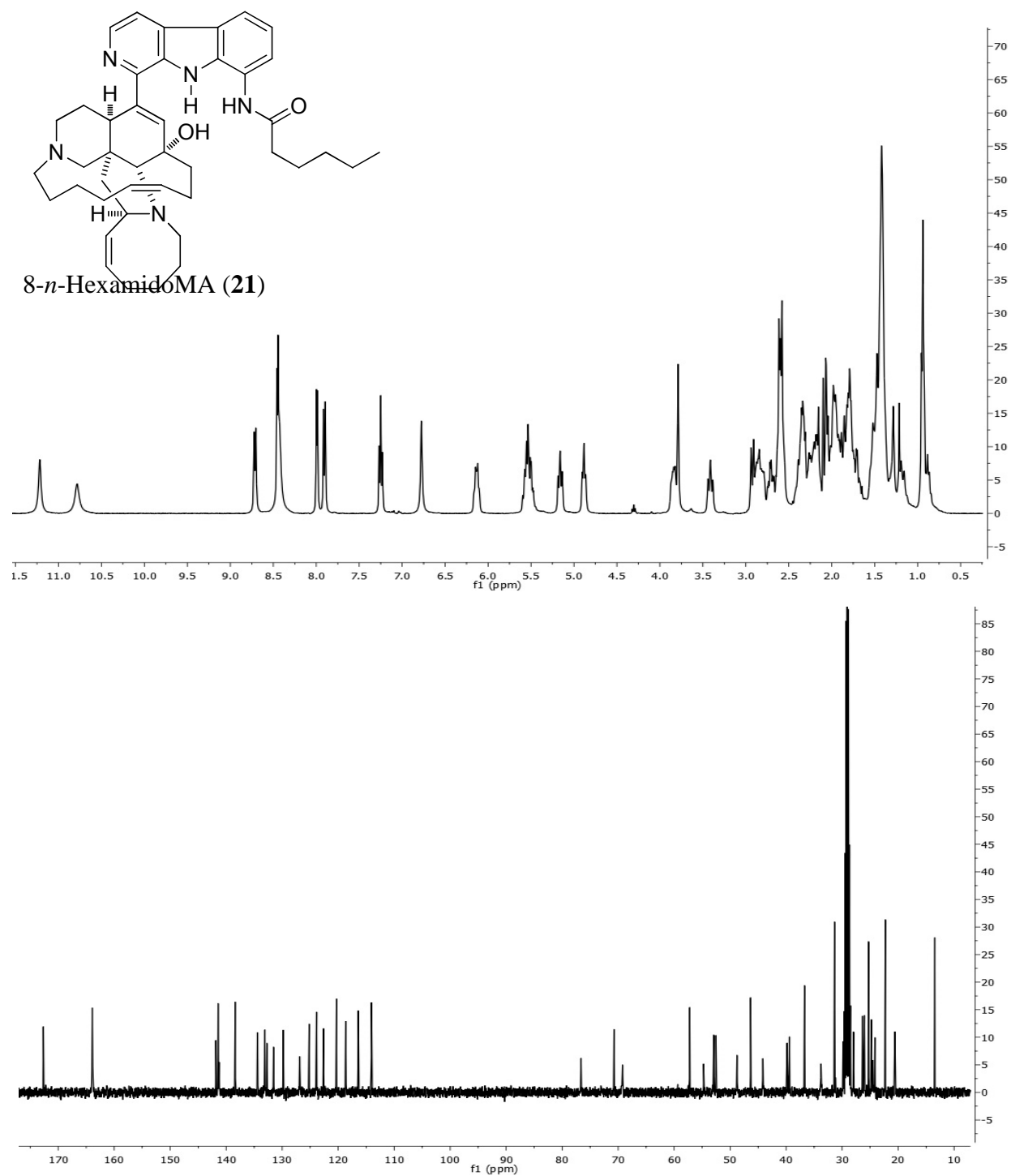
Figure II.35. ^{1}H- and ^{13}C-NMR spectra of 8-*n*-hexamidomanzamine A (**21**) in *d6*-acetone at 400 and 100 MHz, respectively.

111
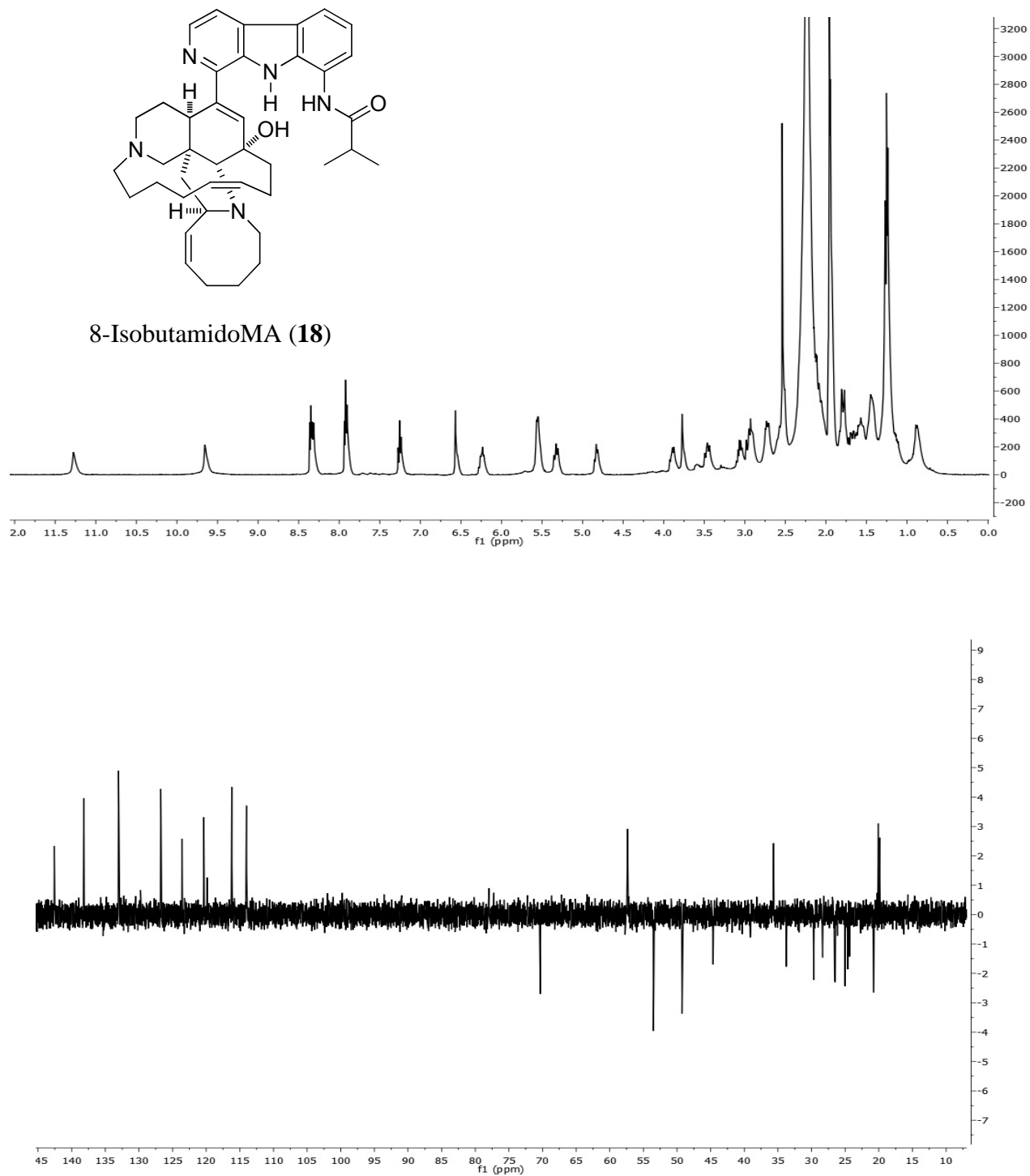
8-IsobutamidoMA (**18**)

Figure II.36. ^{1}H- and [135]DEPT-NMR spectra of 8-isobutamidomanzamine A (**18**) in *d6*-acetone at 400 and 100 MHz, respectively.
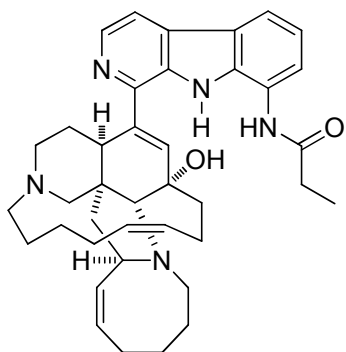
8-*n*-PropamidoMA (**16**)
^{1}H-NMR in CDCl$_3$
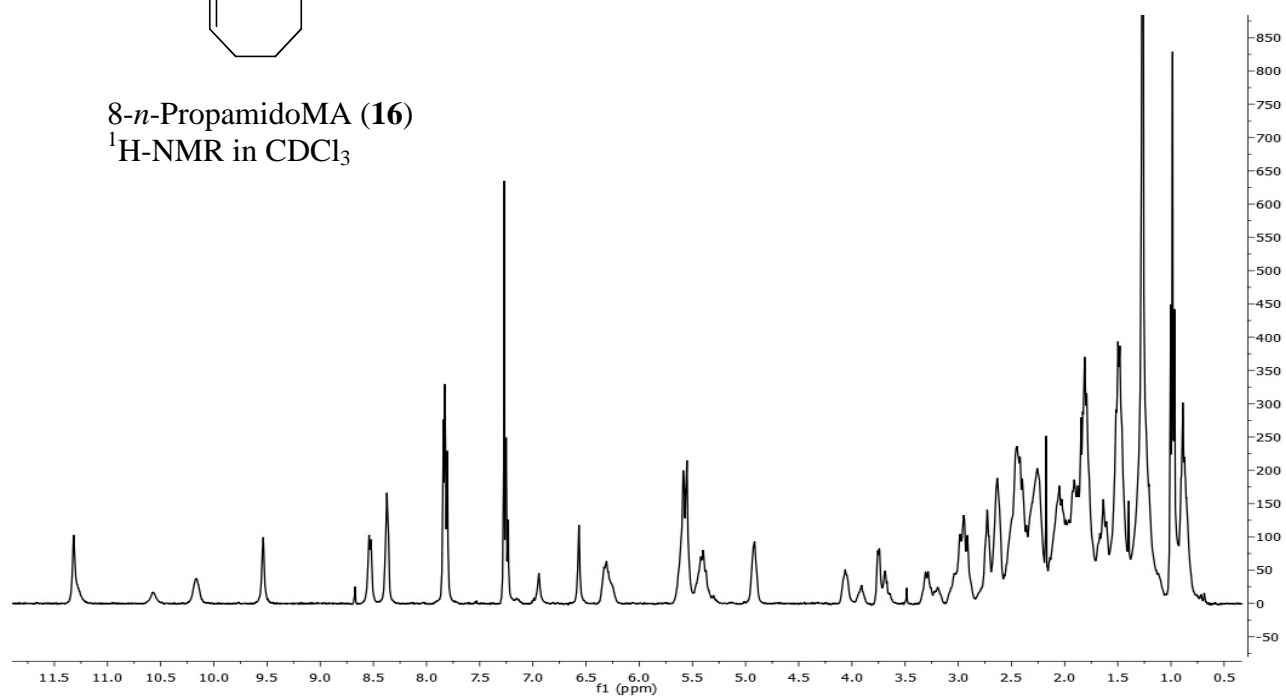
Figure II.37. ^{1}H-NMR spectra of 8-*n*-propamidomanzamine A (**16**) in CDCl$_3$ at 400 MHz.
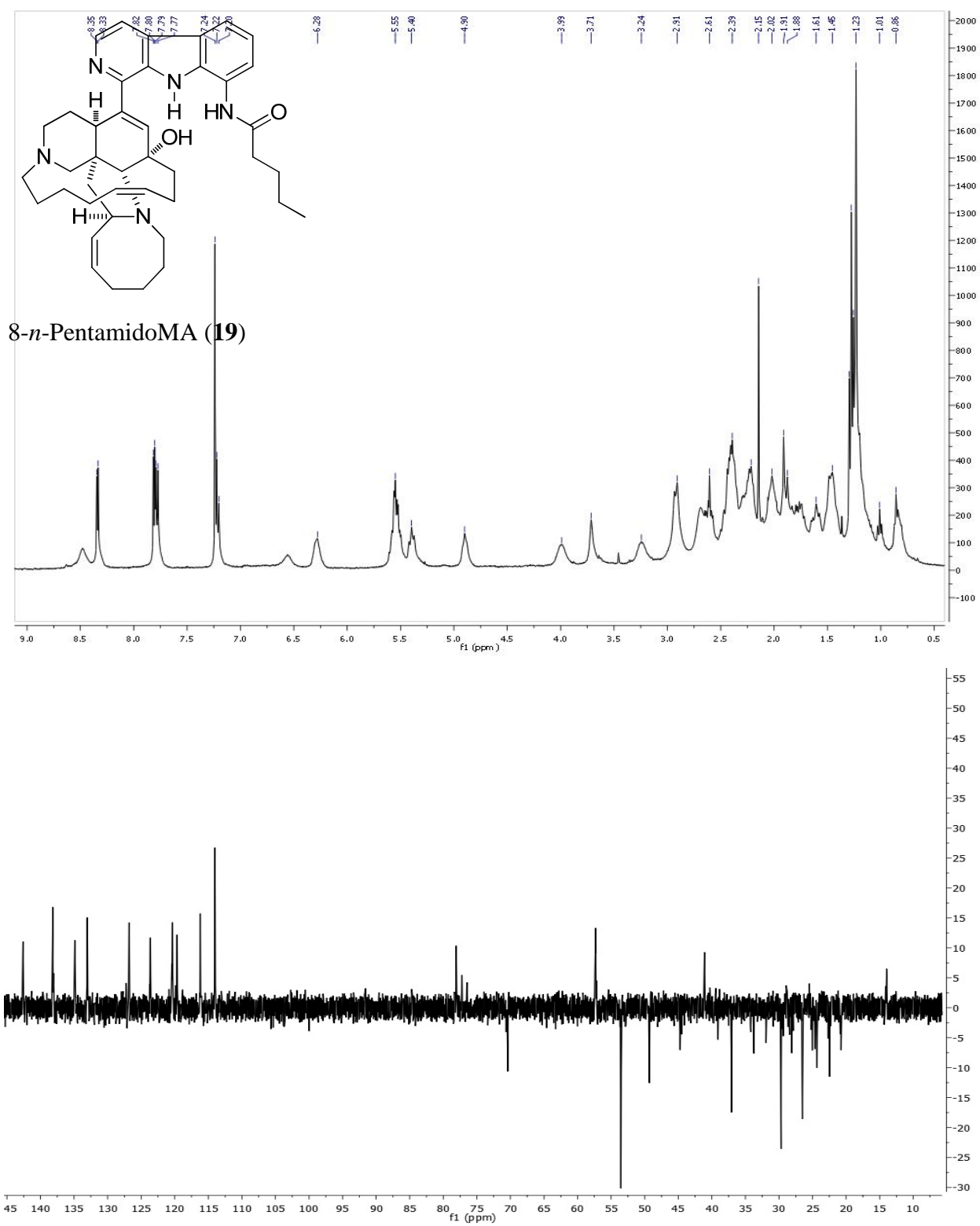
8-*n*-PentamidoMA (**19**)

Figure II.38. ^{1}H- and [135]DEPT-NMR spectra of 8-*n*-pentamidomanzamine A (**19**) in CDCl₃ at

400 and 100 MHz, respectively**.**

CHAPTER II.

SECTION D

SYNTHETIC STUDIES TOWARD THE REPLACEMENT OF THE β-CARBOLINE MOIETY

IN MANZAMINE ALKALOIDS

Introduction:

Nature has served as a gold mine of structurally diverse small molecules utilized for target identification and treatment of human diseases. Over 63% of small molecules reported between 1981 and 2006 are either natural, natural product derived or inspired from natural compounds.[49] However, natural products are not perfectly designed to fit our needs in regard to their application in disease treatment and hence optimization is a key step in the drug development process. Toxicity associated with bioactive natural products is considered a major obstacle in the process of drug discovery. The outstanding diverse biological activities of the manzamine alkaloids, especially for malaria and neuroprotection, support the development of these alkaloids as potential drugs. However, toxicity associated with high dose schedules of MA requires further optimization. The mechanism of MA toxicity as well as the diverse bioactivities is not understood. Thus detailed structure activity studies were completed modifying several moieties in the manzamine structure.[14-18] These SAR studies revealed that the modification of the β-carboline moiety decreases the toxicity and improves biological activities.

Molecular modeling studies showed that MA and several analogs docked well with DNA, suggesting that manzamines act as DNA intercalator and this might be expected from the planar aromatic β-carboline ring found in the manzamines (Figure II.39). This was supported experimentaly by the fact that MA was able to arrest the cell cycle in the S phase.[14] To validate the DNA intercalation hypothesis, we incubated MA with hepG2 cells in order to examine whether or not MA can enter the nucleus and intercalate with DNA. The fluorescence of MA was strong enough to be visualized by fluorescence microscopy and we were able to observe the uptake of MA by the nucleus (Figure II.40).
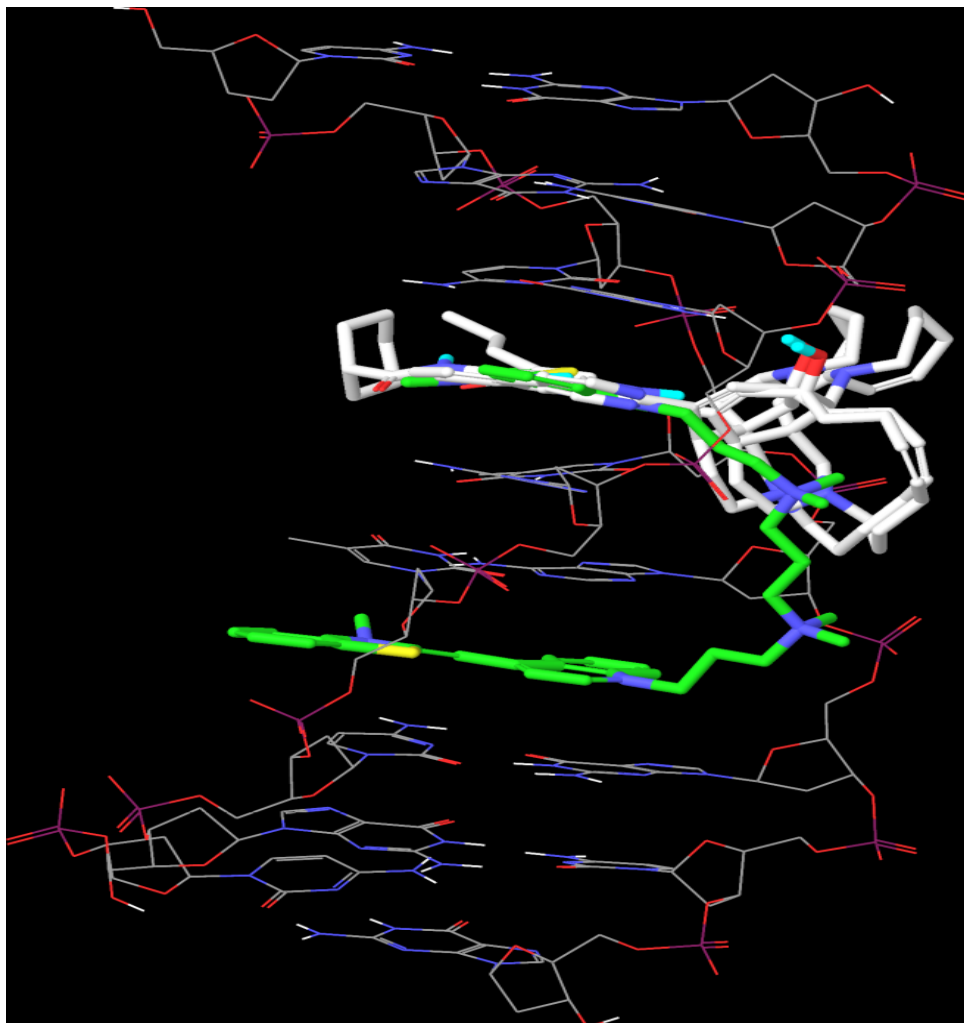
Figure II.39. Docked poses of MA and 1,1'-(4,4,8,8-tetramethyl-4,8-diazaundecamethylene)bis [4-(3-methyl-2,3-dihydrobenzo-1,3-thiazolyl-2-ethylidene)quinolinium] tetraiodide (TOTO) within DNA. TOTO is shown with green carbons and manzamines with white carbons. DNA is shown in wire mode.

	Blue fluorescence	Green fluorescence	Merge

A
Untreated
(negative
control)

B
1 μM MA
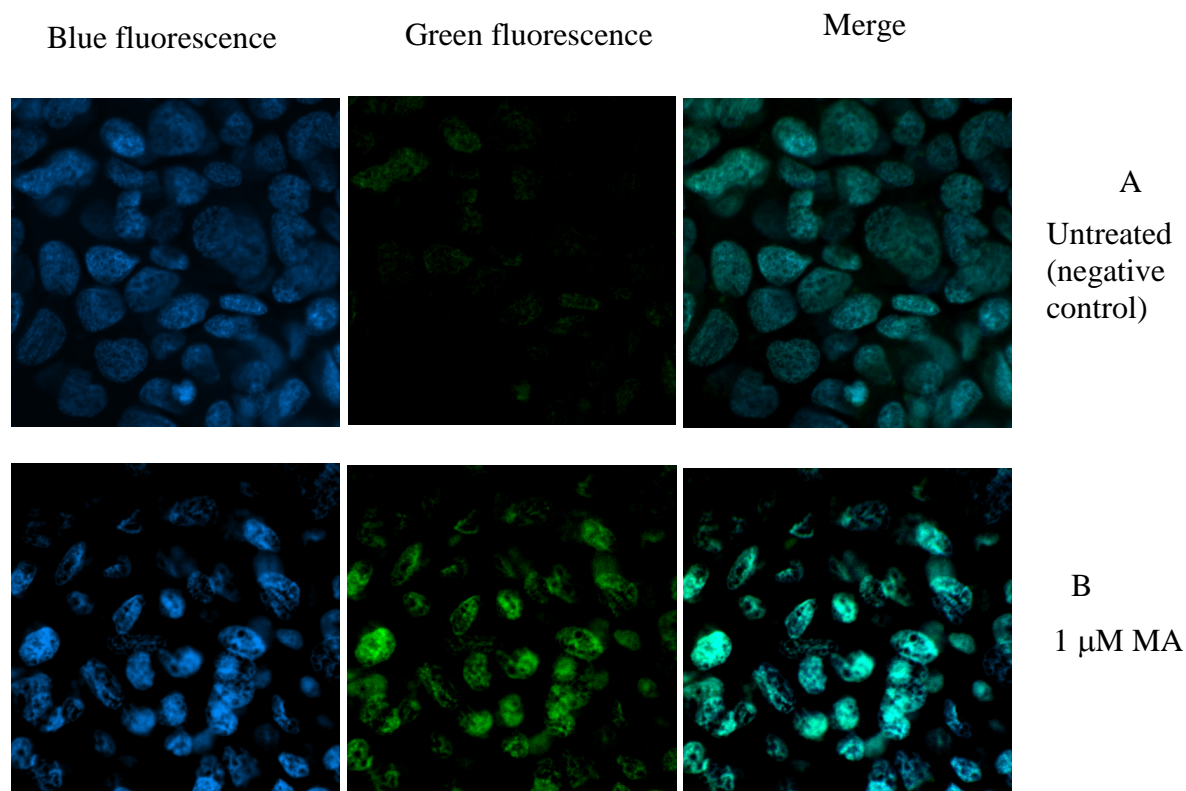
Figure II.40. Manzamine A uptake by the nucleus: A) HepG2 untreated cells (control) stained with DAPI (blue fluorescence). B) HepG2 cells incubated with 1mM MA (green fluorescence) for 4 hours. Cells were visualized by confocal microscopy (40x magnification, Zeiss 510-META).

Based on our SAR studies the replacement of the β-carboline moiety with other heterocycles is the next key step in the lead optimization process. It is important to mention that most naturally reported manzamine alkaloids contain β-carboline moiety but not others, which suggests that generating a manzamine-like analog with different heterocycle will be beyond the biosynthetic manzamine alkaloids.

Synthetic strategies:

Although gram and even kilogram quantities of MA is readily available, removal of the β-carboline moiety from the entire structure is quite difficult to achieve. This is due to the highly conjugated system that tightly linked the β-carboline with the rest of the molecule. Therefore, using MA as a starting material for replacing the β-carboline moiety is not practical. To breakdown the conjugated system, Birch reduction could be utilized. Our goal was to reduce the pyridine ring in the β-carboline as a first step for a retro-Pictet-Spengler approach. However, Birch reduction of MA resulted in the reduction of the Δ^{11} double bond but not the β-carboline itself (Scheme II.3).
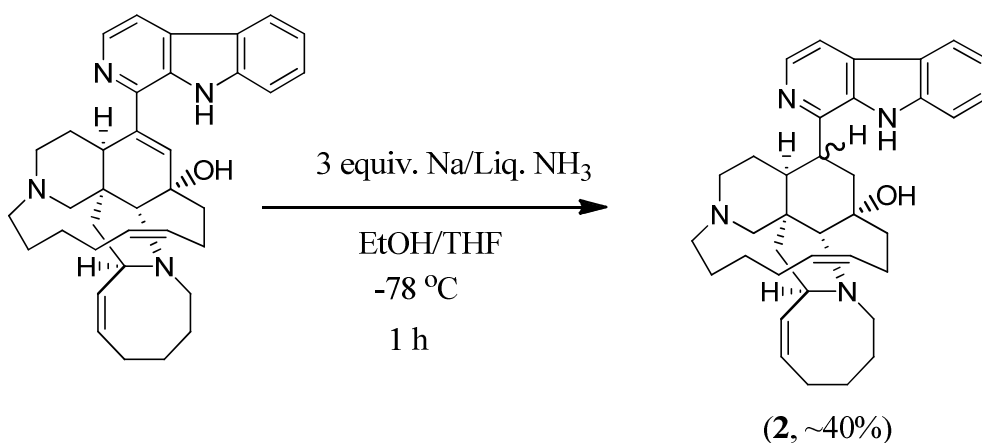
Scheme II.3. Birch reduction of MA.

We then turned our attention to using ircinal A as a starting material instead and C-C coupling reactions. C-C bond formation requires the reaction of two components with opposite polarity: a nucleophile (metal-carbon species) and an electrophile (carbon-halogen or carbon-pseudohalogen bond). In order to utilize a coupling approach, ircinal A should be converted first to either an electrophilic or a nucleophilic partner (Figure II.41). The only disadvantage of using ircinal A is the limited quantities available from the natural source.
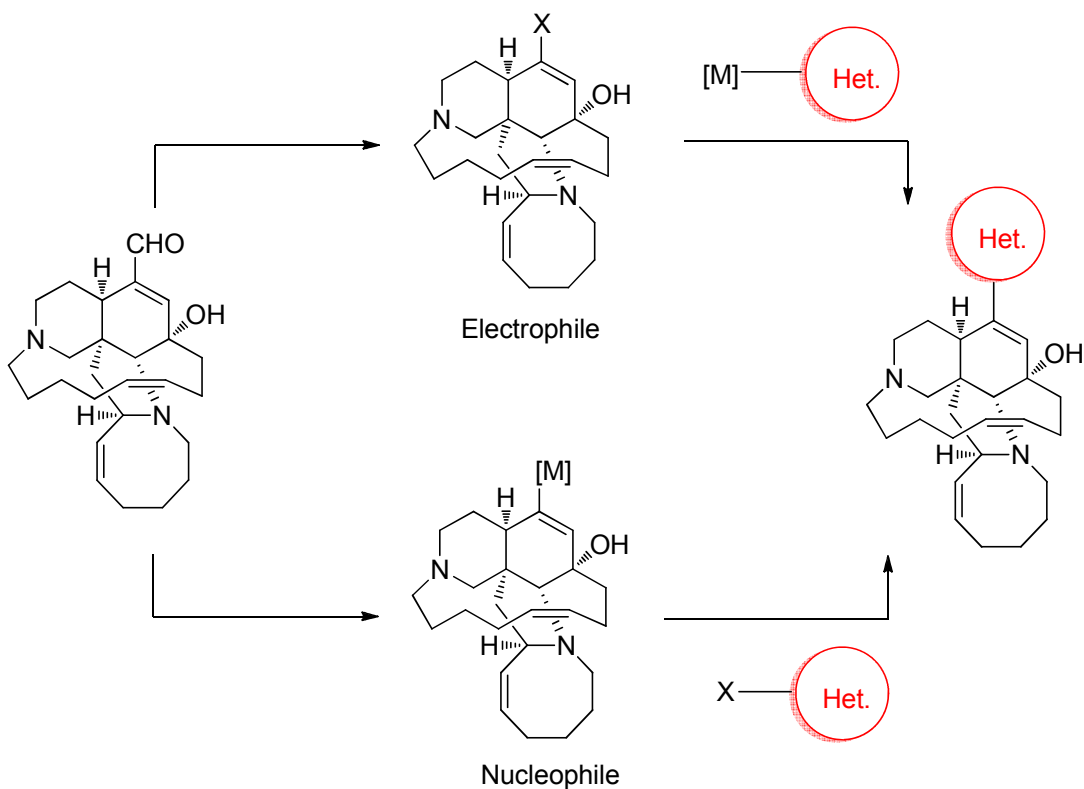
Figure II.41. Different proposed routes for utilizing ircinal A in a C-C coupling reaction.

Ircinal A as a nucleophilic partner:

Decarboxylative cross coupling approach:

Synthetic chemists are always concerned about developing new C-C bond methodologies to construct up complex natural products and medicinally important molecules. Since the discovery of Ullmann reaction (copper catalyzed reductive symmetrical cross coupling of aryl halides), metal catalyzed cross coupling reactions have become the most important tools for C-C construction.[59] Several metals have been used as the nucleophile partner including: palladium, copper, zinc and nickel;[59] however, several drawbacks remains including toxicity and limited commercial availability of some coupling partners. Carboxylic acids are widely available and are easy to make and have been used recently to generate nucleophilic partner through elimination of CO_2.[60] Nilsson reported the first copper catalyzed decarboxylative coupling between *o*-nitrobenzoic acid and iodobenzene in 1966,[61] followed by coupling of 2,6-dinitrobenzoic acid in 1968.[62] Since then, no improvement in regard to copper load or high temperature until more recently when Myers reported in 2002 the palladium catalyzed decarboxylative-Heck type olefination of arene carboxylates,[63] and the palladium catalyzed decarboxylative cross coupling of heteroaromatic carboxylic acids with aryl bromides developed by the Bilodeau's group in 2006.[64] Goossen *et al*. used a palladium source in addition to copper (I) as a cocatalyst to catalyze the extrusion of CO_2 and the generation of the carbon nucleophile; which is subsequently transmetalated to the palladium cycle for coupling with the carbon electrophile (Figure II.42).[64, 65]
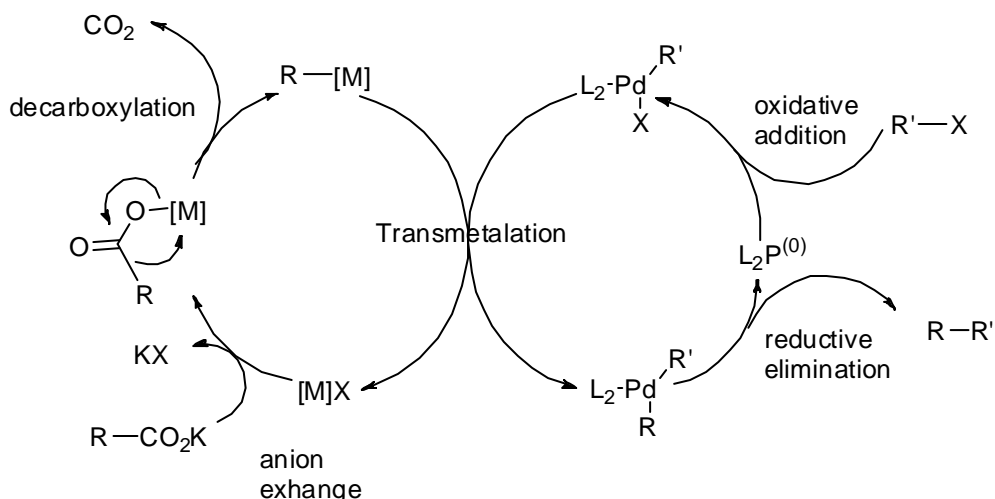
Figure II.42. Cu/Pd catalyzed decarboxylative cross coupling. M=Ag, Cu; R=hetero, aryl, vinyl, acyl; R`=heterocycles, aryl; X=I, Cl, Br, OTf[61-70]

Initial catalyst system developed by Goossen consisted of 10 mol% of CuBr/1,10-phenanthroline and 3 mol% palladium bromide;[64,65] however, several improvements of the catalytic system, substrate and reaction temperature have been made.[66-71] Electrophilic partners were extended from aryl bromides[64,66] to aryl chlorides,[67] aryl triflates[68,69] and aryl tosylates.[70] Silver was shown to be effective metal for the decarboxylative step with lowered reaction temperatures.[71]

The straight forward oxidation of ircinal A to the corresponding carboxylic acid, ircinoic acid, encouraged us to utilize the decarboxylative cross coupling (DCCC) approach for the replacement of the β-carboline moiety. Oxidation of ircinal A was optimized using different oxidizing agents. Perchlorate oxidation as well as silver-catalyzed hydrogen peroxide oxidation gives excellent yields (93%) of ircinoic acid (Scheme II.4).
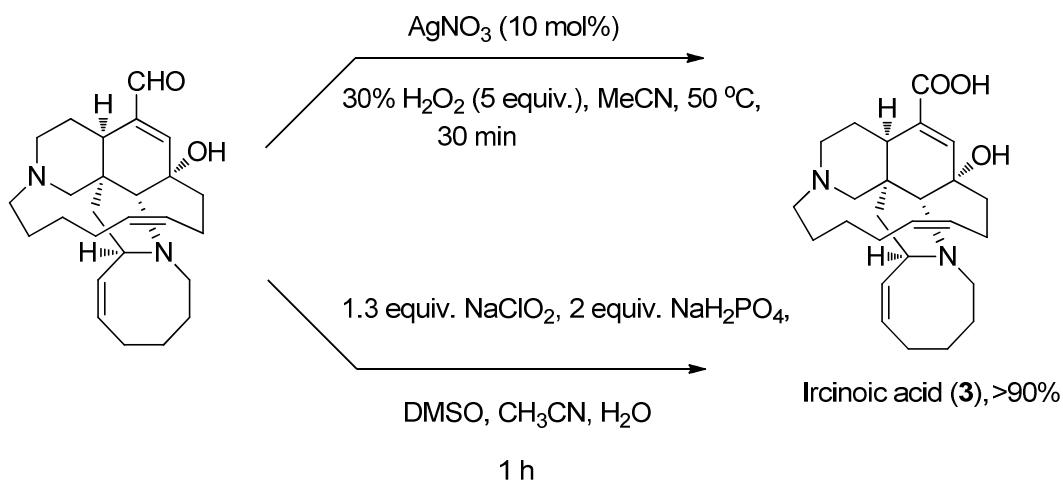
Scheme II.4. Oxidation of ircinal A to ircinoic acid.

We optimized the decarboxylative cross coupling reaction with (*S*)-perillic acid as a model compound with several aryl bromides. Excellent yields were obtained with several aryl halides (Scheme II.5) including the desired hetereocycle 7-bromo-1H-pyrrolo(2,3-*c*)pyridine **4**.
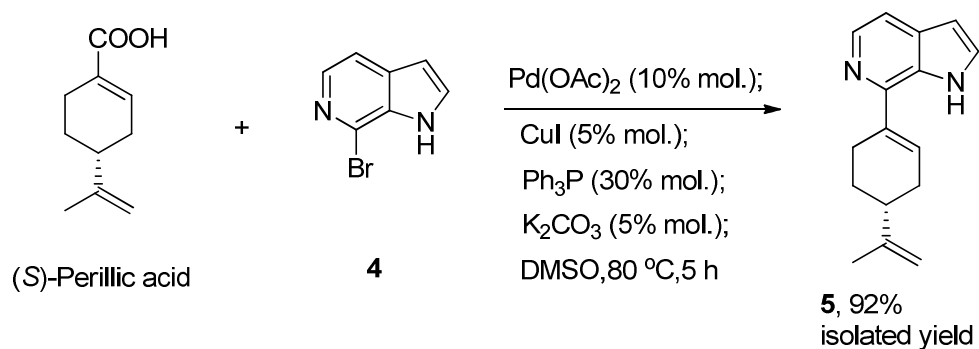
Scheme II.5. Optimized decarboxylative cross coupling conditions with (*S*)-perillic acid

However, the optimized conditions failed with ircinoic acid. Part of this failure is because of complexity of the structure as well as the high basisity of ircinoic acid relative to *S*-perillic acid. Another important issue is that ircinoic acid is placed in contact with two highly activated metals with the possibility of having many side products; especially when having a number of basic nitrogens and double bonds within the structure that could interact with palladium (0). As a result, we decided to optimize the DCCC reaction using ircinoic acid. Our optimization strategy was based on minimizing side reactions as well as reducing reaction temperature to avoid any damage to the ircinal skeleton. Based on the proposed reaction mechanism (Figure II.43), the best approach for minimizing side reactions is to physically separate the two catalytic cycles; in other words, generating the cupric-ircinal like salt **I** separately and allows to react with palladium (0) complex **II** through the transmetalation step. This separation will minimize interaction of ircinoic acid with palladium (0) that will indeed eliminate most side reactions.

Although we obtained the coupled product after several trials, the yield was low (~5%) and the reaction was not reproducible. One explanation is that decarboxylation of ircinoic acid is hard to achieve. These negative results and the limitation of starting material concluded the fact that decarboxylative cross coupling strategy needs further optimizations.
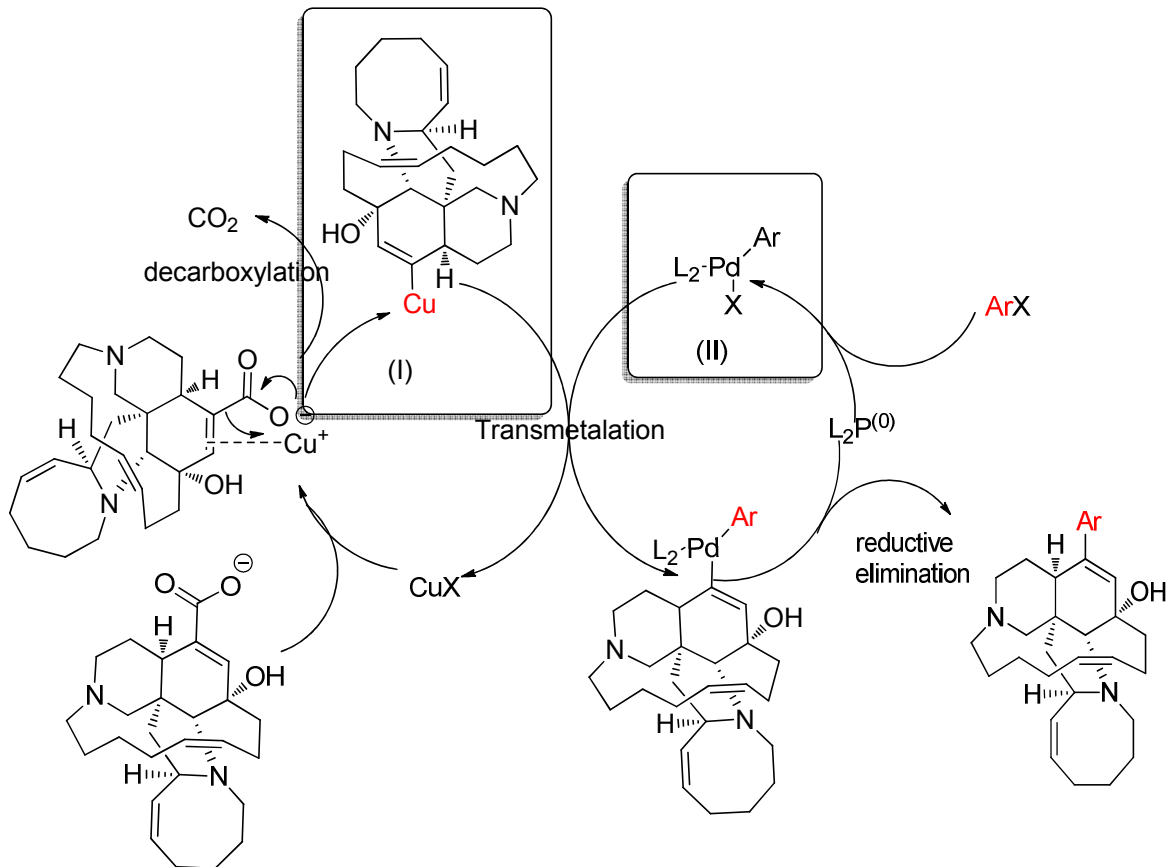
Figure II.43. Proposed mechanism for the decarboxylative cross coupling reaction with ircinoic acid.

Ircinal A as an electrophilic partner:

Ircinal-derived Triflate:

The field of cross coupling reactions is rich in several outstanding synthetic tools for C-C bond construction with a variety of metals as well as nucleophilic partners used. Among these tools Suzuki cross coupling reaction is practical and has been used with a variety of substrates and in the real applications in the field of total synthesis of natural products. In all cases, utilizing ircinal A as an electrophilic partner in C-C cross coupling reaction requires the removal of the

formyl group with insertion of an electron withdrawing group such as a halogen or a triflate group (pseudohalogen) (Figure II.44).
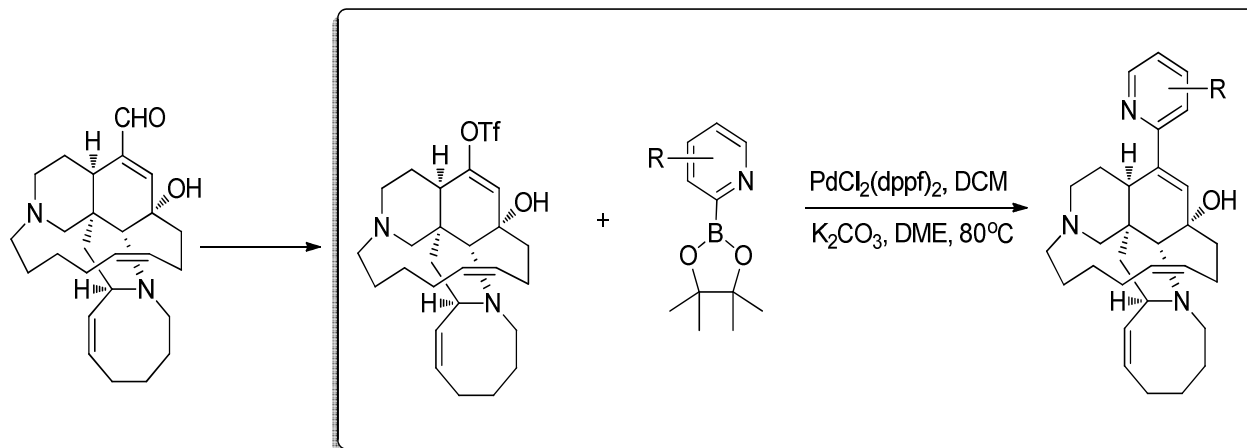
Figure II.44. Suzuki cross coupling approach utilizing ircinal-derived triflate.

Our synthetic approach for this oxidative deformylation is outlines in Figure II.45. Birch reduction of the α,β-unsaturated aldehyde functionality should deliver the reduced ircinal A (**6**) with the generation of a new stereogenic center. An oxidative deformylation reaction will be then utilized to convert this formyl group into the ircinal-derived ketone (**8**) which is very crucial and important intermediate due to its straightforward conversion to the corresponding enolate that could be trapped as a triflate analog (**9**). Oxidative deformylation process starts with enolate formation followed by the reaction with oxygen which after decomposition of the formed adduct will give the keto derivative.[72]

126
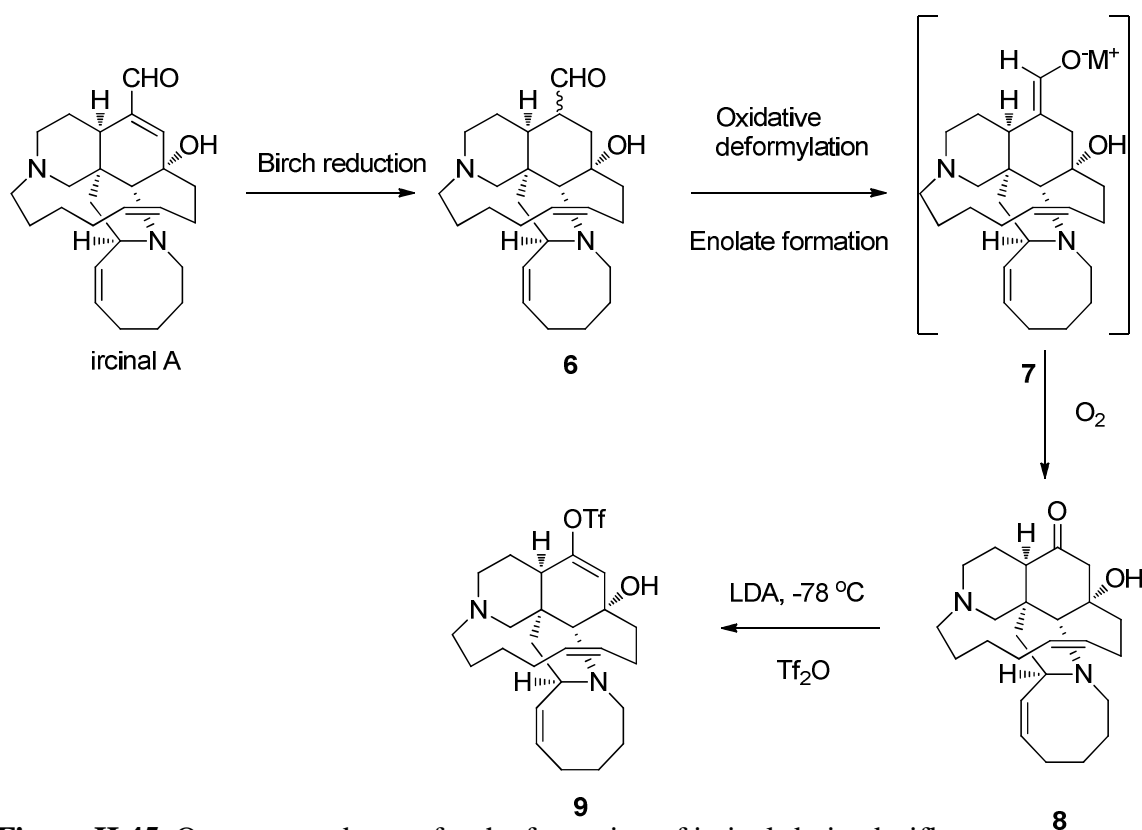
Figure II.45. Our proposed route for the formation of ircinal-derived triflate

However, Birch reduction of ircinal A under atmospheric air resulted in the formation of an interesting and unexpected product **10** (Scheme II.6). The HRESIMS data of **10** (m/z 381.3025 (M+H$^+$)) revealed the loss of a formyl and a hydroxy groups from the ircinal A structure. The presence of the singlet resonance at δ_H 6.08 in the ^{1}H-NMR spectrum of **10** and its HMBC correlation to the carbonyl group C1 (δ_c 197.39) suggested that the newly formed double bond is in conjugation with the carbonyl group. A sequential one-pot Birch reduction-elimination and deformylation reactions were occurred that yielded the unexpected ircinal-derived enone (**10**). A possible mechanism for this sequence is shown in Figure II.46. An electron attack on the β-position of the α,β-unsaturated functionality followed by a proton extraction of the generated enolate will yield radical species (**III**). A second electron attack will occur and then instead of

regular proton abstraction, an elimination of the 3° hydroxy group is more likely to happen that will generate a stabilized conjugated system with the aldehyde group (in the enolate form) (**IV**). In this highly basic conditions, aldehyde group will be in the enolate form (**V**) which will then react with oxygen in a [2+2] cycloaddition way to generate the dioxetane intermediate (**VI**). Rapid decomposition of this intermediate will deliver the unexpected product (**10**) with release of formate salt.
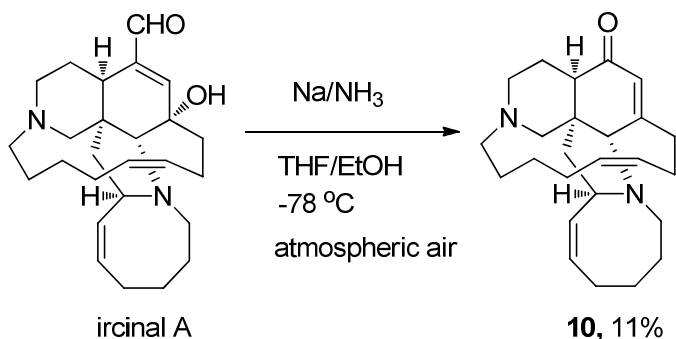
Scheme II.6. Birch reduction of ircinal A

Ircinal-derived enone (**10**) will be useful in generating the deoxy-ircinal-derived triflate (**11**) (Scheme II.7). Although this is not our desired end product, this will give us a chance to optimize the Suzuki cross coupling reaction as well as generating some useful SAR studies at this position. Basically, this enone will be subjected to Birch reduction condition. An enolate (**VII**) will be generated after the second electron attack that could be trapped as a triflate.
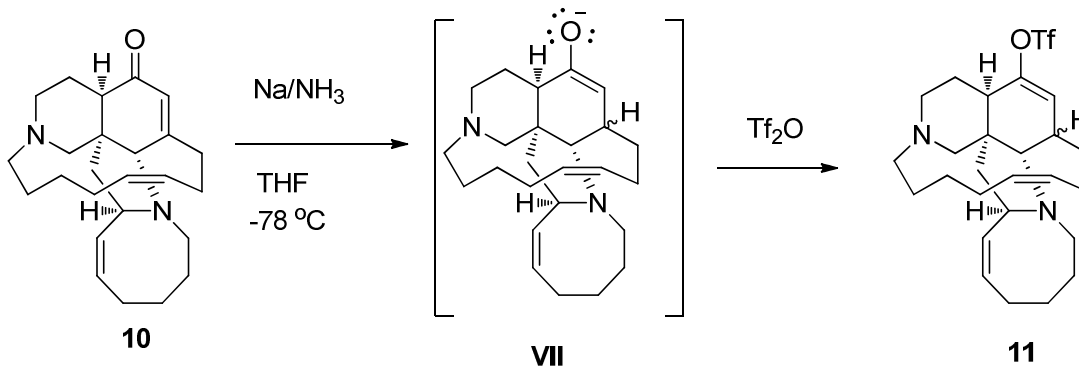
Scheme II.7. Planned Birch reduction for the generation of the deoxyircinal-derived triflate **11.**
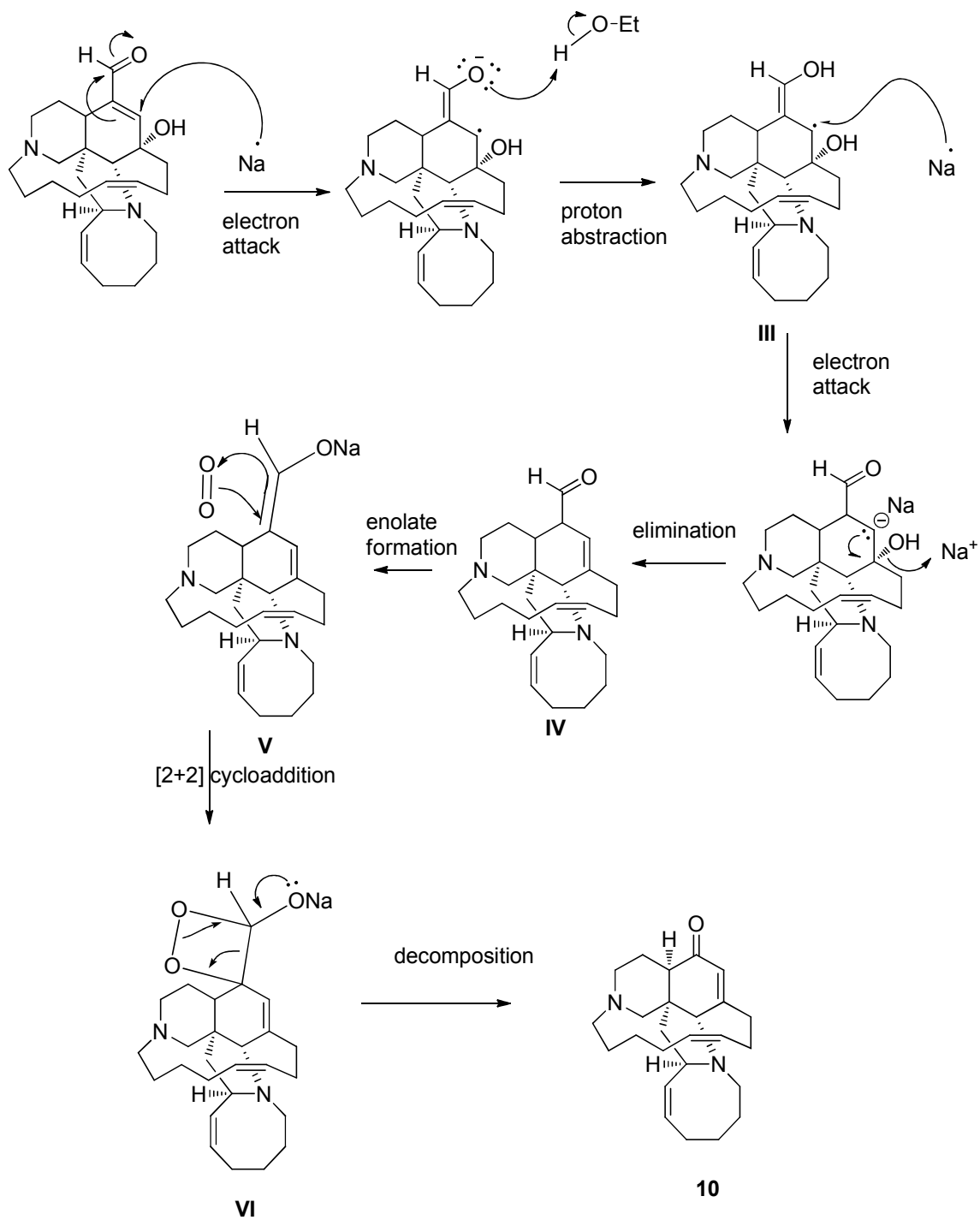
Figure II.46. Proposed mechanism for the formation of the unexpected ircinal-derived enone (**10**).

Conclusion:

In conclusion, the decarboxylative cross coupling reaction is relatively a new approach for the generation of nucleophilic partners in C-C cross coupling reactions. However, this approach was not practical in coupling ircinoic acid with other heterocycles. New and unexpected sequences of reactions were observed in the Birch reduction of ircinal A under atmospheric air. A sequential Birch reduction-elimination-oxidative deformylation were occurred and yielded the unexpected ircinal-derived enone (**10**). This enone will be utilized in another Birch reduction condition in order to trap the generated enolate as a triflate analog. This deoxyircinal-derived triflate will be used for the optimization of a Suzuki coupling reaction.

Experimental:

General Experimental Procedures. The ^{1}H- and ^{13}C-NMR spectra were recorded in CDCl$_3$ or *d6*-acetone on a Bruker DRX NMR spectrometer operating at 400 MHz for ^{1}H and 100 MHz for ^{13}C. Chemical shift (δ) values are expressed in parts per million (ppm) and are referenced to the residual solvent signals of CDCl$_3$ or *d6*-acetone. The high resolution ESI-MS spectra were measured using a Bruker Daltonic (GmbH, Germany) micro-TOF series with electrospray ionization. TLC analysis was carried out on precoated silica gel G254 aluminum plates.

Birth reduction of manzamine A: Ammonia (10 mL) was condensed with sodium (5 equiv.) in a three-neck flask at -78 ^{o}C. A solution of manzamine A (100 mg, 0.182 mmol) dissolved in THF:ethanol (9:1) was first cooled to -78 ^{o}C and then added to ammonia. The reaction mixture was kept stirring at -78 ^{o}C for 30 min. Aqueous NH$_4$Cl was added and ammonia was allowed to evaporate at room temperature. The aqueous solution was extracted with dichloromethane (3x10 mL). The combined organic phases were washed successively with 10% aqueous sodium thiosulphate and brine, dried over MgSO$_4$. The crude product was purified by silica gel column.

10,11-dihydromanzamine A: (2); yellow powder; ^{1}H-NMR (CDCl$_3$) δ 9.04 (1H, d, *J*=2.0 Hz), 8.50 (1H, d, *J*=5.2 Hz) , 8.40 (1H, dd, *J*=9.2, 2.0 Hz), 7.89 (1H, d, *J*=5.2 Hz), 7.77 (1H, d, *J*=9.2 Hz), 6.21 (1H, s), 5.62 (m), 5.42 (t, *J*=10.8 Hz), 4.70 (br), 3.69 (s), 3.25 (1H, t, *J*=11.0 Hz), 2.93 (d, *J*=9.0 Hz), 2.80~2.20 (m), 2.10~1.20 (m); HRESIMS *m/z* calcd for C$_{36}$H$_{37}$N$_5$O (M+H)$^+$ 551.3512, found 551.3645.

Oxidation of Ircinal A: Ircinal A (30 mg, 0.07 mmol) was dissolved in a mixture of t-butanol (5 mL), acetonitrile (2 mL) and water (1 mL). To this solution were added sequentially at room DMSO (excess), NaH$_2$PO$_4$ (144 mg, 1.2 mmol) and NaClO$_2$ (140 mg, 1.2 mmol). The reaction mixture was stirred at room temperature for one hour and NaCl (sat.) solution was added and the mixture was extracted with dichloromethane (3x10 mL).

Ircinoic Acid (3): (29 mg, 93%); white powder; ^{1}H-NMR (CDCl$_3$) δ 9.04 (1H, s), 6.50 (1H, s), 6.21 (1H, s), 5.62 (m), 5.42 (t, *J*=10.8 Hz), 4.70 (br), 3.69 (s), 3.25 (1H, t, *J*=11.0 Hz), 2.93 (d, *J*=9.0 Hz), 2.80~2.20 (m), 2.10~1.20 (m); HRESIMS *m/z* calcd for C$_{26}$H$_{39}$N$_2$O$_3$ (M+H)$^+$ 427.2145, found 427.2456.

Decarboxylative cross coupling of (*S*)-perillic acid with 7-bromo-1H-pyrrolo(2,3-*c*)pyridine (4): (S)-perillic acid (100 mg, 0.602 mmol) and 7-bromo-1H-pyrrolo(2,3-*c*)pyridine (119 mg, 0.031 mmol) were dissolved in dry DMSO (10 mL) in an oven dried two neck round bottom flask under nitrogen atmosphere. To this solution were added subsequently CuI (5 mg, 0.03 mmol), Pd(OAc)$_2$ (13.5 mg, 0.06 mmol), PPh$_3$ (47.3 mg, 0.181 mmol) and anhydrous K$_2$CO$_3$ (4.15 mg, 0.031 mmol). The reaction mixture was heated at 80 ^{o}C for 5 h and the progress of the reaction was monitored by TLC. Water (10 mL) was added and the aqueous phase was extracted with DCM (3x20 mL) and the combined organic layer was dried over Na$_2$SO$_4$ and concentrated under vacuum. The crude product was purified by silica column to afford the coupled product.

7-perillyl-1H-pyrrolo(2,3-*c*)pyridine (5(: (133 mg, 91.7%); white powder; ^{1}H-NMR (CDCl$_3$) δ 8.05 (1H, d, *J*=7.5 Hz), 7.51 (1H, d, *J*=5.0 Hz), 7.44 (1H, d, *J*=5.2 Hz), 7.12 (1H, brd s), 6.66 (1H, brd s), 4.74 (2H, brd s), 2.49~1.10 (m), 1.75 (3H, s); ^{13}C-NMR (CDCl$_3$); 148.86, 141.54, 138.89, 133.93, 132.08, 129.78, 128.46, 125.13, 115.52, 109.40, 103.81, 40.11, 31.38, 27.13, 24.45, 20,86; HRESIMS *m/z* calcd for C$_{16}$H$_{19}$N$_2$ (M+H)$^+$ 238.1491, found 238.1502.

Birch reduction of ircinal A:

Ammonia (5 mL) was condensed with sodium (5 equiv.) in a three-neck flask at -78 ^{o}C. A solution of ircinal A (30 mg, 0.073 mmol) dissolved in THF:ethanol (9:1) was first cooled to -78 ^{o}C and then added to the ammonia solution. The reaction mixture was kept stirring at -78 ^{o}C for 30 min. Aqueous NH$_4$Cl was added and ammonia was allowed to evaporate at room temperature. The aqueous solution was extracted with dichloromethane (3x10 mL). The combined organic phases were washed successively with 10% aqueous sodium thiosulphate and brine, dried over MgSO$_4$. The crude product was purified by silica gel column.

Ircinal-derived enone (10): (3 mg, 11%); ^{1}H-NMR (CDCl$_3$) δ 8.26 (1H, s), 6.08 (1H, d, *J*=5.2 Hz) , 5.97 (1H, s), 5.34 (1H, d, *J*=5.2 Hz), 5.32 (1H, d, *J*=5 Hz), 5.30 (1H, d, *J*=5 Hz), 4.41 (1H, m), 3.37 (1H, m), 3.25 (1H, m), 2.99~1.4 (m); ^{13}C-NMR (CDCl$_3$); 197.39, 136.79, 131.77, 131.49, 130.90, 130.16, 128.15, 64.57, 63.91, 55.19, 53.26, 49.45, 48.33, 45.77, 43.22, 41.48, 37.63, 33.09, 28.40, 27.72, 27.47, 27.38, 25.59, 23.86, 18.73; HRESIMS *m/z* calcd for C$_{25}$H$_{37}$N$_2$O (M+H)$^+$ 381.2877, found 381.3025.
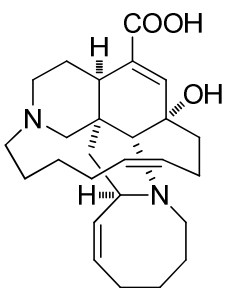
Ircinoic acid
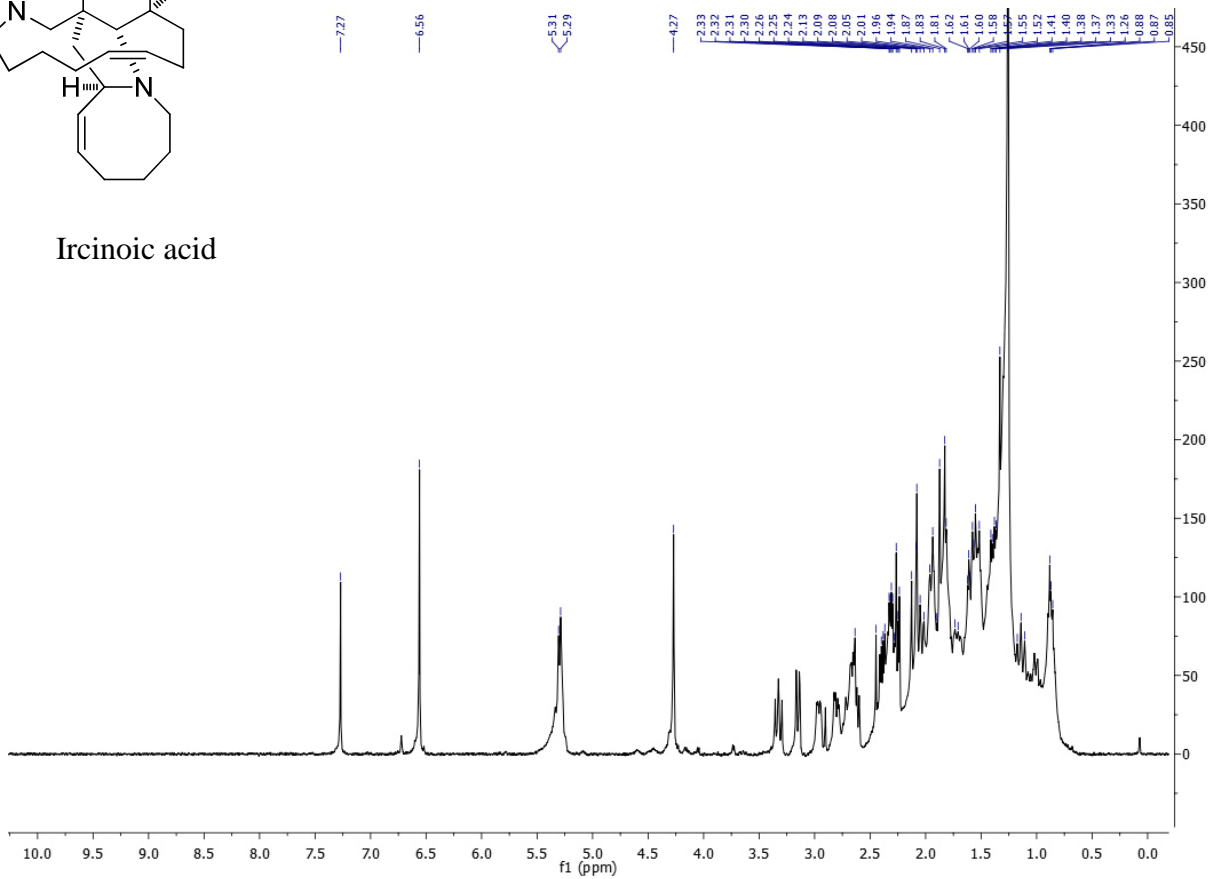
Figure II.47. ^{1}H-NMR of ircinoic acid in CDCl$_3$ at 400 MHz.

7-perillyl-1H-pyrrolo(2,3-*c*)pyridine (**5**)
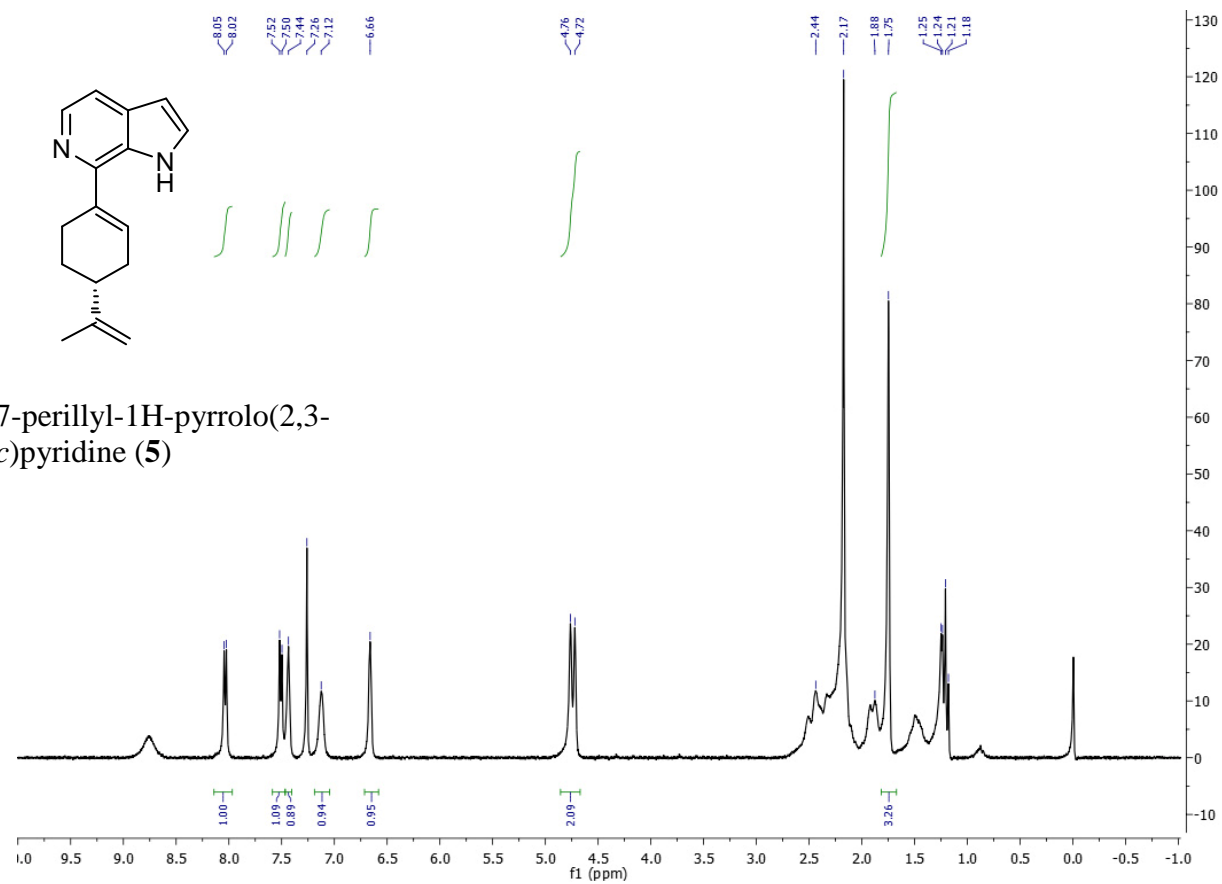
Figure II.48. ^{1}H-NMR of 7-perillyl-1H-pyrrolo(2,3-*c*)pyridine (**5**) in CDCl$_3$ at 400 MHz.

7-perillyl-1H-pyrrolo(2,3-c)pyridine (**5**)
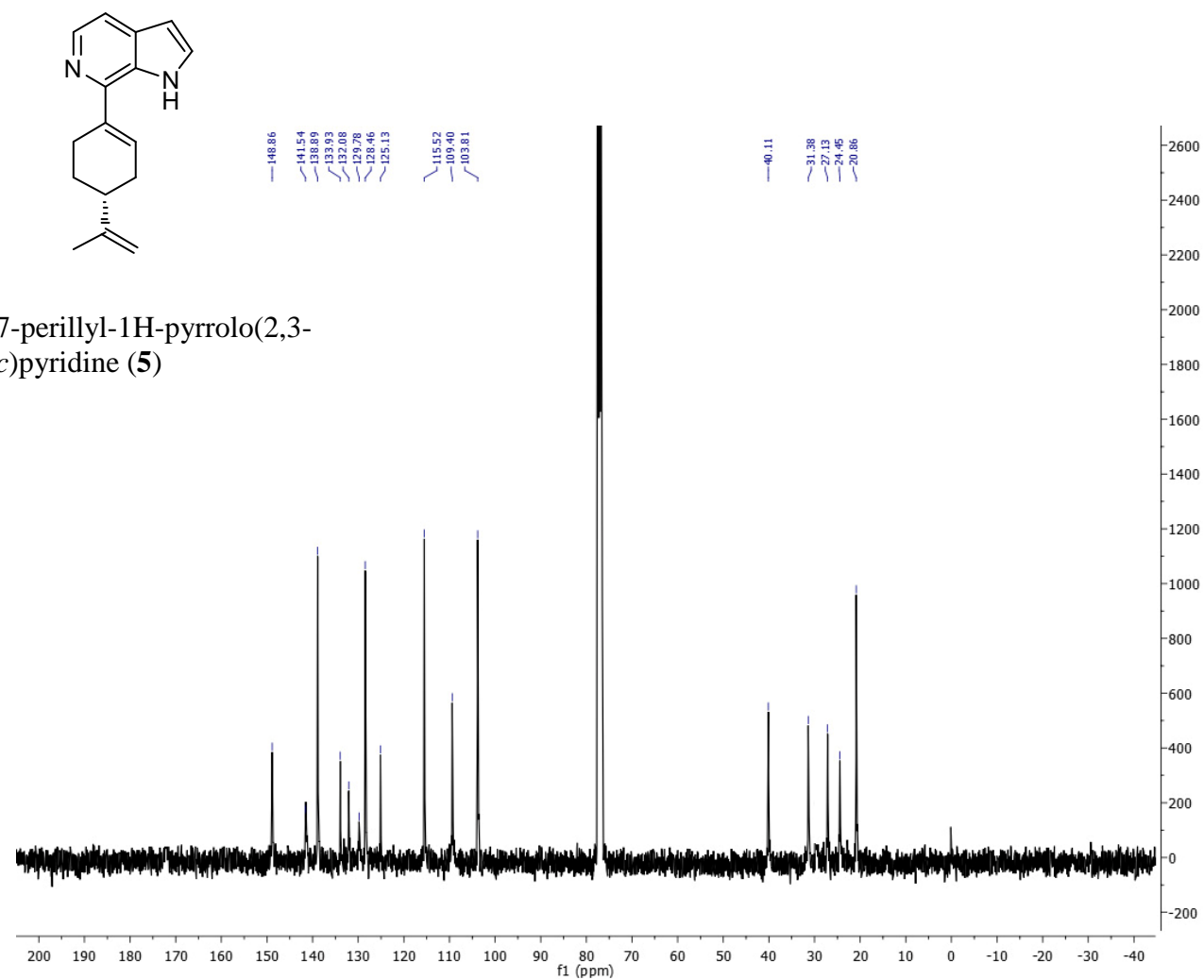
Figure II.49. ^{13}C-NMR of 7-perillyl-1H-pyrrolo(2,3-c)pyridine (**5**) in CDCl$_3$ at 100 MHz.

135

Ircinal-derived enone (**10**)
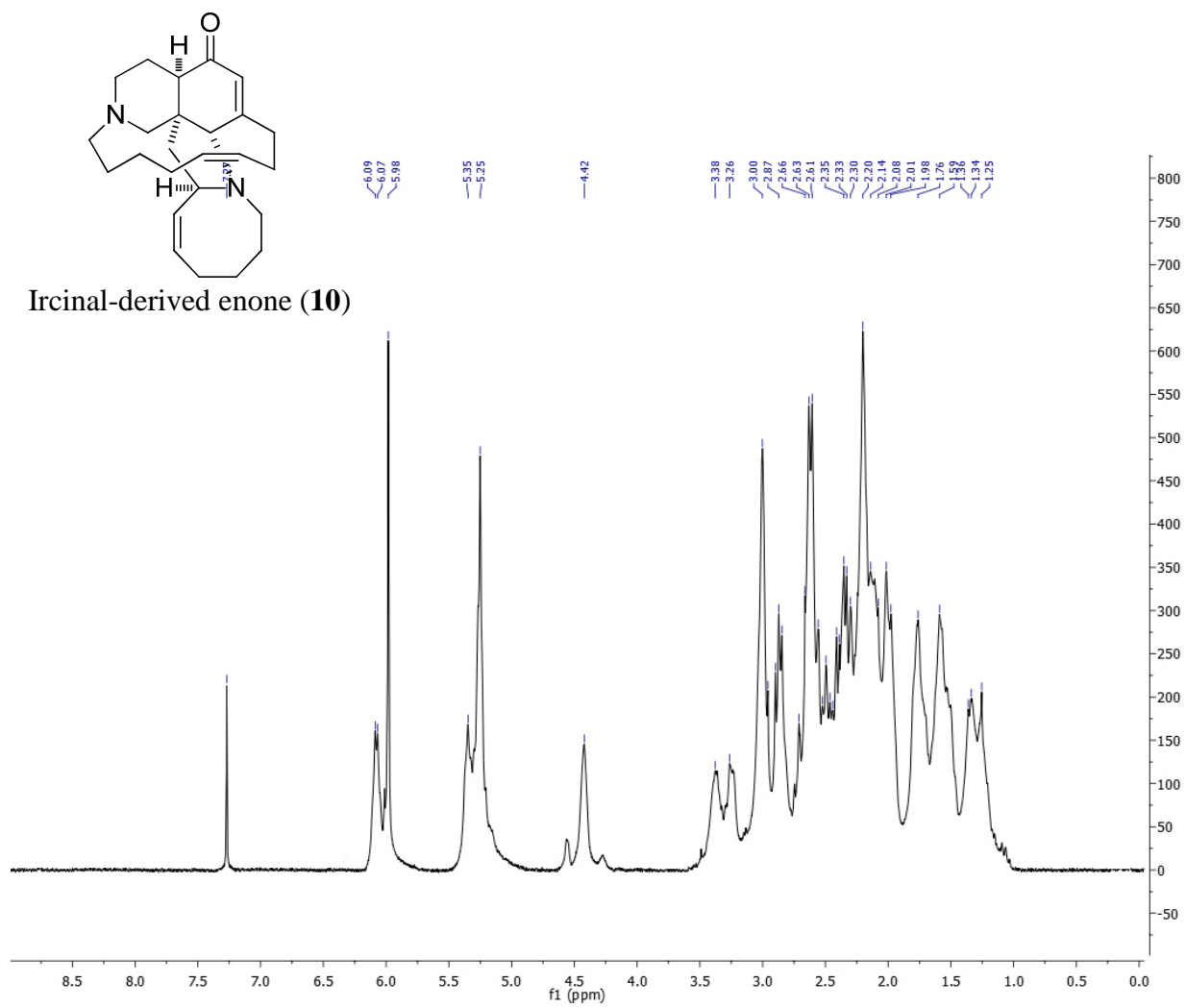
Figure II.50. ^{1}H-NMR of the ircinal-derived enone (**10**) in CDCl$_3$ at 400 MHz.

136
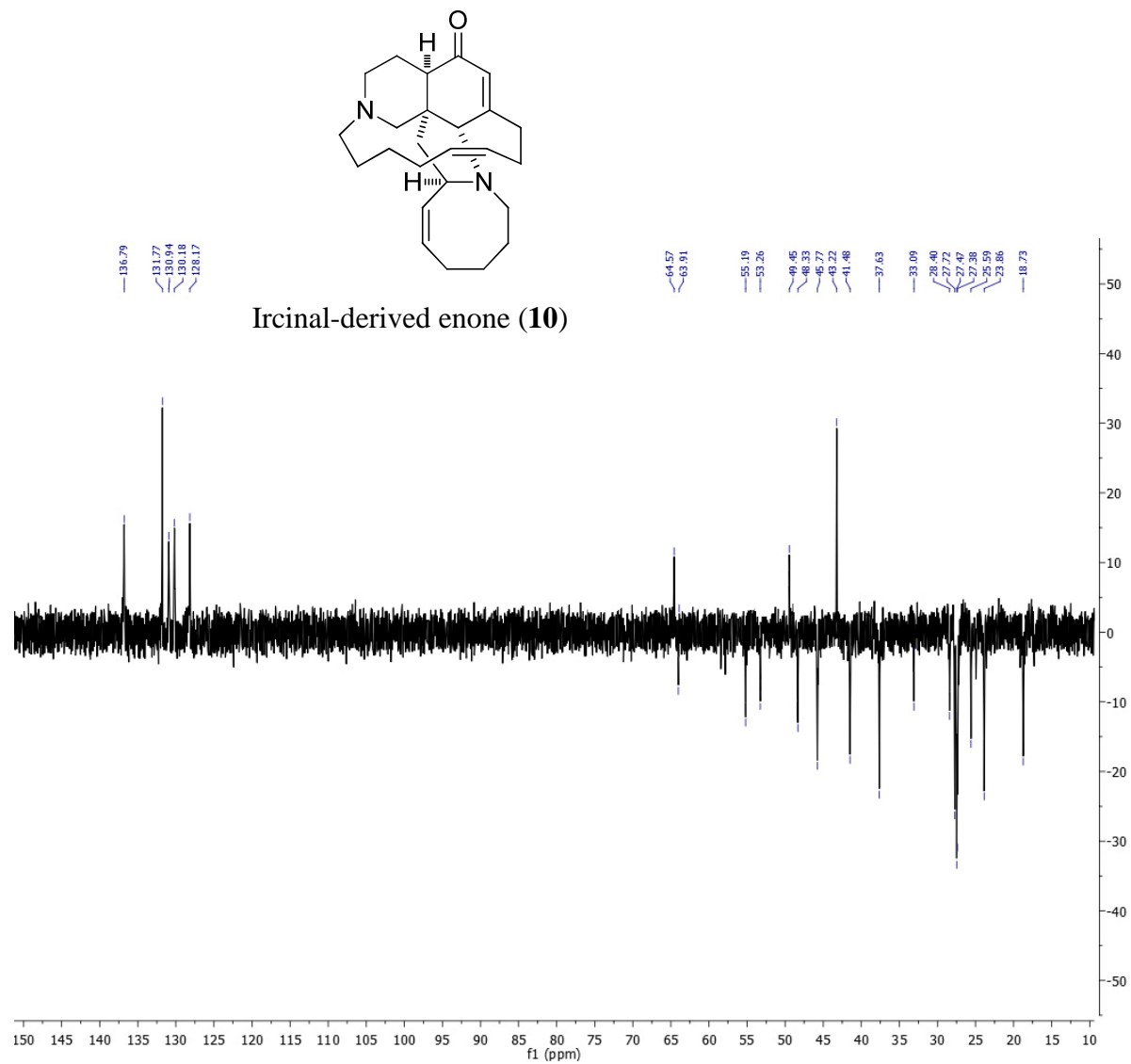
Figure II.51. [145]DEPT-NMR of the ircinal-derived enone (**10**) in CDCl₃ at 100 MHz.

Ircinal-derived enone (**10**)

Figure II.52. HMQC experiment of the ircinal-derived enone (**10**) in CDCl$_3$ at 400 MHz.

Reductive amidation of nitroarenes: a practical approach for the amidation of natural products

Amir E. Wahba [a], Jiangnan Peng [a], Mark T. Hamann [a,b,c,d,*]

CHAPTER III.

REDUCTIVE AMIDATION OF NITROARENES: A PRACTICAL APPROACH FOR THE

AMIDATION OF NATURAL PRODUCTS

Published in Tetrahedron Letters, 2009, 50, 3901-3904.

Authors: Amir E. Wahba, Jiangnan Peng, and Mark T. Hamann

Cited among the 'Best synthetic methods: Oxidation and Reductions, D. F. Taber, Org. Chem.

Highlights 2010, May 24

Abstract: A simple and practical approach for the one-pot conversion of nitroarenes into amide derivatives has been developed. HOAc/Zn are utilized as a reducing agent, and acyl chloride/Et$_3$N are used as the acylating agent in DMF with good yield (~60%) of the amide. This method was applicable to 6-nitromanzamine A, where the yield of 6-cyclohexamidemanzamine A (**7**) was significantly improved (56%) by this approach relative to starting with 6-aminomanzamine A (17%).

Introduction:

Aryl amides are important structural units of many biologically important compounds as well as a number of drug candidates (Figure III.1).[73] Usually, amide is obtained from the corresponding nitro analog in two separate steps: reduction of the nitro group to the corresponding 1° amine, followed by amidation with an activated carboxylic acid. Reduction of the nitro group to the corresponding 1° amine can be completed using a number of approaches. Metal catalyzed reduction is the most common in which a variety of metals/metal oxides/metal sulfides have been reported including: zinc,[74] iron,[75] platinum oxide,[76] palladium,[77] Raney nickel,[78] copper,[79] and ruthenium sulfide.[80]

Although the 1° amine can be purified and subsequently reacted with an activated carboxylic acid, stability of some 1° aromatic amines, especially complex natural product derived 1° amines, may affect the yield of the acylation reaction. Good examples of unstable amines are 6- and 8-aminomanzamine A (**5**, **6**). Manzamine A (**1**), the first representative of the manzamine alkaloids, was isolated by Higa and coworkers in 1986.[12] This class of compounds has shown a variety of bioactivities.[1] Although **1** and its 8-hydroxy analog (**2**) showed an outstanding antimalarial activities both in vitro and in vivo compared to the currently utilized first line antimalarial drugs, chloroquine and artemesinin,[57] their toxicities limited their development as a potential drugs. As part of a continued investigation of SAR and optimization studies of **1** against malaria, we prepared amide analogs of **1** for evaluation in vitro against chloroquine sensitive and resistant *P. falciparum* strains as well as their cytotoxicity (Chapter II.C).
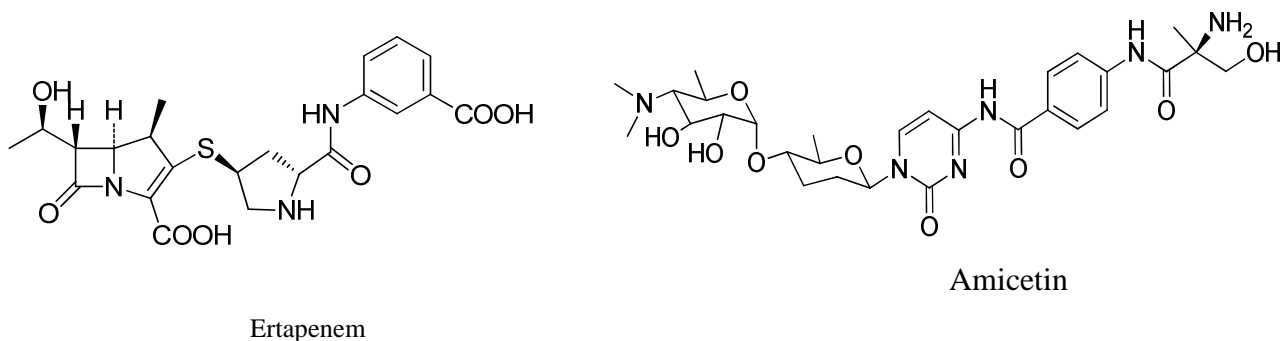
Figure III.1. Drugs that possess aryl amide moieties.

Nitration of **1** (Scheme III.1) by NaNO$_2$ and TFA gave two nitro products: 6- (**3**) and 8-nitromanzamine A (**4**). HOAc/Zn reduction of nitromanzamines afforded the corresponding aminomanzamines (**5, 6**), which were unstable even as the HCl salts. This lack of stability created numerous challenges during the amidation of aminomanzamines. These difficulties were the driving force to explore an effective, practical and gentle one-pot reductive amidation of nitroarenes.

Examples of a one-pot reductive amidation of nitroarenes have been reported. Watanabe using PtCl$_2$(PPh$_3$)$_2$/ tin(IV)chloride/CO/carboxylic acid as a reductive amidation system requires high temperature (180 °C) and pressure (60 atm),[81] and is not applicable to sensitive and complex natural products.
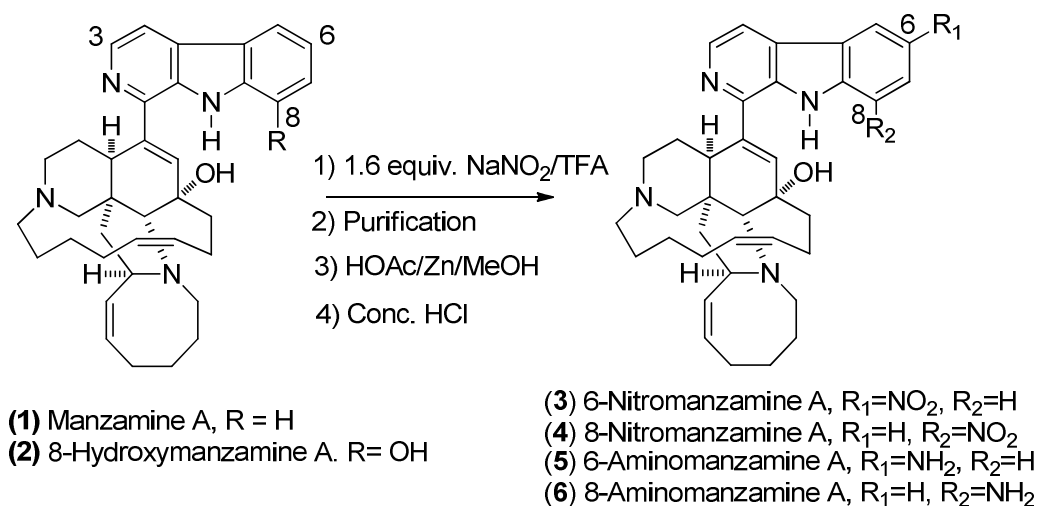
Scheme III.1. Nitration of manzamine A

Samarium diiodide has been used to reduce nitroarenes in the presence of a proton source to generate a nitrogen anion equivalent which can then be acylated with esters.[82] This method is valuable in regard to the use of esters as acylating agents. However the major disadvantage of this method is that the preformed nitrogen anion equivalent is basic enough to generate side reactions in complex natural products which normally have a diverse range of functional groups. Another disadvantage of using samarium diiodide is that it is sensitive to moisture, and requires highly dry reaction conditions. Limited examples for reductive acetamidation are reported. One example uses nucleophilic attack of thioacetate anion at the nitro group,[83] providing acetamide derivative without the intermediate amine. This method could be expanded for the synthesis of amides other than acetamide, but it is not applicable to a complex structure with base sensitive functional groups such as **1.** Dehydration of the allylic 3° hydroxy group at C-12 is always obtained as a byproduct in most of the base mediated reactions of **1**.[84] Kim has used zinc and

acetic anhydride for the conversion of nitroarenes into *N,O*-diacetylated *N*-arylhydroxyamines in good yields. However, the acetamide yields were low.[85] Furthermore, Kim reported high yields of the acetamide derivatives when nitroaromatics were treated with acetic anhydride and acetic acid catalyzed by indium, with trace yield of the diacetylated product.[86] These two methods, although showed selectivity to both products and high yields of each, are not applicable to manzamine A or related structures. Manzamine alkaloids have yielded unexpected rearranged products when treated with acetic anhydride.[17] We report here the reductive amidation of nitroarenes promoted by zinc and acetic acid as the reducing system and acyl chloride and triethylamine as the acylating agent in a one-pot approach. Application to manzamine alkaloids is utilized as an example of the applicability of this method to complex natural products.

Reduction of the nitro group generally requires a protic solvent as a carrier of hydrogen generated in situ. However, amidation reaction using acyl chloride requires aprotic solvent as well as dry conditions to prevent a side reaction with the solvent. In addition, amidation reaction using acyl chlorides require basic conditions, in which the base will neutralize hydrochloric acid librated from the reaction as a by-product. Because of this contrast, we decided to explore the ability of adding 3° amine base (Et$_3$N) in the reduction step, where equimolecular amounts of acetic acid and zinc are used, in addition to the acyl chloride. Once the 1° amine is formed in situ, it will immediately react with the acyl chloride facilitated by the 3° amine base. Solvent optimization of this one-pot reaction was completed using 4-nitroanisole and butyryl chloride as a test reaction (Table III.1).

Table III.1. Solvent optimization for the reductive amidation reaction
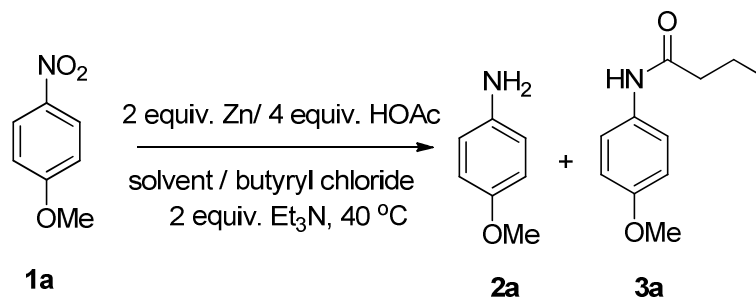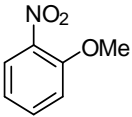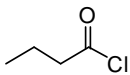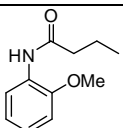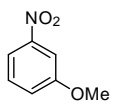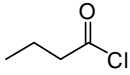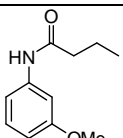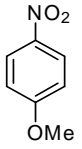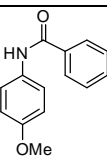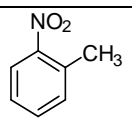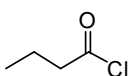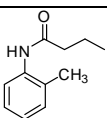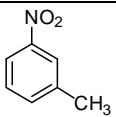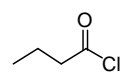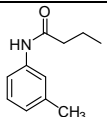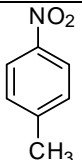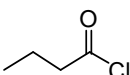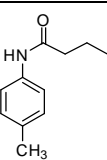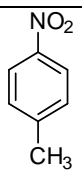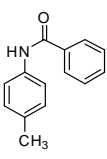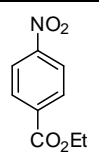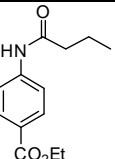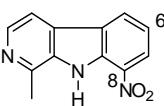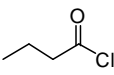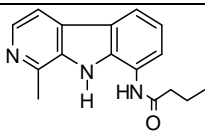
Entry	Solvent	Time (h)	Yield[a] (%)	
			2a	**3a**
1	MeOH	4	98	0
2	DCM	4	80	15
3	DMF	4	30	65
4	Toluene	4	60	37

[a] Isolated yield

All reactions were done using 1.0 mmol of 4-nitroanisole

All reactions showed complete conversion of the starting material

Table III.2. Reductive amidation of several nitroarenes

Entry	Starting material	Acyl chloride	Time (h)	Amide product	Yield[a] (%)
1			4.5		64
2			4		58
3			5		60
4			4		56
5			4		51
6			4.5		62
7			5		64
8			5.5		53
9			0.5		55[b]

| 10 | | | 0.5 | | 58[b] |

---
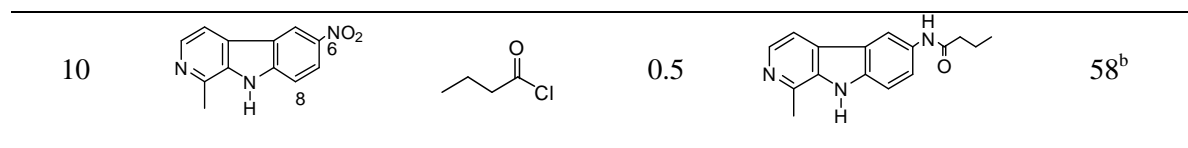
[a] Isolated yields.

[b] Reactions were done using 0.4 mmol of nitroharmanes

All reactions were done using 1.0 mmol of starting material

DMF gave the best results, in which the yield of the amide obtained from the nitro compound was the same as that obtained from the corresponding amine. Using the optimized reaction conditions, we screened several nitro compounds with butyryl chloride as well as other acyl chlorides (Table III.2). All reactions showed 100% conversion of starting material to the corresponding amines and amides, with moderate to good yield of the amides.

After optimizing the reaction conditions, we investigated the applicability of this reaction to the synthesis of 6-cyclohexamidemanzamine A (**7**) (scheme III.2). This amide analog was synthesized from **5** using normal amidation reaction with low yield (17%). This analog showed potent antimalarial activity in vitro with an IC_{50} of 0.032 μM against the D6 clone of *P. falciparum* with no cytotoxicity up to 4.7 μM. It was surprising that the reductive amidation of **3** with cyclohexylcarbonyl chloride (CCC) runs smoothly and quickly (10 min.) without the addition of Et_3N and with a significant improvement in the yield (56%). A reasonable explanation is that nitromanzamines have two internal 3° amino functionalities, which likely accelerate the amidation reaction.

Method A, X=H, yield = 17%

Method B, X=O, yield = 56%

X=H, **5**
X=O, **3**

(**7**)
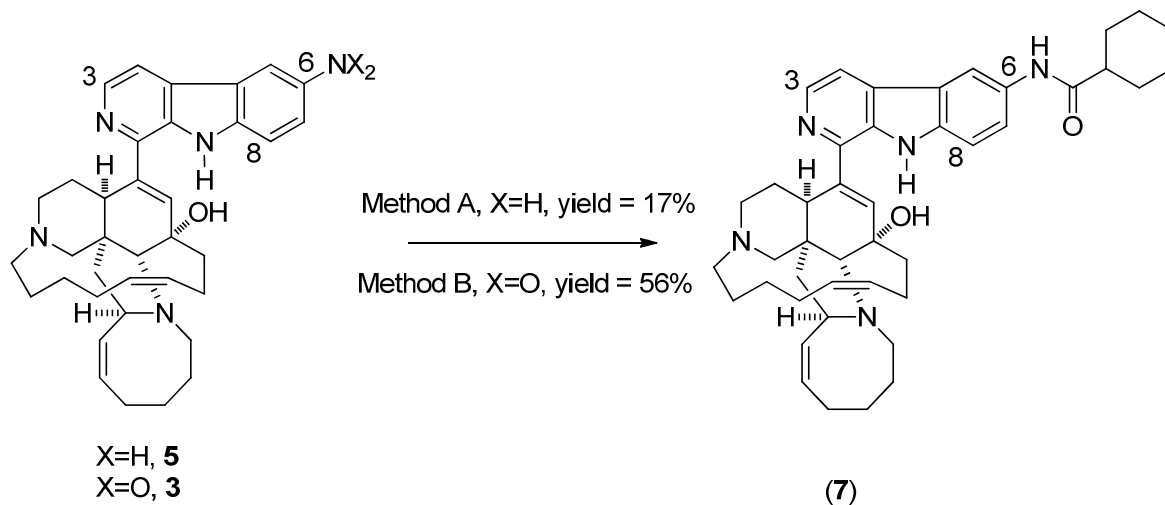
Method A: 1.2 equiv. CCC, 1.1 equiv. Et$_3$N, cat. DMAP, THF, rt, 1 h

Method B: Reductive amidation approach

Scheme III.2. Amidation of manzamine A

To validate this, we utilized harmane (**8**) as a precursor to the synthesis of the closely related model compounds 6-nitroharmane (**9**) and 8-nitroharmane (**10**). Harmane (**8**) was nitrated using the same conditions as **1** (Scheme III.3) which gave **9** and **10** in 45% and 43% yields, respectively. Applying the reductive amidation conditions to **9** and **10** without the addition of Et$_3$N did not gave the amides, even after 12 h of stirring. The amides of **9**, **10** were obtained after the addition of Et$_3$N to the solution (Table III.2, entry 9 and 10). These results clearly validated our explanation regarding the 3° amino capacity of manzamine alkaloids.
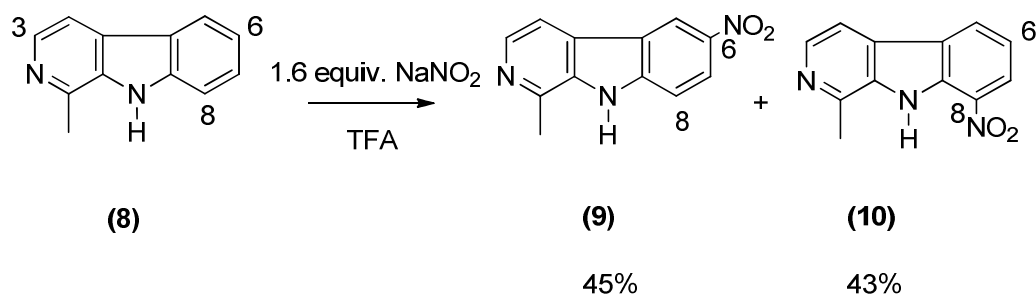
Scheme III.3. Nitration of harmane

In conclusion, this is the first report of using 3° amine base in the reduction step of the nitro compounds in addition to acyl chloride in a one-pot approach to form the corresponding amides. The yields of the amides are reasonable for the model compounds however more significant is that the reaction conditions are mild and well tolerated with **1** and showed significant improvement in the yield of the amide analog of **1**. This reaction is certain to have utility in the optimization studies of various natural product heterocyclic systems.

General Experimental Procedures. ^{1}H- and ^{13}C-NMR spectra were recorded in CDCl₃, *d4*-methanol, or *d6*-acetone on a Bruker Avance NMR spectrometer operating at 400 MHz for ^{1}H and 100 MHz for [13]C. Chemical shift (δ) values are expressed in parts per million (ppm) and are referenced to the residual solvent signals of the solvent used. UV and the high resolution ESI-MS spectra were measured using a Bruker Daltonics (GmbH, Germany) micrO-TOF series with electrospray ionization. TLC analysis was carried out on precoated silica gel G254 aluminum plates. Reagents were purchased from Aldrich and used without further purification. Reactions were carried out in oven-dried glassware.

General procedure for reductive amidation: Et₃N (0.002 mole), zinc (0.002 mole), acetic acid glacial (0.004 mole), and the acyl chloride (0.0013 mole) was added to a solution of the

nitroarene (1 mmol) in anhydrous DMF.[1] The mixture was stirred at 40 $^{\circ}$C for about 5 h. Water (10 mL) was added to the reaction mixture and extracted with ethyl acetate (3x10 mL). The organic layer was dried over anhydrous Na$_2$SO$_4$ and evaporated under vacuum. The crude products were purified by silica column using 98:2 *n*-hexane:acetone.

6-Cyclohexamidemanzmaine A (7):

Method A: 6-aminomanzamine A (100 mg, 0.177 mmol) and catalytic amount of DMAP were dissolved in anhydrous THF (3 mL) under nitrogen atmosphere. Et$_3$N (25 µL, 0.177 mmol) was then added, and the mixture was stirred at room temperature for 10 minutes. Cyclohexylcarbonyl chloride was added (1.2 equiv.), and the reaction mixture was stirred for 1 h. The completion of the reaction was monitored by TLC, then the reaction was quenched with water, and the product was extracted by DCM (3x10 mL). The organic layer was dried over anhydrous sodium sulphate, and then evaporated under reduced pressure. Purification of **7** was carried out on a Phenomenex Luna C8 250x10 mm, 5µm HPLC column using a gradient form CH$_3$CN (0.1% TFA)/water (0.1% TFA) with flow rate of 6 mL/min to give **7** (20 mg, 17.62%)

Method B (reductive amidation method): 6-nitromanzmaine A (100 mg, 0.169 mmol) was utilized with the general reductive amidation procedure above without the addition of Et$_3$N. The crude reaction mixture after evaporation was purified on a Phenomenex Luna C8 250x10 mm, 5 µm HPLC column using a gradient CH$_3$CN (0.1% TFA)/water (0.1% TFA) with flow rate of 6 mL/min to give **7** (63.5 mg, 55.94%).

Nitration of harmane: harmane **(8)** (1 g, 5.494 mmol) was dissolved in TFA (40 ml., 0.538 mmol), and kept at 0 $^{\circ}$C with stirring for 30 min. Sodium nitrite (0.6 g, 8.695 mmol) was added in one portion and allowed to stir at 0 $^{\circ}$C for an additional 3 h. The reaction mixture was poured

---

[1] After the addition of all the reagents, the pH should be around 6. If not, 0.001 mole of Et$_3$N was added.

into water and neutralized by ammonium hydroxide producing a precipitate that was filtered and dried. The crude nitro products of harmane were loaded onto a column packed with 50 g of silica gel. 8-Nitroharmane (**9**) was eluted first with 99:1 DCM:MeOH, followed by 6-nitroharmane (**10**) after the mobile polarity was increased with 95:5 DCM:MeOH (opposite to manzamine A).

6-Nitroharmane (9): (0.56 g, 45.16%); yellow powder; IR: 3020, 2951, 2587, 2079, 1664, 1637, 1534, 1490, 1428, 1402, 1336.93, 1319, 1286, 1266, 1206, 1179, 1131, 1118, 1054, 990, 836, 820, 794, 751, 742, 730 cm^{-1}; ^{1}H-NMR (CDCl$_3$) δ 8.83 (1H, d, *J*=2.4 Hz), 8.13 (1H, d, *J*=2.4 Hz), 8.11 (1H, d, *J*=2.4 Hz), 8.08 (1H, d, *J*=6.8 Hz), 7.96 (1H, d, *J*=6.8 Hz), 7.38 (1H, d, *J*=8.0 Hz), 2.87 (s); ^{13}C-NMR (CDCl$_3$) δ 145.59, 141.93, 139.86, 135.56, 132.58, 130.42, 125.24, 119.59, 119.43, 115.35, 112.63, 15.29; HRESIMS *m/z* calcd for C$_{12}$H$_{10}$N$_3$O$_2$ (M+H)$^+$ 228.0773, found 228.0770.

8-Nitroharmane (10): (0.54 g, 43.54%) yellow powder; IR: 3020, 2951, 2587, 2079, 1664, 1637, 1534, 1490, 1428, 1402, 1336.93, 1319, 1286, 1266, 1206, 1179, 1131, 1118, 1054, 990, 836, 820, 794, 751, 742, 730 cm^{-1}; ^{1}H-NMR (CDCl$_3$) δ 9.87 (s, brd), 8.44 (1H, d, *J*=5.6 Hz), 8.41 (1H, d, *J*=8.0 Hz), 8.37 (1H, d, *J*=8.0 Hz), 7.78 (1H, d, *J*=5.6 Hz), 7.33 (1H, t, *J*=8.0 Hz), 2.86 (s); ^{13}C-NMR (CDCl$_3$) δ 143.32, 140.84, 134.85, 133.97, 133.29, 129.23, 127.58, 126.39, 124.43, 119.61, 112.87, 20.43; HRESIMS *m/z* calcd for C$_{12}$H$_{10}$N$_3$O$_2$ (M+H)$^+$ 228.0773, found 228.0770.

6-*n*-Butamidoharmane (TableIII.2, entry 10): starting from 6-nitroharmane (**9**, 100 mg, 0.441 mmol) and using the general reductive amidation procedure above: (64.35 mg, 54.71%); ^{1}H-NMR (CDCl$_3$) δ 8.56 (s), 8.23 (1H, d, *J*=8.0 Hz), 8.20 (1H, d, *J*=6.0 Hz), 7.75 (1H, d, *J*=8.8 Hz), 7.61(1H, d, *J*=8.0 Hz), 2.97 (s), 2.43 (2H, t, *J*=7.6 Hz), 1.79 (2H, p, *J*=8.0 Hz), 1.06 (3H, t, *J*=8.0 Hz); ^{135}DEPT (CDCl$_3$) δ 130.15 (CH), 126.62 (CH), 115.86 (CH), 114.78 (CH), 113.68 (CH),

39.69 (CH_2), 20.33 (CH_3), 20.03 (CH_2), 13.93 (CH_3). HRESIMS *m/z* calcd for $C_{16}H_{18}N_3O$ (M+H)$^+$ 268.1450, found 268.1448.

8-*n*-Butamidoharmane (TableIII.2, entry 9): starting from 8-nitroharmane (**10**, 100 mg, 0.441 mmol) and using the general reductive amidation procedure: (67.86 mg, 57.69%); ^{1}H-NMR (CDCl$_3$) δ 8.03 (1H, d, *J*=6.0 Hz), 7.72 (1H, d, *J*=8.0 Hz), 7.67 (1H, d, *J*=8.0 Hz), 7.64 (1H, d, *J*=6.0 Hz), 7.05 (1H, t, *J*=8.0 Hz), 2.90 (s), 2.21 (2H, t, *J*=7.2 Hz), 1.73 (2H, p, *J*=8.0 Hz), 0.91 (3H, t, *J*=7.2 Hz); ^{135}DEPT (CDCl$_3$) δ 131.31 (CH), 119.95 (CH), 118.01 (CH), 114.02 (CH), 113.04 (CH), 39.11 (CH_2), 19.71 (CH3), 19.07 (CH_2), 13.79 (CH_3), HRESIMS *m/z* calcd for $C_{16}H_{18}N_3O$ (M+H)$^+$ 268.1450, found 268.1448.

4-(*n*-butamido)anisole (**Table III.2, entry 3**)
^{1}H-NMR (CDCl$_3$)
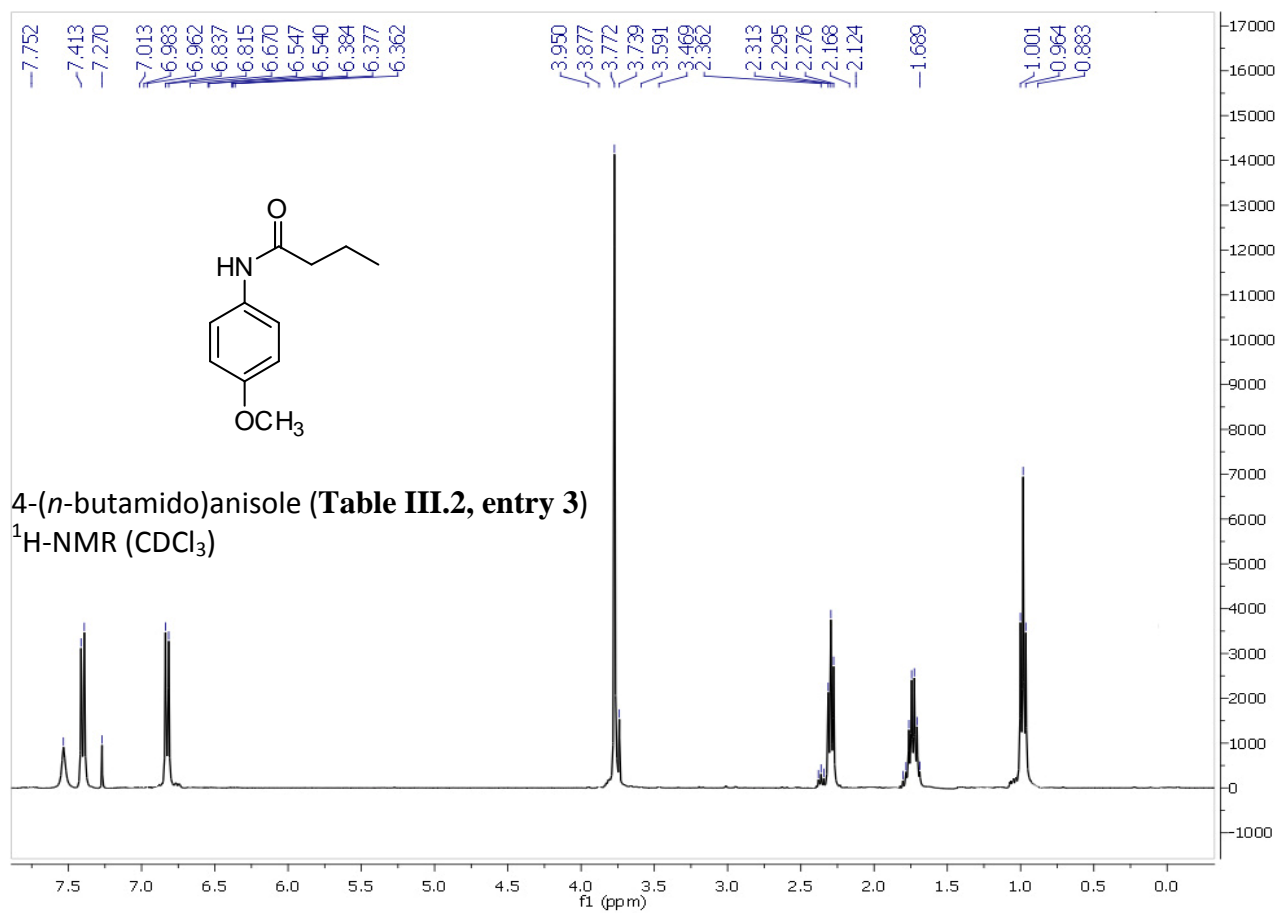
Figure III.2. ^{1}H-NMR of 4-(*n*-butamido)anisole (**Table III.2, entry 3**) in CDCl$_3$ at 400 MHz.

2-(*n*-butamido)anisole (**Table III.2, entry 1**)
^{1}H-NMR (CDCl$_3$)
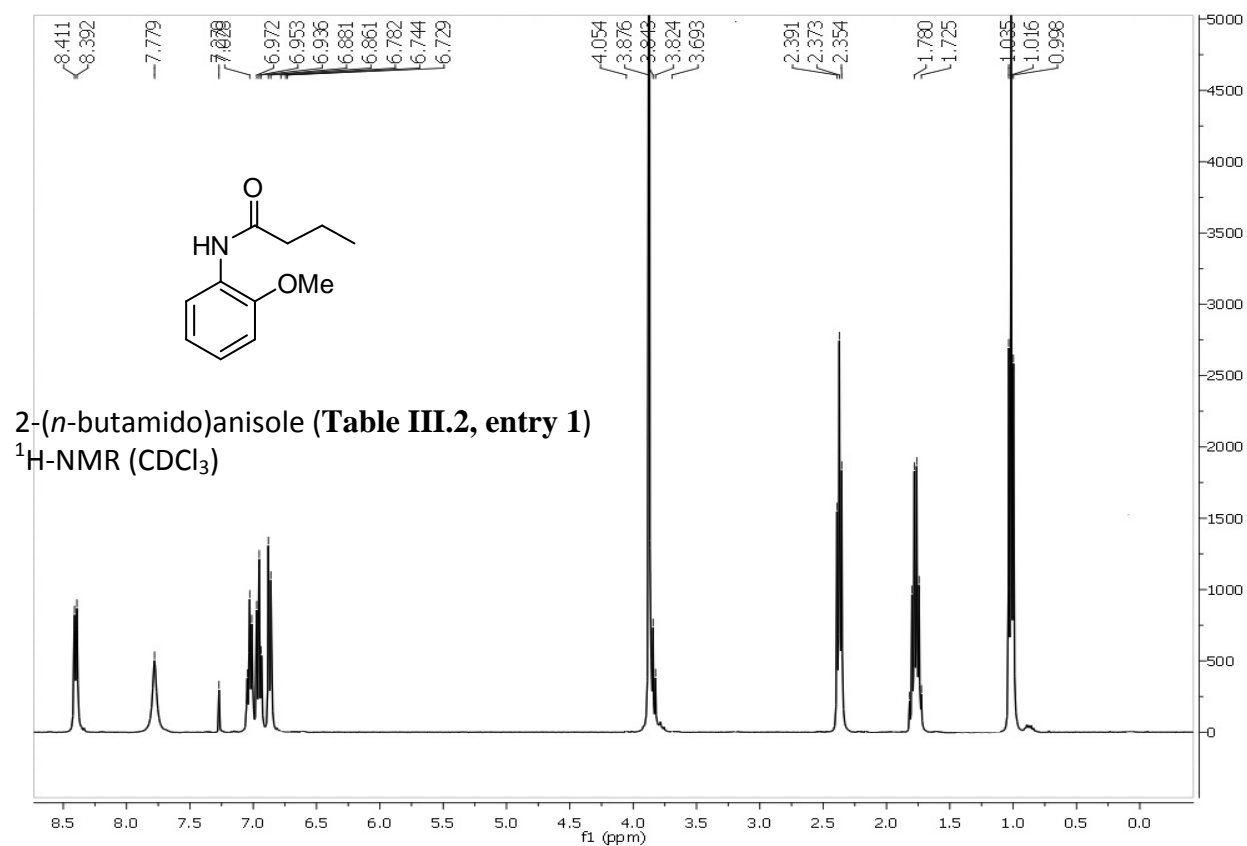
Figure III.3. ^{1}H-NMR of 2-(*n*-butamido)anisole (**Table III.2, entry 1**) in CDCl$_3$ at 400 MHz.

3-(*n*-butamido)anisole (**Table III.2, entry 2**)
^{1}H-NMR (CDCl$_3$)
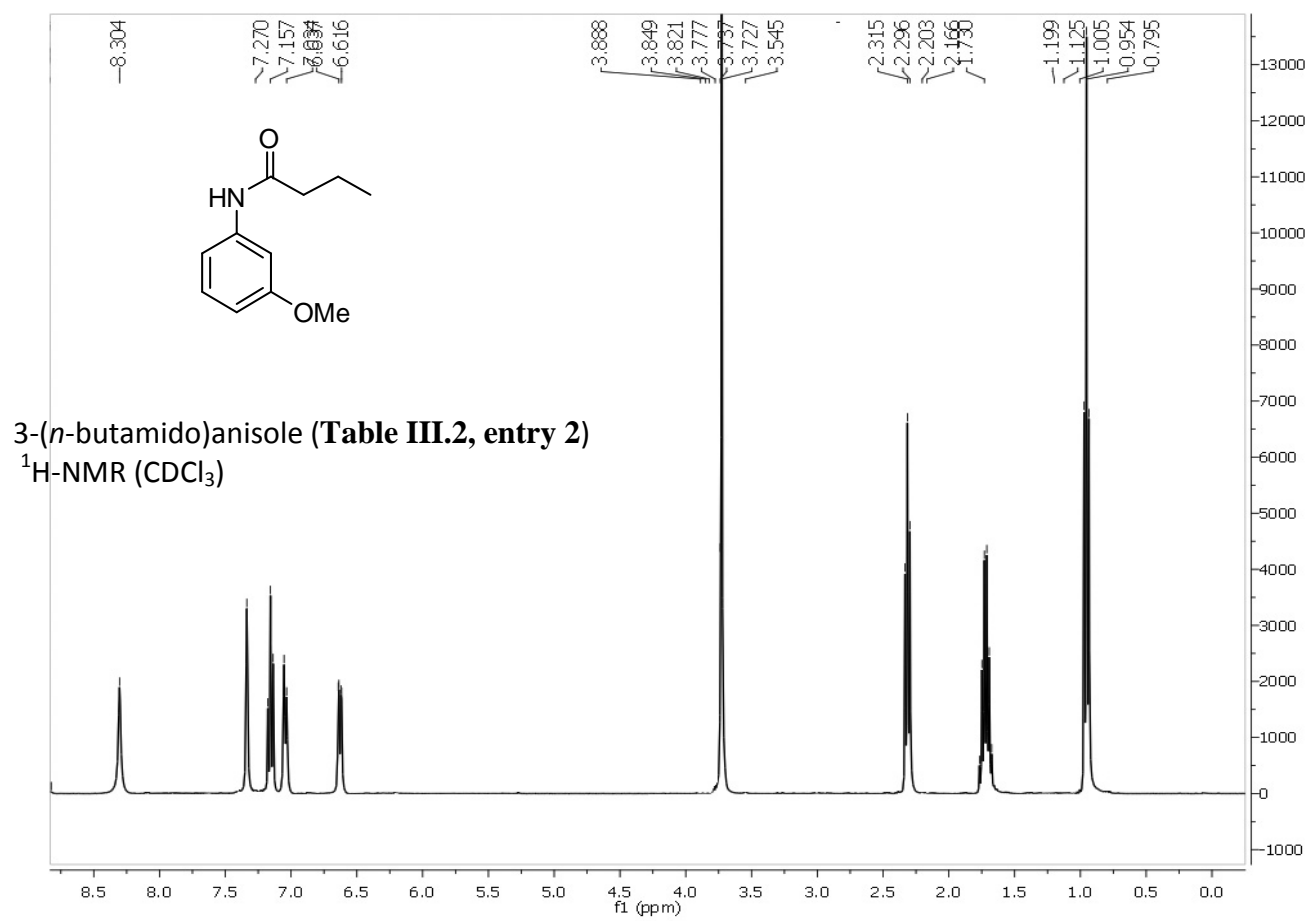
Figure III.4. ^{1}H-NMR of 3-(*n*-butamido)anisole (**Table III.2, entry 2**) in CDCl$_3$ at 400 MHz.

2-(*n*-butamido)toulene (**Table III.2, entry 4**)
¹H-NMR (CDCl₃)
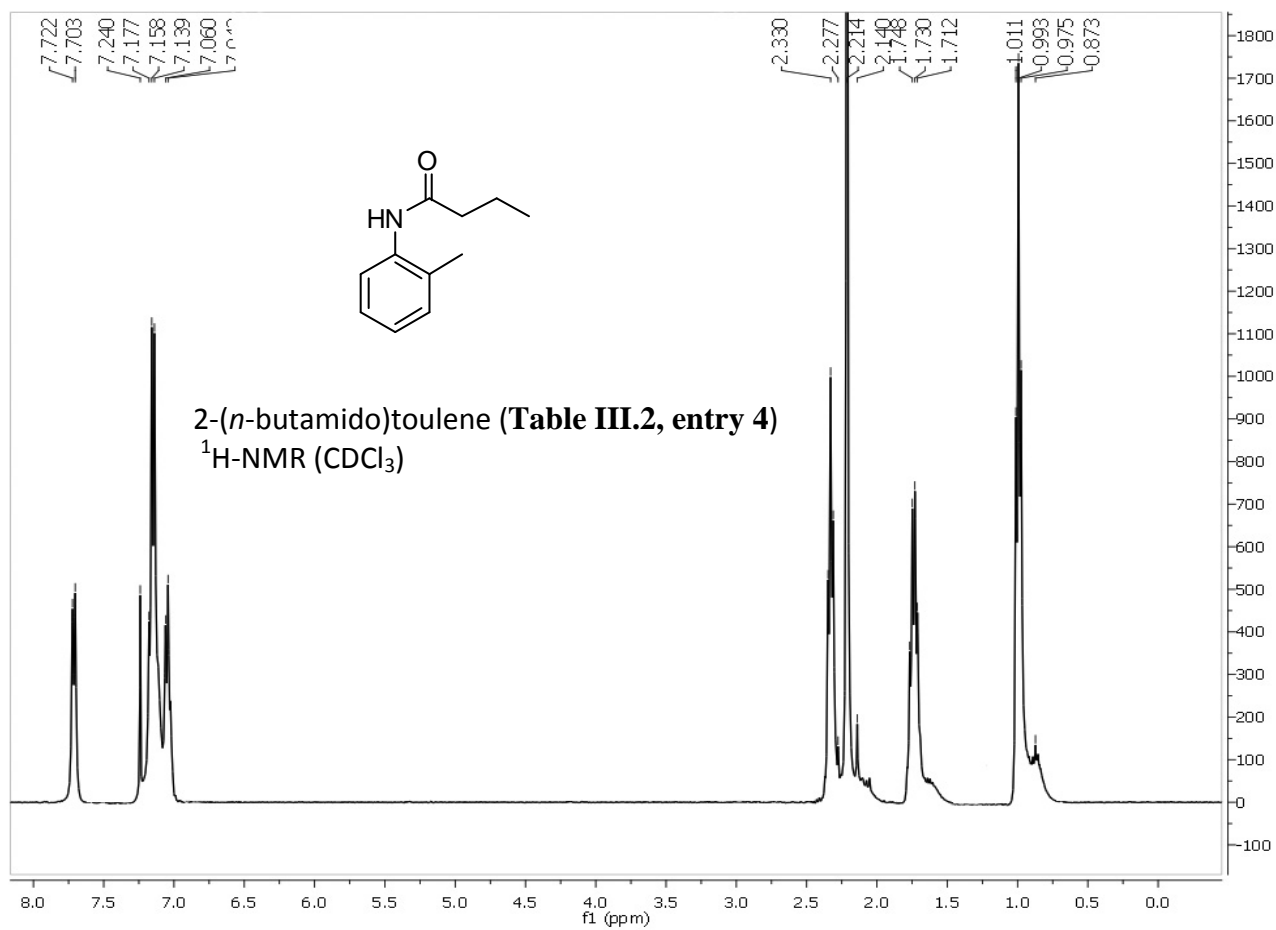
Figure III.5. ¹H-NMR of 2-(*n*-butamido)toulene (**Table III.2, entry 4**) in CDCl₃ at 400 MHz.

3-(*n*-butamido)toulene (**Table III.2, entry 5**)
^{1}H-NMR (CDCl$_3$)
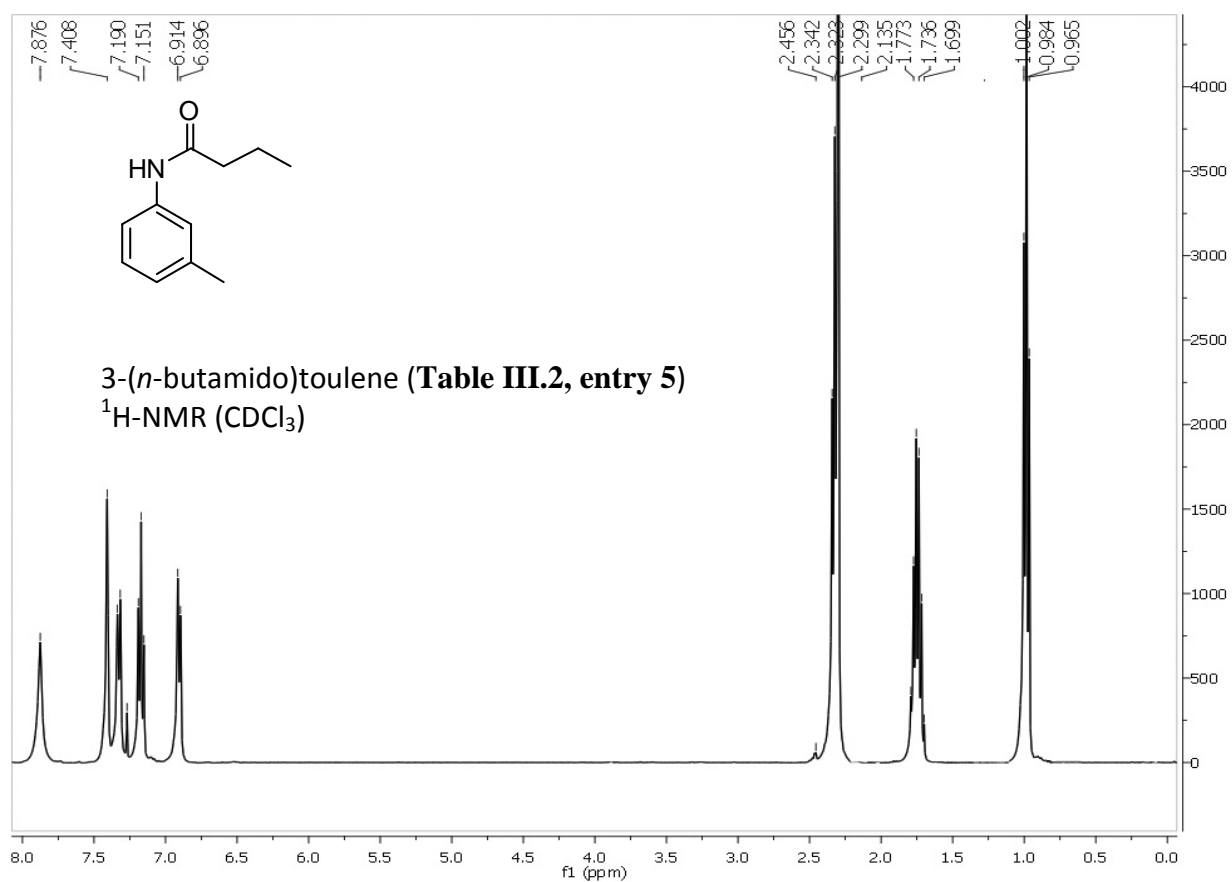
Figure III.6. ^{1}H-NMR of 3-(*n*-butamido)toulene (**Table III.2, entry 5**) in CDCl$_3$ at 400 MHz.

4-(*n*-butamido)toulene (**Table III.2, entry 6**)
^{1}H-NMR (CDCl$_3$)
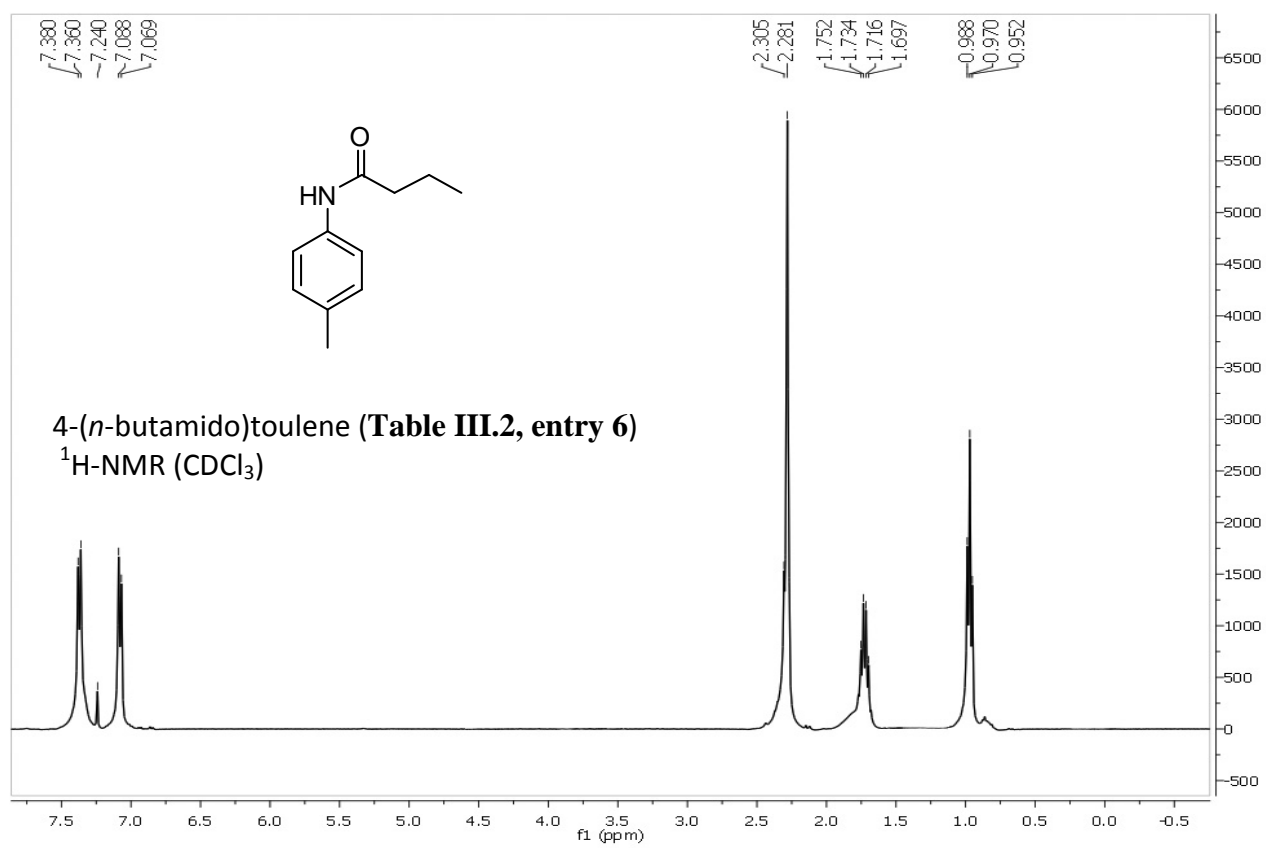
Figure III.7. ^{1}H-NMR of 4-(*n*-butamido)toulene (**Table III.2, entry 6**) in CDCl$_3$ at 400 MHz.

4-(benzamido)toulene (**Table III.2, entry 7**)
^{1}H-NMR (CDCl$_3$)
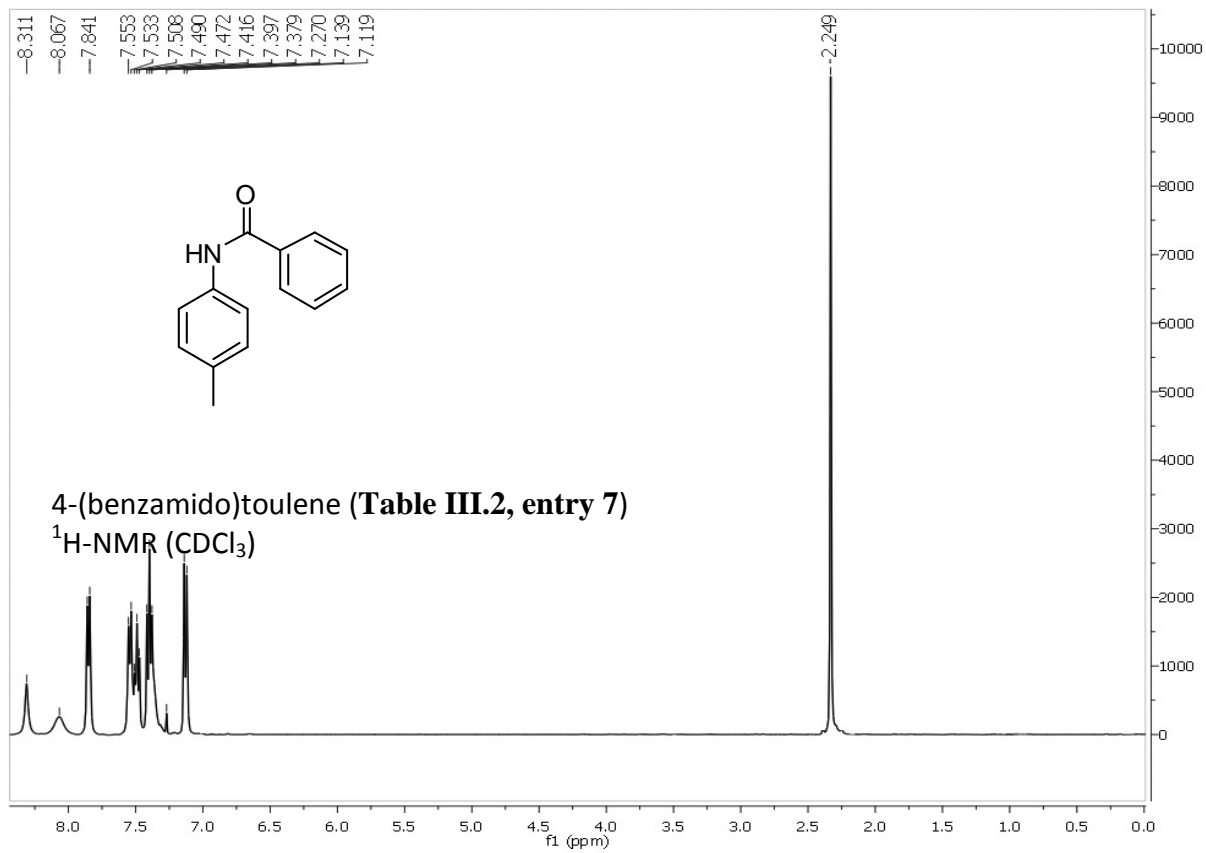
Figure III.8. ^{1}H-NMR of 4-(benzamido)toulene (**Table III.2, entry 7**) in CDCl$_3$ at 400 MHz.
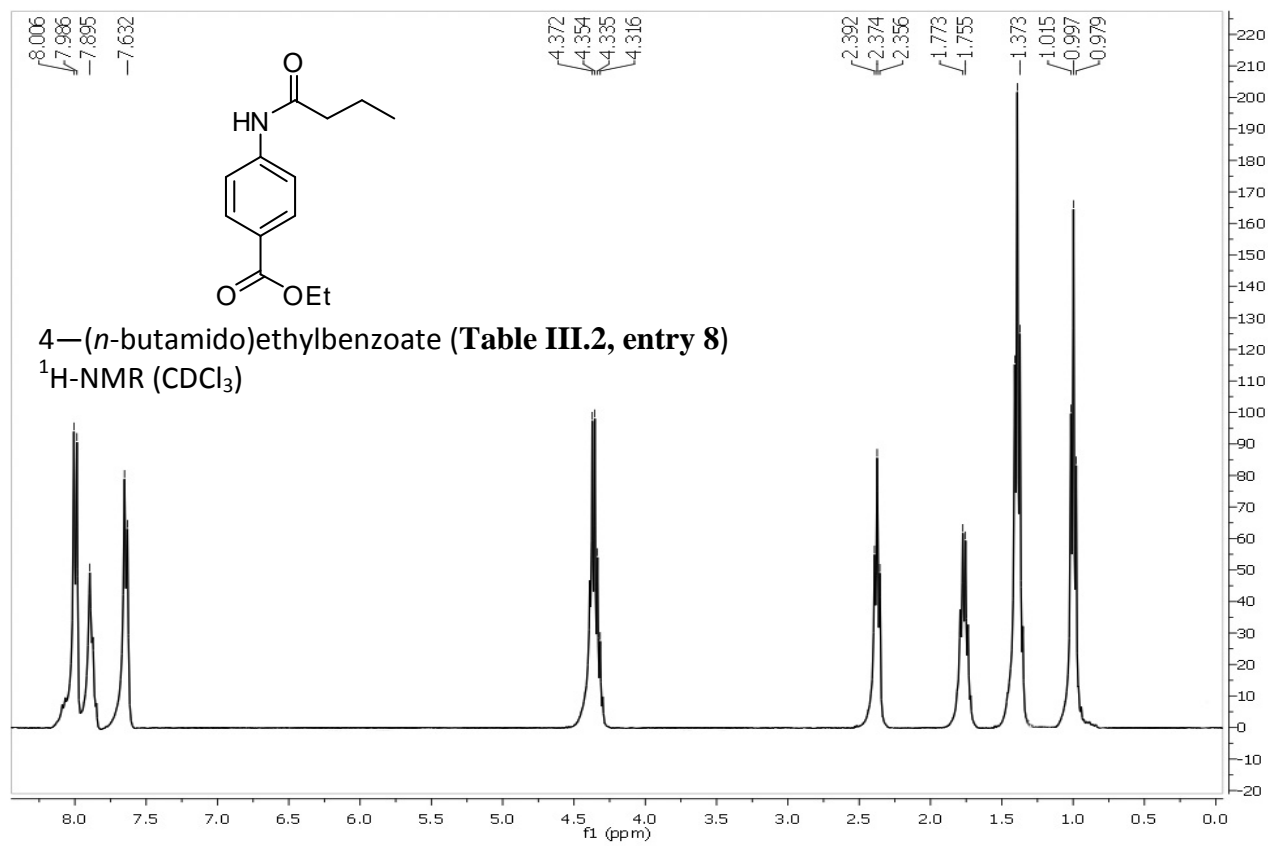
Figure III.9. ^{1}H-NMR of 4-(*n*-butamido)ethylbenzoate (**Table III.2, entry 8**) in CDCl$_3$ at 400

MHz.
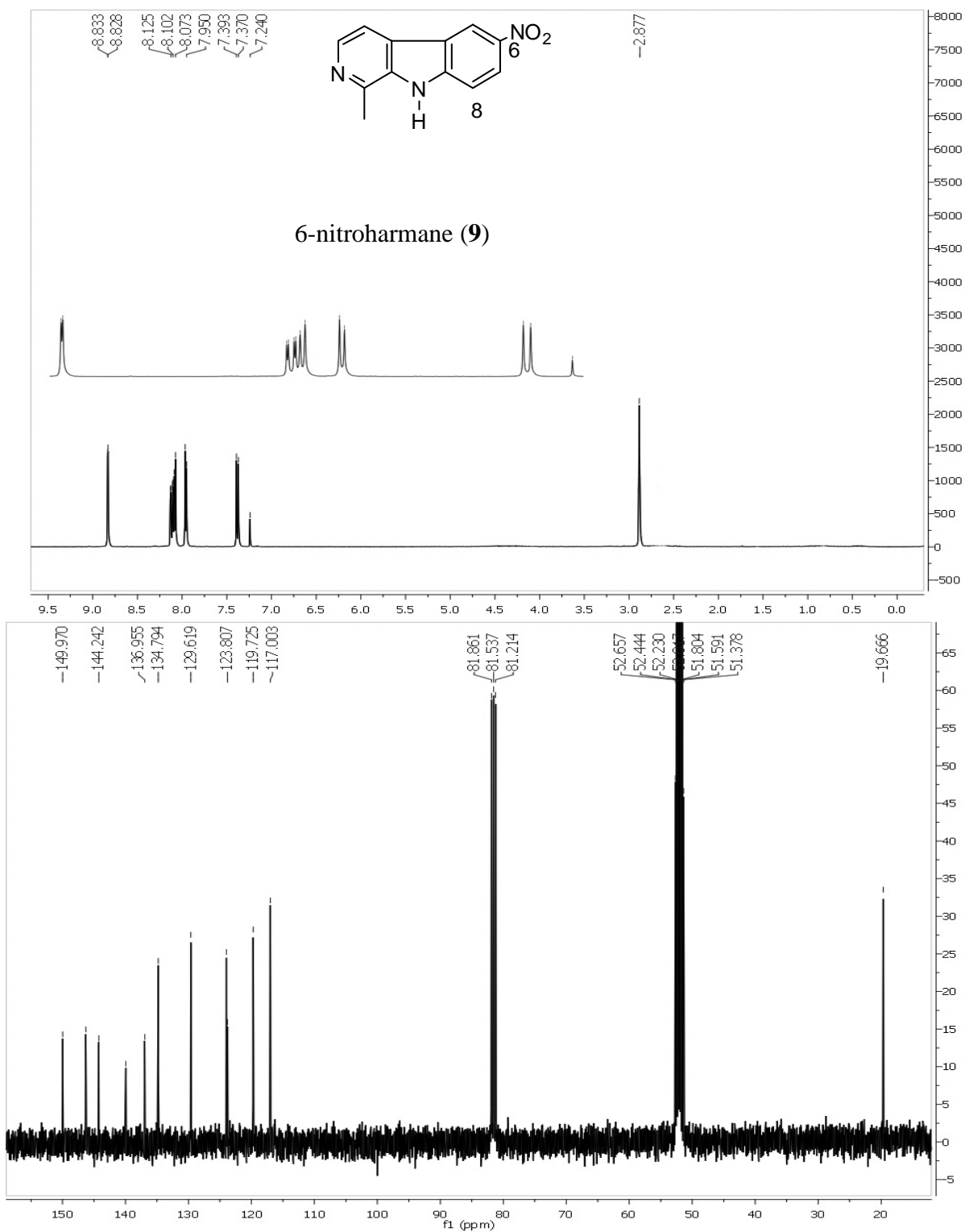
Figure III.10. ^{1}H- and ^{13}C-NMR spectra of 6-nitroharmane (**9**) in CDCl$_3$ at 400 and 100 MHz, respectively.
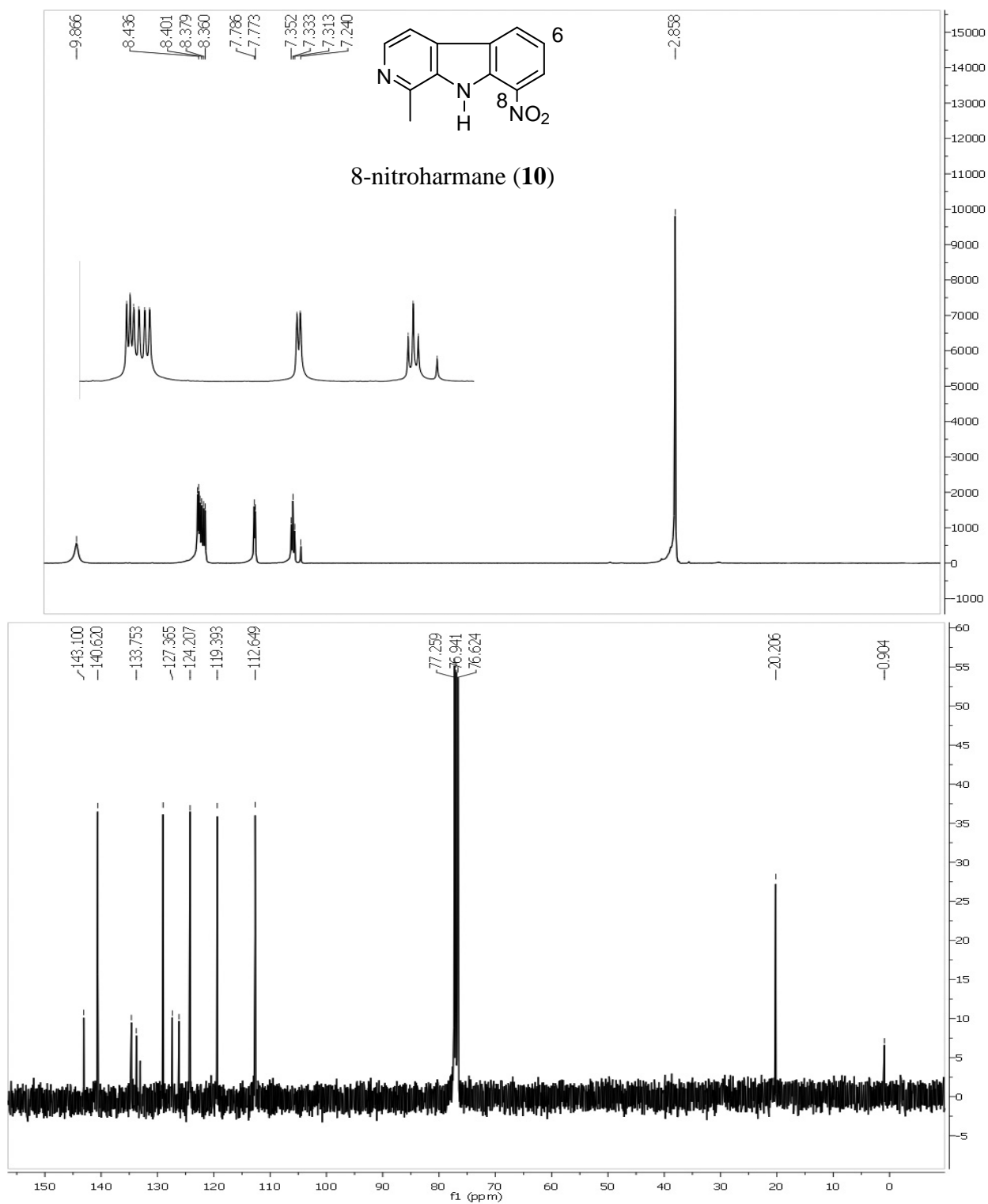
Figure III.11. ^{1}H- and ^{13}C-NMR spectra of 8-nitroharmane (**10**) in CDCl$_3$ at 400 and 100 MHz, respectively.

6-*n*-Butamidoharmane (**Table III.2, entry 10**)
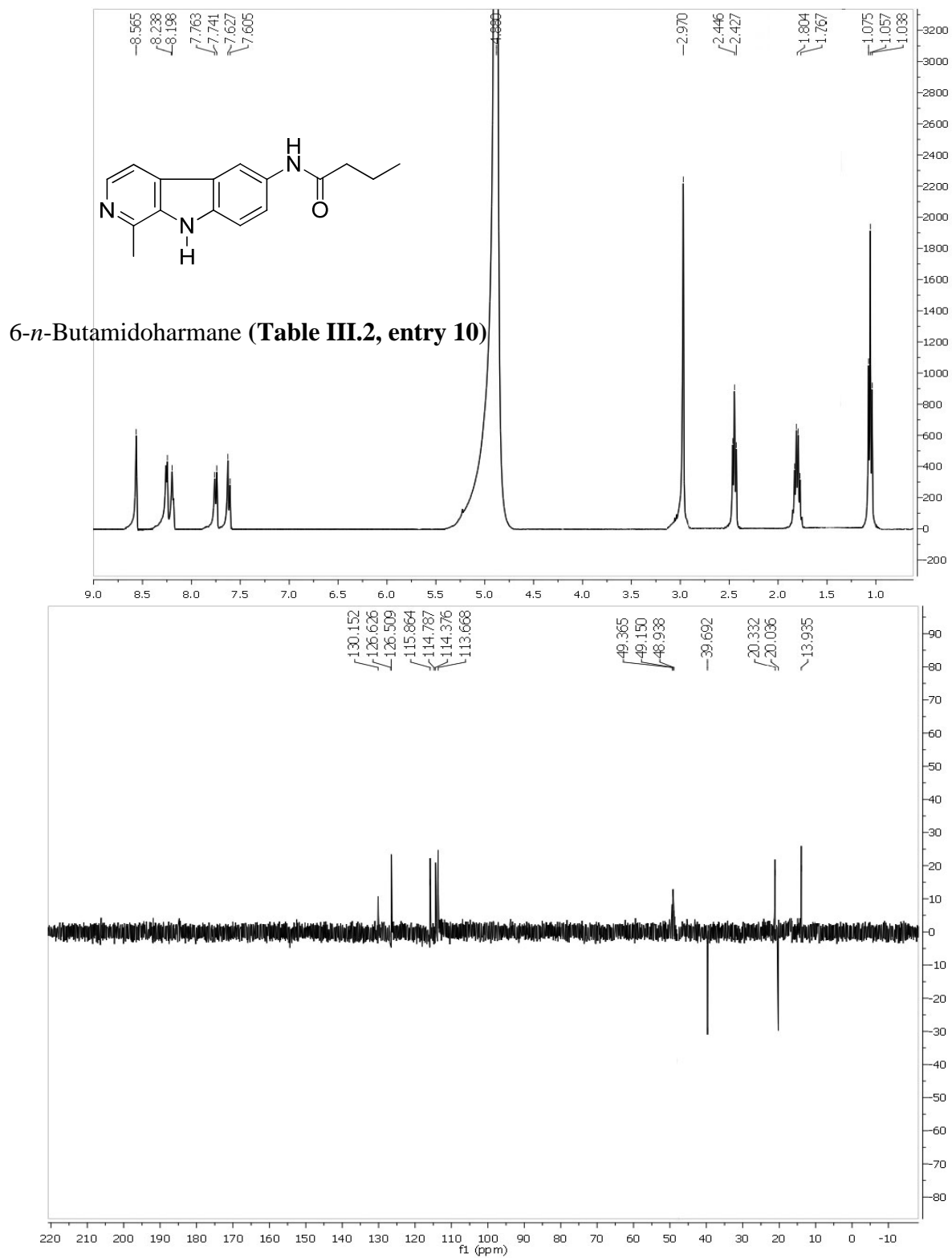
Figure III.12. ^{1}H- and ^{135}DEPT-NMR spectra of 6-*n*-butamidoharmane (**Table III.2, entry 10**) in CDCl$_3$ at 400 and 100 MHz, respectively.

8-*n*-Butamidoharmane (**Table III.2, entry 9**)
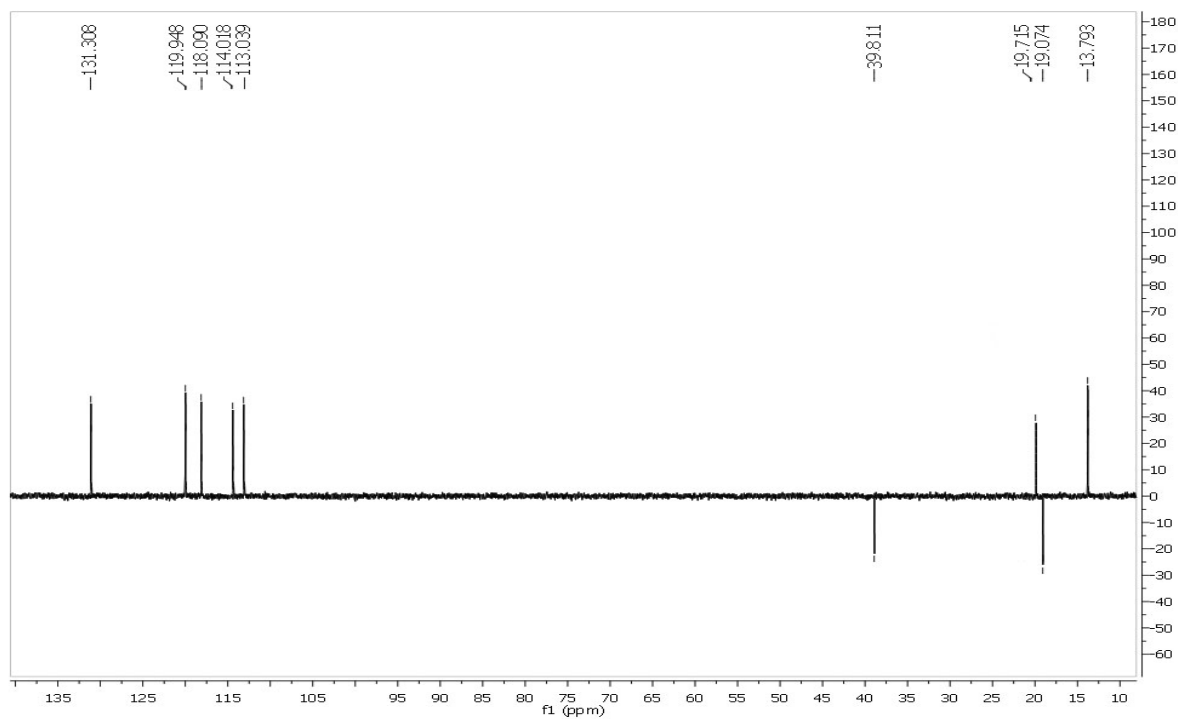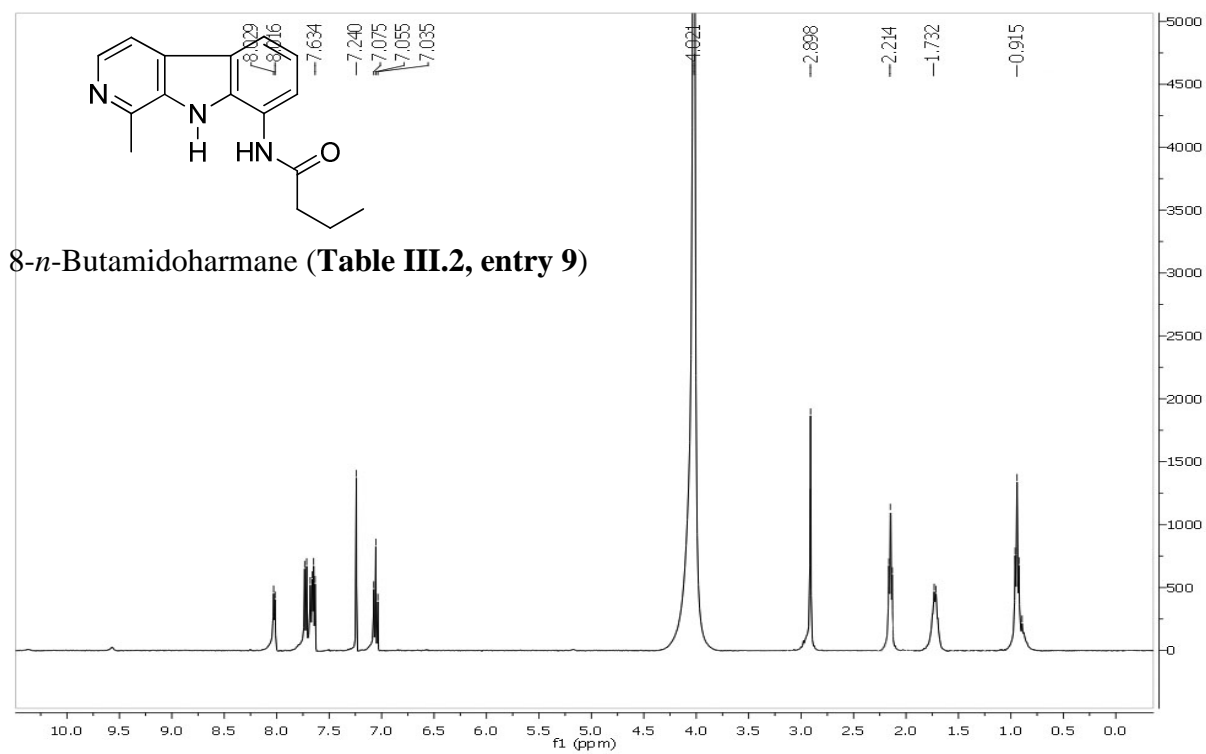
Figure III.13. ^{1}H- and [135]DEPT-NMR spectra of 6-*n*-butamidoharmane (**Table III.2, entry 9**) in CDCl$_3$ at 400 and 100 MHz, respectively.

Reductive *N*-Alkylation of Nitroarenes: A Green Approach for the *N*-Alkylation of Natural Products

Amir E. Wahba[†] and Mark T. Hamann*[†,‡,§,||]

[†]Departments of Pharmacognosy, [‡]Chemistry and Biochemistry, [§]Pharmacology, and [||]National Center for Natural Products Research, The School of Pharmacy, The University of Mississippi, University, Mississippi 38677, United States

CHAPTER IV.

REDUCTIVE *N*-ALKYLATION OF NITROARENES: A PRACTICAL GREEN APPROACH

FOR THE *N*-ALKYLATION OF NATURAL PRODUCTS

Publication in The Journal of Organic Chemistry, 2012, 77, 4578-4584.

Authors: Amir E. Wahba and Mark T. Hamann

ABSTRACT: A simple, mild, cost effective and green approach for the reductive mono N-alkylation of nitroarenes has been developed. HOAc/Zn are utilized as the reducing system together with a carbonyl compound as an alkyl source in methanol. Excellent yields were obtained with stoichiometric control of mono over dialkylated products. Application to five complex natural products demonstrated the practical utility of the method.

Introduction:

One-pot reactions are those in which two or more chemical transformations take place under the same reaction conditions without purification of intermediates and avoiding protection/deprotection steps.[2] Due to this advantage, one-pot reactions are highly practical in organic process development and in the field of total synthesis of complex natural products.[1-10] Indeed the value of such reactions is maximized if they maintain the green chemistry principles such as: waste prevention, atom economy, safer solvents and catalysis selectivity.[87] Simple and gentle chemical modifications are a key element for lead optimization studies where the pharmacological properties of leads must be altered through synthesis or semisynthesis. Nitration of aromatic and heterocyclic compounds is a simple and useful reaction for introduction of a stable nitro group onto a natural product skeleton. The benefit of introducing the nitro group is the ease of conversion to the corresponding amine that can be further alkylated to create primary and secondary aromatic amines. These alkylated amines are important building blocks for drug candidates.

During our detailed structure activity relationship (SAR) and lead optimization studies of manzamine A against malaria and neuroinflammation,[14-18, 88-91] we introduced a nitro group at C-6 and C-8 of the β-carboline moiety. These nitromanzamines are stable while the corresponding amines are not.[15] This instability was the inspiration for development of our one-pot reductive amidation method using Zn/HOAc as the reducing system and acyl chloride/Et$_3$N as the acylating agent in DMF.[19] The same challenges occurred when attempting to *N*-alkylate aminomanzamines by direct and reductive alkylation methods. As a result, we explored the utility of our previously used reducing system (Zn/HOAc) to accomplish an effective one-pot reductive *N*-alkylation of nitroarenes with carbonyl compounds as the alkyl source.

Several examples of one-pot reductive mono *N*-alkylations of nitroarenes with different reducing systems using carbonyl compounds as the alkyl source have been reported. Bae *et al.* used decaborane and 10% Pd/C[92] in methanol as a reducing system with a carbonyl compound as the alkyl source. Although this method showed high yields (~90%) of the mono *N*-alkyl products, it has several drawbacks. Addition of the reducing agent in one batch resulted in an incomplete reaction due to formation of the corresponding ether through reductive etherification. Another report used hydrogen over 10% Pd/C as reducing system and aldehydes as an alkyl source.[93] This method is not selective and not applicable to natural products modification since H_2/10% Pd/C will reduce isolated double bonds. In a similar reaction, ammonium formate was used as in situ hydrogen donor with 5% Pd/C as a reducing system in addition to aldehydes as alkyl source.[94] Xiang *et al* reported the use of aqueous-MeOH as an in situ source of H_2 over an Au-Pd/Al$_2$O$_3$ catalyst for the conversion of nitroarenes into the corresponding imines.[95] Nitriles have also been used as alkylating agents. Hudson *et al.* have used nitriles and ammonium formate with 5% Pd/C as reducing agent in methanol.[96] This approach gave relatively low yields with nitroarenes bearing electron withdrawing groups. Polymethylhydrosiloxane was also used as reducing agent in the presence of Pd(OH)$_2$/C as catalyst and nitriles as alkylating agents.[97] These two methods have the drawback of long reaction time in the first method and an expensive reducing agent in the second method. Other reductive alkylation methods have been reported including: allylic amination of cyclohexene by nitroarenes catalyzed by ruthenium complexes,[98] electrochemical reduction,[99] addition of functionalized arylmagnesium compounds to nitroarenes,[100] the palladium catalyzed coupling of allyl carbonate,[101] the addition of allymagnesium chloride to nitroarenes followed by reduction with LAH,[102] and the zinc promoted reductive alkylation utilizing alkyl halides as the alkyl source.[103]

Apparently, none of the previously reported one-pot reductive *N*-alkylation methods of nitroarenes is suitable for drug development either because of selectivity problems or the use of costly or toxic reagents (i.e., a deviation from green chemistry principles). Moreover, they all lack the application to a real drug lead or natural products. Herein, we report the development of a one-pot reductive *N*-alkylation of nitroarenes using inexpensive zinc metal with acetic acid as a selective reducing system (alkenes are stable under these conditions)[104] and carbonyl compounds as alkyl source with an application to five natural products scaffolds.

Results and discussion:

Solvent optimization using 4-nitroanisole as a model reaction revealed that methanol was the solvent of choice with quantitative yield of the mono N-alkyl product (Table IV.1). We then optimized the reaction conditions using simple nitroarenes and several carbonyl compounds. Mono N-alkyl products were obtained in high yields when one mole of carbonyl compound was used. (Table IV.2). Addition of two equivalents or more of carbonyl compound resulted in the formation of tertiary amines in excellent yields in an atom economical approach.

Table IV.1. Solvent optimization for the reductive mono *N*-alkylation of nitroarenes
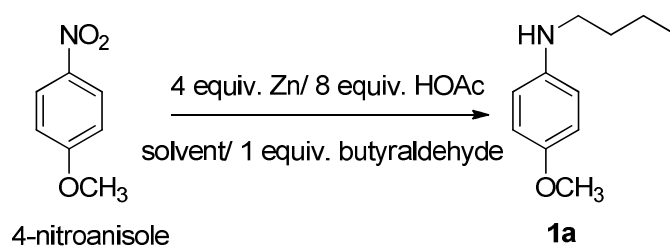
Entry	Solvent	Time (min)	Yield (%)[a]
1	DCM	30	94
2	MeOH	30	Quant.
3	DMF	30	91
4	Toluene	30	86
5	THF	30	87

[a] Isolated yield; All reactions were done using 1 mmol of 4-nitroanisole

Table IV.2. Screening of simple nitroarenes under optimized conditions
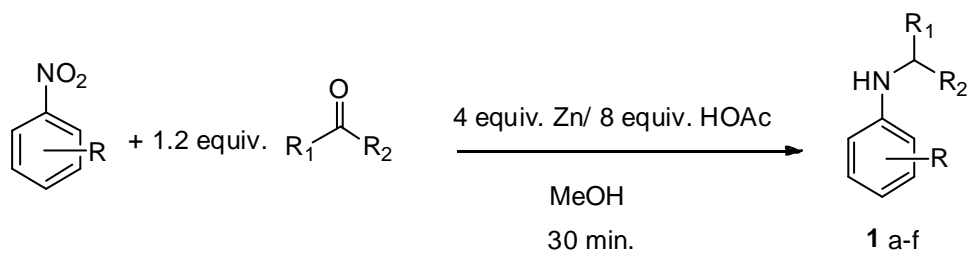
Entry	Nitro compound	Carbonyl compound	Product	Yield (%)[a]
1	NO₂ / OMe	CHO	HN-butyl / OMe **1a**	Quant.
2	NO₂ / OMe	2-methylcyclohexanone	HN-cyclohexyl / OCH₃ **1b**	96
3	NO₂ / OMe	acetone	HN-isopropyl / OCH₃ **1c**	95

171

#			Yield
4	NO$_2$ / CO$_2$Et (ethyl 4-nitrobenzoate)	CHO (butanal)	**1d** (HN-butyl, CO$_2$Et) Quant.
5	NO$_2$ / OMe	OHC–C$_6$H$_4$–Cl (4-chlorobenzaldehyde)	**1e** 97
6	NO$_2$ / OMe	HCHO	**1g** 96[b]
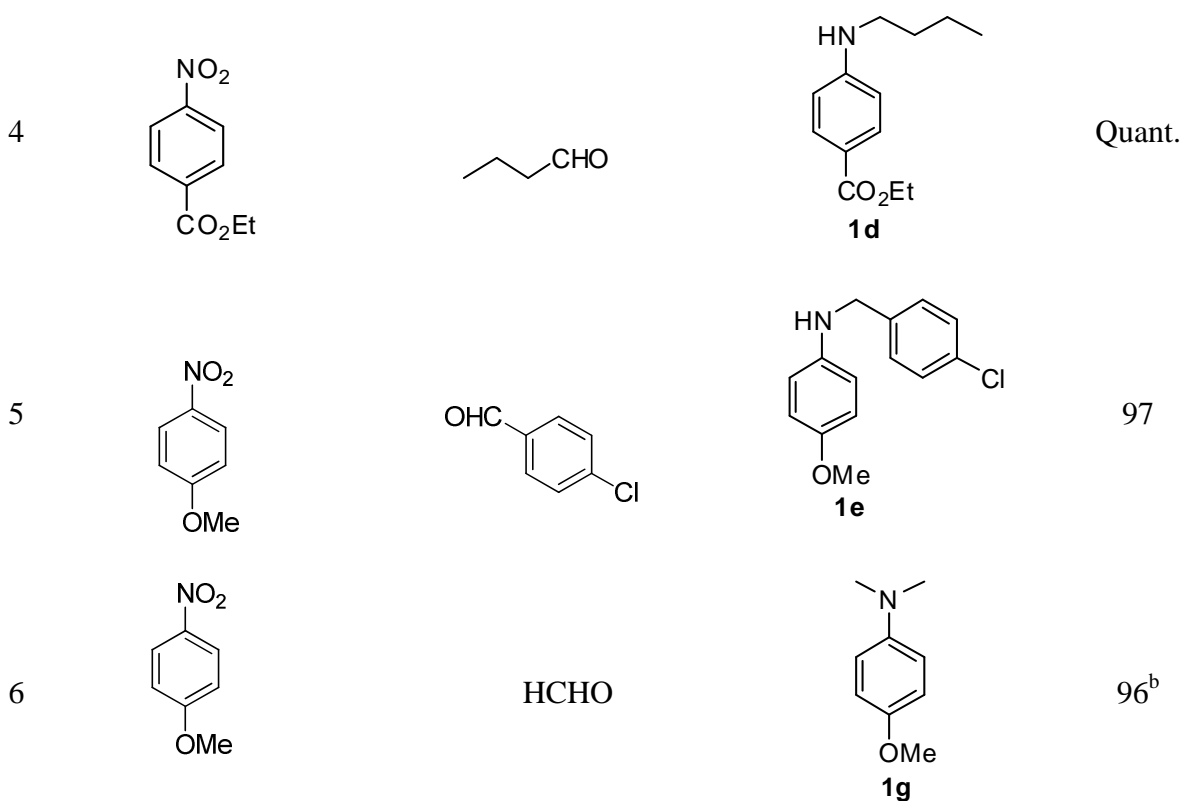
[a] Isolated yields. All reactions were done using 1.0 mmol of starting material

[b] 2.2 equiv. HCHO, 10 equiv. Zn and 20 equiv. HOAc were used. The reaction time was 1 h.

We utilized our optimized conditions for the synthesis of several *N*-alkyl analogs of biologically active natural product scaffolds. Five natural products were nitrated to generate starting nitro materials (Scheme IV.1). Manzamine F (**2**), selected as an example of manzamine alkaloids, yielded upon nitration three nitro products: 7-nitromanzamine F (**3**), 5-nitromanzamine F (**4**) and 5,7-dinitromanzamine F (**5**). The regiochemistry of the nitro group in **3** was assigned based on the strong HMBC correlations of H-5 (δ_H 7.91) to C-4a (δ_c 131.4) and C-4b (δ_c 129.1). Nitration of harmane (**6**), a β-carboline alkaloid, with sodium nitrite gave two nitro products: 8-nitroharmane (**7**) and 6-nitroharmane (**8**). Recently, several β-carboline related alkaloids

identified as prototypes to potent and orally efficient antimalarial leads were synthesized via similar reductive amination chemistry.[105,106] This supports our use of β-carbolines as model compounds. Nitration of the steroid, estradiol (**9**), led to simultaneous nitration of the phenol moiety and oxidation of the C-17 hydroxy functionality to afford 2-nitroestrone (**10)** and the 2,4-dinitro analog (**11**). Nitration of quinine (**12**) resulted in an interesting hydroxynitration of the terminal double bond which led to the formation of compound **13** in moderate yield. The ^{1}H- & ^{13}C-NMR of **13** revealed the absence of the olefinic resonances and the presence of a disubstituted quinoline ring (1H-NMR: δ 8.95, 1H, d, *J*=4.4 Hz; 8.25, 1H, d, *J*=7.7; 8.14, 1H, d, *J*=10.9; 7.74, 1H, d, *J*=10.0 Hz and 7.61, 1H, s) which indicated that the double bond was nitrated instead of the quinoline ring. This could be attributed to the deactivation of the quinoline ring by TFA. The molecular formula of **13** was determined as $C_{20}H_{26}N_3O_5$ $(M+H)^+$ from HRESIMS (*m/z* 388.1872) and the NMR data, which confirmed the addition of a hydroxy group and a nitro group in the molecule. The presence of the methylene resonance at δ 79.2 as well as the oxygenated methine resonance at δ 68.5 in the ^{13}C-NMR spectra confirmed the regiochemistry of the nitro and the hydroxy groups to be at C11 and C10 respectively. Nitration of curcudiol (**14**) gave the mononitro (**15**) and dinitro products (**16**). The nitro group in **15** was assigned at C4 based on the presence of the two singlet resonances at δ 7.51 and 6.31 in the ^{1}H-NMR spectra.

.

(2) → Method A → (3, 20%) + (4, 20%) + (5, 43%)

(9) → Method B → (10, 17%) + (11, 55%)

(12) → Method B → (13, 53%)

(14) → Method A → (15, 20%) + (16, 63%)

174
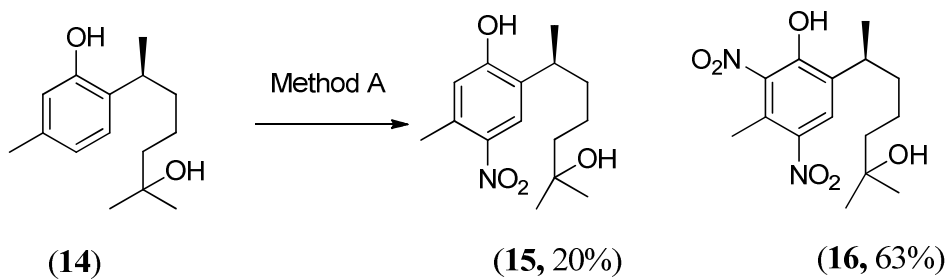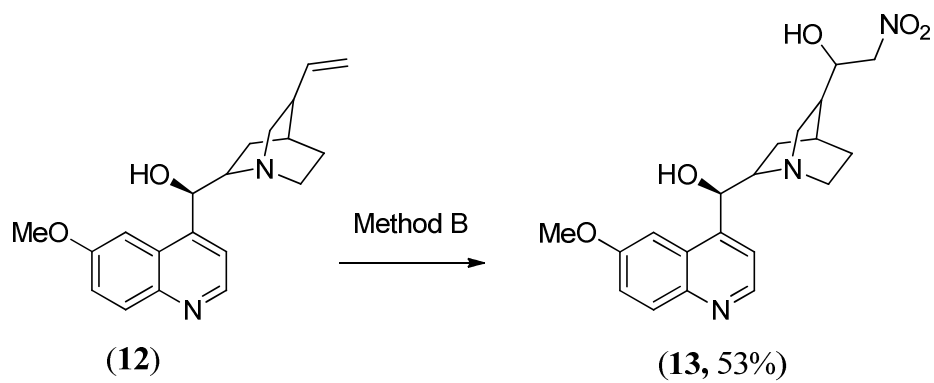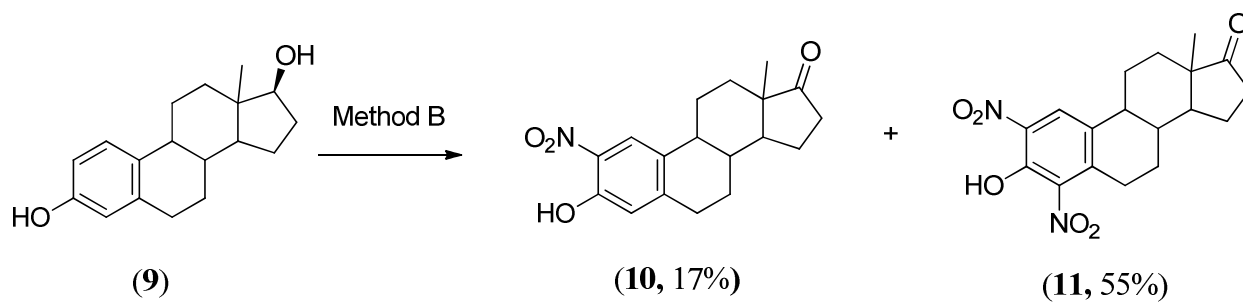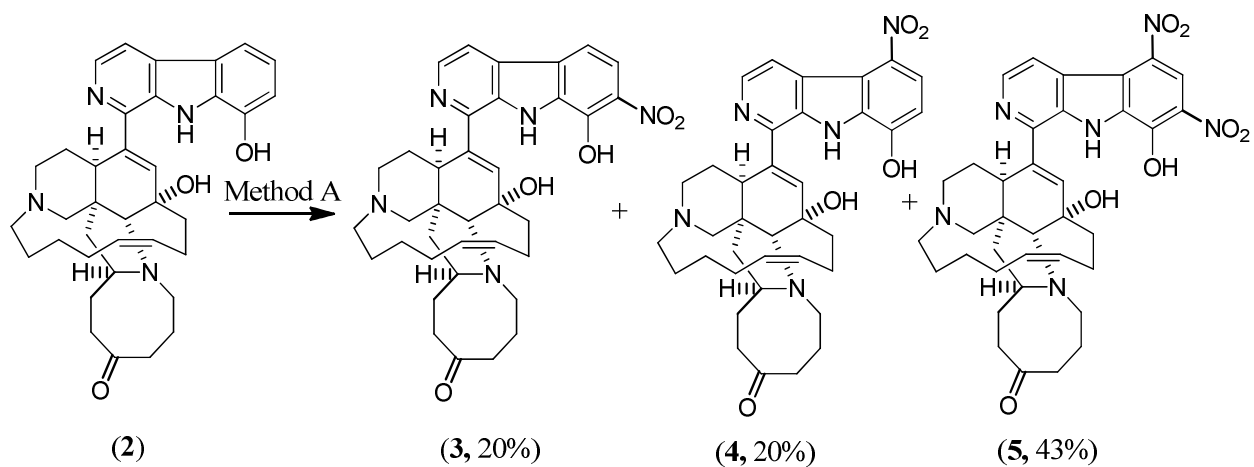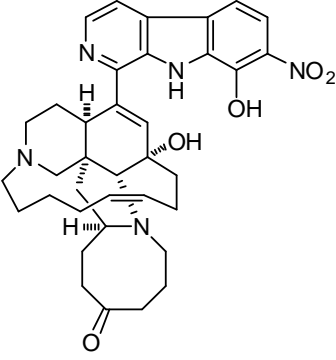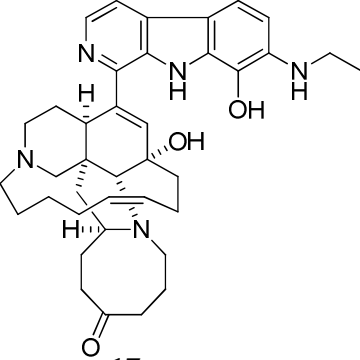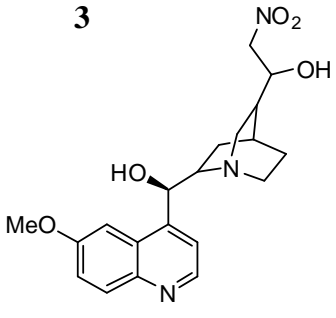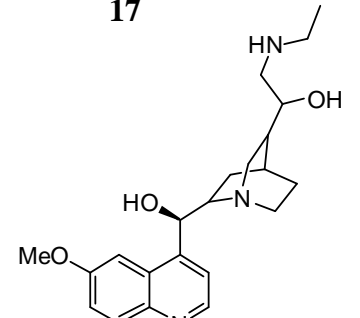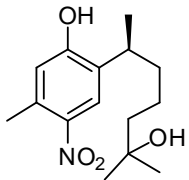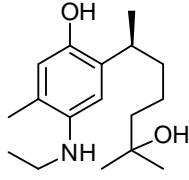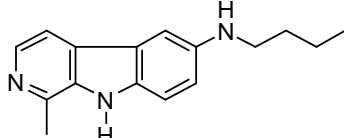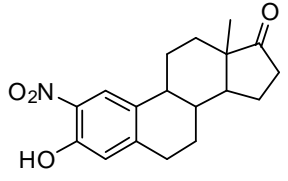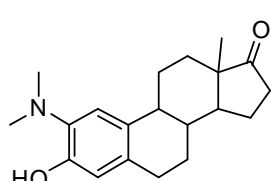
Method A: 1 equiv. of natural product dissolved in TFA, 1.1 equiv. NaNO$_2$, 0 ^{o}C to rt., 1.5 h.

Method B: 1 equiv. of natural product dissolved in HOAc, 3 equiv. HNO$_3$ 0 ^{o}C to rt., 1 h.

Scheme IV.1. Nitration of natural products scaffolds

The optimized reductive *N*-alkylation conditions applied to the nitrated natural products gave moderate to excellent yields (Table IV.3). 7-Nitromanzamine F gave a high yield (91%) of the corresponding 7-*N*-ethylaminomanzamine F (**17**) when one equivalent of acetaldehyde was used. The nitroquinine product **13** gave a moderate yield of 47% of the *N*-ethylamino product **18**. Moreover, nitrocurcudiol **15** gave 64% yield of the *N*-ethylamino analog **19**. A high yield of the 6-*N*-butylaminoharmane (**20**, 97%) was obtained from the reductive alkylation of 6-nitroharmane (**8**). Moreover, a high yield (88%) of the *N,N*-dimethylamino analog **21** was obtained in the case of 2-nitroestrone when reacted with two equivalents of formaldehyde.

Table IV.3. Reductive *N*-alkylation of nitrated natural products

Entry	Nitro products	*N*-alkyl products	Yield (%)[a]
1	**3**	**17**	91
2	**13**	**18**	47
3	**15**	**19**	64
4	R₁=R₂=H: Harmane (**6**) R₁=H, R₂=NO₂: 8-nitroharmane (**7**) R₁=NO₂, R₂=H: 6-nitroharmane (**8**)	**20**	97
5			88[b]

R$_1$=R$_2$=H: Harmane (**6**)
R$_1$=H, R$_2$=NO$_2$: 8-nitroharmane (**7**)
R$_1$=NO$_2$, R$_2$=H: 6-nitroharmane (**8**)

176

	10	21

Isolated yields. 1.2 equiv. of aldehydes were used. Reaction time was 1 h.

ᵇ 2.2 equiv. HCHO, 10 equiv. Zn and 20 equiv. HOAc were used.

Conclusion:

In conclusion, a practical, mild, cost-effective and environmentally benign green method for the one-pot reductive mono N-alkylation of nitroarenes has been developed. This method gives excellent yields with our model compounds with high selectivity for the mono N-alkyl over the dialkylated product in an atom economical approach with easy workup step (no hazardous waste). The reaction conditions were well tolerated by a variety of natural product models and afforded moderate to excellent yields. The major advantage of our method is the use of inexpensive zinc metal and acetic acid as a mild and selective reducing system to nitro group which makes our method greener. When taken in conjunction with the mild reaction conditions, this method may well find applications in drug development

Experimental:

General Experimental Procedures. The ^{1}H- and ^{13}C-NMR spectra were recorded in $CDCl_3$, *d4*-methanol or *d6*-acetone on NMR spectrometer operating at 400 MHz for ^{1}H and 100 MHz for [13]C. Chemical shift (δ) values are expressed in parts per million (ppm) and are referenced to the residual solvent signals of the solvent used. High resolution ESI-MS spectra were measured using electrospray ionization mass spectrometer. TLC analysis was carried out on precoated silica gel G254 aluminum plates. Reagents were purchased from commercial sources and used without further purification. Reactions were carried out in oven-dried glassware.

General procedure for the mono *N*-alkylation of nitroarenes: carbonyl compound (1.2 equiv.), zinc dust (4 equiv.) and acetic acid glacial (8 equiv.) were added to a solution of the nitroarene (1 mmol) in MeOH (2 mL). The mixture was stirred at room temperature for 30 min. Water (5 mL) was added to the reaction mixture and extracted with ethyl acetate (3x10 mL). The organic layer was dried over anhydrous Na_2SO_4 and evaporated under vacuum. The crude products were purified by silica column using 98:2 *n*-hexane:acetone.

4-*N*(*n*-butylamino)anisole (1a):[107] (179 mg, Quant.); yellow oil; ^{1}H-NMR ($CDCl_3$) δ 6.84 (2H, d, *J*=9.1 Hz), 6.63 (2H, d, *J*=9.0 Hz), 3.77 (3H, s), 3.09 (2H, t, *J*=7.6 Hz), 1.61 (2H, t, *J*=7.5 Hz), 1.47 (2H, m), 1.00 (3H, t, *J*=7.5 Hz); HRESIMS *m/z* calcd for $C_{11}H_{18}NO$ (M+H)[+] 180.1388, found 180.1394.

4-*N*(2-methylcyclohexylamino)anisole (1b):[108] (212 mg, 96%); yellow oil; ^{1}H-NMR ($CDCl_3$) δ 6.77 (2H, d, *J*=8.7 Hz), 6.67 (2H, d, *J*=8.9 Hz), 3.76 (3H, s), 1.4-2.2 (2H, m), 1.08 (3H, d, *J*=7.1 Hz); HRESIMS *m/z* calcd for $C_{14}H_{22}NO$ (M+H)[+] 220.1701, found 220.1687.

4-*N*(isopropylamino)anisole (1c):[109] (157 mg, 95%); yellow oil; ^{1}H-NMR (CDCl$_3$) δ 6.78 (2H, d, *J*=8.7 Hz), 6.60 (2H, d, *J*=8.9 Hz), 3.77 (3H, s), 3.56 (1H, m), 1.2 (6H, d, *J*=7.1 Hz); HRESIMS *m/z* calcd for C$_{10}$H$_{16}$NO (M+H)$^+$ 166.1232, found 166.1197.

4-*N*(*n*-butylamino)ethyl benzoate (1d):[110] (221 mg, Quant.); yellowish solid (m.p. 134); ^{1}H-NMR (CDCl$_3$) δ 7.84 (2H, d, *J*=8.9 Hz), 6.55 (2H, d, *J*=8.7 Hz), 4.29 (2H, q, *J*=7.4 Hz), 3.12 (2H, q, *J*=7.1 Hz), 1.58 (2H, m), 1.41 (2H, m), 1.33 (3H, t, *J*=7.0 Hz), 0.93 (3H, t, *J*=7.0 Hz); HRESIMS *m/z* calcd for C$_{13}$H$_{20}$NO$_2$ (M+H)$^+$ 222.1494, found 222.1510.

4-(*p*-chlorobenzylamino)anisole (1e):[111] (240 mg, 97%); yellow oil; ^{1}H-NMR (CDCl$_3$) δ 7.22 (2H, d, *J*=8.6 Hz), 7.07 (2H, d, *J*=8.9 Hz), 6.74 (2H, d, *J*=8.9 Hz), 6.52 (2H, d, *J*=8.9 Hz) 4.42 (1H, brs), 3.72 (3H, s); ^{13}C-NMR (CDCl$_3$): 152.8 (C), 140.7 (C), 140.2 (C), 138.7 (C), 133.3 (CH), 129.0 (CH), 128.9 (CH), 128.6 (CH), 115.7 (CH), 115.7 (CH), 115.0 (CH), 114.9 (CH), 64.6 (CH$_2$), 55.7 (CH$_3$); HRESIMS *m/z* calcd for C$_{14}$H$_{15}$ClNO (M+H)$^+$ 248.0842, found 248.0857.

4-(*N*,*N*-dimethylamino)anisole (1f):[112] (145 mg, 96%); yellowish white oil; ^{1}H-NMR (CDCl$_3$) δ 6.84 (2H, d, *J*=8.6 Hz), 6.75 (2H, d, *J*=8.9 Hz), 2.86 (6H, s), 3.76 (3H, s); HRESIMS *m/z* calcd for C$_9$H$_{14}$NO (M+H)$^+$ 152.1075, found 152.1102.

General methods for the nitration of natural products.

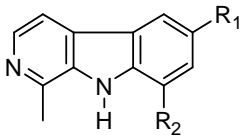**Method A:** 1 equiv. of natural product was dissolved in TFA (3 mL) and stirred for 10 min. at 0 $^{\circ}$C. NaNO$_2$ (1.1 equiv.) was added at once and the reaction mixture was stirred at 0 $^{\circ}$C for 1 h and then for 30 min. at room temperature. The reaction mixture was poured into water and neutralized by ammonium hydroxide producing a precipitate that was filtered and dried. If no

precipitate was formed, the aqueous mixture was extracted with DCM (3x10 mL) and the organic layers were combined and dried over Na_2SO_4 and concentrated under vacuum.

Method B: 1 equiv. of natural product was dissolved in glacial acetic acid (3 mL) and nitric acid (2 equiv.) at 0 °C. The reaction mixture was stirred for 30 min. at 0 °C then for another 30 min at room temperature. The reaction mixture was poured into water and neutralized by ammonium hydroxide producing a precipitate that was filtered and dried. If no precipitate was formed, the aqueous mixture was extracted with DCM (3x10 mL) and the organic layers were combined and dried over Na_2SO_4 and concentrated under vacuum.

Nitration of manzamine F (2): Manzamine F (100 mg, 0.172 mmol) and $NaNO_2$ (13 mg, 0.188 mmol) were reacted by method A. After workup, the crude nitromanzamine F products were purified by silica column chromatography using *n*-hexane:acetone (9:1). Further purification was carried out on a Phenomenex Luna C8 250x10 mm, 5µm Luna reverse-phase HPLC column using gradient CH_3CN (0.1% TFA)/water (0.1% TFA) with flow rate of 6 mL/min to gave the pure nitro analogs.

Manzamine F (2): ^{1}H-NMR (CDCl$_3$) δ 8.41 (1H, d, *J*=7.6 Hz), 7.88 (1H, d, *J*=7.5 Hz), 7.63 (1H, d, *J*=7.6 Hz), 7.61 (1H, d, *J*=7.6 Hz), 7.12 (1H, d, *J*=7.6 Hz), 6.66 (1H, s), 5.60 (2H, m), 3.70 (1H, s), 3.11 (m), 2.92 (m), 2.57 (m), 2.38 (m), 2.10 (m); ^{13}C-NMR (CDCl$_3$) δ 211.0 (C), 143.7 (C), 143.1 (C), 141.3(C), 138.3 (CH), 137.7 (CH), 133.3 (C), 132.6 (C), 130.1 (C), 128.0 (CH), 123.4 (C), 121.1 (CH), 113.8 (CH), 112.2 (CH), 82.1 (CH), 69.6 (C), 63.5 (CH), 53.2 (CH$_2$), 49.8 (CH$_2$), 47.6 (C), 46.7 (CH$_2$), 46.1 (CH$_2$), 45.1 (CH$_2$), 42.5 (CH), 39.9 (CH$_2$), 38.9 (CH$_2$), 34.2 (CH$_2$), 32.7 (CH$_2$), 26.9 (CH$_2$), 25.7 (CH$_2$), 25.2 (CH$_2$), 24.6 (CH$_2$), 21.5 (CH$_2$).

7-nitromanzamine F (3): (21 mg, 20%); $[\alpha]_D^{25}$ +11.5 (*c* 0.05, MeOH); yellow solid; (R$_f$ = 0.6, 9:1 DCM:MeOH); IR: 3534 (br), 3211, 3050, 2959, 2924, 2852, 1711, 1650, 1574, 1507, 1457,

1421, 1260, 1072, 1024, 911, 802, 729 cm^{-1}; ^{1}H-NMR (*d6*-acetone) δ 8.55 (1H, d, *J*=7.6 Hz), 8.38 (1H, d, *J*=7.5 Hz), 8.18 (1H, d, *J*=7.6 Hz), 7.91 (1H, d, *J*=7.6 Hz), 6.71 (1H, s), 5.65 (2H, m), 3.70 (1H, s), 3.44 (m), 3.29 (m), 3.14 (m), 2.92 (m), 2.72 (m), 2.53 (m), 2.34 (m), 2.24 (m) 2.08 (s), 2.03 (m), 1.96 (m), 1.74 (m), 1.48 (m); ^{13}C-NMR (*d6*-acetone) δ 211.0 (C), 150.9 (C), 139.6 (C), 136.1 (CH), 135.2 (CH), 133.7 (CH), 132.6 (C), 131.4 , 129.1 (CH), 122.3 (C), 121.7 (C), 121.6 (C), 119.6 (C), 115.4 (CH), 113.3 (CH), 79.8 (CH), 70.6 (C), 69.2 (CH$_2$), 58.8 (CH$_2$), 55.7 (CH), 51.1 (CH$_2$), 47.3 (CH$_2$), 45.6 (CH$_2$), 41.6 (CH$_2$), 36.6 (CH$_2$), 36.3 (CH$_2$), 34.7 (CH$_2$), 28.1 (CH$_2$), 25.1 (CH$_2$), 24.3 (CH$_2$), 22.9 (CH$_2$), 20.7 (CH$_2$); HRESIMS *m/z* calcd for C$_{36}$H$_{44}$N$_5$O$_5$ (M+H)$^+$ 626.3342, found 626.3335.

5-nitromanzamine F (4): (21 mg, 20%); $[\alpha]_D^{25}$ +12.1 (*c* 0.05, MeOH); pale orange solid; (R$_f$ = 0.50, 9:1 DCM:MeOH); IR: 3194 (br), 3090, 2964, 2930, 2854, 2802, 1710, 1671, 1649, 1560, 1456, 1417, 1335, 1202, 1194, 1073, 1026, 911, 820, 805, 729 cm^{-1}; ^{1}H-NMR (*d6*-acetone) δ 8.70 (1H, d, *J*=7.6 Hz), 8.53 (1H, d, *J*=7.5 Hz), 8.12 (1H, d, *J*=7.6 Hz), 7.12 (1H, d, *J*=7.6 Hz), 6.99 (1H, s), 5.65 (2H, m), 3.70 (1H, s), 3.44 (m), 3.29 (m), 3.14 (m), 2.92 (m), 2.72 (m), 2.53 (m), 2.34 (m), 2.24 (m) 2.08 (s), 2.03 (m), 1.96 (m), 1.74 (m), 1.48 (m); ^{13}C-NMR (*d6*-acetone) δ 211.0 (C), 149.3 (C), 141.7 (C), 141.0 (C), 136.0 (CH), 135.1 (C), 132.5 (CH), 131.9 (CH), 129.4 (C), 122.5 (C), 121.7 (C), 118.0 (CH), 117.1 (CH), 115.2 (CH), 114.0 (CH), 79.0 (CH), 72.0 (CH$_2$), 67.5 (CH$_2$), 56.6 (CH$_2$), 56.3 (CH), 53.5(CH$_2$), 52.2 (CH$_2$), 49.3 (CH$_2$), 46.3(CH$_2$), 42.4 (CH), 36.8(CH$_2$), 36.6 (CH$_2$), 33.4 (CH$_2$), 30.6 (CH$_2$), 29.6 (CH$_2$), 29.2 (CH$_2$), 28.6 (CH$_2$), 27.5 (CH$_2$), 25.2 (CH$_2$), 22.1 (CH$_2$), 20.0 (CH$_2$); HRESIMS *m/z* calcd for C$_{36}$H$_{44}$N$_5$O$_5$ (M+H)$^+$ 626.3342, found 626.3335.

5,7-dinitromanzamine F (5): (46 mg, 43%); $[\alpha]_D^{25}$ +18.5 (*c* 0.1, MeOH); orange solid; (R$_f$ = 0.4, 9:1 DCM:MeOH); IR: 3239 (br), 3050, 2932, 2854, 2797, 1693, ,1562, 1446, 1418, 1365, 1330,

1271, 1245, 1112, 1075, 823, 789 cm^{-1}; ^{1}H-NMR (*d6*-acetone) δ 8.59 (1H, d, *J*=7.6 Hz), 8.21 (1H, d, *J*=7.5 Hz), 8.20 (1H, s), 6.52 (1H, s), 5.36 (2H, m), 3.70 (1H, s), 3.44 (m), 3.29 (m), 3.14 (m), 2.92 (m), 2.72 (m), 2.53 (m), 2.34 (m), 2.24 (m) 2.08 (s), 2.03 (m), 1.96 (m), 1.74 (m), 1.48 (m); ^{13}C-NMR (*d6*-acetone) δ 212.0 (C), 151.1 (C), 143.6 (C), 141.5 (C), 138.4 (CH), 137.7 (CH), 136.9 (C), 133.5 (C), 131.8 (CH), 130.2 (CH), 128.3 (C), 124.1 (C), 120.2 (C), 114.3 (CH), 109.3 (CH), 80.5 (CH), 70.1 (CH$_2$), 69.9 (CH$_2$), 57.1 (CH$_2$), 55.7 (CH$_2$), 53.9 (CH), 51.4 (CH$_2$), 46.8 (CH$_2$), 43.3 (CH), 39.7 (CH$_2$), 36.6 (CH$_2$), 36.4 (CH$_2$), 34.6 (CH$_2$), 32.7 (CH$_2$), 27.3 (CH$_2$), 25.2 (CH$_2$), 24.3 (CH$_2$), 22.1 (CH$_2$), 21.0 (CH$_2$); HRESIMS *m/z* calcd for C$_{36}$H$_{43}$N$_6$O$_7$ (M+H)$^+$ 671.3193, found 671.3207.

Nitration of harmane (6): Harmane (100 mg, 0.440 mmol) and NaNO$_2$ (33.4 mg, 0.480 mmol) were reacted by method A. After workup, the crude nitro products of harmane were loaded onto a column packed with 15 g of silica gel. 8-Nitroharmane (**7**) was eluted first with 99:1 DCM:MeOH, followed by 6-nitroharmane (**8**) after the mobile polarity was increased with 95:5 DCM:MeOH.

8-Nitroharmane (7):[113] (54 mg, 43%); yellow powder (m.p. 211-212 ^{o}C; lit. 209-210 ^{o}C); (R$_f$ = 0.8, 9:1 DCM:MeOH); IR: 3087, 3044, 2974, 2865, 2784, 1660, 1640, 1530,1491, 1339, 1288, 1202, 1184, 1131, 833 cm^{-1}; ^{1}H-NMR (CDCl$_3$) δ 9.87 (s, brd), 8.44 (1H, d, *J*=5.6 Hz), 8.40 (1H, d, *J*=8.0 Hz), 8.37 (1H, d, *J*=8.0 Hz), 7.78 (1H, d, *J*=5.6 Hz), 7.33 (1H, t, *J*=8.0 Hz), 2.86 (s); ^{13}C-NMR (CDCl$_3$) δ 143.3 (C), 140.6 (CH), 134.8 (C), 134.0 (C), 133.7 (C), 127.4 (CH), 127.6 (C), 126.4 (C), 124.2 (CH), 119.4 (CH), 112.6 (CH), 20.2 (CH$_3$); HRESIMS *m/z* calcd for C$_{12}$H$_{10}$N$_3$O$_2$ (M+H)$^+$ 228.0773, found 228.0770.

6-Nitroharmane (8):[113] (56 mg, 45%); yellow powder (m.p. 297-299 ^{o}C; lit. 299-300 ^{o}C); (R$_f$ = 0.7, 9:1 DCM:MeOH); IR: 3305, 3086, 2869, 1673, 1640, 1531, 14942, 1434, 1338, 1201, 1138,

832 cm^{-1}; ^{1}H-NMR (CDCl$_3$) δ 8.83 (1H, d, *J*=2.4 Hz), 8.13 (1H, d, *J*=2.4 Hz), 8.11 (1H, d, *J*=2.4 Hz), 8.08 (1H, d, *J*=6.8 Hz), 7.96 (1H, d, *J*=6.8 Hz), 7.38 (1H, d, *J*=8.0 Hz), 2.87 (s); ^{13}C-NMR (CDCl$_3$) δ 150.0 (C), 144.2 (C), 137.0 (C), 134.8 (CH), 129.6 (CH), 123.8 (CH), 119.7 (CH), 119.4 (CH), 117.0 (CH), 19.6 (CH$_3$); HRESIMS *m/z* calcd for C$_{12}$H$_{10}$N$_3$O$_2$ (M+H)$^+$ 228.0773, found 228.0770.

Nitration of β-estradiol (9): β-estradiol (100 mg, 0.36 mmol) was nitrated with method B. After workup, the crude nitro products was purified with silica column eluted with DCM:MeOH (95:5). The hydroxy group was oxidized under these conditions.

2-nitroestrone (10):[114] (19.8 mg, 17%); $[\alpha]_D^{25}$ +96.2 (*c* 0.1, DCM); yellow powder (m. p. 178-179 ^{o}C; lit. 178-180 ^{o}C); (R$_f$ = 0.56, 100% DCM) ; IR: 3078, 2928, 2857, 1736, 1631, 1525, 1479, 1433, 1374, 1310, 1263, 1053, 897, 734, 703 cm^{-1}; ^{1}H-NMR (CDCl$_3$) δ 7.99 (1H,s), 6.88 (1H,s), 2.97 (2H, m), 2.53 (1H, dd, *J*=17.0, 8.3 Hz), 2.46 (1H, m), 2.31-1.97 (6H, m), 1.75-1.40 (8H, m), 0.91 (3H,s); ^{13}C-NMR (CDCl$_3$) δ 220.1 (C), 153.0 (C), 148.9 (C), 133.2 (C), 131.7 (C), 121.7 (CH), 119.1 (CH), 50.5 (CH), 48.0 (C), 43.6 (CH), 37.8 (CH), 35.9 (CH$_2$), 31.4 (CH$_2$), 29.8 (CH$_2$), 26.0 (CH$_2$), 25.8 (CH$_2$), 21.7 (CH$_2$), 13.9 (CH$_3$); HRESIMS *m/z* calcd for C$_{18}$H$_{22}$NO$_4$ (M+H)$^+$ 316.1549, found 316.1552.

2,4-dinitroestrone (11):[114] (64 mg, 55%); $[\alpha]_D^{25}$ +90.1 (*c* 0.1, DCM); yellow powder (m. p. 186-188 ^{o}C; lit. 185-188 ^{o}C); (R$_f$ = 0.4, 100% DCM); IR: 3350, 3008, 2987, 1734, 1631, 1532, 1345, 1308, 1259, 1061, 897 cm^{-1}; ^{1}H-NMR (CDCl$_3$) δ 8.14 (1H,s), 2.88 (2H, m), 2.53 (1H, dd, *J*=17.0, 8.3 Hz), 2.46 (1H, m), 2.31-1.97 (6H, m), 1.75-1.40 (8H, m), 0.91 (3H,s); ^{13}C-NMR (CDCl$_3$) δ 220.1 (C), 144.8 (C), 141.7 (C), 139.2 (C), 133.6 (C), 132.1 (C), 122.7 (CH), 50.0 (CH), 47.7 (C), 43.5 (CH), 37.0 (CH), 35.7 (CH$_2$), 31.2 (CH$_2$), 28.2 (CH$_2$), 25.8 (CH$_2$), 24.9

(CH$_2$), 24.8, 21.5 (CH$_2$), 13.7 (CH$_3$); HRESIMS m/z calcd for C$_{18}$H$_{21}$N$_2$O$_6$ (M+H)$^+$ 361.1399, found 361.1402.

Nitration of quinine (12): Quinine (100 mg, 0.31 mmol) was nitrated by method B. After workup, the crude product was fractionated using solid phase extraction (SPE-C18) and the fraction eluted with H$_2$O:MeOH (80:20) was further purified on a Phenomenex Luna C8 250x22 mm, 5μm Luna reverse-phase HPLC column using gradient CH$_3$CN (0.1% TFA)/water (0.1% TFA) with flow rate of 20 mL/min to gave the pure nitro analog.

Quinine (12): ^{1}H-NMR (*d4*-methanol) δ 8.61 (1H, d, *J*=8.0 Hz), 7.90 (1H, d, *J*=8.0 Hz), 7.65 (1H, d, *J*=4.0 Hz), 7.36 (1H, s), 7.33 (1H, s), 6.23 (1H, d, *J*=4.0 Hz), 5.65 (1H, m), 5.56 (1H, m), 4.82 (1H, m), 3.92 (3H, s), 3.65 (1H, m), 3.07 (2H, m), 2.63 (2H, m), 2.26 (1H, m), 1.82 (2H, m), 1.70 (1H, m), 1.52 (1H, m), 1.36 (1H, m); ^{13}C-NMR (*d4*-methanol) δ 159.5 (C), 150.6 (C), 148.0 (CH), 144.7 (C), 142.7 (CH), 131.4 (CH), 131.3, 128.0 (C), 123.2 (CH), 120.0 (CH), 119.9, 114.9 (CH$_2$), 102.3 (CH), 72.2 (CH), 60.1 (CH), 57.7 (CH$_2$), 56.4 (CH$_3$), 44.1 (CH$_2$), 40.1 (CH), 29.2 (CH), 28.2 (CH$_2$), 21.6 (CH$_2$).

11-nitro-10-hydroxyquinine (13): (63 mg, 53%); $[\alpha]_D^{25}$ +133.0 (*c* 1, MeOH); yellow-orange powder m. p. 167-170 ^{o}C); (R$_f$ = 0.5, 100% DCM); IR: 3368, 3007, 2971, 2839, 1672, 1621, 1556, 1510, 1473, 1242, 1229, 1133, 1027, 834, 799 cm^{-1}; ^{1}H-NMR (*d4*-methanol) δ 8.95 (1H, d, *J*=4.4 Hz), 8.25 (1H, d, *J*=7.7 Hz), 8.14 (1H, d, *J*=10.9 Hz), 7.74 (1H, d, *J*=10.0 Hz), 7.61 (1H, s), 6.23 (1H, m), 4.50 (2H, t, *J*=9.8 Hz), 4.29 (1H, m), 4.04 (3H, s), 3.88 (1H, m), 3.49 (1H, m), 3.25 (1H, m), 2.33-1.50 (6H, m); ^{13}C-NMR (*d4*-methanol) δ 162.9 (C), 162.5 (C), 162.3 (C), 157.0 (C), 142.4 (CH), 135.8 (C), 129.0 (C), 128.8 (CH), 124.7 (CH), 121.3 (CH), 119.3 (CH), 102.8 (CH), 98.9 (C), 89.0 (C), 81.5 (C), 79.2 (CH$_2$), 68.5 (CH), 67.1 (CH), 61.0 (CH), 57.4

(CH), 53.6 (CH$_2$), 53.4 (CH$_2$), 45.5 (CH$_2$), 38.3 (C), 38.1 (CH$_2$), 25.8 (CH$_2$), 25.5 (CH$_2$), 20.0 (CH$_2$); HRESIMS m/z calcd for C$_{20}$H$_{26}$N$_3$O$_5$ (M+H)$^+$ 388.1872, found 388.1859.

Nitration of curcudiol (14): Curcudiol (100 mg, 0.423 mmol) and NaNO$_2$ (32 mg, 0.463 mmol) were reacted by method A. After workup, the crude products were purified by silica column eluted with n-hexane:acetone (85:15).

Curcudiol (14): ^{1}H-NMR (CDCl$_3$) δ 7.04 (1H, d, J=8.0 Hz), 6.70 (1H, d, J=8.0 Hz), 3.14 (1H,t, J=7.2 Hz), 2.25 (3H, s), 1.64-1.20 1.20 (8H, m), 1.20-1.18 (9H, m); ^{13}C-NMR (CDCl$_3$) δ 153.8 (C), 136.6 (C), 131.2 (C), 127.2 (CH), 121.7 (CH), 116.8 (CH), 72.2 (C), 43.9 (CH$_2$), 38.2 (CH$_2$), 31.6, 31.3 (CH), 29.9 (CH$_3$), 29.1 (CH$_3$), 22.6 (CH$_2$), 21.6 (CH$_3$).

4-nitrocurcudiol (15): (24 mg, 20%); $[\alpha]_D^{25}$ +8.3 (c 0.2, MeOH); yellow powder (m. p. 103 ^{o}C); (R$_f$ = 0.6, 7:3 hexane:EtOAc); IR: 3365, 3177, 3067, 2919, 2850, 2793, 2298, 1776, 1714, 1638, 1602, 1571, 1443, 1370, 1216, 1151, 1134, 1030, 997, 851, 814, 762 cm^{-1}; ^{1}H-NMR (CDCl$_3$) δ 7.51 (1H, s), 6.31 (1H, s), 3.00 (1H,m), 2.17 (3H, s), 1.6-1.2 (12H, m), 1.20 (6H, s), 1.12 (3H, d, J=5.3 Hz); ^{13}C-NMR (CDCl$_3$) δ 187.4 (C), 150.8 (C), 148.3 (C), 146.1 (C), 129.6 (C), 119.5 (CH), 89.4 (C), 40.4 (CH$_2$), 36.3 (CH$_2$), 31.5 (CH), 29.9 (CH$_3$), 25.7 (CH$_3$), 21.9 (CH$_3$), 19.9 (CH$_2$), 17.2 (CH$_3$); HRESIMS m/z calcd for C$_{15}$H$_{22}$NO$_4$ (M-H)$^-$ 280.1548, found 280.1541.

2,4-dinitrocurcudiol (16): (24 mg, 20%); $[\alpha]_D^{25}$ +10.1 (c 0.1, MeOH) ; yellow powder (m. p. 125 ^{o}C); (R$_f$ = 0.3, 7:3 hexane:EtOAc); IR: 3329, 3013, 2928, 2863, 1705, 1618, 1585, 1518, 1453, 1420, 1374, 1288, 1228, 1150, 1108, 944, 909, 859, 775, 766 cm^{-1}; ^{1}H-NMR (CDCl$_3$) δ 8.20 (1H, s), 2.95 (1H,m), 2.12 (3H, s), 1.6-1.2 (12H, m), 1.16 (6H, s), 1.07 (3H, d, J=5.3 Hz); ^{13}C-NMR (CDCl$_3$) δ 186.5 (C), 152.1 (C), 149.9 (C), 148.4 (C), 129.2 (C), 119.1 (C), 71.6 (C), 43.6 (CH$_2$), 36.6 (CH$_2$), 31.5 (CH), 29.1 (CH$_3$), 25.7 (CH$_3$), 21.9 (CH$_2$), 19.9 (CH$_3$), 17.0 (CH$_3$); HRESIMS m/z calcd for C$_{15}$H$_{21}$N$_2$O$_6$ (M-H)$^-$ 325.1399, found 325.1392.

Reductive *N*-alkylation of natural products scaffolds:

7-*N*-ethylaminomanzamine F (17): 7-nitromanzamine F (**3,** 21 mg, 0.034 mmol) and acetaldehyde (2.0 µL, 0.040 mmol) were reacted by the general reductive alkylation method (0.2 mL of DCM was added as a cosolvent). The reaction mixture was stirred for 1 h at room temperature under nitrogen atmosphere. The crude product was purified on a Phenomenex Luna C8 250x10 mm, 5µm Luna reverse-phase HPLC column using gradient CH_3CN (0.1% TFA)/water (0.1% TFA) with flow rate of 6 mL/min to gave the pure *N*-ethylamino analog. **7-*N*-ethylaminomanzamine F:** (19 mg, 91%); $[\alpha]_D^{25}$ +17.2 (*c* 0.1, MeOH); pale yellow powder; (R_f = 0.5, 9:1 DCM:MeOH); IR: 3239, 3210, 3050, 2932, 2854, 2797, 1693, 1562, 1446, 1418, 1365, 1330, 1271, 1245, 1112, 1075, 823, 789 cm^{-1}; ^{1}H-NMR ($CDCl_3$) δ 8.46 (1H, d, *J*=7.6 Hz), 7.71 (1H, d, *J*=7.5 Hz), 7.35 (1H, d, *J*=7.6 Hz), 7.03 (1H, d, *J*=7.6 Hz), 6.50 (1H, s), 5.53 (2H, m), 3.50 (1H, s), 3.44 (m), 3.01 (m), 2.60 (m), 2.40 (m), 2.35 (m), 2.34 (m), 1.70 (m), 1.56 (m), 1.35 (3H, t, *J*=10 Hz); ^{13}C-NMR ($CDCl_3$) δ 211.0 (C), 142.2 (C), 140.6 (C), 137.1 (CH), 137.7 (CH), 135.9 (C), 132.2 (CH), 131.9 (CH), 130.3 (C), 129.4 (C), 126.5 (C), 121.4 (C), 115.1 (CH), 112.4 (CH), 111.9 (CH), 109.4 (CH), 81.5 (CH), 70.1 (CH_2), 63.2 (CH_2), 55.9 (CH), 55.0 (CH_2), 51.1 (CH_2), 44.8 (CH), 38.2 (CH_2), 35.8 (CH_2), 35.6 (CH_2), 34.7 (CH_2), 27.3 (CH_2), 26.0 (CH_2), 25.3 (CH_2), 23.5 (CH_2), 20.8 (CH_2), 14.1 (CH_3); HRESIMS *m/z* calcd for $C_{38}H_{50}N_5O_3$ (M+H)$^+$ 624.3913, found 624.3932.

10-*N*-ethylamino-11-hydroxyquinine (18): 10-nitro-11-hydroxyquinine (**13,** 50 mg, 0.129 mmol) and acetaldehyde (9.0 µL, 0.155 mmol) were reacted by the general reductive alkylation method The reaction mixture was stirred for 1 h at room temperature under nitrogen atmosphere. The crude product was purified on a Phenomenex Luna C8 250x10 mm, 5µm Luna reverse-phase HPLC column using gradient CH_3CN (0.1% TFA)/water (0.1% TFA) with flow rate of 6

mL/min to gave the pure *N*-ethylamino analog. **10-*N*-ethylamino-11-hydroxyquinine:** (23 mg, 47%); $[\alpha]_D^{25}$ +140.9 (*c* 1, DCM); brown powder (m. p. 156-158 ^{o}C); (R$_f$ = 0.3, 100% DCM); IR: 3345, 3239, 3156, 3007, 2932, 1620, 1591, 1552, 1509, 1469, 1448, 1430, 1371, 1332, 1324, 1228, 1174, 1136, 1082, 1025, 988, 953, 827, 760 cm^{-1}; ^{1}H-NMR (*d4*-methanol) δ 8.95 (1H, d, *J*=4.4 Hz), 8.20 (1H, d, *J*=7.7 Hz), 8.14 (1H, d, *J*=10.9 Hz), 7.74 (1H, d, *J*=10.0 Hz), 7.61 (1H, s), 6.27 (1H, m), 4.50 (2H, t, *J*=9.8 Hz), 4.29 (1H, m), 4.06 (3H, s), 3.78 (1H, m), 3.49 (1H, m), 3.33 (1H, m), 2.99 (2H, q, *J*=10.0 Hz), 2.33-1.50 (6H, m), 1.23 (3H, t, *J*=10.0 Hz); ^{13}C-NMR (*d4*-methanol) δ 162.0 (C), 162.5 (C), 162.3 (C), 157.0 (C), 142.4 (CH), 135.8 (C), 128.9 (CH), 128.8 (C), 124.7 (CH), 121.3 (C), 119.3 (CH), 102.8 (CH), 98.9 (C), 89.0 (C), 81.5 (CH), 70.2 (CH$_2$), 68.5 (CH), 61.0 (CH), 57.4 (CH$_2$), 53.6 (CH$_2$), 53.4 (CH$_2$), 45.5 (CH$_2$), 44.0 (CH$_2$), 38.3 (CH$_2$), 38.1 (CH$_2$), 25.8 (CH$_2$), 25.5 (CH$_2$), 20.0 (CH$_2$), 11.1 (CH$_3$); HRESIMS *m/z* calcd for C$_{22}$H$_{32}$N$_3$O$_3$ (M+H)$^+$ 386.2443, found 386.2424.

4-*N*-ethylaminocurcudiol (19): 4-nitrocurcudiol (**15**, 20 mg, 0.071 mmol) and acetaldehyde (5.0 µL, 0.085 mmol) were reacted by the general reductive alkylation method The reaction mixture was stirred for 1 h at room temperature under nitrogen atmosphere. The crude product was purified on a Phenomenex Luna C8 250x10 mm, 5µm Luna reverse-phase HPLC column using gradient CH$_3$CN (0.1% TFA)/water (0.1% TFA) with flow rate of 6 mL/min to gave the pure *N*-ethylamino analog. **4-*N*-ethylaminocurcudiol (19):** (13 mg, 64%); $[\alpha]_D^{25}$ +4.7 (*c* 0.05, DCM); pale-yellow oil; (R$_f$ = 0.7, 7:3 hexane:EtOAc);IR: 3402(brd), 3012, 2960, 2932, 2873, 2359, 2341, 1775, 1705, 1637, 1513, 1420, 1367, 1219, 1164, 1091, 1009, 987, 830 cm^{-1}; ^{1}H-NMR (CDCl$_3$) δ 6.50 (1H, s), 6.39 (1H, s),3.14 (2H, q, *J*= Hz), 3.02 (1H,m), 2.13 (3H, s), 1.79-1.56 (12H, m), 1.47 (6H, s), 1.21 (3H, d, *J*=5.3 Hz); ^{13}C-NMR (CDCl$_3$) δ 155.7 (C), 149.4 (C), 135.6 (C), 133.8 (C), 132.1 (C), 118.1 (CH), 89.4 (C), 43.1 (CH$_2$), 40.1 (CH$_2$), 36.8 (CH$_2$), 31.6 (CH),

29.5 (CH3), 25.4 (CH$_3$), 22.2 (CH$_2$), 21.5 (CH$_3$), 20.6 (CH$_3$), 16.6 (CH$_3$), 12.8 (CH$_3$); HRESIMS *m/z* calcd for C$_{17}$H$_{28}$NO$_2$ (M-H)$^-$ 278.2120, found 278.2131.

6-*N*-*n*-butylaminoharmane (20): 6-nitroharmane (**8**, 50 mg, 0.220 mmol) and butyraldehyde (24.0 μL, 0.264 mmol) were reacted by the general reductive alkylation method The reaction mixture was stirred for 1 h at room temperature under nitrogen atmosphere. The crude product was purified on a Phenomenex Luna C8 250x10 mm, 5μm Luna reverse-phase HPLC column using gradient CH$_3$CN (0.1% TFA)/water (0.1% TFA) with flow rate of 6 mL/min to gave the pure *N*-ethylamino analog. **6-*N*-*n*-butylaminoharmane** (55 mg, 98%); brownish oil; (R$_f$ = 0.6, 100% DCM); IR: 3258, 3012, 2941, 2587, 2079, 1664, 1637, 1534, 1490, 1428, 1402, 1336.93, 1319, 1286, 1266, 1206, 1179, 1131, 1118, 1054, 990, 836, 820, 794, 751, 742, 730 cm^{-1}; ^{1}H-NMR (CDCl$_3$) δ 8.26 (1H, d, *J*=8.0 Hz), 7.74 (1H, d, *J*=7.8 Hz), 7.29 (1H, d, *J*=8.0 Hz), 7.25 (1H, d, *J*=8.0 Hz), 6.90 (1H, d, *J*=8.0), 3.19 (2H, t, *J*=7.6 Hz), 2.75 (s), 2.43 (2H, t, *J*=7.6 Hz), 1.66 (2H, q, *J*=8.0 Hz), 1.43 (2H, p, *J*=8.0 Hz), 1.00 (3H, t, *J*=8.0 Hz); ^{13}C-NMR (CDCl$_3$) δ 143.2 (C), 141.7, 136.9 (CH), 135.4 (C), 134.5 (C), 128.4 (C), 122.9 (CH), 118.3 (CH), 113.2 (CH), 112.7 (C), 102.8 (CH), 45.1 (CH$_2$), 32.0 (CH$_2$), 20.6 (CH$_2$), 21.0 (CH$_3$), 14.2 (CH$_3$). HRESIMS *m/z* calcd for C$_{16}$H$_{20}$N$_3$ (M+H)$^+$ 254.1657, found 254.1649.

2,2-*N*,*N*-dimethylaminoestrone (21): 2-nitroestrone (**10**, 20 mg, 0.062 mmol) and formaldehyde (17 μL, 0.140 mmol) were reacted by the general reductive alkylation method (0.2 mL of DCM was added as a cosolvent). The reaction mixture was stirred for 1 h at room temperature under nitrogen atmosphere. The crude product was purified on a Phenomenex Luna C8 250x10 mm, 5μm Luna reverse-phase HPLC column using gradient CH$_3$CN (0.1% TFA)/water (0.1% TFA) with flow rate of 6 mL/min to gave the pure analog. **2,2-*N*,*N*-dimethylaminoestrone:** (17 mg, 88%); $[\alpha]_D^{25}$ +148.8 (*c* 1, DCM); yellow powder (m. p. 162-165

^{o}C); (R$_f$ = 0.4, 100% DCM); IR: 3362, 3016, 2928, 2862, 2784, 1737, 1581, 1502, 1453, 1260, 1081, 801 cm^{-1}; ^{1}H-NMR (CDCl$_3$) δ 7.07 (1H,s), 6.66 (1H,s), 2.61 (6H, s), 2.53 (1H, dd, J=17.0, 8.3 Hz), 2.46 (1H, m), 2.31-1.97 (6H, m), 1.59-1.23 (8H, m), 0.89 (3H,s); ^{13}C-NMR (CDCl$_3$) δ 221.0 (C), 149.3 (C), 138.3 (C), 134.1 (C), 131.1 (C), 117.4 (CH), 113.8 (CH), 50.4 (CH), 48.0 (C), 45.3 (CH$_3$), 44.2 (CH$_3$), 38.3 (CH), 35.8 (CH$_2$), 31.5 (CH), 29.6 (CH$_2$), 29.2 (CH$_2$), 26.5 (CH$_2$), 26.1 (CH$_2$), 21.5 (CH$_2$), 13.8 (CH$_3$); HRESIMS m/z calcd for C$_{20}$H$_{28}$NO$_2$ (M+H)$^+$ 314.2120, found 314.2101.

4-(*n*-butylamino)anisole (**1a**)
^{1}H-NMR (CDCl$_3$)
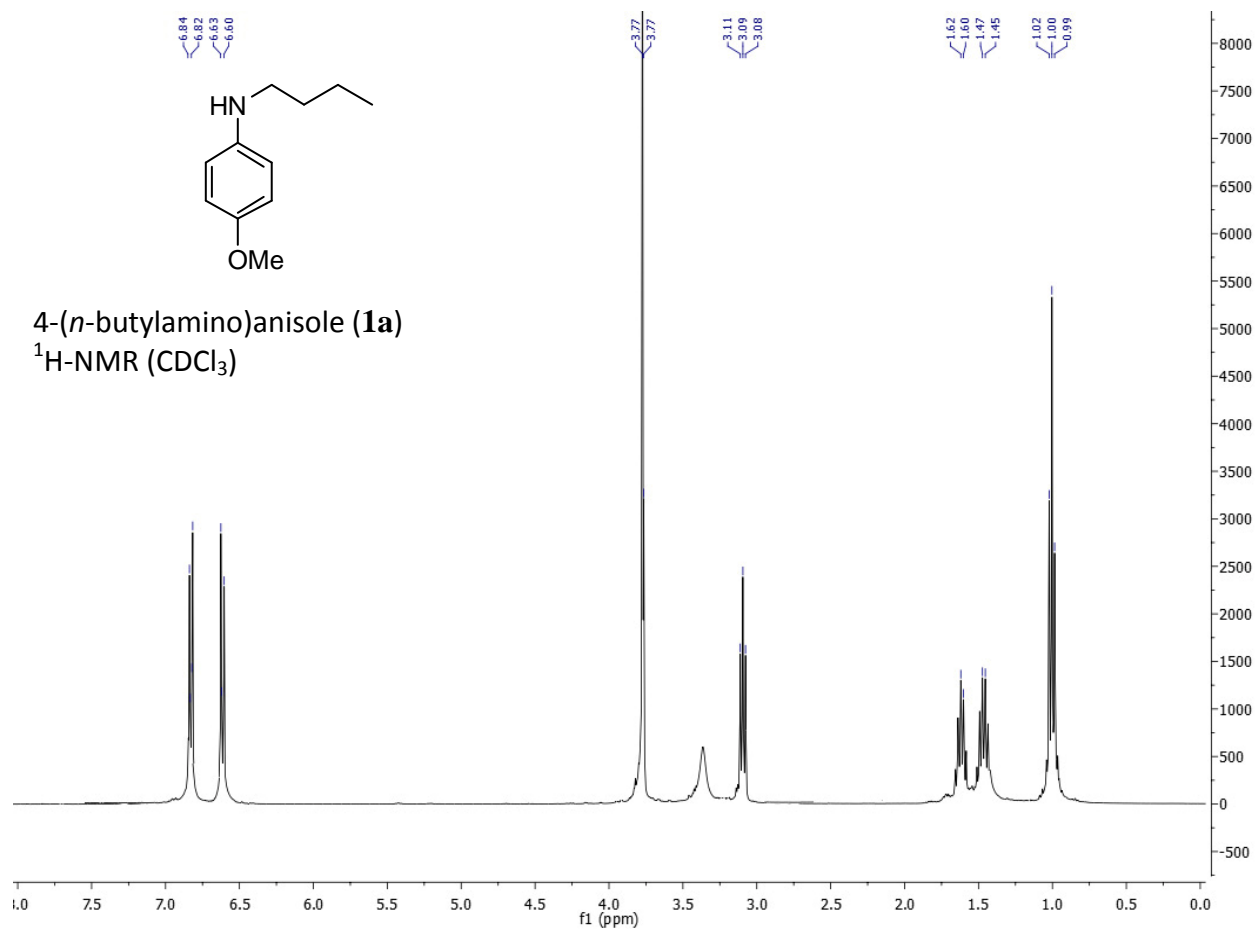
Figure IV.1. ^{1}H-NMR of 4-(*n*-butylamino)anisole (**1a**) in CDCl$_3$ at 400 MHz.

Racemic mixture;
Complete conversion

4-(2-methylcyclohexylamino)anisole (**1b**) ^{1}H-NMR (CDCl$_3$)
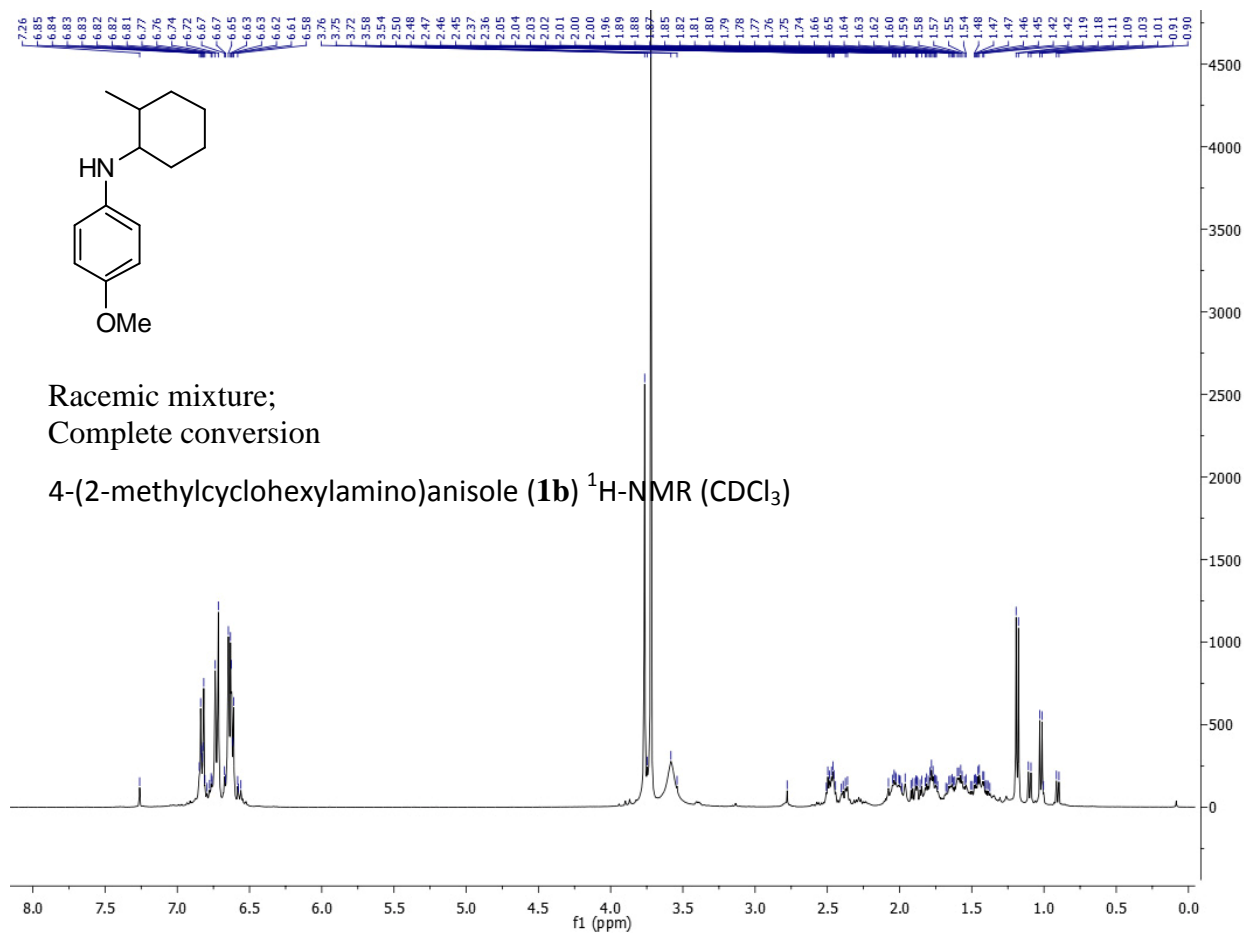
Figure IV.2. ^{1}H-NMR of 4-(2-methylcyclohexylamino)anisole (**1b**) in CDCl$_3$ at 400 MHz.
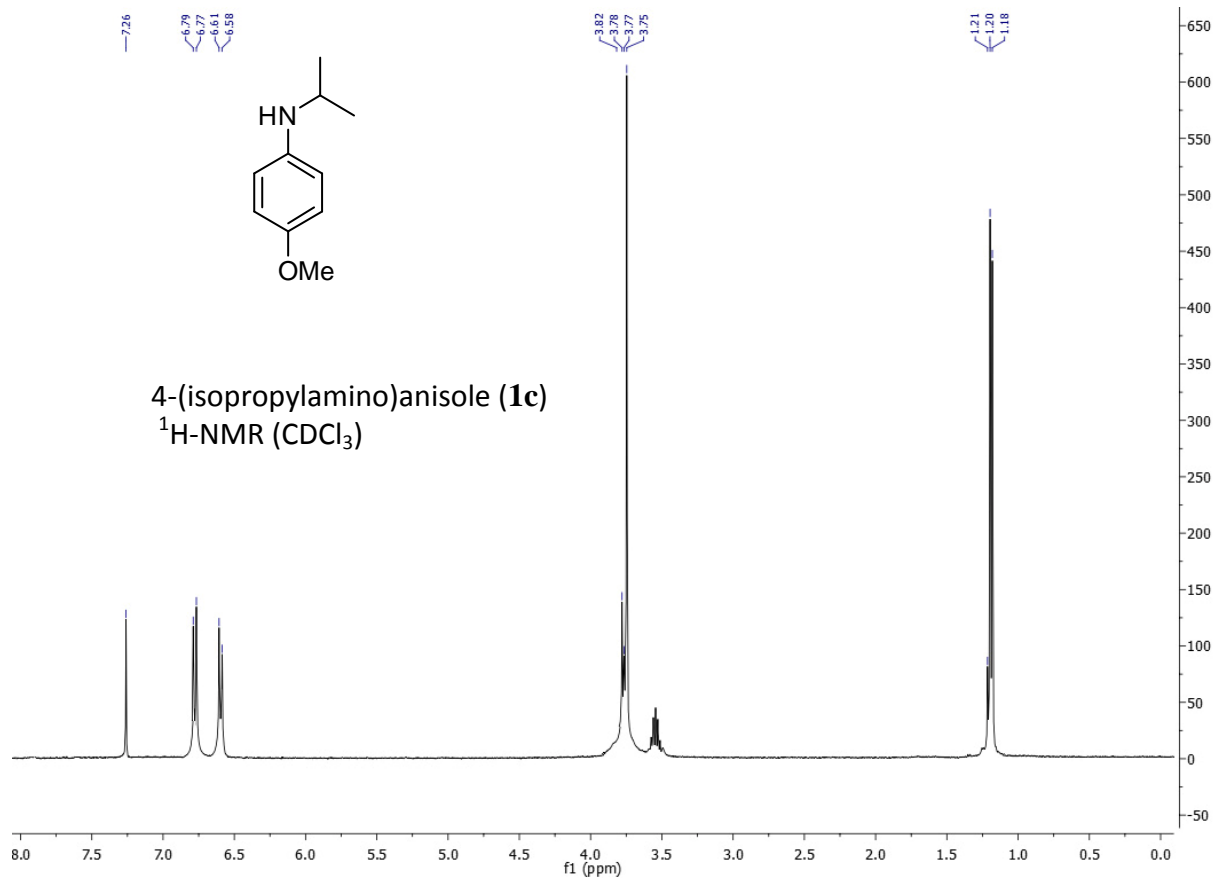
Figure IV.3. ^{1}H-NMR of 4-(isopropylamino)anisole (**1c**) in CDCl$_3$ at 400 MHz.

4-(*n*-butylamino)ethylbenzoate (**1d**)
^{1}H-NMR (CDCl$_3$)
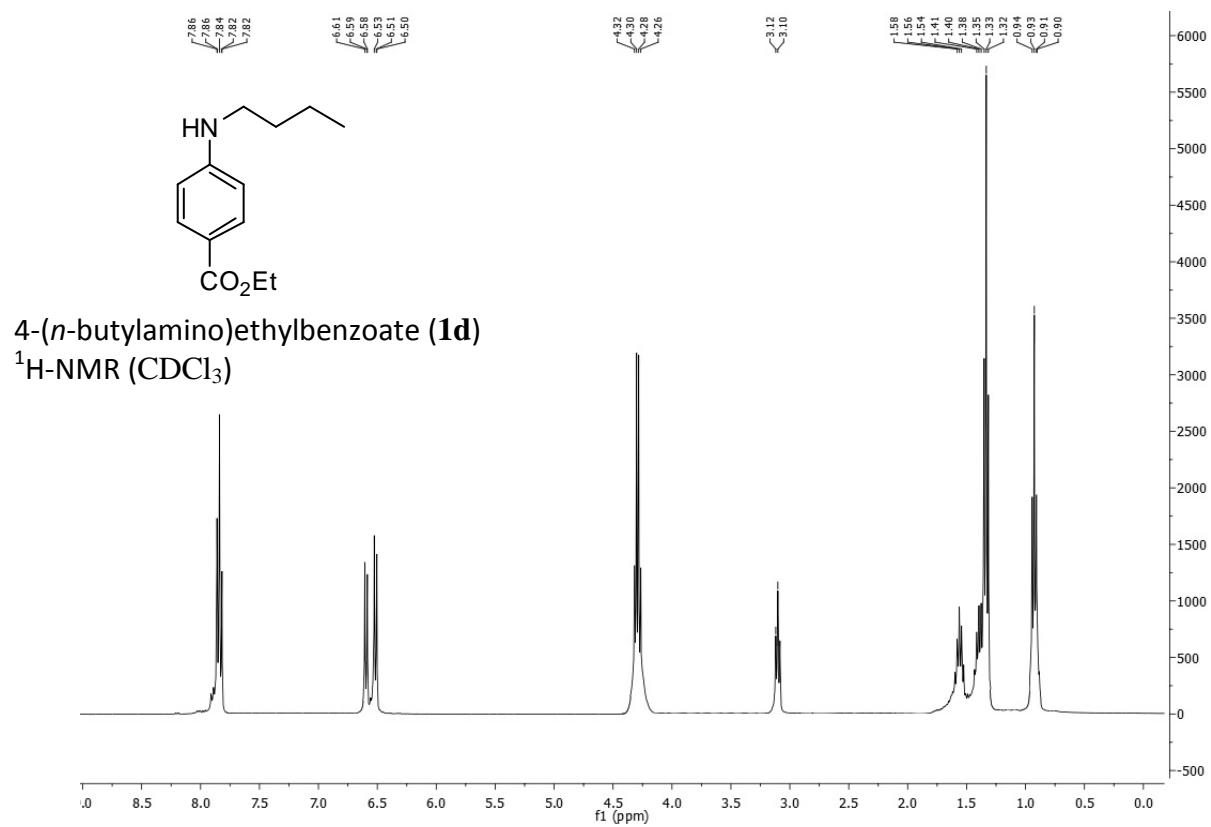
Figure IV.4. ^{1}H-NMR of 4-(*n*-butylamino)ethylbenzoate (**1d**) in CDCl$_3$ at 400 MHz.

4-(*p*-chlorobenzylamino)anisole (**1e**)
^{1}H-NMR (CDCl$_3$)
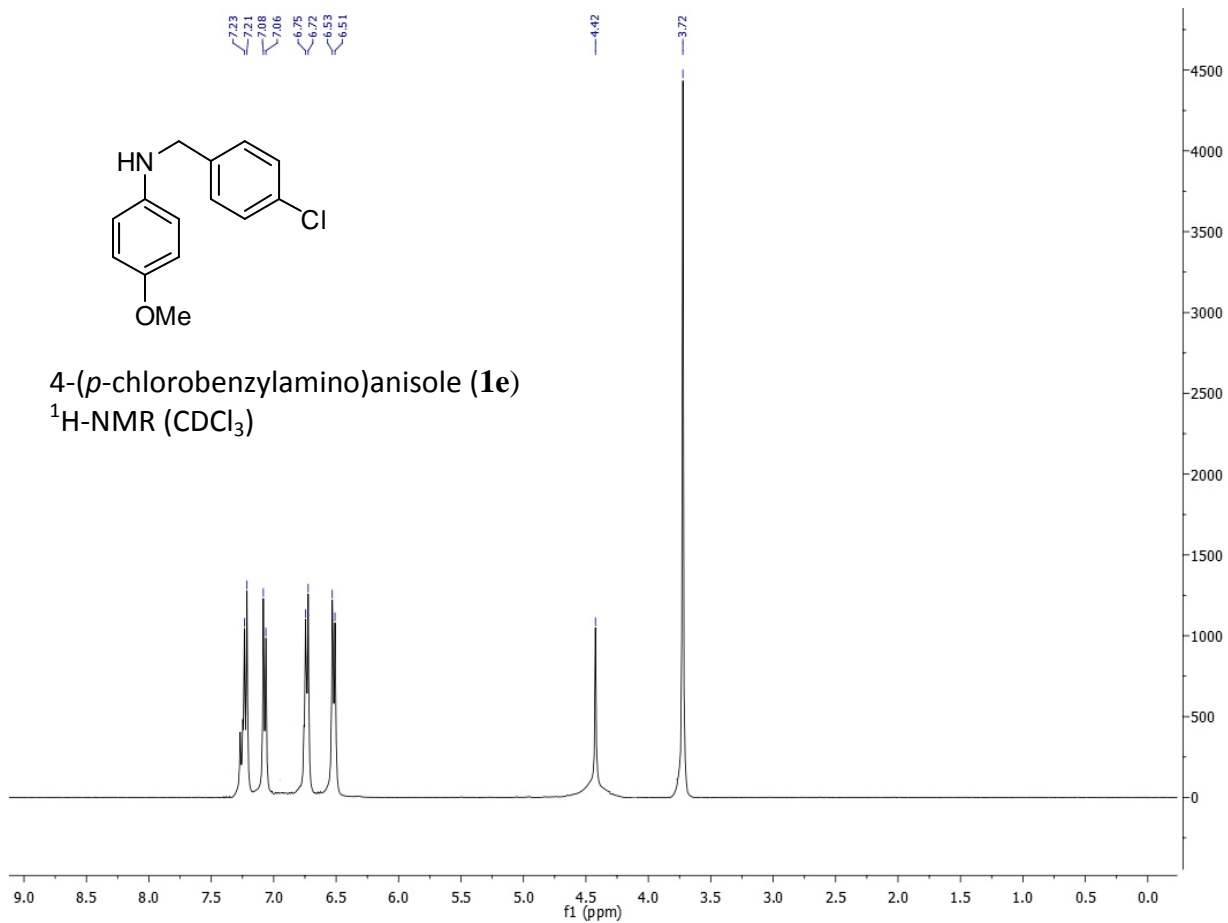
Figure IV.5. ^{1}H-NMR of 4-(*p*-chlorobenzylamino)anisole (**1e**) in CDCl$_3$ at 400 MHz.

4,4-*N*,*N*-dimethylaminoanisole **(1f)**
^{1}H-NMR (CDCl$_3$)
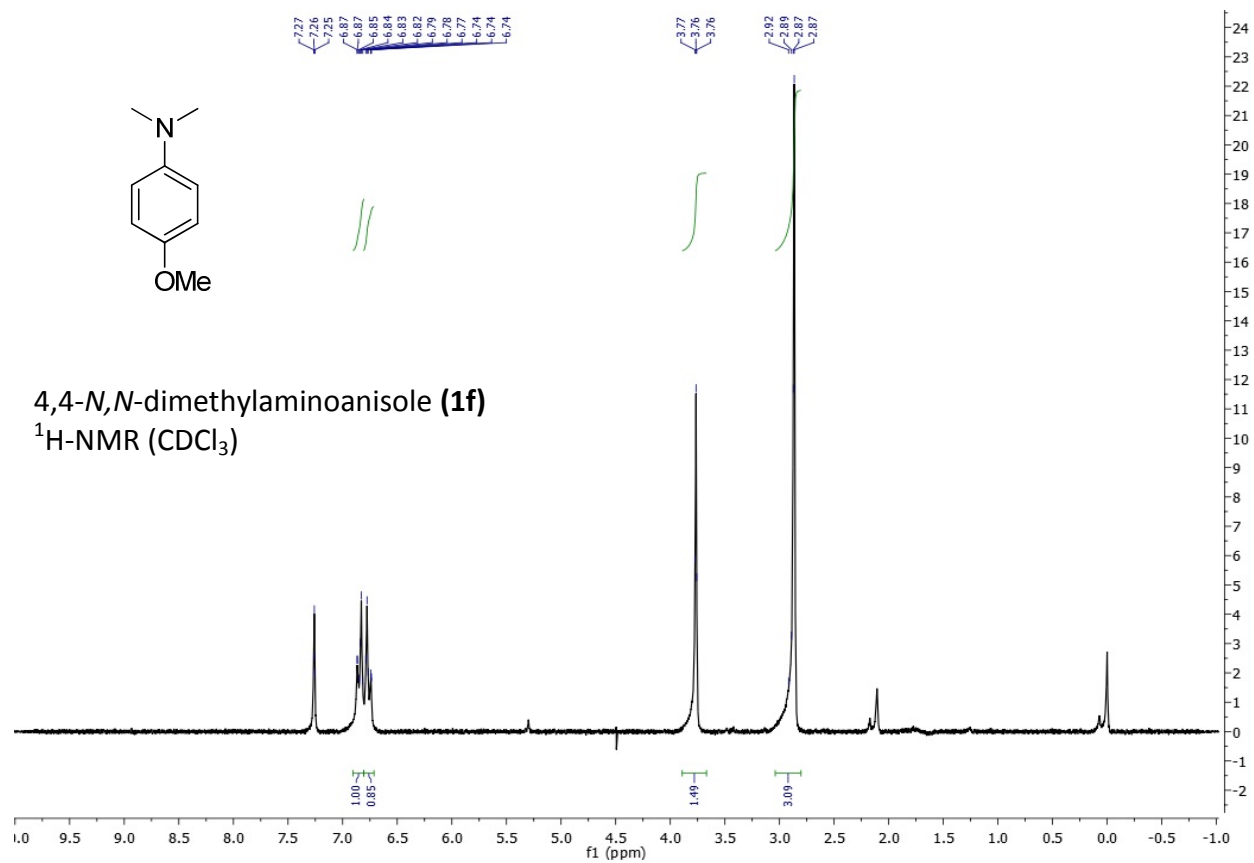
Figure IV.6. ^{1}H-NMR of 4,4-*N*,*N*-dimethylaminoanisole **(1f)** in CDCl$_3$ at 400 MHz.
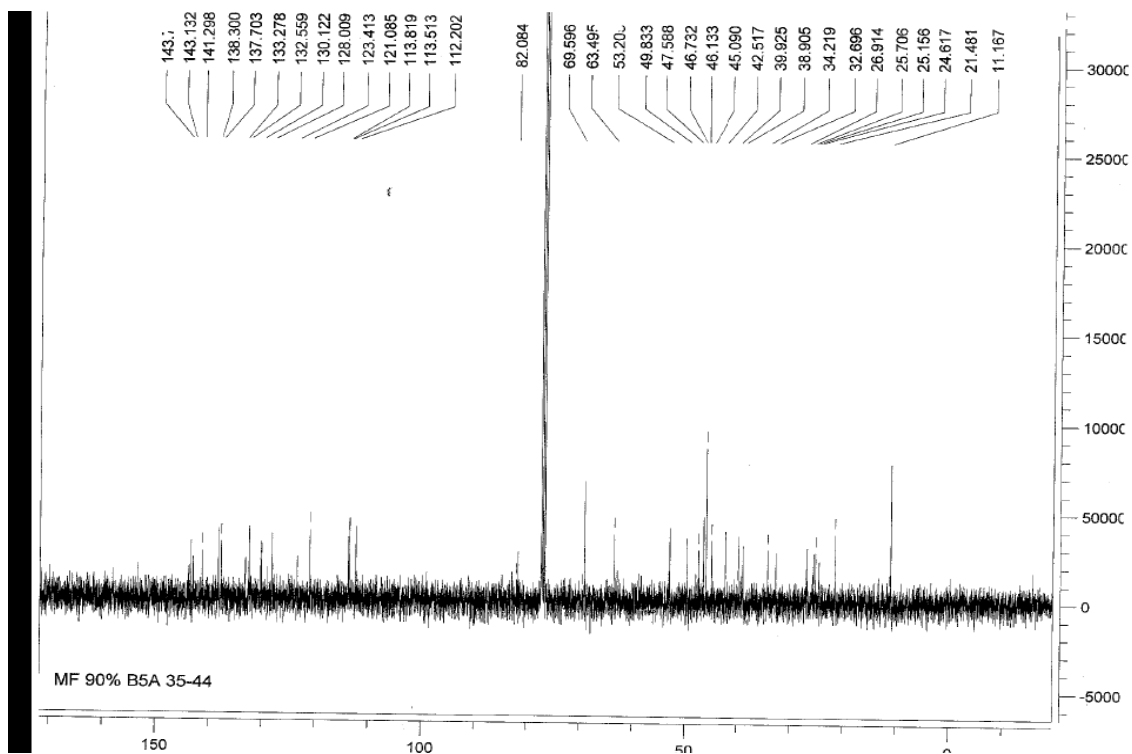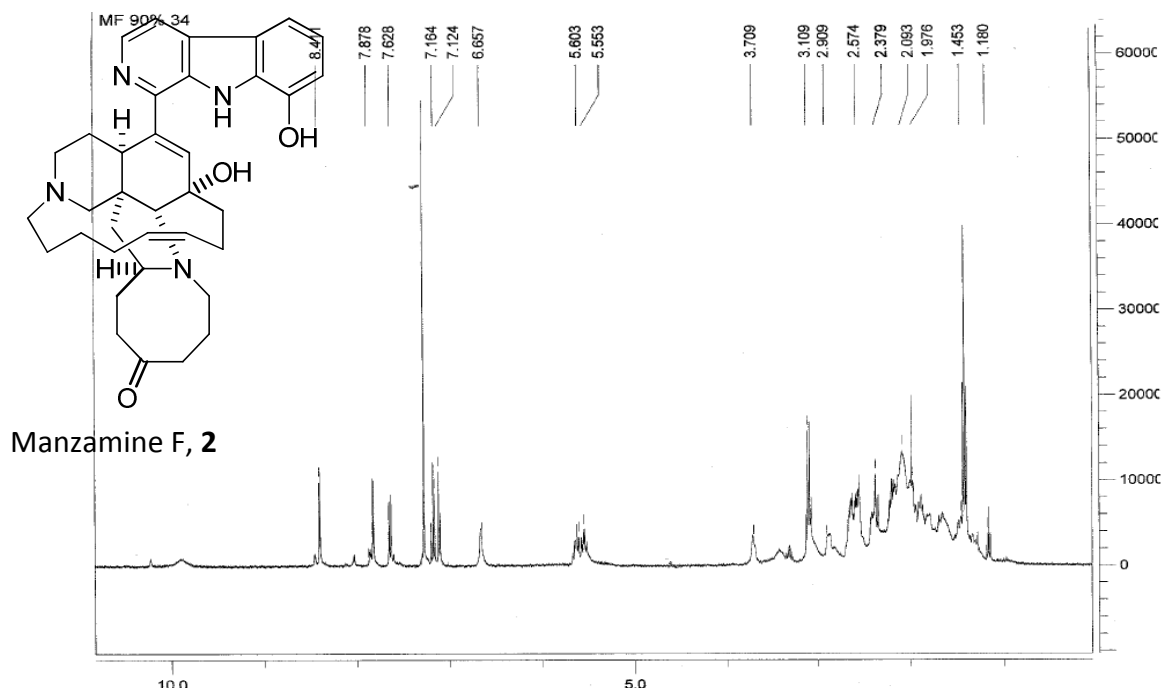
Figure IV.7. ^{1}H- and ^{13}C-NMR spectra of manzamine F (**2**) in CDCl$_3$, at 400 and 100 MHz, respectively.
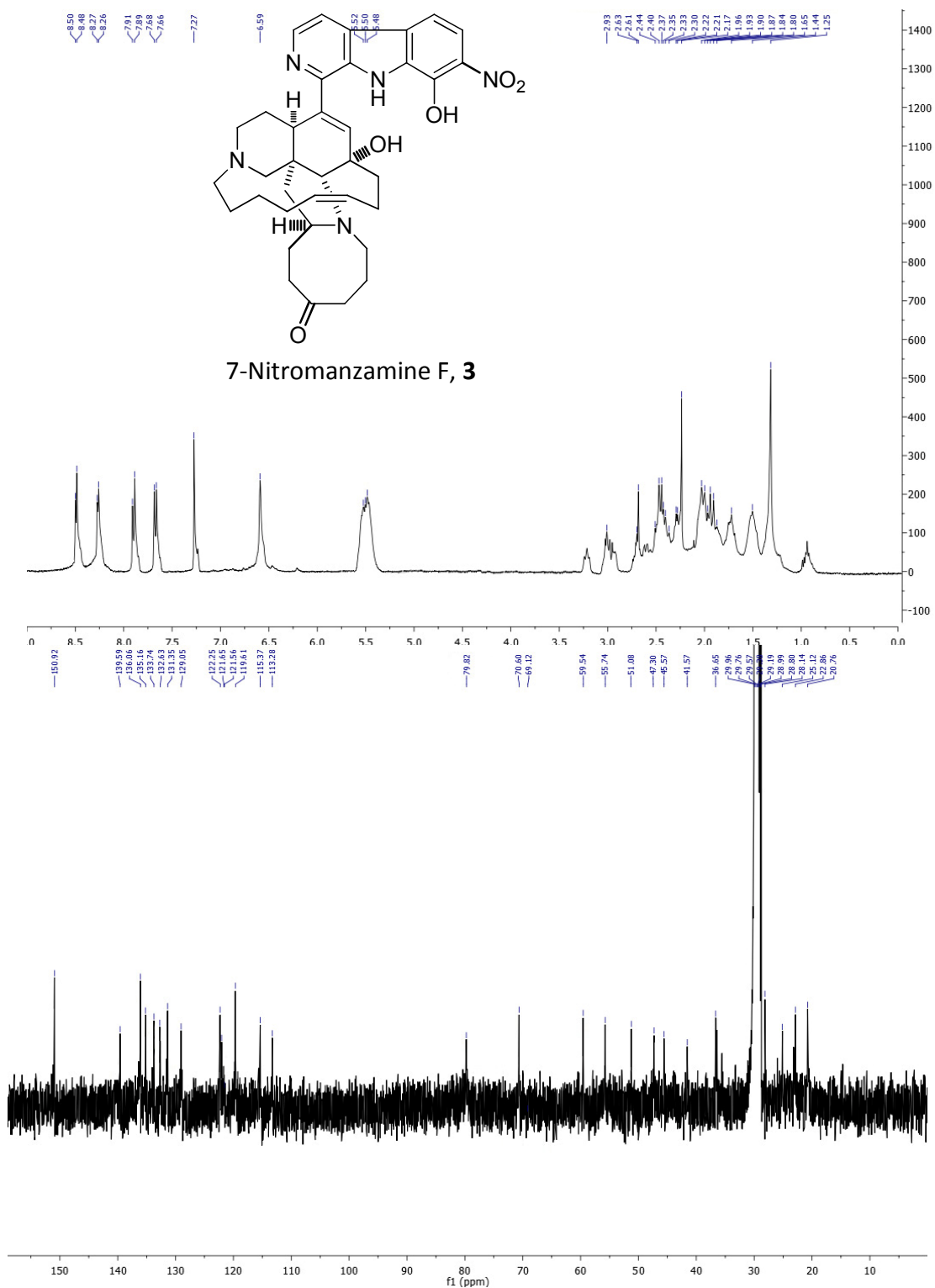
Figure IV.8. ^{1}H- and ^{13}C-NMR spectra of 7-nitromanzamine F (**3**) in *d6*-acetone, at 400 and 100 MHz, respectively.
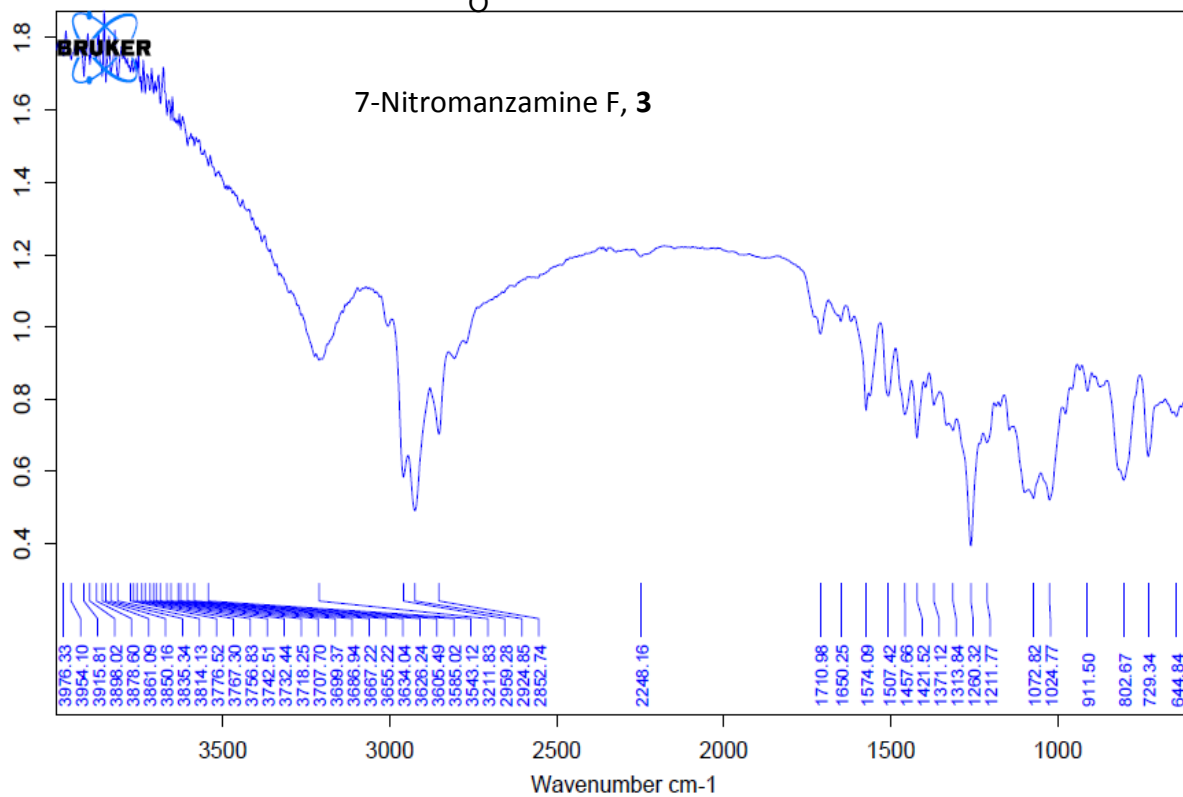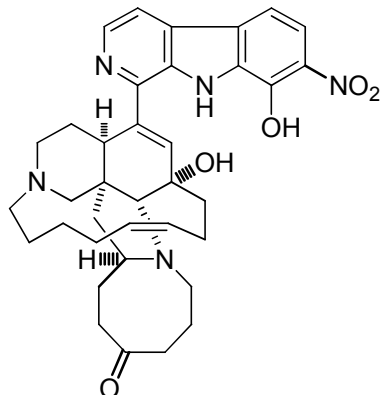
Figure IV.9. IR spectra (neat) of 7-nitromanzamine F (**3**).
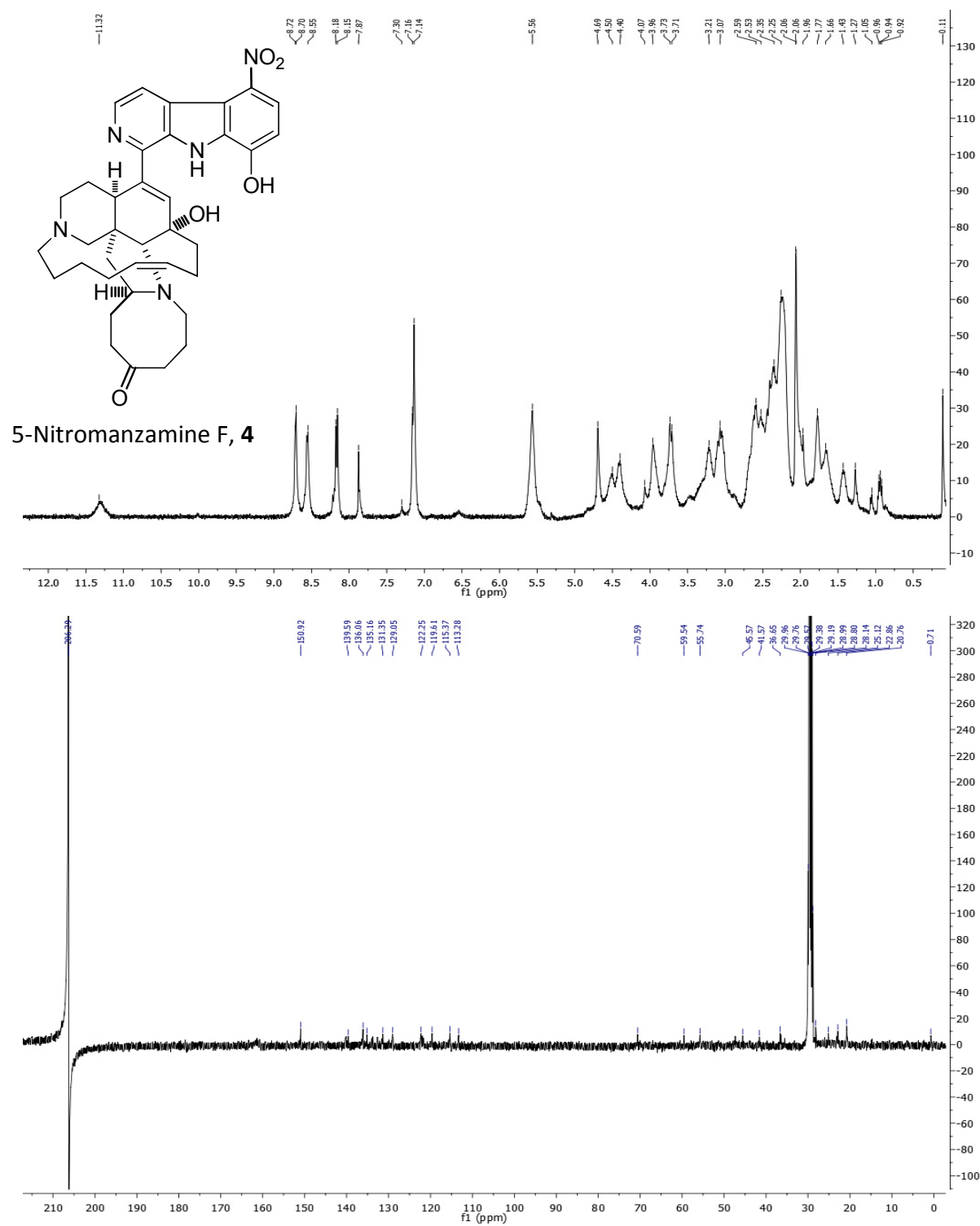
Figure IV.10. ^{1}H- and ^{13}C-NMR spectra of 5-nitromanzamine F (**4**) in *d6*-acetone, at 400 and 100 MHz, respectively.
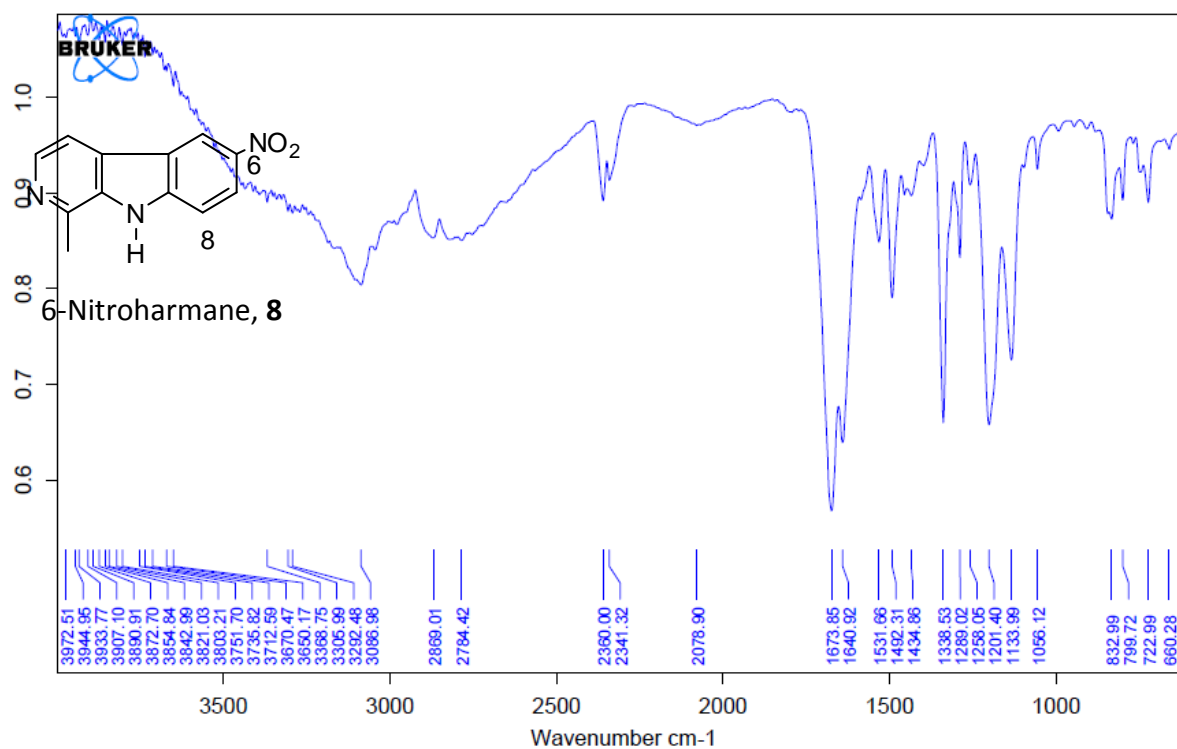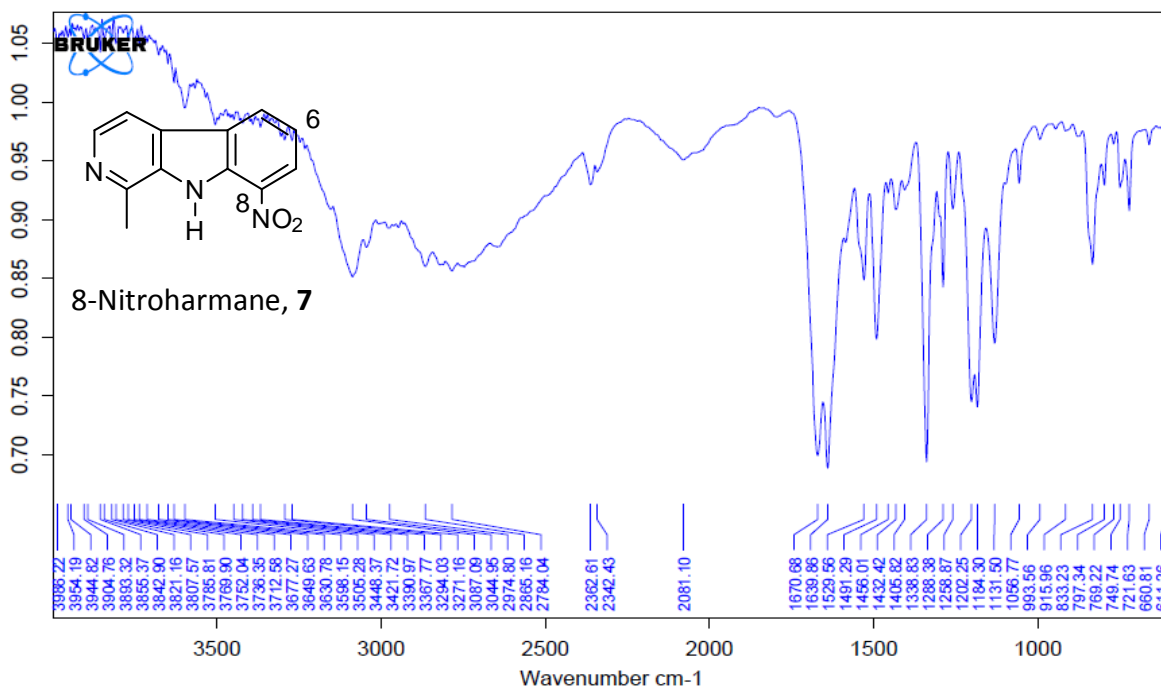
Figure IV.11. IR spectra (neat) of 8-nitroharmane (**7**) and 6-nitroharmane (**8**).
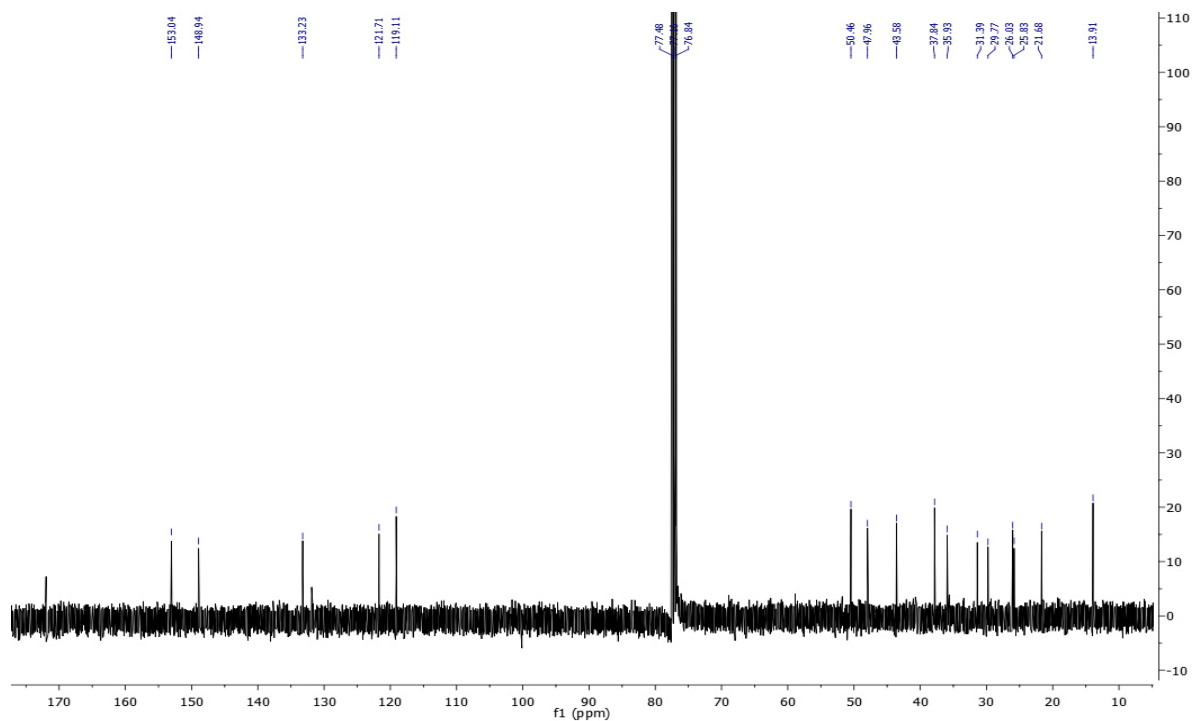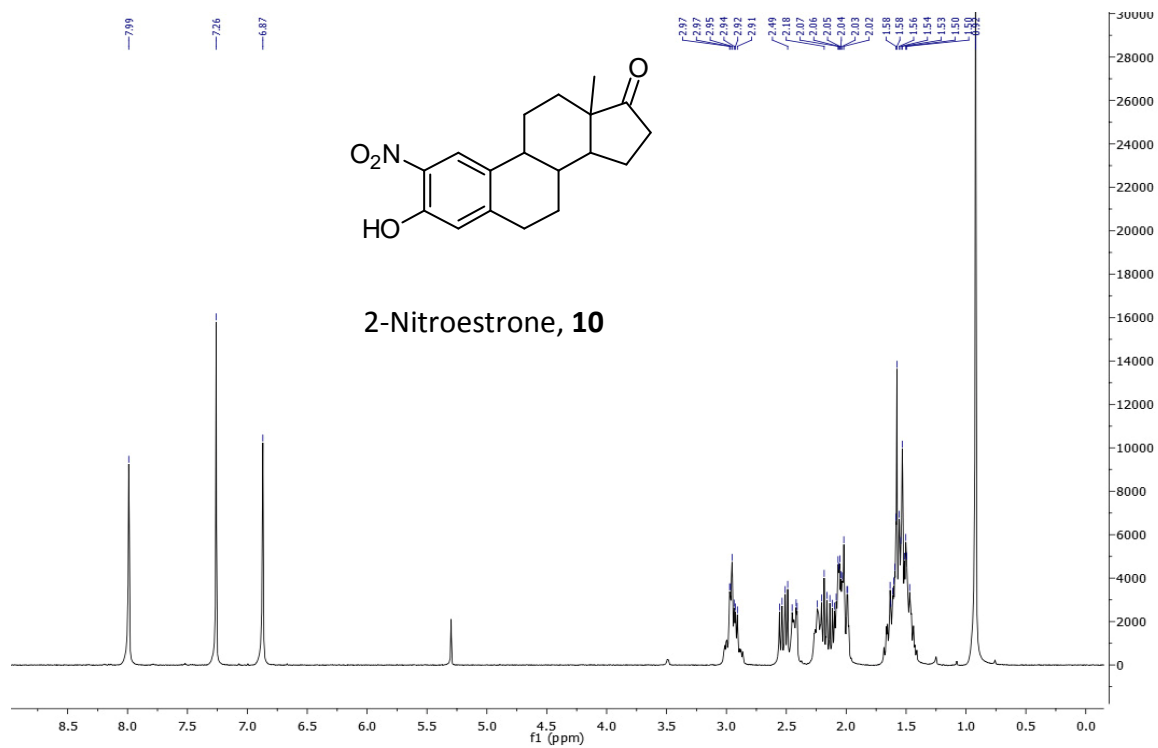
Figure IV.12. ^{1}H- and ^{13}C-NMR spectra of 2-nitroestrone (**10**) in CDCl$_3$ at 400 and 100 MHz, respectively.
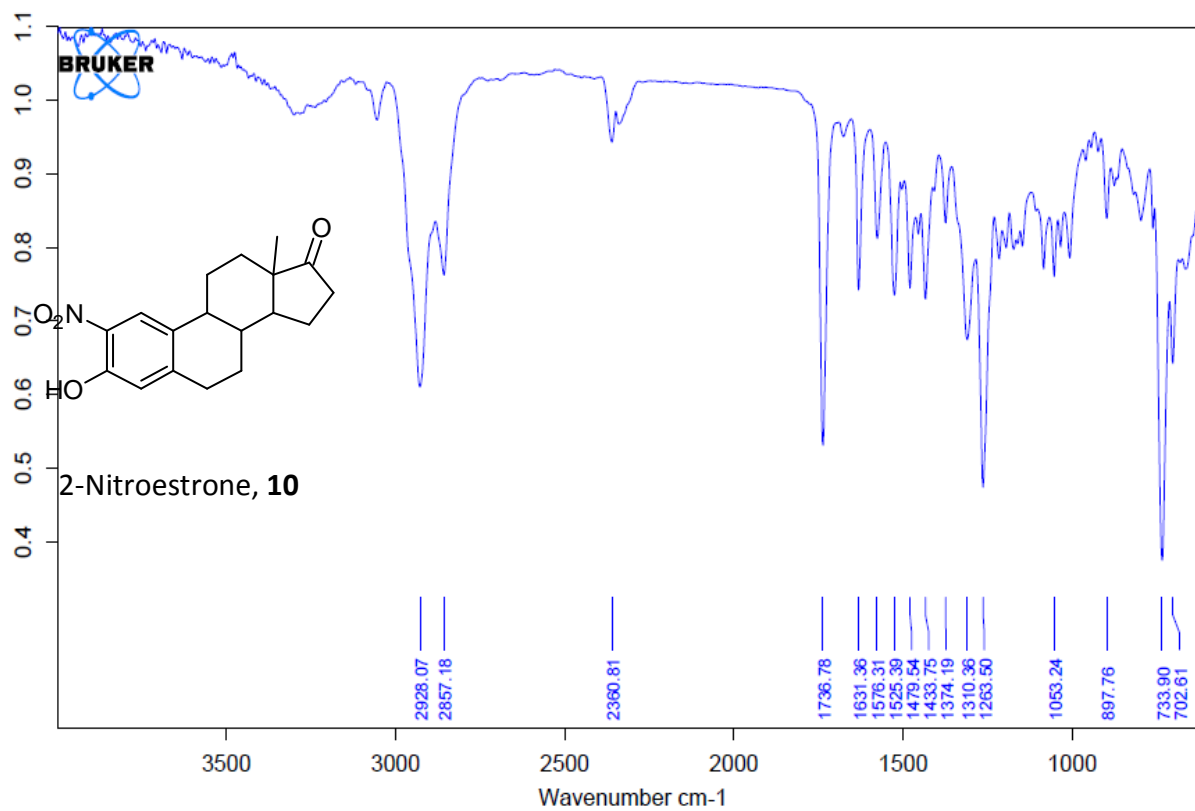
Figure IV.13. IR spectra (neat) of 2-nitroestrone (**10**).

2,4-Dinitroestrone, **11**
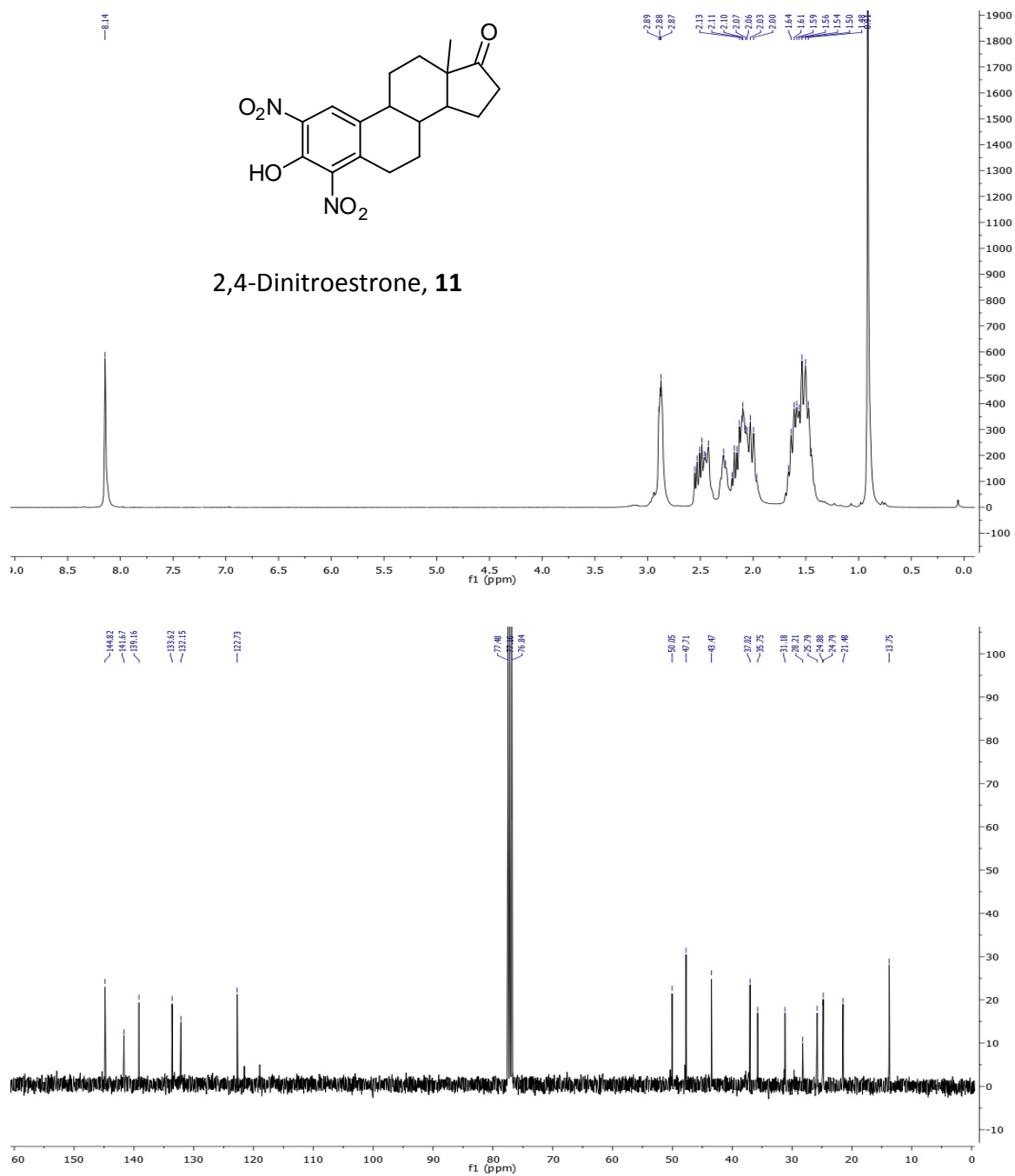
Figure IV.14. ^{1}H- and ^{13}C-NMR spectra of 2,4-dinitroestrone (**11**) in CDCl$_3$ at 400 and 100 MHz, respectively.
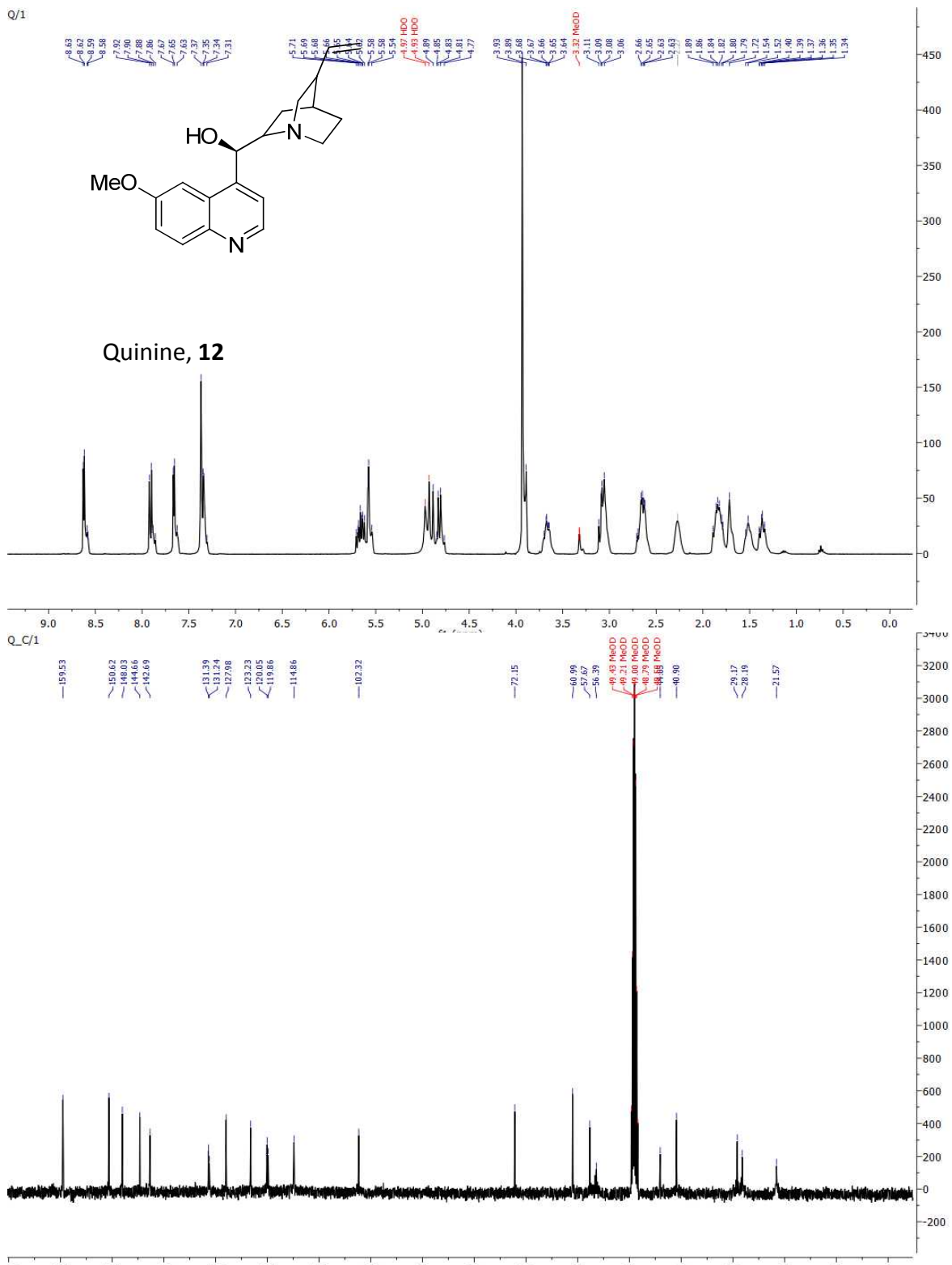
Figure IV.15. ^{1}H- and ^{13}C-NMR spectra of quinine (**12**) in $d4$-methanol at 400 and 100 MHz, respectively.

11-Nitro-10-hydroxyquinine, **13**
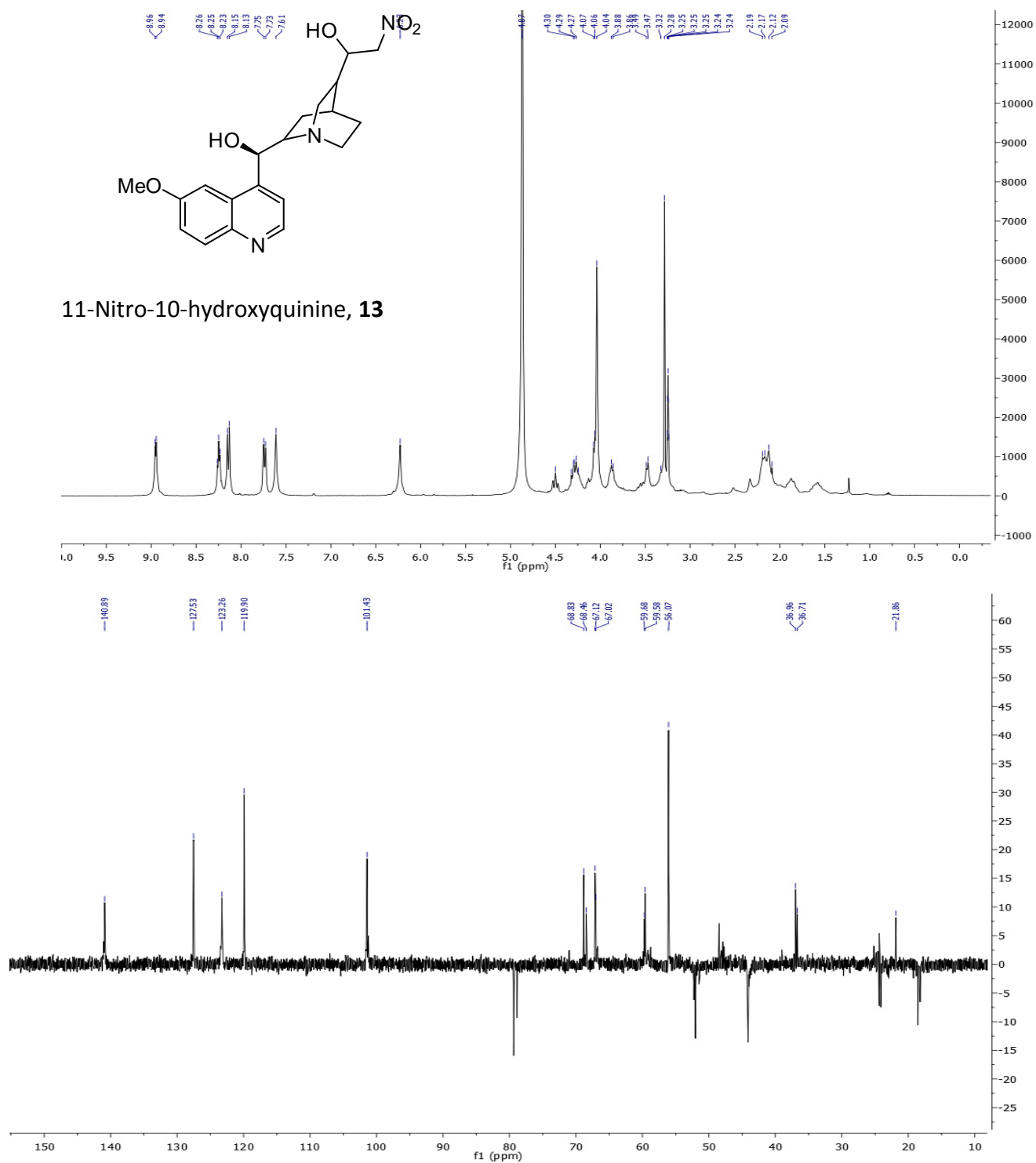
Figure IV.16. ^{1}H- and ^{135}DEPT-NMR spectra of 11-nitro-10-hydroxyquinine (**13**) in *d4*-methanol at 400 and 100 MHz, respectively.
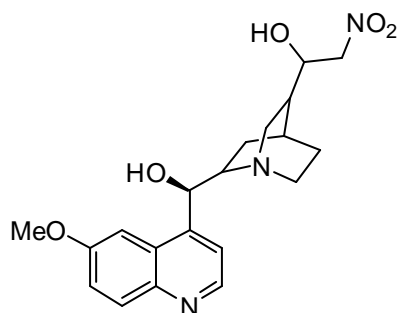
11-Nitro-10-hydroxyquinine, **13**
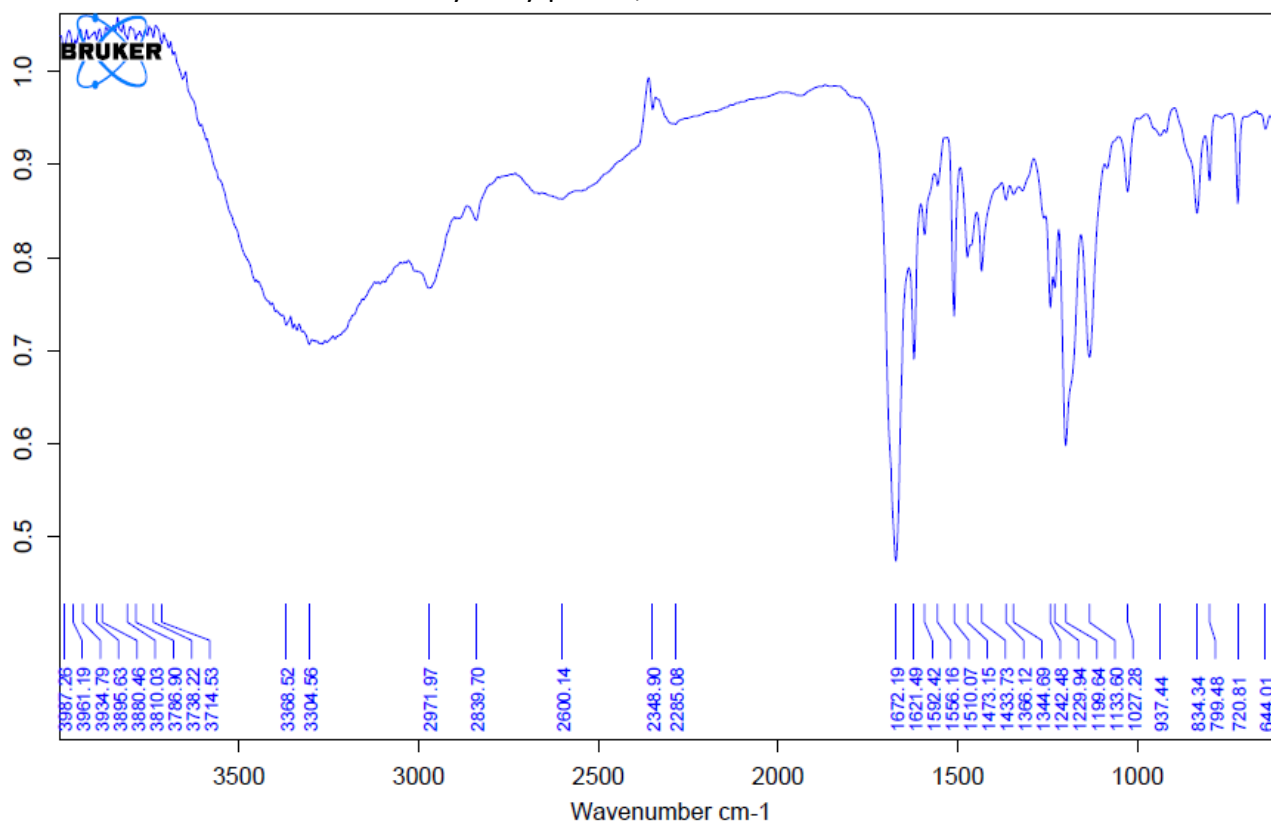
Figure IV.17. IR spectra (neat) of 11-Nitro-10-hydroxyquinine (**13**).
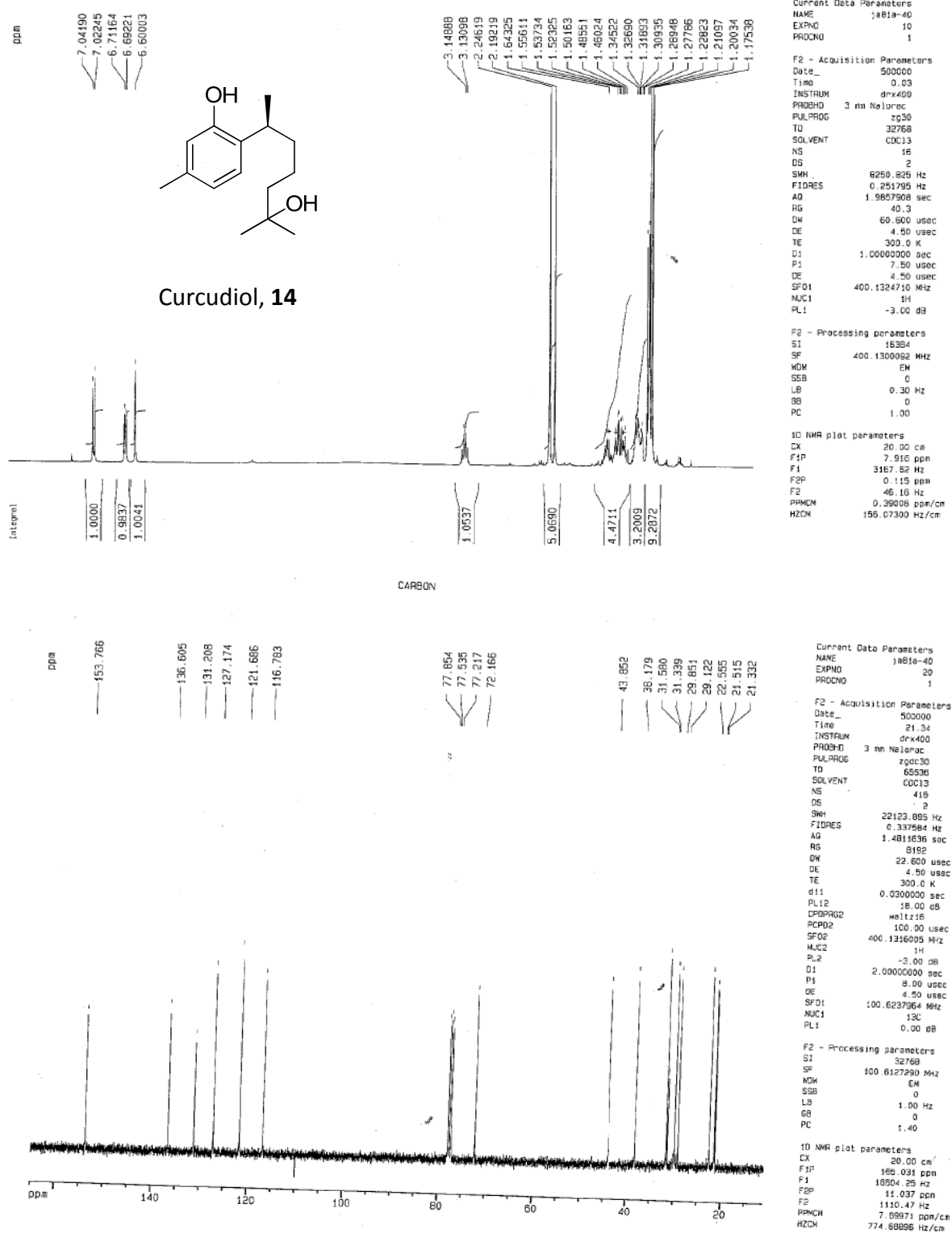
Figure IV.18. ^{1}H- and ^{13}C-NMR spectra of curcudiol (**14**) in CDCl$_3$ at 400 and 100 MHz, respectively.
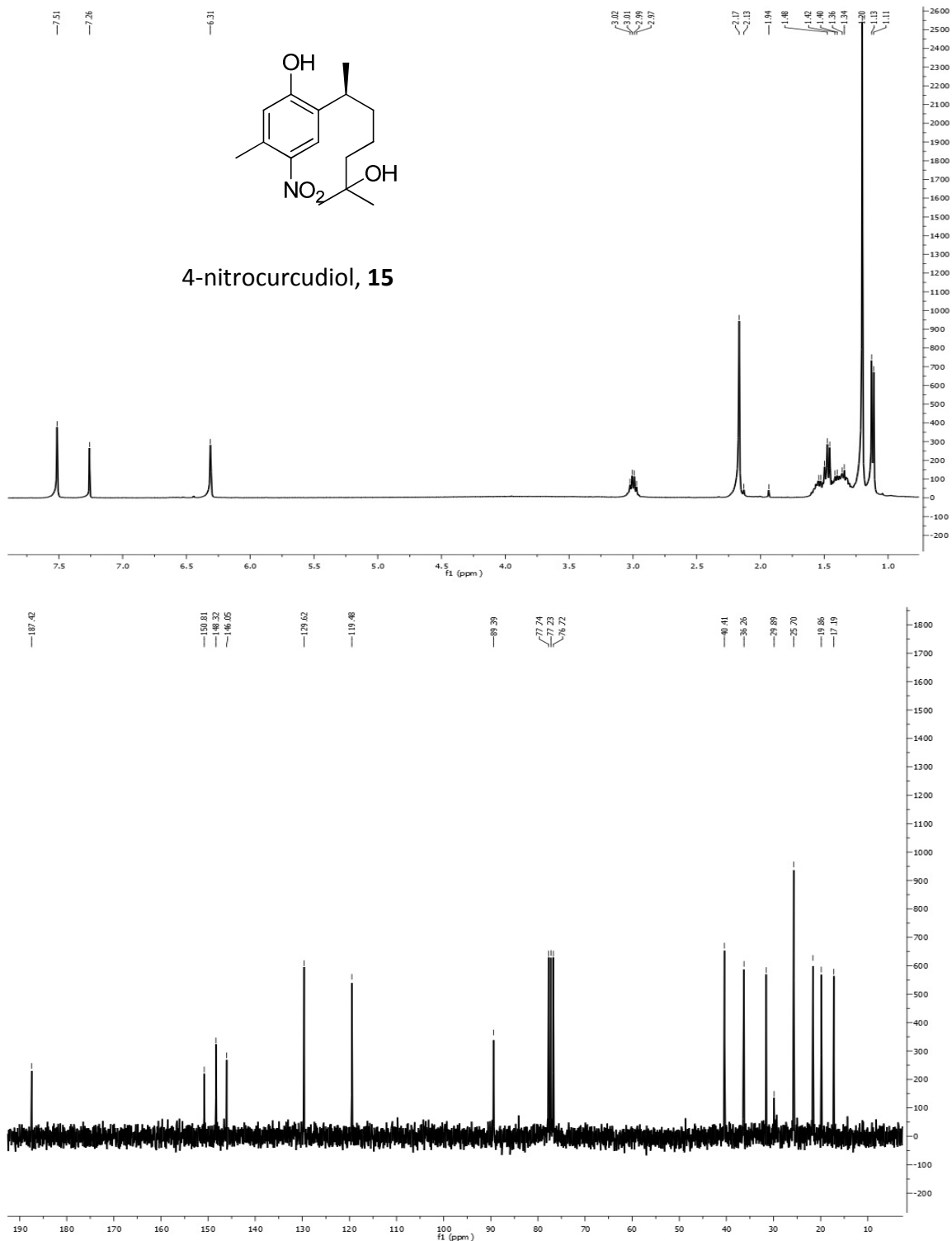
Figure IV.19. ^{1}H- and ^{13}C-NMR spectra of 4-nitrocurcudiol (**15**) in CDCl$_3$ at 400 and 100 MHz, respectively.
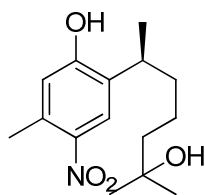
4-nitrocurcudiol, **15**
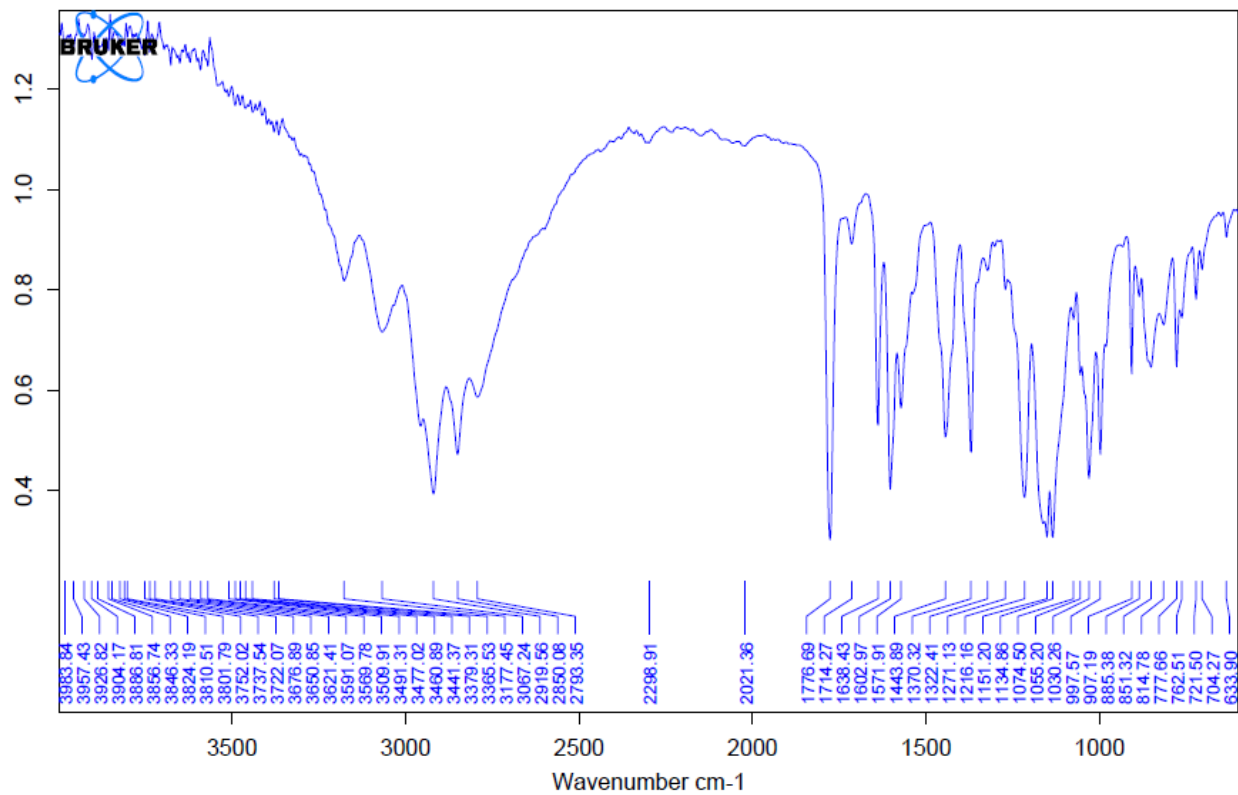
Figure IV.20. IR spectra (neat) of 4-nitrocurcudiol (**15**).

7-*N*-ethylaminomanzamine F **(17)**
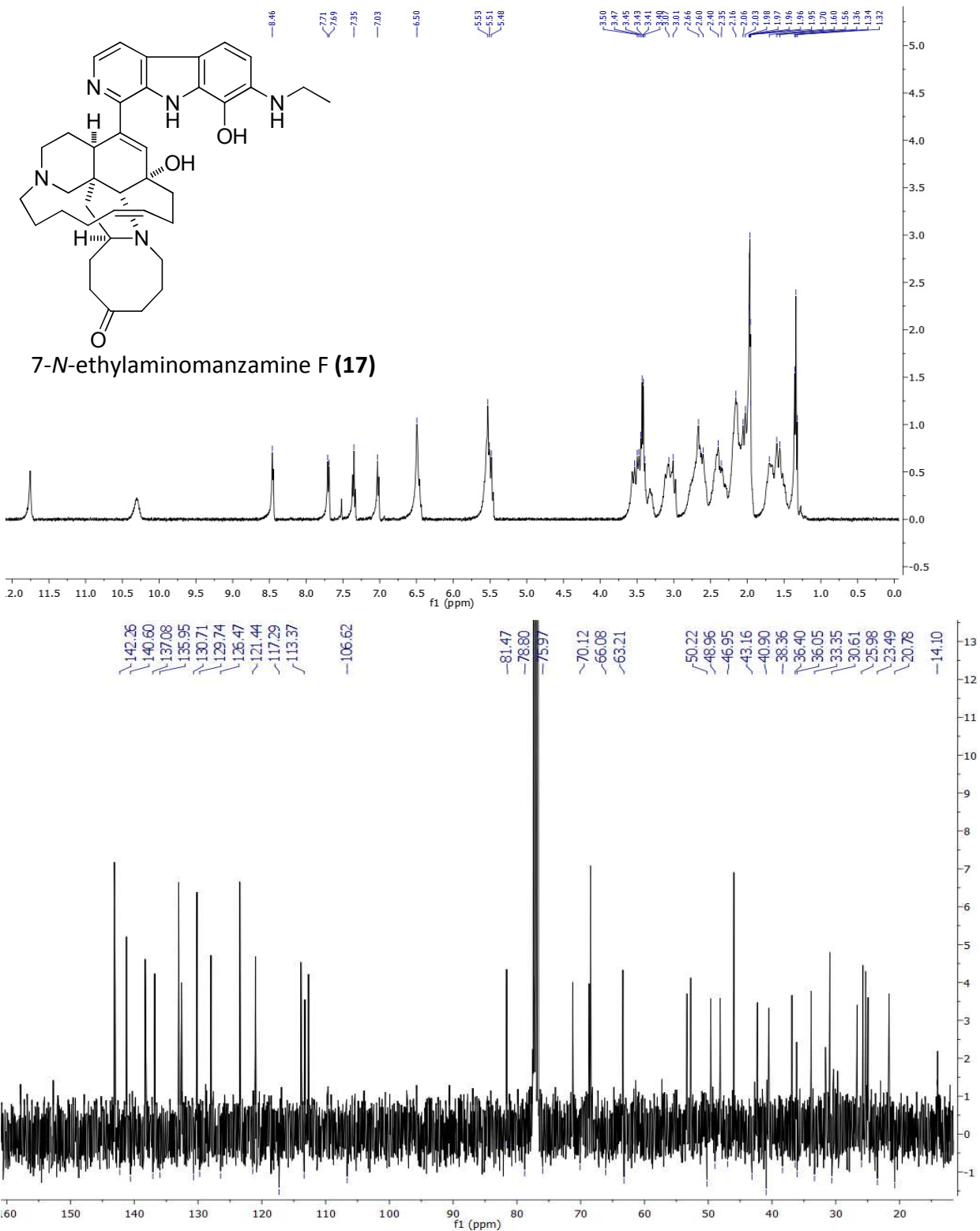
Figure IV.21. ^{1}H- and ^{13}C-NMR spectra of 7-*N*-ethylaminomanzamine F (**17**) in CDCl$_3$ at 400

and 100 MHz respectively.

11-*N*-ethylamino-10-hydroxyquinine **(18)**
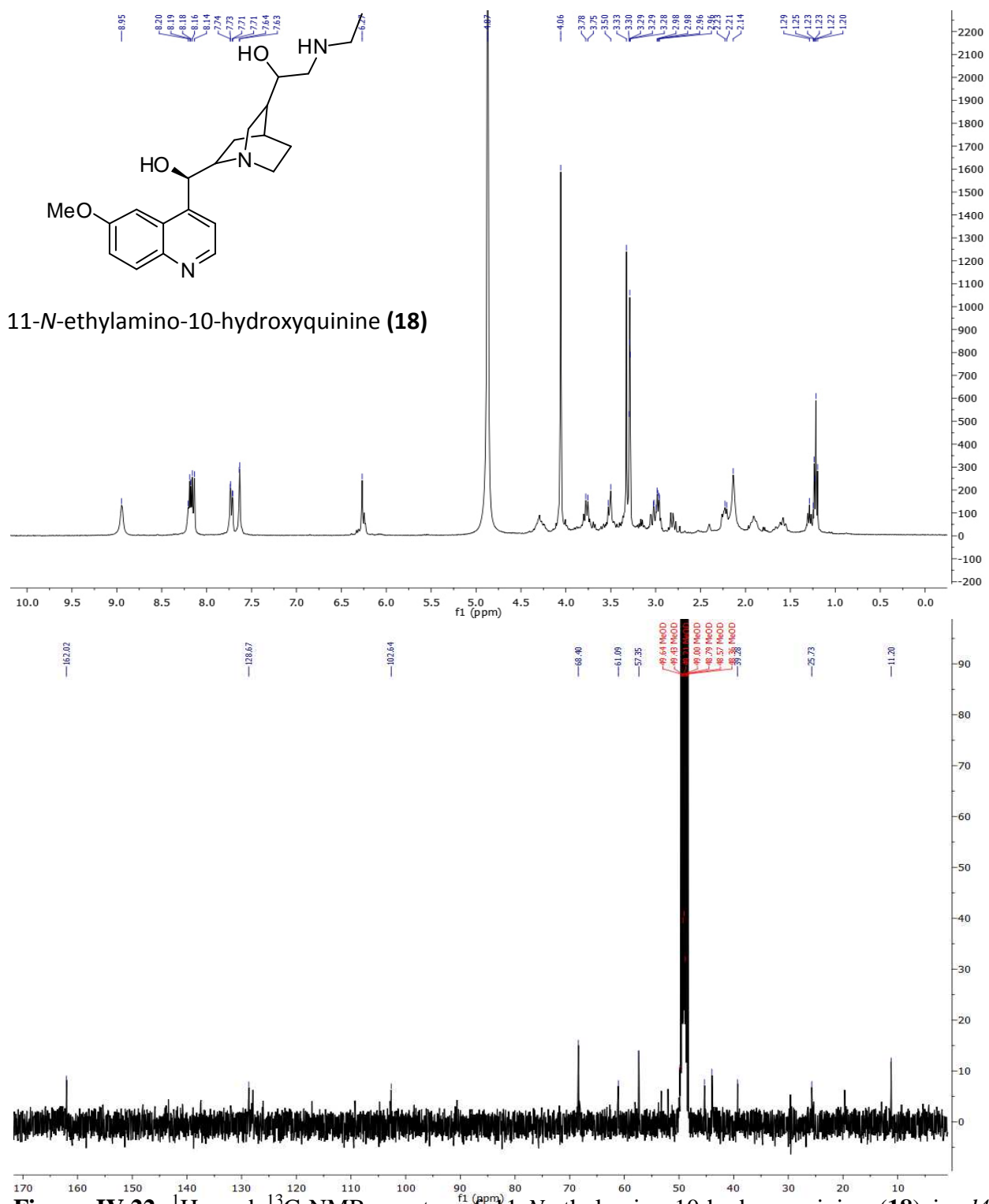
Figure IV.22. ¹H- and ¹³C-NMR spectra of 11-*N*-ethylamino-10-hydroxyquinine (**18**) in *d4*-methanol at 400 and MHz respectively.

211

4-*N*-ethylaminocurcudiol **(19)**

Figure IV.23. ¹H- and ¹³C-NMR spectra of 4-*N*-ethylaminocurcudiol (**19**) in CDCl₃ at 400 and 100 MHz respectively.
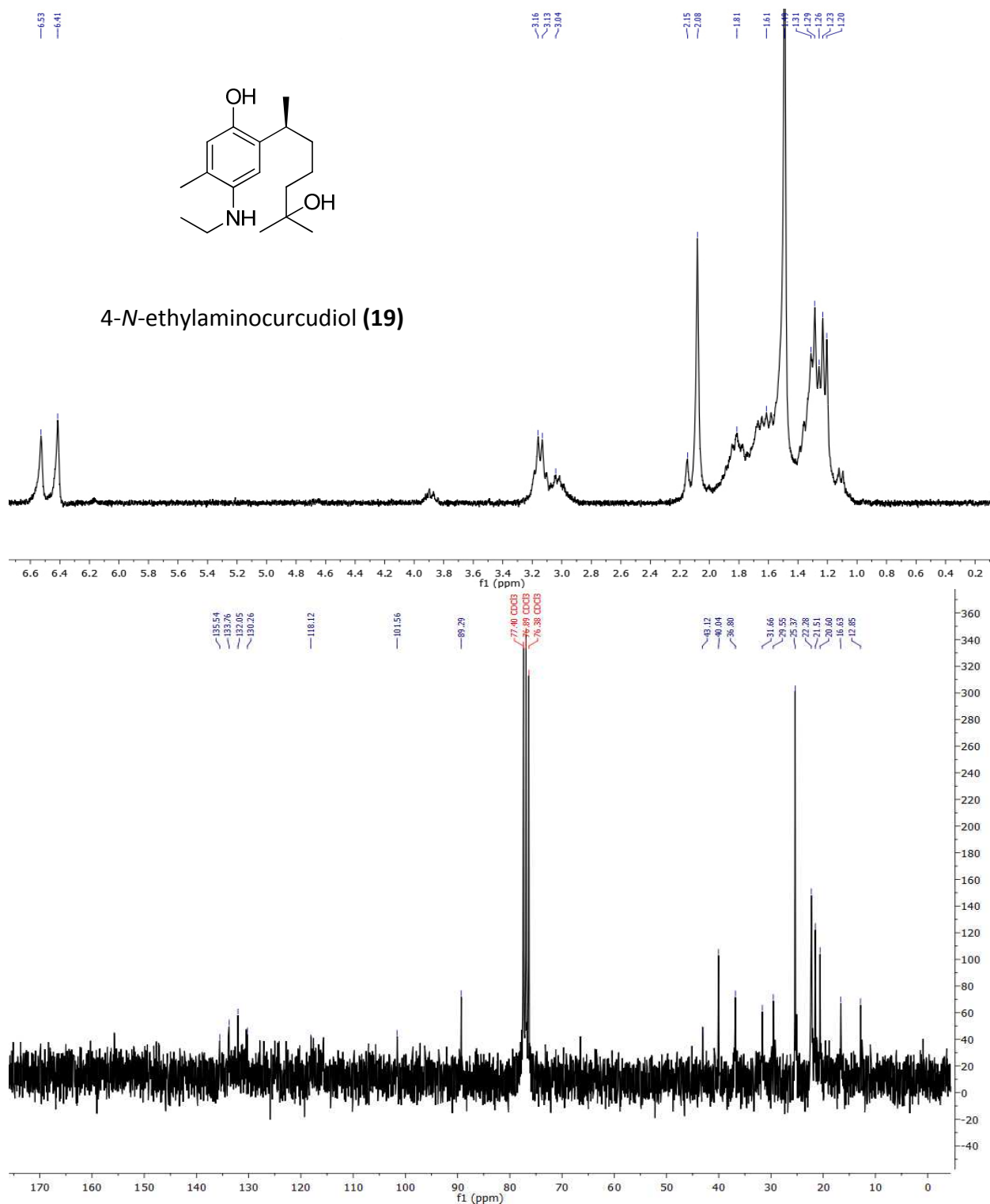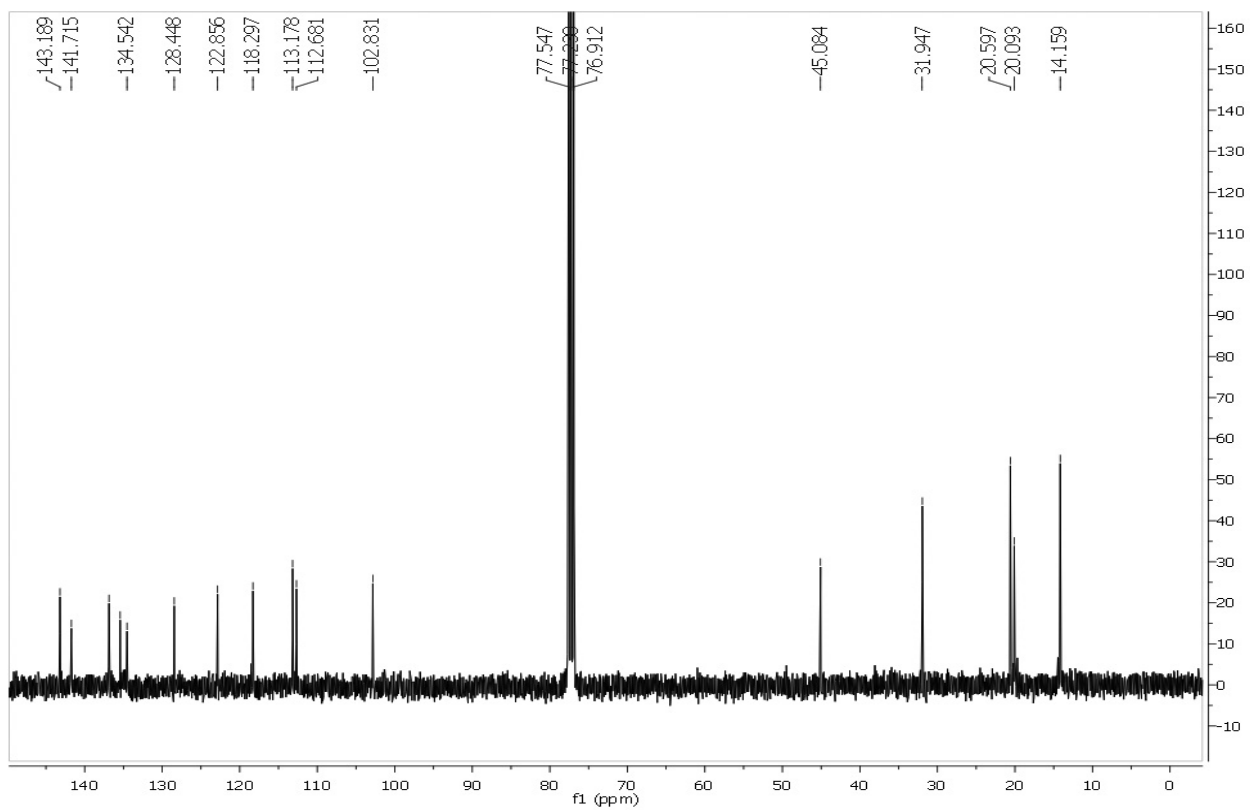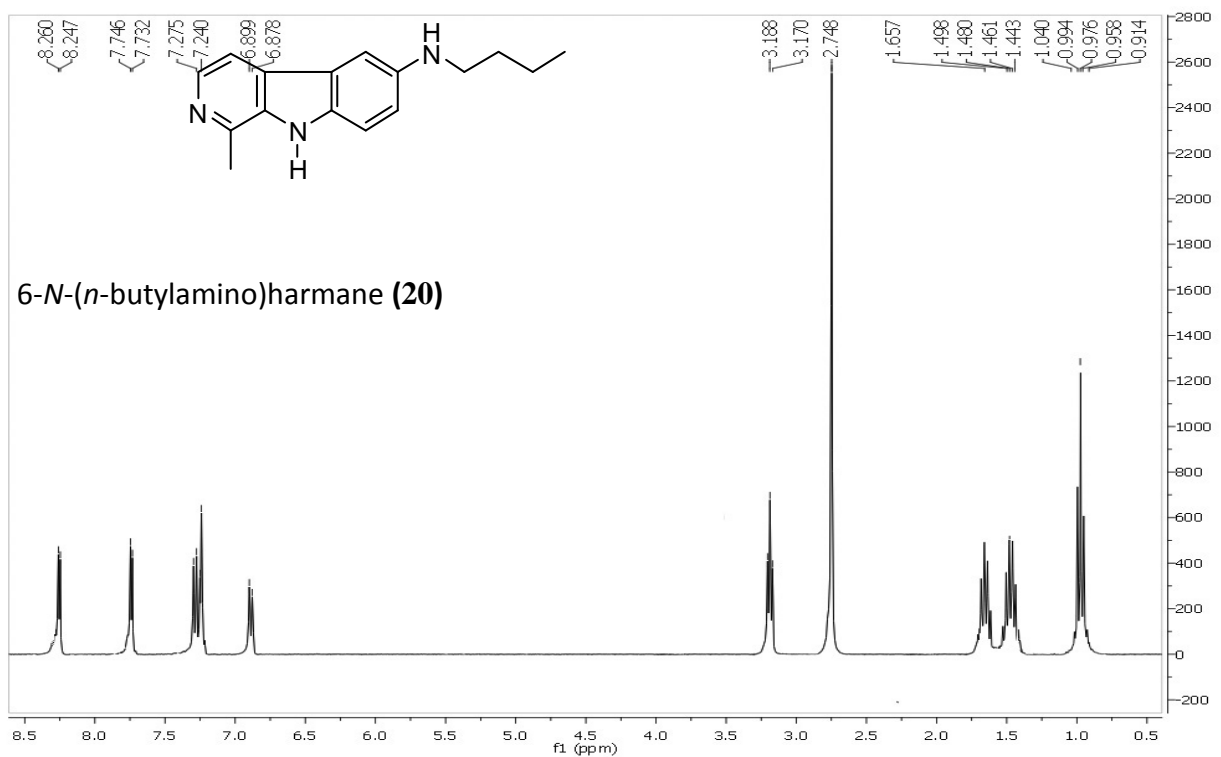
Figure IV.24. ^{1}H- and ^{13}C-NMR spectra of 6-*N*-*n*-butylaminoharmane (**20**) in CDCl$_3$ at 400 and 100 MHz, respectively.

Figure IV.25. ^{1}H- and ^{13}C-NMR spectra of 2-*N,N*-dimethylaminoestrone (**21**) in CDCl$_3$ at 400 and 100 MHz respectively.

BIBLIOGRAPHY

1. Peng, J.; Rao, K.V.; Choo, Y.M.; Hamann, M.T. Manzamine alkaloids. In *Modern Alkaloids*; Fattorusso, E., Taglialatela-Scafati, O., Eds.; Wiley-VCH Verlag GmbH & Co. KgaA: Weinheim, Germany, **2007**; pp. 189–232.

2. Tietze, L.F. Domino reactions in organic synthesis. *Chem. Rev.,* **1996**, *96*, 115–136.

3. Tietze, L.F.; Beifuss, U. Sequential transformations in organic chemistry: a synthetic strategy with a future. *Angew. Chem. Int. Ed. Engl.*, **1993**, *32*, 131–163.

4. Nicolaou, K.C.; Montagnon, T.; Snyder, S.A. Tandem reactions, cascade sequences, and biomimetic strategies in total synthesis. *Chem. Commun.,* **2003**, *5*, 551-564.

5. Nicolaou, K.C.; Edmonds, D.J.; Bulger, P.G. Cascade reactions in total synthesis. *Angew. Chem. Int. Ed. Engl.,* **2006**, *45*, 7134–7186.

6. Nicolaou, K.C.; Chen, S.J. The art of total synthesis through cascade reactions. *Chem. Soc. Rev.,* **2009**, *38*, 2993–3009.

7. Pellissier, H. Asymmetric domino reactions. Part A: reactions based on the use of chiral auxiliaries. *Tetrahedron,* **2006**, *62*, 1619–1665.

8. Pellissier, H. Asymmetric domino reactions. Part B: reactions based on the use of chiral catalysts and biocatalysts. *Tetrahedron,* **2006**, *62*, 2143–2173.

9. Padwa, A. Domino reactions of rhodium(II) carbenoids for alkaloid synthesis. *Chem. Soc. Rev.*, **2009**, *38*, 3072–3081.

10. Padwa, A.; Bur, S.K. The domino way to heterocycles. *Tetrahedron,* **2007**, *63*, 5341–5378.

11. Kibayashi, C. Development of new synthetic methods and its applications to total synthesis of nitrogen-containing bioactive natural products. *Chem. Pharm. Bull.,* **2005**, *53*, 1375–1386.

12. Sakai. R.; Higa, T.; Jefford, C.W.; Bernardinelli, G. Manzamine A, a novel antitumor alkaloid from a sponge. *J. Am. Chem. Soc.,* **1986**, *108*, 6404–6405.

13. Rao, K.V.; Kasanah, N.; Wahyuono, S.; Tekwani, B.L.; Schinazi, R.F.; Hamann, M.T. Three new manzamine alkaloids from a common Indonesian sponge and their activity against infectious and tropical parasitic diseases. *J. Nat. Prod.,* **2004**, *67*, 1314–1318.

14. Peng, J.; Kudrimoti, S.; Prasanna, S.; Odde, S.; Doerksen, R.J.; Pennaka, H.K.; Choo, Y.; Rao, K.V.; Tekwani, B.L.; Madgula, V.; Khan, S.I.; Wang, B.; Mayer, A.M.S.; Jacob, M.R.; Tu., L.C.; Gertsch, J.; Hamann. M.T. Structure–activity relationship and mechanism of action studies of manzamine analogues for the control of neuroinflammation and cerebral infections. *J. Med. Chem.,* **2010**, *53*, 61–76.

15. Wahba, A.E.; Peng, J.; Kudrimoti, S.; Tekwani, B.L.; Hamann, M.T. Structure activity relationship studies of manzamine A: amidation of positions 6 and 8 of the β-carboline moiety. *Bioorg. Med. Chem.,* **2009**, *17*, 7775–7782.

16. Shilabin, A.G.; Kasanah, N.; Tekwani, B.L.; Hamann, M.T. Kinetic studies and bioactivity of potential manzamine prodrugs. *J. Nat. Prod.,* **2008**, *71*, 1218–1221.

17. El-Sayed, K.A.; Khalil, A.A.; Yousaf, M.; Labadie, G.; Kumar, G.M.; Franzblau, S.G.; Mayer, A.M.S.; Avery, M.A.; Hamann, M.T. Semisynthetic studies on the manzamine alkaloids. *J. Nat. Prod.,* **2008**, *71*, 300–308.

18. Ibrahim, M.A.; Shilabin, A.G.; Prasanna, S.; Jacob, M.; Khan, S.I.; Doerksen, R.J.; Hamann, M.T. 2-Methyl modifications and SAR studies of manzamine A. *Bioorg. Med. Chem.,* **2008**, *16*, 6702–6706.

19. Wahba, A.E.; Peng, J.; Hamann, M.T. Reductive amidation of nitroarenes: a practical approach for the amidation of natural products. *Tetrahedron Lett.,* **2009**, *50*, 3901–3904.

20. De Oliveira, J.H.H.L.; Nascimento, A.M.; Kossuga, M.H.; Cavalcanti, B.C.; Pessoa, C.O.; Moraes, M.O.; Macedo, M.L.; Ferreira, A.G.; Hajdu, E.; Pinheiro, U.S.; Berlinck, R.G.S. Cytotoxic alkylpiperidine alkaloids from the Brazilian marine sponge *Pachychalina alcaloidifera. J. Nat. Prod.,* **2007**, *70*, 538–543.

21. Matsunaga, S.; Miyata, Y.; Van Soest, R.W.M.; Fusetani, N. Tetradehydrohalicyclamine A and 22-hydroxyhalicyclamine A, new cytotoxic bis-piperidine alkaloids from a marine sponge *Amphimedon sp. J. Nat. Prod.,* **2004**, *67*, 1758–1760.

22. Ishiguro, Y.; Kubota, T.; Ishiuchi, K.; Fromont, J.; Kobayashi, J. Plakoridine C, a novel piperidine alkaloid from an Okinawan marine sponge *Plakortis sp. Tetrahedron Lett.*, **2009**, *50*, 3202–3204.

23. Escolano, C.; Amat, M.; Bosch, J. Chiral Oxazolopiperidone Lactams: versatile intermediates for the enantioselective synthesis of piperidine-containing natural products. *Chem. Eur. J.,* **2006**, *12*, 8198–8207.

24. Felpin, F.; Lebreton, J. Recent advances in the total synthesis of piperidine and pyrrolidine natural alkaloids with ring-closing metathesis as a key step. *Eur. J. Org. Chem.,* **2003**, *2003*, 3693–3712.

25. Laschat, S.; Dickner, T. Stereoselective synthesis of piperidines. *Synthesis,* **2000**, *2000*, 1781–1813.

26. Sun, X.; Sengupta, S.; Petersen, J.L.; Wang, H.; Lewis, J.P.; Shi, X. Intermolecular cross-double-Michael addition between nitro and carbonyl activated olefins as a new approach in C-C bond formation. *Org. Lett.,* **2007**, *9*, 4495–4498.

27. Chen, Y.; Zhong, C.; Petersen, J.L.; Akhmedov, N.G.; Shi, X. One-pot asymmetric synthesis of substituted piperidines by exocyclic chirality induction. *Org. Lett.,* **2009**, *11*, 2333–2336.

28. Franzen, J.; Fisher, A. Asymmetric alkaloid synthesis: a one-pot organocatalytic reaction to quinolizidine derivatives. *Angew. Chem. Int. Ed. Engl.,* **2009**, *48*, 787–791.

29. Takada, K.; Uehara, T.; Nakao, Y.; Matsunaga, S.; van Soest, R.W.; Fusetani, N. Schulzeines A-C, new α-glucosidase inhibitors from the marine sponge *Penares schulzei*. *J. Am. Chem. Soc.,* **2004**, *126*, 187–193.

30. Enders, D.; Grondal, C.; Huttl, A.R.M. Asymmetric organocatalytic domino reactions. *Angew. Chem. Int. Ed. Engl.,* **2007**, *46*, 1570–1581.

31. Wang, Y.; Kumano, T.; Kano, T.; Maruoka, K. Organocatalytic approach to enantioselective one-pot synthesis of pyrrolidine, hexahydropyrrolizine, and octahydroindolizine core structures. *Org. Lett.,* **2009**, *11*, 2027-2029.

32. El-Naggar, M.; Piggott, A.M.; Capon, R.J. Bistellettazines A-C and bistellettazole A: new terpenyl-pyrrolizidine and terpenyl-imidazole alkaloids from a southern Australian marine sponge, S*telletta sp*. *Org. Lett.,* **2008**, *10*, 4247–4250.

33. Biard, J.F.; Guyot, S.; Roussakis, C.; Verbist, J.F.; Vercauteren, J.; Weber, J.F.; Boukef, K. Lepadiformine, a new marine cytotoxic alkaloid from *Clavelina lepadiformis* mueller. *Tetrahedron Lett.,* **1994**, *35*, 2691-2694.

34. Castagnoli, N.J. *N*-acylenamines from oxazolines. New route to 2-acetamidogylcals. *J. Org. Chem.,* **1969**, *34*, 3187–3189.

35. Cushman, M.; Abbaspour, A.; Gupta, Y.P. Total synthesis of (±)-14-epicorynoline, (±)-corynoline, and (±)-6-oxocorynoline. *J. Am. Chem. Soc.,* **1983**, *105*, 2873–2879.

36. Masse, C.E.; Ng, P.Y.; Fukase, Y.; Sanchez-Rosello, M.; Shaw, J.T. Divergent structural complexity from a linear reaction sequence: synthesis of fused and spirobicyclic γ-lactams from common synthetic precursors. *J. Comb. Chem.,* **2006**, *8*, 293–296.

37. Wei, J.; Shaw, J.T. Diastereoselective synthesis of γ-lactams by a one-pot, four-component reaction. *Org. Lett.,* **2007**, *9*, 4077–4080.

38. Tang, Y.; Fettinger, J.C.; Shaw, J.T. One-step synthesis of complex nitrogen heterocycles from imines and alkyl-substituted maleic anhydrides. *Org. Lett.,* **2009**, *11*, 3802–3805.

39. Peng, J.; Shen, X.; El-Sayed, K.A.; Dunbar, D.C.; Perry, T.L.; Wilkins, S.P.; Hamann, M.T. Marine natural products as prototype agrochemical agents. *J. Food & Agr. Chem.,* **2003**, *51*, 2246-2252.

40. Nakamura, H.; Deng, S.; Kobayashi, J.; Ohizumi, Y.; Tomotake, Y.; Matsuzaki, T. Physiologically active marine natural products from porifera. XV. keramamine-A and -B, novel antimicrobial alkaloids from the okinawan marine sponge *Pellina sp. Tetrahedron Lett.,* **1987**, *28*, 621-624.

41. Hamann, M.T.; Alonso, D.; Martin-Aparicio, E.; Fuertes, A.; Perez-Puerto, M.J.; Castro, A.; Morales, S.; Navarro, M.L.; Del Monte-Millan, M.; Medina, M.; Pennaka, H.; Balaiah, A.; Peng, J.; Cook, J.; Wahyuono, S.; Martinez, A. Glycogen synthase kinase-3 (GSK-3) inhibitory activity and structure–activity relationship (SAR) studies of the manzamine alkaloids. Potential for alzheimer's disease, *J. Nat. Prod.,* **2007,** *70*, 1397-1405.

42. Ward, P.; Equinet, L.; Packer, J.; Doerig, C. Protein kinases of the human malaria parasite plasmodium falciparum: the kinome of a divergent eukaryote. *BMC Genomics,* **2004,** *5*, 79.

43. Liu, F.; Liang, Z.; Shi, J.; Yin, D.; El-Akkad, E.; Grundke-Iqbal, I.; Iqbal, K.; Gong, C.X. PKA modulates GSK-3β and cdk5-catalyzed phosphorylation of tau in situ and kinase specific manners. *FEBS Lett.,* **2006,** *580*, 6269.

44. Ang, K.K; Holmes, M.J; Higa, T.; Hamann, M.T.; Kara, U.A. In vivo antimalarial activity of the β-carboline alkaloid manzamine A. *Antimicrob. Agents Chemother.,* **2000**, *44*, 1645-1649.

45. Yousaf, M.; Hammond, N.L.; Peng, J.; Wahyuono, S.; McIntosh, K.A.; Charman, W.N.; Mayer, A.M.S.; Hamann, M.T. New manzamine alkaloids from an Indo-pacific sponge. Pharmacokinetics, oral availability, and the significant activity of several manzamines against HIV-I, AIDS opportunistic infections, and inflammatory diseases. *J. Med. Chem*., **2004**, *47*, 3512-3517.

46. a) Becke, A.D. A new mixing of Hartree-Fock and local density-functional theories. *J. Chem. Phys.,* **1993**, 98, 1372-1377; b) Schaefer, A.; Horn, H.; Ahlrichs, R. Fully optimized contracted Gaussian-basis sets for atoms Li to Kr. *J. Chem. Phys.,* **1992**, *97*, 2571-2577; c) Schaefer, A.; Huber, C.; Ahlrichs, R. Fully optimized contracted Gaussian-basis sets of triple zeta valence quality for atoms Li to Kr, *J. Chem. Phys.,* **1994,** *100*, 5829-5835.

47. Panosian, C.B. Economic access to effective drugs for falciparum malaria, *Clin. Infect. Dis.*, **2005**, *40*, 713-717.

48. Ridley, R.G. Medical need, scientific opportunity and the drive for antimalarial drugs, *Nature*, **2002**, *415*, 686-693.

49. Newman, D.J.; Crag, G.M. Natural products as source of new drugs over the last 25 years. *J. Nat. Prod*., **2007**, 70, 461-477.

50. Rao, K.V.; Santarsiero, B.D.; Mesecar, A.D.; Schinazi, R.F.; Tekwani, B.L.; Hamann, M. T. New manzamine alkaloids with activity against infectious and tropical parasitic diseases from an Indonesian sponge. *J. Nat. Prod.,* **2003**, *66*, 823-828.

51. Hamann, M.T.; El-Sayed, K.A. Application: WOWO Patent, **2001**, US27035 2002017917**.**

52. El-Sayed, K.A.; Kelly, M.; Kara, U.A.K.; Ang, K.K.H.; Katsuyama, I.; Dunbar, D.C.; Khan, A.A.; Hamann, M.T. New manzamine alkaloids with potent activity against infectious diseases. *J. Am. Chem. Soc.,* **2001**, *123*, 1804-1808.

53. Longley, R.E.; McConnell, O.J.; Essich, E.; Harmody, D. Evaluation of marine sponge metabolites for cytotoxicity and signal transduction activity. *J. Nat. Prod.,* **1993,** *56*, 915-920.

54. Mayer, A.M.S.; Gunasekera, S.P.; Pomponi, S.A.; Sennett, S.H. Anti-inflammatory uses of Manzamines. *U S Patent,* **2003**, 6, 602, 881.

55. Mayer, A.M.S.; Gunasekera, S.P.; Pomponi, S.A.; Sennett, S.H. Anti-inflammatory uses of Manzamines. *U S Patent,* **2002**, 6, 387, 916.

56. Hamann, M.T. The manzamines as an example of the unique structural classes available for the discovery and optimization for infectious disease controls based on marine natural products. *Curr. Pharm. Des.*, **2007**, *13*, 653-660.

57. Rao, K.V.; Kasanah, N.; Wahyuono, S.; Tekwani, B.L.; Schinazi, R.F.; Hamann, M.T. Three new manzamine alkaloids from a common Indonesian sponge and their activity against infectious and tropical parasitic diseases. *J. Nat. Prod.,* **2004**, *67*, 1314-1318.

58. Rao, K.V.; Donia, M.S.; Peng, J.; Garcia-Palomero, E.; Alonso, D.; Martinez, A.; Medina, M.; Franzblau, S.G.; Tekwani, B.L.; Khan, S.I.; Wahyuono, S.; Willett, K.L.; Hamann, M.T. Manzamine B and E and ircinal A related alkaloids from an Indonesian

Acanthostrongylophora sponge and their activity against infectious, tropical, and Alzheimer's diseases. *J. Nat. Prod.,* **2006,** *69*, 1034-1040.

59. For reviews on C-C bond formation: a) Hassan, J.; Sevignon, M.; Gozzi, C.; Schulz, E.; Lemaire, M. Aryl-aryl bond formation one century after the discovery of the Ullmann reaction. *Chem.Rev*., **2002**, *102*, 1359–1469; b) Miyaura, N.; Suzuki, A. Palladium-catalyzed cross-coupling reactions of organoboron compounds. *Chem. Rev*., **1995**, *95*, 2457–2483; c) Suzuki, A. In Metal-Catalyzed Cross-Coupling Reactions; Diederich, F., Stang, P.J. Eds.; Wiley-VCH: Weinheim, Germany, **1998**; p 49.d) Cross-coupling reactions: a practical guide, Vol. 219 (Ed.: N. Miyaura), Springer, Berlin, **2002**; e) Metal-catalyzed cross-coupling reactions (Eds.: A. de Meijere, F.Diederich), Wiley-VCH, Weinheim, **2004**.

60. For a review: Goossen, L.J.; Rodriguez, N.; Goossen, K. Carboxylic acids as substrates in homogeneous catalysis. *Angew Chem. Int. Ed*., **2008**, *47*, 3100-3120.

61. Nilsson, M. A new biaryl synthesis illustrating a connection between the Ullmann biaryl synthesis and copper-catalyzed decarboxylation. *Acta Chem. Scand.,* **1966**, *20*, 423-426; b) Bjorklund, C.; Nilsson, M. Decarboxylative couplings of 2,6-dinitrobenzoic acid. *Acta Chem. Scand.,* **1968**, *22*, 2585-2588.

62. Myers, A.G.; Tanaka, D.; Mannion, M.R. Development of a decarboxylative palladium reaction and its use in a Heck-type olefination of arene carboxylates. *J. Am. Chem. Soc.,* **2002**, *124*, 11250-11251.

63. Forgione, P.; Brochu, M.; St-Onge, M.; Thesen, K.H.; Bailey, M.D.; Bilodeau, F. Unexpected intermolecular Pd-catalyzed cross-coupling reaction employing heteroaromatic carboxylic acids as coupling partners. *J. Am. Chem. Soc.,* **2006**, *128*, 11350-11351.

64. Goossen, L.J.; Deng, G.; Levy, L.M. Synthesis of biaryls via catalytic decarboxylative coupling. *Science,* **2006**, *313*, 662-664.

65. Goossen, L.J.; Rodriguez, N.; Melzer, B.; Linder, C.; Deng, G.; Levy, L.M. Biaryl synthesis via Pd-catalyzed decarboxylative coupling of aromatic carboxylates with aryl halides. *J. Am. Chem. Soc.,* **2007**, *129*, 4824-4833.

66. Goossen, L.J.; Rudolphi, F.; Oppel, C.; Rodriguez, N. Synthesis of ketones from alpha-oxocarboxylates and aryl bromides by Cu/Pd catalyzed decarboxylative cross-coupling. *Angew. Chem. Int. Ed.*, **2008**, *47*, 3043–3045.

67. Goossen, L.J.; Zimmermann, B.; Knauber, T. Palladium/copper-catalyzed decarboxylative cross-coupling of aryl chlorides with potassium carboxylates. *Angew. Chem. Int. Ed.*, **2008**, *47*, 7103–7106.

68. Goossen, L.J.; Rodriguez, N.; Linder, C. Decarboxylative biaryl synthesis from aromatic carboxylates and aryl triflates. *J. Am. Chem. Soc.,* **2008**, *130*, 15248–15249.

69. Goossen, L.J.; Linder, C.; Rodrguez, N.; Lange, P.P. Biaryl and aryl ketone synthesis via Pd-catalyzed decarboxylative coupling of carboxylate salts with aryl triflates. *Chem. Eur. J.*, **2009**, *15*, 9336–9349.

70. Goossen, L.J.; Rodriguez, N.; Lange, P.P.; Linder, C. Decarboxylative cross-coupling of aryl tosylates with aromatic carboxylate salts. *Angew. Chem. Int. Ed.*, **2010**, *49*, 1111–1114.

71. Goossen, L.J.; Lange, P.P.; Rodriguez, N.; Linder, C. Low temperature Ag/Pd-catalyzed decarboxylative cross-coupling of aryl triflates with aromatic carboxylate salts. *Chem. Eur. J.*, **2010**, *16*, 3906–3909.

72. Tokunaga, M.; Aoyama, H.; Shirogane, Y.; Obora, Y.; Tsuji, Y. Oxidative cleavage of C-C bond of 2-phenylpropioanldehyde using molecular oxygen. *Catal .Today*, **2006**, *117*, 138-140.

73. Merck index, 14 ed.; Budavari, S., Ed.; Merck, **2006**, 397, 3673.

74. Tsukinoki, T.; Tsuzuki, H. Organic reaction in water. Part 5. Novel synthesis of anilines by zinc metal-mediated chemoselective reduction of nitroarenes. *Green Chem*., **2001**, *3*, 37–38.

75. Hodgson, H.H.; Whitehurst, J.S. Preparation of 1:5- and 1:8-naphthylenediamine and related compounds. *J. Chem. Soc*., **1945**, 202–204.

76. Nishimura, S. Hydrogenation and hydrogenolysis. V. Rhodium-platinun oxide as a catalyst for the hydrogenation of organic compounds. *Bull. Chem. Soc. Jpn*., **1961**, *34*, 32–36.

77. Mendenhall, G.D.; Smith, P.A.S. 2-nitrocarbazole. *Org. Syn. Coll.,* **1973**, *5*, 829–833.

78. Adkins, H.; Billica, H.R. Preparation of Raney nickel catalysts and their use under conditions comparable with those for platinum and palladium catalysts. *J. Am. Chem. Soc*., **1948**, *70*, 695–698.

79. Adkins, H.; Connor, R. Catalytic hydrogenation of organic compounds over copper chromite. *J. Am. Chem. Soc.,* **1931**, *53*, 1512-1520**.**

80**.** Broadbent, H.S.; Slaugh, L.H.; Jarvis, N.L. Rhenium sulfides as liquid-phase hydrogenation catalysts. A comparison with molybdenum sulfide and cobalt polysulfide. *J. Am.Chem. Soc*., **1954**, *76*, 1519–1523.

81. Watanabe, Y.; Tsuji, Y.; Kondo, T.; Takeuchi, R. Platinum complex catalyzed reductive N-acylation of nitro compounds. *J. Org. Chem*., **1984**, *49* , 445–4455.

82. Wang, X.; Guo, H.; Xie, G.; Zhang, Y. One-pot synthesis of amides from N-acylation of nitroarenes with esters mediated by samarium diiodide. *Syn. Comm*., **2005**, *34*, 3001-3008.

83. Bhattacharya, A.; Purohit, V.C.; Suarez, V.; Tichkule, R.; Parmer, G.; Rinald, F. One-step reductive amidation of nitro arenes: application in the synthesis of acetaminophen. *Tetrahedron Lett.*, **2006**, *47*, 186–1864.

84. Unpublished results with manzamine alkaloids.

85. Kim, B.H.; Jun, Y.M.; Suh, S.W.; Baik, W.; Lee, B.M. Reduction of nitroaromatics with zinc and acetic anhydride. *J. Chem. Res.(S)*, **1998**, 46-47.

86. Kim, B.H.; Han, R.; Piao, F.; Jun, Y.; M.; Baik, W.; Lee, B.M. Indium-mediated one-pot reductive conversion of nitroarenes to *N*-arylacetamides. *Tetrahedron Lett.*, **2003**, *44*, 77-79.

87. U.S. Environmental Protection Agency: http://www.epa.gov/gcc/pubs/principles.html, accessed March 24, 2011.

88. Choo, Y.; Hamann, M.T. An improved Pictet-Spengler condensation: a convenient synthetic route to bioactive manzamine derivatives. *Heterocycles,* **2007**, *71*, 245-252.

89. Winkler, J.D.; Londregan, A.T.; Hamann, M.T. Antimalarial activity of a new family of analogues of manzamine A. *Org. Lett*. **2006**, *8*, 2591-2594.

90. Winkler, J.D.; Londregan, A.T.; Ragains, J.R.; Hamann, M.T. Synthesis and biological evaluation of manzamine analogues. *Org. Lett*. **2006**, *8*, 3407-3409.

91. Winkler, J.D.; Londregan, A.T.; Hamann, M.T. Synthetic medification of manzamine A via Grubbs metathesis. Novel structures with enhanced antibacterial and antiprotozoal properties. *Org. Lett*. **2007**, *9*, 4467-4469.

92. Bae, J.W.; Cho, Y.J.; Lee, S.H.; Yoon, C.M.; Yoon, C.M. A one-pot synthesis of *N*-alkylaminobenzenes from nitroaromatics: reduction followed by reductive amination using $B_{10}H_{14}$. *Chem. Commun.*, **2000**, 1857-1858.

93. Sydnes, M.O.; Isobe, M. One-pot reductive monoalkylation of nitro aryls with hydrogen over Pd/C. *Tetrahedron Lett.*, **2008**, *49*, 1199-1202.

94. Byun, E.; Hong, B.; Castro, K.A.D.; Lim, M.; Rhee, H. One-pot reductive mono-*N*-alkylation of aniline and nitroarene derivatives using aldehydes. *J. Org. Chem.*, **2007**, *72*, 9815-9817.

95. Xiang, Y.; Meng, Q.; Li, X.; Wang, J. In situ hydrogen from aqueous-methanol for nitroarene reduction and imine formation over an Au-Pd/Al$_2$O$_3$ catalyst. *Chem.Commun.,* **2010**, *46*, 5918-5920.

96. Nacario, R.; Kotakonda, S.; Fouchard, D.M.D.; Tillekeratne, L.M.V.; Hudson, R.A. Reductive monoalkylation of aromatic and aliphatic nitro compounds and the corresponding amines with nitriles. *Org. Lett.* **2005**, *7*, 471-474.

97. Reddy, C.R.; Vijeender, K.; Bhusan, P.B.; Madhavi, P.P.; Chandrasekhar, S. Reductive *N*-alkylation of aromatic amines and nitro compounds with nitriles using polymethylhydrosiloxane. *Tetrahedron Lett.*, **2007**, *48*, 2765-2768.

98. Cenini,S.; Ragaini, F.; Tollari, S.; Paone, D. Allylic amination of cyclohexene catalyzed by ruthenium complexes. A new reaction involving an intermolecular C-H functionalization. *J. Am. Chem. Soc.*, **1996**, *118*, 11964-11965.

99. Degrand,C.; Compagnon, P.L.; Belot, G.; Jacquin, D. Synthesis and structure of products of hydroxylamine acylation with 3-carboxy-2,2,5,5-tetramethylpyrrolinoxyl derivatives. *J. Org. Chem.*, **1980**, *45*, 1189-1196.

100. Sapountzis, I.; Knochel, P. A new general preparation of polyfunctional diarylamines by the addition of functionalized arylmagnesium compounds to nitroarenes. *J. Am. Chem. Soc.*, **2002**, *124*, 9390-9391.

101. Kamijo, S.; Jin, T.; Yamamoto, Y. Novel synthetic route to allyl cyanamides: palladium-catalyzed coupling of isocyanides, allyl carbonate, and trimethylsilyl azide. *J. Am. Chem. Soc.*, **2001**, *123*, 9453-9454.

102. Bartoli, G.; Marcantoni, E. Unexpected reactivity of allyl magnesium chloride with nitroarenes. A general method of synthesis of N-allyl-N-arylhydroxylamines and N-allylanilines. *Tetrahedron Lett.* **1988**, *29*, 2251-2254.

103. Bieber, L.W.; da-Costa, R.C.; da-Silva, M.F. Reductive alkylation of nitrobenzene promoted by zinc and tin in protic solvents. *Tetrahedron lett.* **2000**, *41*, 4827-4830.

104. Lin, H.; Ng, F.W.; Danishefsky, S.J. The synthesis of (±)-gelsemine. *Tetrahedron lett.* **2002**, *43*, 549-551.

105. Rottmann, M.; McNamara, C.; Yeung, B.K.S.; Lee, M.C.S.; Zou, B.; Russell, B.; Seitz, P.; Plouffe, D.M.; Dharia, N.V.; Tan, J.; *et al*. Spiroindolones, a potent compound class for the treatment of malaria. *Science*, **2010**, *329*, 1175-1180.

106. Yeung, B.K.S. Rottmann, M.; Lakshminarayana, S.B.; Ang, S.H.; Leong, S. Y.; Tan, J.; Wong, J.; Keller-Maerki, S.; Fischi, C.; *et.al.* Spirohydro B-carbolines (spiroindolones): a new class of potent and orally efficacious compounds for the treatment of malaria. *J. Med. Chem.*, **2010**, *53*, 5155-5164.

107. Watson, A.J.A.; Maxwell, A.C.; Williams, J.M.J. Borrowing hydrogen methodology for amine synthesis under solvent free microwave conditions. *J. Org. Chem.* **2011**, *76*, 2328-2331.

108. Wakchaure, V.N.; Zhou, J.; Hoffmann, S.; List, B. Catalytic asymmetric reductive amination of α-branched ketons. *Angew. Chem. Int. Ed.* **2010**, *49*, 4612- 4614.

109. Saidi, O.; Blacker, A.J.; Farah, M.M.; Marsden, S.P.; Williams, J.M.J. Selective amine-cross coupling using iridium catalyzed "borrowing hydrogen" methodology. *Angew. Chem. Int. Ed.* **2009,** *48,* 7375-7378.

110. Byun, E.; Hong, B.; De Castro, K.A.; Lim, M.; Rhee, H. One-pot reductive mono *N*-alkylation of aniline and nitroarene derivatives using aldehydes. *J. Org. Chem.* **2007**, *72*, 9815–9817.

111. Pratt, E.; Frazza, E. Disproportionative condensations II. The *N*-alkylation of anilines with primary alcohols. *J. Am. Chem. Soc*. **1954**, *76*, 6174-6179.

112. Satoh, T.; Osawa, A.; Ohbayashi, T.; Kondo, A. A new method for generation of non-stabilized α-amino-substituted carbanions by the reaction of magnesium carbenoids with N-lithioarylamines: their reactivity and a new synthesis of α-amino acid derivatives. *Tetrahedron*, **2006**, *62*, 7892-7901.

113. Snyder, H.R.; Parmerter, S.M.; Katz, L. The synthesis of derivatives of β-carboline. III. The nitration of harmane. *J. Am. Chem. Soc.* **1948**, *70*, 222-225.

114. Bose, A.; Sanjoto, W.P.; Villarreal, S.; Aguilar, H.; Banik, B.K. Novel nitration of estrone by metal nitrates. *Tetrahedron Lett.* **2007**, *48*, 3945-3947.

LIST OF APPENDICES

APPENDIX: A

Kudrimoti, S.; Ahmed, S.; Daga, P.R.; **Wahba, A.E.;** Khalifa, S.I.; Doerksen, R.J.; Hamann, M.T. Semisynthetic Latrunculin B Analogs: Latrunculin–Actin Docking Explains Poor Bioactivity. *Bioorganic and Medicinal Chemistry*, **2009**, *17*, 7517-7522.

Semisynthetic latrunculin B analogs: Studies of actin docking support a proposed mechanism for latrunculin bioactivity

Sucheta Kudrimoti[a], Safwat A. Ahmed[f], Pankaj R. Daga[d], Amir E. Wahba[a], Sherief I. Khalifa[g], Robert J. Doerksen[d,e], Mark T. Hamann[a,b,c,e,*]

[a] Department of Pharmacognosy, The University of Mississippi, University, MS 38677-1848, United States
[b] Department of Pharmacology, The University of Mississippi, University, MS 38677-1848, United States
[c] Department of Chemistry and Biochemistry, The University of Mississippi, University, MS 38677-1848, United States
[d] Department of Medicinal Chemistry, The University of Mississippi, University, MS 38677-1848, United States
[e] The National Center for Natural Products Research, The University of Mississippi, University, MS 38677-1848, United States
[f] Department of Pharmacognosy, Faculty of Pharmacy, Suez Canal University, Ismailia, Egypt
[g] Department of Pharmacy Practice and Clinical Pharmacy, Faculty of Pharmacy, Msir International University, Cairo, Egypt

ARTICLE INFO

ABSTRACT

Latrunculins are unique macrolides containing a thiazolidinone moiety. Latrunculins A, B and T and 16-epi-latrunculin B were isolated from the Red Sea sponge Negombata magnifica. N-Alkylated, O-methylated analogs of latrunculin B were synthesized and biological evaluation was performed for antifungal and antiprotozoal activity. The natural latrunculins showed significant bioactivity, while the semisynthetic analogs did not. Docking studies of these analogs into the X-ray crystal structure of G-actin showed that, in comparison with latrunculins A and B, N-alkylated latrunculins did not dock satisfactorily. This suggests that the analogs do not fit well into the active site of G-actin due to steric clashes and provides an explanation for the absence of bioactivity.

Published by Elsevier Ltd.

1. Introduction

Latrunculins are architecturally unique marine metabolites which were first isolated from the Red Sea sponge Negombata magnifica (formerly Latruncilin magnifica).[1] Coral reefs of the Red Sea are densely populated with colonies of the N. magnifica sponge, which are apparently free from predation due to chemical defense.[2] Squeezing this sponge leads to a secretion of a reddish fluid which has been shown to cause poisoning in fish. A detailed study of this excretion by Kashman's group led to the discovery of latrunculins, which are 14- and 16-membered lactones and the first natural products known to contain a 2-thiazolidinone moiety, 1–4 (Fig. 1).[2,3] These macrolides were also later found in taxonomically unrelated organisms from different geographic locations, signifying that the actual producer or origin of these curious secondary metabolites could be symbiotic microbes.[4]

Over the past years macrolides of marine source have continued to be of interest due to their varied biological activities. In addition to the significant ichthyotoxic properties, the latrunculins are also cytotoxic to tumor cells and antiviral.[5] The significant physiological properties of latrunculins has led to their extensive utilization as biochemical tools. Latrunculins alter cell shape and inhibit the microfilament mediated processes of meiosis, fertilization, early development, force development in muscles, and even influence protein kinase C signaling.[6] These metabolites play an important interfering role in actin polymerization[7] and cytoskeletal coordination which are essential in cell locomotion and many forms of motility, including phagocytosis and cytokinesis. Actin-binding proteins control the contractile machinery of smooth muscle cells and play a significant role in controlling the structural framework that surrounds and supports the contractile apparatus. Actin-binding proteins regulate the dynamic equilibrium that exists between actin monomers (G-actin) and actin polymers or filaments (F-actin). A recent report shows that aging skin appears to look younger when treated with this type of metabolite.[8] It was shown that the increasing volume of filamentous F-actin fibers is a major source of the stiffness of human epithelial cells and repairing the elasticity in skin cells can be achieved by chemically halting F-actin polymerization. The treatments evaluated contained compounds known to intervene with F-actin polymerization such as cytochalasin B, cytochalasin D, and latrunculins A and B. These studies furnish insight and potential for both biological and pharmaceutical applications for these natural products. Skin treated with cytochalasin B progressively became softer with fewer wrinkles.[8] Recent progress in the study of actin interaction with small marine molecules

* Corresponding author. Tel.: +1 662 915 5930; fax: +1 662 915 6975.
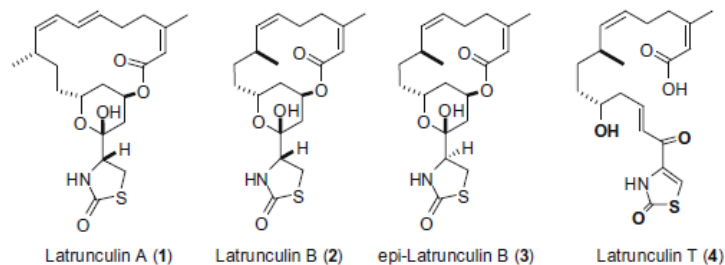E-mail address: mthamann@olemiss.edu (M.T. Hamann).

232

Figure 1. Latrunculin macrolides.

prompted our design and synthesis of modified analogs. Previous studies have focused on the synthesis of analogs with an aromatic and sulfonyl functional group attached at the hydroxy group. The majority of these analogs were surprisingly inactive against various cancer cell lines as well as bacteria and protozoa. These data have shown that the pyran ring hydroxy group is clearly essential for cytotoxicity and actin binding.[9]

In this study, we report the synthesis and biological evaluation of a small series of N-alkyl, O-methyl derivatives of latrunculin B having a varying-length carbon chain substituted at the nitrogen of the thaizolidinone moiety. Since previous studies have shown the importance of a free hydroxy group for the biological activity, we also carried out hydrolysis of the protected hydroxy group of the N-decyl, O-methyl derivative to check if protection of this OH in the molecules was responsible for the weaker activity. We used computational docking studies to study the predicted binding mode of the newly synthesized analogs to G-actin.

2. Results and discussion

2.1. Natural latrunculins isolation

Analysis of the crude extract of N. magnifica by TLC indicated the presence of latrunculin B and other related metabolites. Flash column chromatography (normal-phase) of the methanol/dichloromethane extract provided several fractions. After several extensive chromatographic steps, **2** was afforded as the major metabolite as well as **1**, **3**, and **4** as minor metabolites. Compounds **1–4** were identified by comparison of their spectroscopic properties to those in the literature.[2a,10,11]

2.2. Synthesis of N-alkylated analogs

Synthetic derivatives were prepared using latrunculin B (**2**) as a starting material. Latrunculins are known to be highly sensitive to both acidic and basic conditions.[12] This instability can be consider-

ably reduced through the acetalization of the lactol functionality by protection of the hydroxy group of the tetrahydropyran (THP) ring. This protection was accomplished through the treatment of **2** with methanol in the presence of a catalytic amount of boron-trifluoro-etherate to yield **5** (Scheme 1). N-Alkylation of thiazolidine ring was then carried out on the amidic nitrogen of **5** by using sodium hydride in the presence different alkyl halides in tetrahydrofuran (THF) under nitrogen atmosphere (Scheme 1). The N-alkylated products (**6–11**) were confirmed by ^{1}H NMR data in which N-alkylation was confirmed by the absence of an N–H peak at 5.90 ppm. N-Decyllatrunculin B (**12**) was obtained by the catalytic acid hydrolysis of the acetal functionality in **11**.

2.3. Biological testing

The isolated compounds **1–4**, O-methylated latrunculin B (**5**) (Table 1), and N-alkylated derivatives (**6–12**) were evaluated for anti-fungal and anti-protozoal activity (Saccharomyces cerevisiae NRRL Y-2034, Aspergillus flavus NRRL 501, and Candida albicans) using the twofold dilution method.[13] Latrunculin T (**4**) was found to be more active than other isolated latrunculins against S. cerevisiae NRRL Y-2034 (MIC = 32 μg/M). Latrunculin A (**1**) was found to be active against C. albicans (MIC = 60 μg/M), and A. flavus NRRL 501 (MIC = 60 μg/M). The alkylated latrunculin B derivatives **5–12** were evaluated for antimalarial and antimicrobial activity but were found to be inactive.

2.4. Actin docking studies
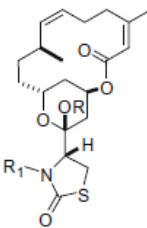
2.4.1. Actin X-ray structure

To check the effect of the substitutions on G-actin docking and by implication on actin binding, stepwise docking studies were carried out. Docking of latrunculins A and B has been reported recently by Fürstner et al.[14] using AUTODOCK followed by optimization. Fürstner et al. used 1ESV,[15] a complex of actin with latrunculin A (2.00 Å resolution), for their docking studies. How-
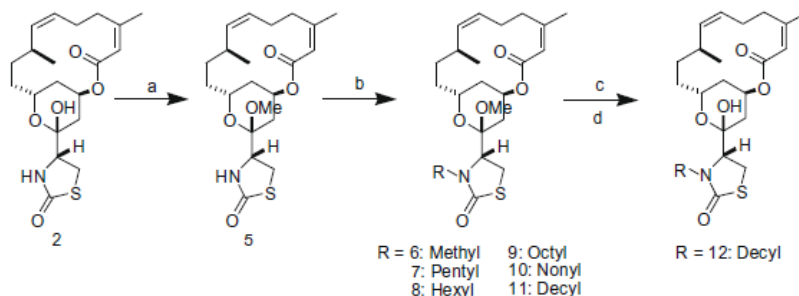
Scheme 1. Synthesis of the N-alkyl derivatives of latrunculin B. Reagents and conditions: (a) BF₃·OEt₂, MeOH, rt; (b) NaH, THF, R–X, 0 °C, rt; (c) concd H₂SO₄ (10 μL), THF, rt; (d) H₂O.

Table 1
GOLD docking scores for the latrunculin B analogs

Analog	R	R₁	GOLD Score
2	H	H	70.2
5	Me	H	48.0
6	Me	Methyl	21.7
7	Me	Pentyl	18.1
8	Me	Hexyl	21.1
9	Me	Octyl	23.1
10	Me	Nonyl	28.5
11	Me	Decyl	32.1
12	H	Decyl	35.5

ever, one of the active site amino acids showing hydrogen bonding interaction with the ligand, Glu207, is not resolved in 1ESV. Hence, docking into that crystal structure is unreliable. We instead used an alternative co-crystal structure of latrunculin A in actin, 1RDW (2.30 Å),[16] in our work.

2.4.2. Latrunculins A (1) and B (2)

As part of our research on latrunculins reported recently,[17] GOLD[18] was able to dock **1** into the G-actin ATP binding site in a manner similar to that of the actin–latrunculin A co-crystal structures. Merging of the docked pose with the protein structure extracted from the crystal structure and minimization of the complex resulted in the same hydrogen bonding and van der Waals interactions as those in the crystal structure. Compound **2**, using the same procedure for docking and minimization, yielded a very similar pose to that of **1**. All the hydrogen bonding interactions observed in the X-ray co-crystal structure of **1** in actin were reproduced for **1** and for **2** as well (Fig. 2). The overlay of the two

latrunculins with the crystal structure is shown in Figure 3. The docking scores (Table 1) were 90.7 (**1**) and 70.0 (**2**) for the two molecules. The binding energies calculated were −84.8 and −74.5 kcal/mol for **1** and **2**, respectively.

2.4.3. O-Methylated latrunculin B (5)

In this work, latrunculin B was then modified by replacing the hydroxy group on the pyran ring with methoxy to obtain O-methylated latrunculin B (**5**). The docking pose obtained for **5** was reasonably similar to that of **1** and **2**. The docking score for this analog was 48.0 while that of **2** was 70.2. The ligand was then merged into the active site and minimization was carried out. The binding energy was calculated to be −53.1 kcal/mol, so it is predicted not to bind as well as **2**. The final minimized binding pose of **5** is shown in Figure 4. Minimization of the complex resulted in the side chain of the Glu207 residue moving by ≈0.71 Å and that of Tyr69 moving by ≈1.2 Å away from their original position in the crystal structure. Hence we predict that the O-methylated analog will best bind to
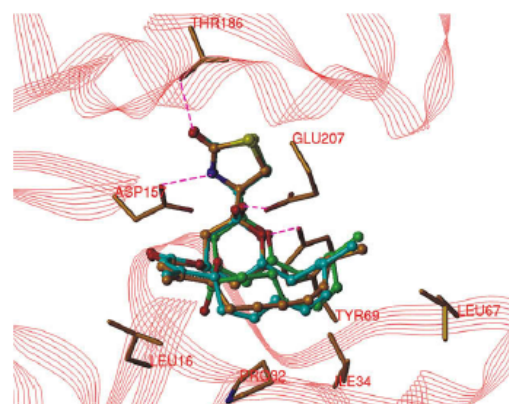
Figure 3. Optimized binding pose of latrunculin A (**1**) (ball-and-stick, C cyan) and latrunculin B (**2**) (ball-and-stick, C green) in actin (red ribbon mode), shown overlapped with **1** from 1RDW (ball-and-stick, C gold); key H-bonds are shown (pink dashed lines).
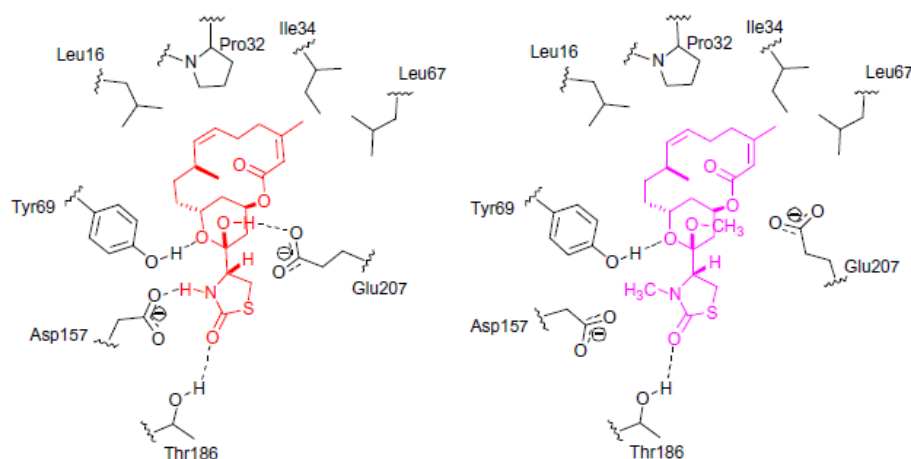
Figure 2. Schematic representation of the non-bonding interactions shown by latrunculin B (**2**) (left) and compound **6** (right) with actin.

234
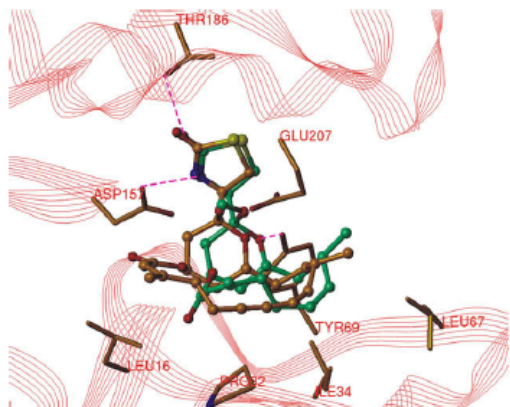
Figure 4. Optimized binding pose of O-methylated latrunculin B (**5**) (ball-and-stick, C bluegreen) in actin (red ribbon mode), shown overlapped with optimized latrunculin A (**1**) (ball-and-stick, C gold, from 1RDW.pdb); key H-bonds are shown (pink dashed lines). Glu207 and Tyr69 residues have moved away from the binding site compared to the crystal structure.

the actin active site if there is some movement of active site residue side chains. The methyl substitution pushed the ligand slightly away from the location of **2** in its docked pose. All the hydrogen bonding interactions observed in the X-ray co-crystal structure of **1** in actin were also seen for **5** except for that with Glu207, which is to the pyran ring hydroxyl in **1**.

2.4.4. N-Alkylated latrunculins

Each of the semi-synthetic latrunculins (**6–12**) were docked into the active site using the same procedure. GOLD produced 10 different conformations for each molecule. Depending upon the position of the five-membered thiazolidinone ring and macrocyclic lactone ring, all the docked conformations collectively could be divided into three different clusters. Representatives of the three different docking poses are shown in Figure 5. In all clusters, the thiazolidinone ring moved away from the binding pocket it occupies for **1** or **2**, and in the pose shown in Figure 5a the pyran ring also was greatly displaced. One of the docked conformations (shown in Fig. 5c) was closest to the crystal structure. However, only two of the hydrogen bonding interactions, observed for **1** bound into G-actin in 1RDW, were reproduced: the carbonyl oxygen was found to be H-bonded to Thr186 and the pyran ring O showed H-bonding interaction with Tyr69. Figure 2 illustrates that methylation of the amidic nitrogen and the hemiacetal functionality in **6** resulted in loss of two hydrogen bonding interactions, with

Asp157 and Glu207, respectively, while the hydrogen bonding interactions with Tyr69 and Thr186 and hydrophobic interactions with Leu16, Pro32, Ile34, and Leu67 found for **2** were maintained for **6**. The macrocyclic ring was found to be shifted also. In the two other cases (Fig. 5a and b), it was obvious that GOLD was not able to dock these molecules into the active site of G-actin. The docking scores for the N-alkylated latrunculins are shown in Table 1. In comparison with latrunculins A and B, **6–12** showed very low scores between 18 and 36, suggesting that these molecules have extremely low binding affinity toward G-actin. The docking poses show that they would not be able to fit well into the active site of G-actin due to steric clashes. There is a slight increase in docking score with increase in alkyl chain length but this can be attributed to the increase in van der Waals binding of the alkyl sidechain with hydrophobic groups away from the thiazolidinone binding pocket and in fact the longer side chains make it harder for the N-alkylated latrunculins to fit into the actin binding pocket.

3. Conclusions

We have synthesized O-methylated-N-alkylated-latrunculin B analogues and evaluated their cytotoxicity and antimicrobial activity. The docking studies demonstrated why free NH and OH groups of latrunculin B (**2**) are essential to have any activity for the above synthesized compounds. The O-methylated **5** had reduced binding to G-actin since it had one fewer hydrogen bond. The O-methylated-N-alkylated analogues could not fit into the G-actin latrunculin binding pocket.

4. Experimental

4.1. General experimental procedures

The ^{1}H and ^{13}C NMR spectra were recorded in CDCl$_3$ on a Bruker DRX NMR spectrometer operating at 400 MHz for ^{1}H and 75 MHz for ^{13}C. Chemical shift (δ) values are expressed in parts per million (ppm) and are referenced to the residual solvent signals of CDCl$_3$. Optical rotations were measured with a JASCO DIP-310 digital polarimeter. The high resolution ESI-MS spectra were measured using a Bruker Daltonic (GmbH, Germany) micro-TOF series with electrospray ionization.

4.2. Isolation and characterization

The specimen of the sponge *N. magnifica* utilized for this study was collected by SCUBA at a depth of 15 m off Hurghada in the Egyptian Red Sea. The sponge material was frozen immediately
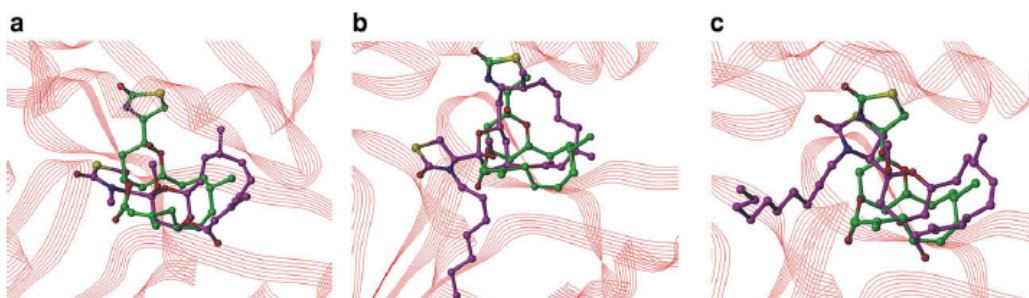
Figure 5. Three different binding pose clusters predicted by GOLD for N-alkylated latrunculin B analogs (represented by (a) **6**; (b) **10**; and (c)) **11**. The images portray that these analogs do not bind to the active site in a similar pose to those of **1** (X-ray structure shown, C green) and **2**. One of the docked conformations, (c), was the closest to the pose of **1** in the crystal structure, though even in that case not all the hydrogen bonding interactions observed in 1RDW were reproduced.

S. Kudrimoti et al./Bioorg. Med. Chem. 17 (2009) 7517–7522

7521

and kept frozen at −20 °C until processed. The voucher specimen is deposited at the Zoological Museum of the University of Amsterdam, under the registration no. ZMAPOR 18968. The sponge occurs as branching, red colored colonies at a depth of 6.0–15.0 m. Colonies of these sponges grow attached to exposed rocks or descending rocky slopes. Single branches usually measure 30–40 cm long and 1.5–2.0 cm thick. The sponges (in the dried state) are erect and composed of short, curved, flanged, narrow fans of different lengths with a restricted base of attachment. Surface textures of dry sponges are fibrous and roughened. The specimen of sponge viewed microscopically revealed that megascleres are arranged uniformly within fibers and clearly differentiated into primary and secondary tracts. The sponge material was identified and confirmed by Professor Rob W. M. VanSoest, Faculty of Science, Zoological Museum, Amsterdam. The sponge sample was freeze-dried (1 kg dry weight), ground and extracted with a mixture of MeOH/CH$_2$Cl$_2$ (1:1) (3 × 2 L) at room temperature. The extract was evaporated under vacuum to give 250 g of red oil. This extract was subjected to vacuum liquid chromatography on flash silica using hexane, ethyl acetate, and methanol gradient. Fractions eluted from 30% to 60% ethyl acetate in hexane were combined and concentrated to afford 60 g of material. Purification of this fraction was carried out by flash column chromatography on silica gel using hexane/ethyl acetate (85:15). Relatively non-polar fractions were combined. Final purification was carried out on RP-C18-HPLC using a mobile phase consisting of acetonitrile and water (60:40 v/v) to afford 1 (5 mg), 2 (4 g), and 3 (2 mg).

The polar fractions were combined and rechromatographed by flash column chromatography on silica gel using 2% methanol in chloroform. Final purification was carried out on sephadex LH-20 using methanol/chloroform (1:1) to afford 4 (14 mg).

4.3. Acetalization of 2

To a solution of 2 (0.395 g, 0.001 mmol) in MeOH, a catalytic amount of Et$_2$O–BF$_3$ was added. The mixture was stirred overnight and was neutralized with 10% aq.NaHCO$_3$ solution. The crude product was extracted with DCM (3 × 30 mL) and the organic layer was dried over anhydrous Na$_2$SO$_4$ then evaporated under reduced pressure. The residue was purified by silica column (9:1 hexane/acetone).

4.3.1. 15-MethoxyLat B (5)

(0.327 g, 80%); $[\alpha]_D^{25}$ 23.9 (c 0.11, MeOH); ^{1}H NMR (CDCl$_3$) δ (ppm): 5.9 (s, NH), 5.70 (s, 2-H), 5.17 (br s, 13-H), 5.25 (td, J = 11.4, 3.3, 6-H), 5.05 (td, J = 11.4, 1.6, 7-H), 4.2 (br t, J = 11.4, 11-H), 3.80 (dd, J = 12.0, 2.2, 16H), 3.40 (dd, J = 12.0, 2.2, 17-H), 3.29 (s, OCH$_3$), 2.75–1.0 (m, 5,5′, 4,4′, 9,9′′, 10,10′, 12,12′, 14,14′-H), 1.90 (s, 20-CH$_3$), 0.90 (s, 19-CH$_3$). HRMS m/z calcd for C$_{21}$H$_{32}$NO$_5$S (M+H$^+$) 410.2001, found 410.1997.

4.4. Alkylation of nitrogen of the thiazolidinone

To a suspension of sodium hydride (0.062 mmol) in dry THF, was slowly added methoxy Lat-B (0.045 mmol) at 0 °C. The mixture was stirred for one hour, then alkyl halide (2.4 mmol) was added and the reaction mixture stirred for 6–8 h under nitrogen atmosphere. Ether and water were added and the organic layer was dried over anhydrous Na$_2$SO$_4$. The residue was purified by column chromatography to yield pure N-alkyl derivative of Lat-B.

4.4.1. 15-Methoxy-N-methyl-Lat B (6)

(10 mg, 53%); $[\alpha]_D^{25}$ 27.2 (c 0.11, MeOH); ^{1}H NMR (CDCl$_3$) δ (ppm): 5.70 (s, 2-H), 5.17 (br s, 13-H), 5.25 (td, J = 11.4, 3.3, 6-H), 5.05 (td, J = 11.4, 1.6, 7-H), 4.24 (br t, J = 11.4, 11-H), 3.80 (dd, J = 12.0, 2.2, 16-H), 3.40 (dd, J = 12.0, 2.2, 17-H), 3.29 (s, OCH$_3$),

3.20 (s, N-CH$_3$), 2.75–1.00 (m, 5,5′, 4,4′, 9,9′, 10,10′, 12,2′, 14,14′-H), 1.90 (s, 20-CH$_3$), 0.90 (s, 19-CH$_3$). HRMS m/z calcd for C$_{22}$H$_{33}$NO$_5$SNa (M+Na$^+$) 446.1977, found 446.1981.

4.4.2. 15-Methoxy-N-pentyl-Lat B (7)

(11 mg, 52%); $[\alpha]_D^{25}$ 22.1 (c 0.11, MeOH); ^{1}H NMR (CDCl$_3$) δ (ppm) 5.70 (s, 2-H), 5.17 (br s, 13-H), 5.25 (td, J = 11.4, 3.3, 6-H), 5.05 (td, J = 11.4, 1.6, 7-H), 4.24 (br t, J = 11.4, 11-H), 3.80 (dd, J = 12.0, 2.2, 16-H), 3.40 (dd, J = 12.0, 2.2, 17-H), 3.29 (s, OCH$_3$), 3.15 (t, N-CH$_2$), 2.75–1.0 (m, 5,5′, 4,4′, 9,9′, 10,10′, 12,12′, 14,14′-H, CH$_3$ and (CH$_2$)$_3$), 1.91 (s, 20-CH$_3$), 0.92 (s, 19-CH$_3$). HRMS m/z calcd for C$_{26}$H$_{41}$NO$_5$SNa (M+Na$^+$) 502.2603, found 502.2611.

4.4.3. 15-Methoxy-N-hexyl-Lat B (8)

(11 mg, 51%); $[\alpha]_D^{25}$ 27.5 (c 0.11, MeOH); ^{1}H NMR (CDCl$_3$) δ (ppm) 5.70 (s, 2-H), 5.17 (br s, 13-H), 5.25 (td, J = 11.4, 3.3, 6-H), 5.05 (td, J = 11.4, 1.6, 7-H), 4.24 (br t, J = 11.4, 11-H), 3.80 (dd, J = 12.0, 2.2, 16-H), 3.40 (dd, J = 12.0, 2.2, 17-H), 3.29 (s, OCH$_3$), 3.19 (s, N-CH$_2$), 2.75–1.00 (m, 5,5′, 4,4′, 9,9′, 10,10′, 12,12′, 4,14′-H, CH$_3$ and (CH$_2$)$_4$), 1.90 (s, 20-CH$_3$), 0.90 (s, 19-CH$_3$). HRMS m/z calcd for C$_{27}$H$_{43}$NO$_5$SNa (M+Na$^+$) 516.2760, found 516.2769.

4.4.4. 15-Methoxy-N-octyl-LatB (9)

(12 mg, 52%); $[\alpha]_D^{25}$ 29.8 (c 0.11, MeOH); ^{1}H NMR (CDCl$_3$) δ (ppm) 5.70 (s, 2-H), 5.17 (br s, 13-H), 5.25 (td, J = 11.4, 3.3, 6-H), 5.05 (td, J = 11.4, 1.6, 7-H), 4.24 (br t, J = 11.4, 11-H), 3.80 (dd, J = 12.0, 2.2, 16-H), 3.40 (dd, J = 12.0, 2.2, 17-H), 3.29 (s,OCH$_3$), 3.21 (t, N-CH$_2$), 2.75–1.00 (m, 5,5′, 4,4′, 9,9′, 10,10′, 12,12′, 14,14′-H, CH$_3$ and (CH$_2$)$_6$), 1.90 (s, 20-CH$_3$), 0.90 (s, 19-CH$_3$). HRMS m/z calcd for C$_{29}$H$_{47}$NO$_5$SNa (M+Na$^+$) 544.3072, found 544.3083.

4.4.5. 15-Methoxy-N-nonyl-Lat B (10)

(13 mg, 55%); $[\alpha]_D^{25}$ 27.2 (c 0.11, MeOH); ^{1}H NMR (CDCl$_3$) δ (ppm) 5.70 (s, 2-H), 5.17 (br s, 13-H), 5.25 (td, J = 11.4, 3.3, 6-H), 5.05 (td, J = 11.4, 1.6, 7-H), 4.24 (br t, J = 11.4, 11-H), 3.80 (dd, J = 12.0, 2.2, 16-H), 3.40 (dd, J = 12.0, 2.2, 17-H), 3.29 (s, OCH$_3$), 3.21 (t, N-CH$_2$), 2.75–1.00 (m, 5,5′, 4,4′, 9,9′, 10,10′, 12,12′, 14,14′-H, CH$_3$ and (CH$_2$)$_7$), 1.90 (s, 20-CH$_3$), 0.90 (s, 19-CH$_3$). HRMS m/z calcd for C$_{30}$H$_{49}$NO$_5$SNa (M+Na$^+$) 558.3229, found 558.3234.

4.4.6. 15-Methoxy-N-decyl-Lat B (11)

(12 mg, 50%); $[\alpha]_D^{25}$ 31.1 (c 0.11, MeOH); ^{1}H NMR (CDCl$_3$) δ (ppm) 5.70 (s, 2-H), 5.17 (br s, 13-H), 5.25 (td, J = 11.4, 3.3, 6-H), 5.05 (td, J = 11.4, 1.6, 7-H), 4.2 (br t, J = 11.4, 11-H), 3.80 (dd, J = 12.0, 2.2, 16-H), 3.40 (dd, J = 12.0, 2.2, 17-H), 3.29 (s, OCH$_3$), 3.21 (t, N-CH$_2$), 2.75–1.00 (m, 5,5′, 4,4′, 9,9′, 10,10, 12,12′, 14,14′-H, CH$_3$ and (CH$_2$)$_8$), 1.90 (s, 20-CH$_3$), 0.90 (s, 19-CH$_3$). HRMS m/z calcd for C$_{31}$H$_{51}$NO$_5$SNa (M+Na$^+$) 572.3385, found 572.3377.

4.5. Hydrolysis of (11)

To a solution of 11 (0.062 mmol) in dry THF, H$_2$SO$_4$ (20 μmL) was added at room temperature. The mixture was stirred for one hour under nitrogen atmosphere, then poured into H$_2$O (10 mL). The crude product was extracted with ether (3 × 10 mL) and the organic layer was dried over anhydrous Na$_2$SO$_4$. The residue was purified by column chromatography to yield pure N-decyl derivative of Lat- B (12).

4.5.1. N-Decyl-Lat B (12)

(8 mg, 24%); $[\alpha]_D^{25}$ 19.1 (c 0.11, MeOH); ^{1}H NMR (CDCl$_3$) δ (ppm) 5.70 (s, 2-H), 5.17 (br s, 13-H), 5.25 (td, J = 11.4, 3.3, 6-H), 5.05 (td, J = 11.4, 1.6, 7-H), 4.2 (br t, J = 11.4, 11-H), 3.80 (dd, J = 12.0, 2.2, 16-H), 3.40 (dd, J = 12.0, 2.2, 17-H), 3.21 (t, N-CH$_2$), 2.75–1.00 (m, 5,5′, 4,4′, 9,9′, 10,10, 12,12′, 14,14′-H, CH$_3$ and (CH$_2$)$_8$), 1.90 (s, 20-CH$_3$),

236

0.90 (s, 19-CH$_3$). HRMS m/z calcd for C$_{30}$H$_{49}$NO$_5$SNa (M+Na$^+$) 558.3229, found 558.3221.

5. Computational details

Hydrogen atoms were added to the protein crystal structure complex containing actin, ATP and latrunculin A and the resultant structure was used for the docking studies with GOLD 2.0.[18] For docking, the active site of the protein was defined as the pocket formed by atoms within a 10 Å sphere centered on the O of Glu207, which is involved in H-bonding to the ligand. For each docking run, GOLD's genetic algorithm was used to generate 100,000 solutions. The number of populations was set to 5. The selection pressure was 1.1. Two different scoring functions were used for the docking studies: GOLD Score and ChemScore. Both the scoring functions produced a similar docking conformation, so we reported only the GOLD Scores (higher score implies better binding). The docked conformation was merged into the binding cavity and the complex was then minimized in sybyl 7.2[19] using the MMFF94 force field and charges, including only residues having any atom within an 8 Å sphere of Glu207 in the minimization (this included ATP). The binding energy (lower energy implies better binding) of ligands was calculated using the formula:

$$E_{binding} = E_{complex} - (E_{protein} + E_{ligand}).$$

References and notes

1. Neeman, I.; Fishelson, L.; Kashman, Y. *Mar. Biol.* **1975**, *30*, 293.
2. (a) Kashman, Y.; Groweiss, A.; Shmueli, U. *Tetrahedron Lett.* **1980**, *21*, 3629; (b) Gillor, O.; Carmeli, A.; Rahamim, Y.; Fishelson, Z.; Ilan, M. *Mar. Biotechnol.* **2000**, *2*, 213; (c) Hadas, E.; Shpigel, M.; Ilan, M. *Aquaculture* **2005**, *244*, 159; (d) Vilzny, B.; Amagata, T.; Mooberry, S. L.; Crew, P. *J. Nat. Prod.* **2004**, *67*, 1055.
3. Kashman, Y.; Groweiss, A.; Shmueli, U.; Lidor, R.; Blasberger, D.; Carmely, S. *Tetrahedron* **1985**, *41*, 1905.
4. Okuda, R. K.; Scheuer, P. J. *Experientia* **1985**, *41*, 1355.
5. (a) Spector, I.; Shochet, N. R.; Kashman, Y.; Groweiss, A. *Science* **1983**, *219*, 493; (b) Longley, R. E.; McConnell, O. J.; Essich, E.; Harmody, D. *J. Nat. Prod.* **1993**, *56*, 915; (c) Allingham, J. S.; Klenchin, V. A.; Rayment, I. *Cell. Mol. Life Sci.* **2006**, *18*, 1.
6. Coue, M.; Brenner, S. L.; Spector, I.; Korn, E. D. *FEBS Lett.* **1987**, *213*, 316.
7. Cimini, D.; Fioravanti, D.; Tanzarella, C.; Degrassi, F. *Chromosoma* **1998**, *107*, 479.
8. (a) Sokolov, I.; Iyer, S.; Woodworth, C. D. *Nanomedicine* **2006**, *2*, 31; (b) Sokolov, I. *Chem. Eng. News* **2006**, *84*, 34.
9. Wilkin, S. P. Ph.D. Thesis. *Isolation, Structure Elucidation and High-Throughput Lead Optimization Studies of Bioactive Secondary Metabolites from marine Invertebrates*; 2000 May.
10. Hoye, T. R.; Ayyad, S. N.; Eklov, B. M.; Hashish, N. E.; Shier, W. T.; El Sayed, K. A.; Hamann, M. T. *J. Am. Chem. Soc.* **2002**, *124*, 7405.
11. El Sayed, K. A.; Youssef, D. T.; Marchetti, D. *J. J. Nat. Prod.* **2006**, *69*, 219.
12. Blasberger, D.; Carmely, S.; Cojocaru, M.; Spector, I.; Shochet, N. R.; Kashman, Y. *Liebigs Ann. Chem.* **1989**, *12*, 1171.
13. Hansen, M. B.; Nielsen, S. E.; Berg, K. *J. Immunol. Methods* **1989**, *119*, 203.
14. Fürstner, A.; Kirk, D.; Fenster, M. D. B.; A, C.; De Souza, D.; Nevado, C.; Tuttle, T.; Thiel, W.; Müller, O. *Chem. Eur. J.* **2007**, *13*, 135.
15. Morton, W. M.; Ayscough, K. R.; McLaughlin, P. J. *Nature Cell Biol.* **2000**, *2*, 376–378.
16. Reutzel, R.; Yoshioka, C.; Govindasamy, L.; Yarmola, E. G.; Agbandje-McKenna, M.; Bubb, M. R.; McKenna, R. *J. Struct. Biol.* **2004**, *146*, 291.
17. Ahmed, S. A.; Odde, S.; Daga, P. R.; Bowling, J. J.; Mesbah, M. K.; Youssef, D. T.; Khalifa, S. I.; Doerksen, R. J.; Hamann, M. T. *Org. Lett.* **2007**, *9*, 4773.
18. Verdonk, M. L.; Cole, J. C.; Hartshorn, M. J.; Murray, C. W.; Taylor, R. D. *Proteins* **2003**, *52*, 609–623.
19. sybyl 7.2, Tripos: 1699 South Hanley Rd., St. Louis, Missouri, 63144, USA.

VITA

I was born in Kuwait in 1977 to an Egyptian family originally from Mansoura City, Egypt. I received my B.S. degree in Major Chemistry from Mansoura University (Chemistry Department, Damietta Faculty of Science), Egypt in 1999. I was then appointed as a TA in the same department in 2000 and completed my master degree in Organic Chemistry (Natural Products) in 2004. In 2006, I was granted a predoctoral fellowship from the Egyptian Government to obtain my Ph.D. in the field of marine natural products. In my free time I enjoy reading about history and watch the History Channel. I also like to play soccer and Tennis as well. Beside my work in the chemical field, I was interested in computer programming.